Universitat de Lleida

Genomic instability associated to impairment of Fe-S clusters synthesis in Saccharomyces cerevisiae yeast cells

José Carlos Aires Maria

Dipòsit Legal: L.1237-2014
http://hdl.handle.net/10803/275980

Genomic instability associated to impairment of Fe-S clusters synthesis in *Saccharomyces cerevisiae* yeast cells

Universitat de Lleida
Departament de Ciències
Mèdiques Bàsiques

José Carlos Aires Maria

(Graduate in Microbiology)

JULY, 2014

Thesis submitted to fulfill the requirements for the degree of Doctor, held under the scientific guidance of

Dr. Enric Herrero **Dr. Gemma Bellí**

Ao meu anjo da guarda

It is like life and destiny: we think we know the story, but we have read only half the tale.

Pedra filosofal

Eles não sabem que o sonho é uma constante
da vida tão concreta e definida
como outra coisa qualquer,
como esta pedra cinzenta em que me sento e descanso,
como este ribeiro manso em serenos sobressaltos,
como estes pinheiros altos
que em verde e ouro se agitam,
como estas aves que gritam
em bebedeiras de azul.
Eles não sabem que o sonho
é vinho, é espuma, é fermento,
bichinho álacre e sedento, de focinho pontiagudo,
que fossa através de tudo num perpétuo movimento.
Eles não sabem que o sonho
é tela, é cor, é pincel, base, fuste, capitel,
arco em ogiva, vitral, pináculo de catedral,
contraponto, sinfonia, máscara grega, magia,
que é retorta de alquimista,
mapa do mundo distante, rosa dos ventos, infante,
caravela quinhentista, que é Cabo da Boa Esperança,
ouro, canela, marfim,
florete de espadachim, bastidor, passo de dança,
Colombina e Arlequim, passarola voadora, pára-raios,
locomotiva, barco de proa festiva, alto-forno, geradora,
cisão do átomo, radar, ultra som, televisão
desembarque em foguetão na superfície lunar.
Eles não sabem, nem sonham,
que o sonho comanda a vida.
Que sempre que um homem sonha
o mundo pula e avança
como bola colorida
entre as mãos de uma criança.

António Gedeão, Movimento Perpétuo (1956)

ACKNOWLEDGMENTS

Researchers are awkwardly social beings, but, in spite of that, they can not live isolated from the society in which they work. They are afflicted by the same injustices, struggles and lack of social awareness as other citizens, have problems, questions, suffer from loneliness, are happy in various degrees, receive a certain degree of support in the pursuit of their goals, have or have no friends. Despite the difficulties with which PhD candidates are confronted (economic, isolation, loneliness), the thesis presented here and the investigation that led to it had numerous supporters - some unexpected, some more expected, and others because of intense friendships. It is, therefore, my pleasure to list each supporter and gratefully acknowledge their contribution.

This thesis is not only the result of extensive hours of study, reflection and work during the many phases that were required for its completion. It is also the culmination of an academic goal that I pursue. It would not have been possible without the help of a considerable number of people.

Començo agraint als meus directors, primer al Dr Enric Herrero per acceptar-me en el seu laboratori i donar-me la possibilitat d'entrar en aquesta aventura que va començar fa gairebé 5 anys. Gràcies per la teva paciència, la teva preocupació pel meu benestar i per compartir la teva saviesa i, sobretot, aquesta inquietud contagiosa que t'envolta. En segon lloc, la Dra Gemma Belli que més que una consellera vaig tenir el plaer de tenir-te com una companya. Gràcies pel teu consell, la crítica i la teva disposició a suavitzar sempre els mals resultats que estava tenint. També una paraula d'agraïment a la Dra Celia Casas per la seva preocupació constant en fer les coses bé i més que res en la raó per fer-les.

Una paraula afectuosa als meus companys de laboratori que amb el temps es van convertir en amics, la Laia, la Judit, la Maria, el Jordi, el David, l' Andrés, el Sergi i el Fernando per fer d'aquest meu segon llar un lloc més agradable.

També vull agrair a les meves segones mans perquè sense la seva participació aquest treball no es va fer d'una manera suau, em refereixo a la Mireia, a la Esther, a la Meri i a la Sílvia, les hi dono les gràcies per la seva ajuda i disponibilitat.

Agradeço aos meus pais, às minhas madrinhas (em principal a "madrinha" Cecília) e ao resto da minha família por me terem dado todas as oportunidades para que pudesse chegar onde estou. Uma palavra de apreço ao "pai" Guerra que foste tu o principal culpavél de estar nesta situação e mais recentemente ao meu "veio" Zé Luis que com a tua boa disposição contagiante fizeste desta minha travessia um passeio na praia de Copacabana.

A Liliana que és a minha sombra, companheira e ladra do meu coração que sem ti esta aventura nunca teria chegado a bom porto. Só tu sabes o quanto sofremos juntos para chegarmos a este final. Espero que a partir de agora possa pagar a minha eterna divida que tenho contigo. Aos teus pais por primeiro te terem trazido a este mundo e depois por serem uns grandes amigos.

Ao Rui, a Ester, a Alexandra pela vossa ajuda em tudo que pedia, por serem muito mais que amigos e por conseguirem sempre tirar-me uma gargalhada quando só via tormentas. E mais recentemente ao Rui Benfeitas por nesta reta final me trazer um pouco do ar luso que tanto falta sinto.

La Moma i l'Anabel per la seva amistat, suport i constant preocupació per mi.

A la Ana y a José mi "tocayo" guatemalteco por aguantarme y por hacereme sentir que no soy un extraño, sino uno más como ellos. José con tu buen gusto por los coches, comida, música y programas de tele me has hecho olvidar que eres de los maristas.

To Charu, Disha, Upasana and Arindam for accepting me into your circle of friends and show me the beauty that is the Indian culture. I am eternally grateful to consider me as a friend.

To Hiren, Rinku and Venky for sharing a bit of their lives with me.

Ana con tu "broken english" y amistad, gracias por compartir las cenas, alegrías y penas.

Alejandra, Ayax y Eric, guardaré vuestra amistad mexicana en el corazón con mucho cariño.

Bernarda, ha sido con un enorme placer conocerte y muchas gracias desde el corazón por tu amistad.

Ingrid, estimada amiga gràcies per l'acollida afectuosa a Avignon i Dublín. En tots dos viatges ens has fet sentir com a casa. Sergi gràcies per ser un bon guia i per ajudar-me en els aspectes tècnics d'aquesta tesi.

A la familia Camarasa, René, Sandra, madre, Tere, Lay, Moni y Héctor por haberme hecho sentir parte de vuestra familia muy divertida y peculiar en la que me considero un miembro más.

Aan Paula, die ik beschouw als een goede vriend, een speciaal woord van dank voor het laten meebeleven van vele onvergetelijke en ontstressende wandelingen.

Ao "Ti Alex" que de Barcelona foste a melhor recordação que mantenho no coração. Quem diria que uma década depois estaria nesta posição de defender uma tese, hein? E a sua respectiva e doce QiaoQiao que com a sua amizade nos cativou para sempre.

A minha "primeira filhota" Tânia que desde o nosso encontro aqui em Lleida nunca mais deixamos de estar em contacto. Um abraço forte ao Bruno e ao vosso rebento.

Aos meus velhos amigos de sempre, Sidónio, Sérgio, Pedro, Martinha, Pedro Reis e Chicão que como eu sabem o que é ser emigrante e o que isso representa.

Por último mas não menos importante, a minha família portuguesa aqui em Lleida, Filipe, Tânia e Alex, um muito, mas muito obrigado por me terem adotado como mais um membro da família e me fazerem sentir amado e mimado.

Distracted like I am, more names should appear here but it would extend the number of pages and increase the price of this thesis and that my advisor would not thing so funny, so...

To all, my sincere thanks.

SUMMARY

Grx5 is one of eight proteins of the glutaredoxin (GRX) family in *Saccharomyces cerevisiae*. GRXs are thiol oxidoreductases widely spread among prokaryotic and eukaryotic organisms. Yeast Grx5 is located at the mitochondrial matrix and participates in the synthesis of iron-sulphur clusters (ISCs), which are co-factors required for several essential cellular processes, such as respiration, photosynthesis, nitrogen fixation, ribosome biogenesis, regulation of gene expression and DNA-RNA metabolism. Cells lacking Grx5 display several phenotypes: (i) inability to grow on minimal medium or in the presence of a non-fermentable carbon source, (ii) hypersensitivity to external oxidants, (iii) iron accumulation inside the cell, (iv) increase in protein oxidative damage, and (v) defects in the activity of enzymes requiring ISCs as cofactors, like aconitase or succinate dehydrogenase. These phenotypes are similar to those of other ISC mutants. Some ISC proteins are involved in DNA metabolism, more precisely in DNA replication and/or repair processes. Recent works reported that defects in ISC metabolism compromise the stability of the cellular genome, and this instability is associated to human predisposition towards multiple types of cancers. Using the yeast *grx5* mutant as a model we wanted to gain further insight in the relationship between genomic instability and defects in ISC biosynthesis.

In the present study we demonstrated that cells lacking Grx5 display increased recombination and spontaneous mutation frequencies, leading to a genetic instability. These phenotypes are independent of the iron overload observed in the *Δgrx5* mutant. Furthermore, a significant increase in Rad52-associated foci formation was observed in mutant cells, indicating DNA repair clustered lesions. We have also shown that *Δgrx5* mutant cells are hypersensitive to several DNA-damaging agents and that this phenotype is independent of the oxidant conditions found in the medium. Overexpressing the chaperone Ssq1, another ISC biosynthesis pathway protein, rescues the sensitivity phenotype of the *Δgrx5* mutant against genotoxic agents. Defects in cell cycle progression observed in *Δgrx5* mutant cells as a consequence of genetic instability are specific of the S-phase. We studied various DNA damage pathways and found that only the Homologous Recombination (HR) pathway seems to play an important role in repairing DNA damage in *Δgrx5* mutant cells. This was shown by the severe additive effects (compared to the single mutants) observed in the double mutants *Δgrx5Δrad50* and *Δgrx5Δrad52* with respect to the hypersensitivity to DNA-damaging agents. This is confirmed by the additive

hypersensitivity of these two double mutants in the presence of the antitumor drug camptothecin, which causes double strand breaks DNA damage. Finally, the hypersensitivity of the *Δgrx5* mutant cells to the genotoxic agents was proved to be independent of defects in the assembly/maturation of ISC in several proteins that participate in the DNA repair pathways, such as Pri2, Rad3 or Ntg2.

RESUMEN

La proteína Grx5 de *Saccharomyces cerevisiae* es una de las ocho proteínas de la familia de las glutaredoxinas (GRXs) en esta especie de levadura. Las GRXs son tiol oxidoreductasas ampliamente distribuídas entre organismos procariotas y eucariotas. La proteína Grx5 de levadura se encuentra en la matriz mitocondrial y participa en la síntesis de los centros hierro-azufre (ISCs), que son co-factores necesarios para varios procesos celulares esenciales, tales como la respiración, la fotosíntesis, la fijación de nitrógeno, la biogénesis de los ribosomas, la regulación de la expresión génica y el metabolismo del ADN-ARN. Las células de levadura que carecen de Grx5 muestran varios fenotipos: (i) incapacidad para crecer en medio mínimo o en presencia de una fuente de carbono no fermentable, (ii) hipersensibilidad a oxidantes externos, (iii) acumulación de hierro dentro de la célula, (iv) aumento del daño oxidativo en las proteínas, y (v) defectos en la actividad de enzimas que requieren ISCs como cofactores, tales como la aconitasa o la succinato deshidrogenasa. Estos fenotipos son similares a los de otros mutantes en la biogénesis de ISCs. Algunas proteínas asociadas a ISCs están involucradas en el metabolismo del ADN, más precisamente en su replicación o en procesos de reparación del mismo. Trabajos recientes demostraron que los defectos en el metabolismo de ISCs comprometen la estabilidad del genoma celular, y esta inestabilidad está asociada a la predisposición a múltiples cánceres humanos. Mediante el uso de un mutante *Δgrx5* de *S. cerevisiae* como modelo de estudio quisimos abordar la comprensión de la relación entre la inestabilidad genómica y los defectos en la biosíntesis de ISCs.

En el presente estudio hemos demostrado que las células que carecen de Grx5 tienen aumentada la frecuencia de recombinación y de mutación cromosómicas, lo que conduce a una inestabilidad genética elevada. También se demostró que estos fenotipos no dependen de la acumulación de hierro en el mutante *Δgrx5*. Además, se observó un aumento significativo en la formación de "foci" (áreas del núcleo donde el ADN está dañado) asociados a la proteína Rad52 en las células mutantes, indicando lesiones en las zonas de reparación del ADN. También hemos demostrado que las células mutantes *Δgrx5* son hipersensibles a varios agentes que dañan el ADN y que este fenotipo es independiente de las condiciones oxidantes del mutante. Se ha demostrado que la sobreexpresión de otra proteína implicada en la ruta de biosíntesis de ISCs (Ssq1) rescata el fenotipo de sensibilidad presentado por el mutante *Δgrx5* frente a agentes genotóxicos. Además, los defectos en la progresión del ciclo celular observados en las

células mutantes *Δgrx5* son específicos de la fase S. Entre las diferentes vías de daño en el DNA estudiadas, sólo la vía de recombinación homóloga (HR) parece jugar un papel importante en la reparación de daño del ADN en las células mutantes *Δgrx5*, tal como se muestra por los efectos aditivos (en comparación con los mutantes individuales) observados en los dobles mutantes *Δgrx5Δrad50* y *Δgrx5Δrad52* con respecto a la hipersensibilidad a agentes que dañan el ADN. Esto se ha confirmado también a través de la hipersensibilidad aditiva de estos dos dobles mutantes en presencia del fármaco antitumoral camptotecina, que causa roturas de doble cadena en el ADN. Por último, la hipersensibilidad de las células mutantes *Δgrx5* a los agentes genotóxicos se demostró no ser debida a defectos en el ensamblaje/maduración de varias proteínas asociadas a ISCs que se sabe que participan en los procesos de reparación del ADN, tales como Pri2, Rad3 o Ntg2.

RESUM

La proteïna Grx5 de *Saccharomyces cerevisiae* és una de les vuit proteïnes de la família de les glutaredoxines (GRX) en aquesta espècie de llevat. Les GRXs són tiol oxidoreductases àmpliament repartides entre organismes procariotes i eucariotes. La Grx5 de llevat es troba a la matriu mitocondrial i participa en la síntesi dels centres ferro-sofre (ISCs), que són co-factors necessaris per a diversos processos cel·lulars essencials, com ara la respiració, la fotosíntesi, la fixació de nitrogen, la biogènesi del ribosoma, la regulació de l'expressió gènica i el metabolisme de l'ADN-ARN. Les cèl·lules de llevat que no tenen Grx5 mostren diversos fenotips: (i) incapacitat per créixer en medi mínim o en presència d'una font de carboni no fermentable, (ii) hipersensibilitat a oxidants externs, (iii) acumulació de ferro dins la cèl·lula, (iv) augment de dany oxidatiu de proteïnes, i (v) defectes en l'activitat d'enzims que requereixen ISCs com a cofactors, com són l'aconitasa o la succinat deshidrogenasa. Aquests fenotips són similars als d'altres mutants en la biogènesi de ISCs. Algunes proteïnes amb ISCs estan involucrades en el metabolisme de l'ADN, més precisament en la replicació de l'ADN o en els processos de reparació del mateix. Treballs recents van demostrar que els defectes en el metabolisme de ISCs comprometen l'estabilitat del genoma cel·lular, i aquesta inestabilitat està associada a la predisposició a múltiples càncers humans. Mitjançant l'ús d'un mutant *Δgrx5* de *S. cerevisiae* com a model d'estudi vam intentar entendre millor la relació entre la inestabilitat genòmica i els defectes en la biosíntesi de ISCs.

En el present estudi hem demostrat que les cèl·lules que no tenen Grx5 augmenten les freqüències de recombinació i mutació cromosòmiques, el que condueix a una inestabilitat genètica elevada. També es va demostrar que aquests fenotips no depenen de l'acumulació de ferro en el mutant *Δgrx5*. A més, es va observar un augment significatiu en la formació de "foci" (àrees del nucli on l'ADN està danyat) associats a la proteïna Rad52 en les cèl.lules mutants, indicant lesions en les zones de reparació de l'ADN. També hem demostrat que les cèl·lules mutants *Δgrx5* són hipersensibles a diversos agents que danyen l'ADN i que aquest fenotip és independent de les condicions oxidants que es troben en el mutant. S'ha demostrat que la sobreexpressió d'una altra proteïna implicada en la ruta de biosíntesi de ISCs (Ssq1) rescata el fenotip de sensibilitat del mutant *Δgrx5* front aquests agents genotòxics. A més, els defectes en la progressió del cicle cel·lular observats en les cèl·lules mutants *Δgrx5* són específics de la fase S. Entre les diferents vies de dany en el DNA estudiades només la via de recombinació homòloga

(HR) sembla jugar un paper important en la reparació de dany de l'ADN en les cèl.lules mutants *Δgrx5*, com es mostra pels efectes additius (en comparació amb els mutants individuals) observats en els dobles mutants *Δgrx5Δrad50* i *Δgrx5Δrad52* pel que fa a la hipersensibilitat a agents que danyen l'ADN. Això s'ha confirmat també per la hipersensibilitat additiva d'aquests dos dobles mutants en presència del fàrmac antitumoral camptotecina, que causa trencaments de doble cadena en l'ADN. Per últim, la hipersensibilitat de les cèl.lules mutants *Δgrx5* als agents genotòxics es va demostrar no ser deguda a defectes en l'assemblatge/maduració de diverses proteïnes amb ISCs que se sap que participen en els processos de reparació de l'ADN, com ara Pri2, Rad3 o Ntg2.

RESUMO

A Grx5 de *Saccharomyces cerevisiae* é uma das oito proteínas que compoêm a família glutaredoxina (GRX) desta espécie de levedura. As GRXs são tiol-oxidorredutases amplamente espalhadas entre os organismos procariotas e eucariotas. A Grx5 de levedura está localizada na matriz mitocondrial e participa na síntese de "clusters" ferro-enxofre (ISCs), que são co-factores necessários para vários processos celulares essenciais, tais como a respiração, a fotossíntese, a fixação de azoto, a biogénese ribossomal, a regulação de expressão génica e no metabolismo de ADN-ARN. As células de levedura sem Grx5 exibem vários fenótipos: (i) incapacidade de crescer em meio mínimo ou em presença de uma fonte de carbono fermentável, (ii) hipersensibilidade aos oxidantes externos, (iii) acumulação de ferro no interior da célula, (iv) aumento do dano oxidativo nas proteínas, e (v) defeitos na atividade das enzimas que requerem ISC como cofator, como por exemplo a aconitase ou o succinato desidrogenase. Estes fenótipos são semelhantes aos de outros mutantes involucrados na síntese de ISC. Algumas proteínas com este tipo de "clusters" estão envolvidas no metabolismo do ADN, mais precisamente na replicação ou em processos de reparação do ADN. Trabalhos recentes relataram que os defeitos no metabolismo destes "clusters" comprometem a estabilidade do genoma celular e esta instabilidade está associada á predisposição humana a vários tipos de cancro. Usando como modelo de estudo um mutante de levedura onde a proteína Grx5 foi retirada queríamos obter mais informações sobre a relação entre a instabilidade genética e os defeitos na biossíntese dos ISCs.

Neste estudo foi demonstrado que células de leveduras sem a proteína Grx5 exibem um aumento nas frequências de mutação e de recombinação, que tem como consequencia um aumento na instabilidade genética do organismo. Também foi demonstrado que estes fenótipos não são dependentes da acumulação de ferro por mutantes *Δgrx5*. Além disso, foi observado um aumento significativo na formação de "foci" (zonas do núcleo onde o ADN se encontra danificado) nos mutantes *Δgrx5* associados á proteína repórter rad52, indicando lesões na reparação do ADN. Mostrámos também que as células do mutante *Δgrx5* são hipersensíveis a vários agentes que danificam o ADN e que este fenótipo é independente das condições oxidantes ás quais está exposto o mutante. Ficou também demonstrado neste trabalho que a sobrexpressão da proteina chaperona Ssq1, envolvida também na via de biossíntese dos ISC, resgata o fenótipo de sensibilidade apresentada pelo mutante *Δgrx5* contra os agentes

genotóxicos. Além do mais ficou comprovado que os defeitos da progressão do ciclo celular observados em células mutantes *Δgrx5* eram específicos da fase S.

Entre as diferentes vias de reparação do ADN, apenas a via de recombinação homóloga (HR) parece desempenhar um papel importante na reparação de danos no ADN em células mutantes *Δgrx5* como demonstrado pelos efeitos acentuados (em comparação com os mutantes simples) observados nos mutantes duplos *Δgrx5Δrad50* e *Δgrx5Δrad52* no que diz respeito à hipersensibilidade aos agentes que danificam o ADN, como é o caso do fármaco anti-tumoral denominado camptotecina que provoca quebras de cadeia dupla de dano de ADN. Finalmente, demonstrou-se que a hipersensibilidade apresentada das células mutantes *Δgrx5* aos agentes genotóxicos não era provocada por defeitos de montagem ou de maturação dos ISCs de várias proteínas do ISCs que são conhecidos por participar no sistema de reparação do ADN, tais como Pri2, Rad3 ou Ntg2.

ABBREVIATIONS

5-FOA – 5-Fluorotic acid
AP – apurinic/apyrimidinic
AcLi – lithium acetate
BER – base excision repair
BPS – bathophenanthrolinedisulfonic acid
CDK – cyclin-dependent kinase
CIA – cytosolic iron–sulphur protein assembly
CPD – cyclobutane pyrimidine dimers
CPT – camptothecin
ctDNA – chloroplasts DNA
DDR – DNA damage response
DIG-dUDP – dioxigenin-dUDP
dNTP – deoxyribonucleotide triphosphate
DSB – double strand break
dsDNA – double-stranded DNA
FACS – fluorescence-activated cell sorting
Fe-S – iron sulphur
FRDA – Friedreich ataxia
GG-NER – global genomic NER
GPX – glutathione peroxidase
GRX – glutaredoxin
GSH – glutathione
GSSG – oxidized glutathione
GST – glutathione-S-transferase
HR – homologous recombination
HU – hydroxyurea
ICL – interstrand cross-linked repair
ISC – Fe-S cluster
MDA – malondialdehyde
MetO – methionine sulfoxide
MMS – methyl methane sulfonate
NAC – N-acetyl cysteine
NER – nucleotide excision repair
NIF – nitrogen fixation
MMR – mismatch repair
MSR – methionine sulphoxide reductase
mtDNA – mitochondrial DNA
nDNA – nuclear DNA
NHEJ – nonhomologous end join
PAPS – 3'-phosphoadenosine 5'-phosphosulphate
PCNA – proliferating cell nuclear antigen

PCR – polymerase chain reaction
PEG – polyethylene glycol
PHGPX – phospholypid hydroperoxide GPXs
PRR – post-replication repair
PRX – thioredoxin peroxidase
RPA – replication protein A
RNAP II – RNA polymerase II
RNR – ribonucleotide reductase
RNS – reactive nitrogen species
ROS – reactive oxygen species
SOD – superoxide dismutase
SUF – sulphur mobilization
ssDNA – single-stranded DNA
UV – ultraviolet
***t*-BOOH** – *ter*-butyl hydroperoxide
TC-NER – transcription coupled NER
TD – thymine dimer
TLS – translesion synthesis
TRX – thioredoxin
XP – xeroderma pigmentosum
YFP – yellow fluorescence protein

LIST OF TABLES

LIST OF FIGURES

TABLE OF CONTENTS

PART I

INTRODUCTION

1. OXIDATIVE STRESS

1.1. General concepts

In an oxidative environment like the one we live in, aerobic life generates oxidants. As a consequence, both photosynthetic and non-photosynthetic organisms are exposed to potential damage by these oxidants to diverse cell components including membrane lipids, proteins and DNA. Various oxidants can be generated under oxidative stress, which occurs when the concentration of these oxidants increases beyond the antioxidant buffering capacity of the cell, as well as during the course of normal metabolism in certain cell compartments (Michelet *et al.*, 2006). There are two main oxidant categories: reactive oxygen species (ROS), and reactive nitrogen species (RNS). Oxygen-cotaining chemical species where that oxygen can assume various oxidation states that include the singlet oxygen, the superoxide anion (O_2^-), hydrogen peroxide (H_2O_2), the highly reactive hydroxyl radical (OH·) and peroxide radicals are considered ROS (Toledano *et al.*, 2003). In contrast, when oxygen is combined with nitrogen and forms nitric oxide radicals (NO^-) and peroxynitrite radicals ($ONOO^-$), these species are described as RNS. To protect their cell components against these oxidants different organisms have evolved several defence mechanisms. Understanding all the processes that are involved in the oxidative stress is of critical importance in biomedical research, since oxidative damage has been related to major human diseases including atherosclerosis, diabetes, cardiovascular diseases, cancer, neurodegenerative disorders (such as Alzheimer, Parkinson, Huntington or Friedreich ataxia), or chronic liver and lung diseases (Ames *et al.*, 1993).

1.2. Damage to cellular components

Fig. 1 shows the different types of damage to cellular components caused by ROS. The most highly reactive ROS is the OH· radical. This high reactivity limits its diffusion in biological systems, causing OH· to generate cellular damage on target molecules proximal to the site where the radical is generated. With respect to O_2^- the most deleterious effect

is associated to its ability to release iron from proteins containing iron-sulphur (Fe-S) clusters (ISCs), like aconitase, which leads to both damage of these proteins and further generation of other ROS through autocatalytic cyclic reactions. Nevertheless, this toxicity might be associated to an iron deprived state due to increased demand for reassembling dissociated ISCs (Toledano *et al.,* 2003).

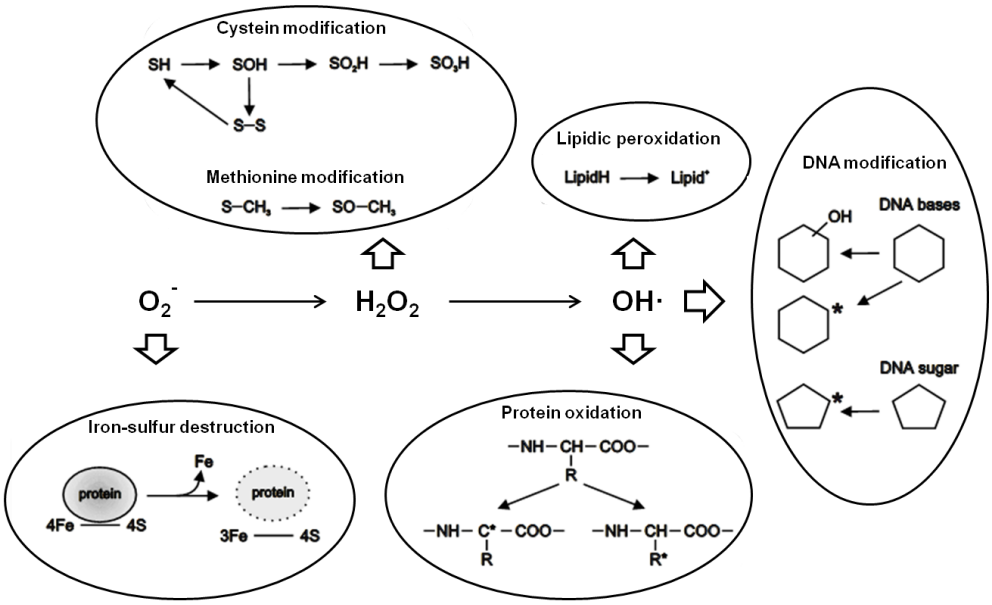

Fig. 1. Scheme of the ROS reactivity with biological molecules.

1.2.1. Lipids

A lipid peroxidation chain reaction is initiated with the formation of OH· starting with the hydrogen removal from an unsaturated lipid side chain. As a consequence, a first radical is produced which can accept a dioxygen (O_2) molecule to form a peroxyl radical (LOO·) and be transformed to an alkoxyl radical (LO·) to carry on an autocatalytic peroxidation chain reaction. This reaction will be interrupted when two lipid radical molecules combine or in the presence of radical scavengers like alpha-tocopherol (Toledano *et al.,* 2003). The products derived from lipid peroxidation and some of their by-products, such as 4-hydroxynonenal and malondialdehyde (MDA), quickly react with other biological molecules, mainly forming adducts with proteins and DNA bases (Møller *et al.,* 2007).

1.2.2. Proteins

ROS and RNS cause various types of chemical modifications on proteins. These modifications, if irreversible, are often associated with permanent loss of function and lead to the elimination or the accumulation of the damaged proteins. Modifications of cysteine residues may be reversible and have a dual role in the protection from

irreversible oxidation of these same cysteine residues and the modulation of protein function (Ghezzi and Bonetto, 2003). Depending on the ROS exposure, aggregation or fragmentation of proteins *in vitro* can occur. Generally, OH· preferentially promotes protein aggregation, but in the presence of O_2, it mainly leads to protein fragmentation. Under *in vitro* conditions, OH· initiates protein damage by either attacking the alpha carbon or the amino acid side chain of proteins, forming a carbon radical which initiates an autocatalytic chain reaction that is somewhat similar to that described for lipids. In addition to the generic damage just described, OH· radicals cause the hydroxylation of some amino acids, such as phenylalanine, tyrosine, arginine, histidine and lysine (Toledano *et al.,* 2003). There are several classes of damage that ROS and RNS can cause to protein. These classes are described below.

Carbonylation: Protein carbonylation is an irreversible oxidative damage which leads to a loss of protein function. The oxidation of proteins by ROS generates reactive carbonyl derivatives. These derivates are formed by a variety of oxidative pathways, such as direct oxidation of the protein backbone leading to the formation of protein fragments with an N-terminal α-ketoacyl amino acid residue, oxidation of some amino acid side chains (particularly, histidine, arginine or lysine) into ketone or aldehyde derivatives, reaction with products of lipid peroxidation (such as 4-hydroxy-2-nonenal), or conjugation with reducing sugars (glycation) or their oxidation products (glycoxidation). Protein carbonylation is considered a good indicator of the oxidative damage extent associated with various conditions of oxidative stress, aging and physiological disorders, including neurodegenerative diseases (Ghezzi & Bonetto, 2003; Dalle-Donne *et al.,* 2006).

Nitrosylation: This process can be reversed by protective mechanisms. The covalent attachment of the NO^- to cysteine thiol is a post-translational modification that potentially regulates protein functions (Jaffrey *et al.,* 2001). Protein and glutathione thiols can react with NO^- derivatives leading to a variety of products including disulfides, sulfenic, sulfinic and sulfonic acids, as well as S-nitrosothiols (Costa *et al.,* 2003). The most common NO^- derivative peroxynitrite ($ONOO^-$) is formed by the reaction $NO^- + O_2^- \rightarrow ONOO^-$. This NO^- derivative can cause depletion of sulphydryl groups and other modifications including lipid oxidation, DNA bases deamination, nitration of aromatic amino acid residues, and oxidation of methionine to its sulfoxide (Møller *et al.,* 2007).

Disulfide-bond formation: Formation of disulfide bonds from the free thiols of the protein is a reversible process. The stability of the disulfide bond is of biological importance for protein structure and function. The ability to form and break a specific bond under suitable biological conditions depends on the oxidant or reductant nature,

the disulfide stability, forward and reverse reactions kinetics, and the nature and redox state of the environment where the reaction occurs (Gilbert, 1995). The oxidation of thiol to disulfide provoked by different ROS (for example H_2O_2) is a very important metabolic redox regulation mechanism. Intra/intermolecular disulfide bonds can be formed between cysteine side chains, and the reduced form can be regenerated with the participation of diverse reductases such as the thioredoxin (TRX) or glutaredoxin (GRX) systems (Møller *et al.,* 2007), which will be explained later in detail.

1.2.3. DNA

DNA molecules do not suffer damage directly by O_2^- and H_2O_2 themselves; instead, damage occurs through Haber Weiss and Fenton-catalyzed OH· production (Toledano *et al.,* 2003). As DNA is negatively charged it binds transition metal cations (such as iron) which catalyze the above reactions. Moreover, other radicals which are formed from protein and lipid peroxidation can also induce DNA damage, such as adducts formed from MDA. At least sixty different DNA modifications by the OH· radical are known (Boiteux, 1997), including single and double DNA strand breaks (DSB), abasic site formation, direct base modifications, and DNA cross-links. It has been estimated that endogenous ROS can cause approximately 50,000 to 200,000 apurinic/apyrimidinic (AP) sites per mammalian cell per day (Martin, 2008). Mitochondrial DNA (mtDNA) holds higher steady-state damage compared with nuclear DNA (nDNA). This accumulation is probably caused by local ROS formation and also by the lack of chromatin protection provided by histones (Szczesny *et al.,* 2003).

1.3. Cellular effects of ROS in *Saccharomyces cerevisiae*

The studies described in this thesis have been carried out with the model organism *S. cerevisiae* since this yeast provides the combination and integration of cell biological, biochemical, genetic, and genome-wide experimental approaches that allow us to describe the cellular effects of ROS and analyse the mechanisms of defence against oxidative stress. The cellular tolerance of yeast cells to ROS toxicity differs between growth stages. In stationary phase (when nutrients are exhausted) they show higher resistance to stress, including oxidative and thermal ones, than cells in exponential phase (Toledano *et al.,* 2003). Also, cells grown in non-fermentable medium (glycerol), and therefore forced to respire, are more resistant to H_2O_2 and menadione (a generator of superoxide) than cells grown in glucose medium (Flattery-O'Brien *et al.,* 1993). Respiring cells display higher protein carbonyl content (Cabiscol *et al.,* 2000). During respiration,

the major oxidized targets are mitochondrial proteins, in accordance with the fact that mitochondria become the main source of ROS during respiration (Cabiscol *et al.,* 2000). Menadione and H_2O_2 have distinctive effects on cells at different cell cycle stages. In asynchronous cell populations H_2O_2 arrests cells in G2 phase while menadione does it in G1 (Flattery-O'Brien, 1998). A detailed study examining the cell death induced by high doses of H_2O_2 reported the presence of several key features of apoptosis (Madeo *et al.,* 1999).

1.4. Defence systems against oxidants

To maintain the adequate cellular redox state and minimize the damaging effects of ROS, aerobic organisms evolved diverse non-enzymatic and enzymatic antioxidant defence systems. We will start by describing the former type and then review the later type of antioxidant defences.

1.4.1. Non-enzymatic defence systems

Non-enzymatic defence systems typically consist of small molecules acting as antioxidants, which are soluble in either an aqueous or a lipid environment. These defence systems include for example vitamin E, polyamines, ascorbic acid, lipid-soluble antioxidants, metallothioneins, flavohaemoglobin and glutathione.

Vitamin E: Vitamin E functions as an essential lipid-soluble antioxidant that prevents the propagation of free radicals including lipid peroxyl, alkoxyl and hydroxyl radicals. Yeast cells treated with Trolox, a soluble compound analogue of α-tocopherol (the most biologically active form of vitamin E), revealed decreased intracellular oxidation during normal metabolism (Raspor *et al.,* 2005).

Polyamines: Polyamines are small molecules derived from amino acids implicated in protecting yeast against oxidant stress (by holding some ROS, especially O_2^-). As they are positively charged, they can interact with negatively charged molecules such as DNA, RNA and proteins. In *S. cerevisiae*, the polyamines spermine and spermidine have been found to be essential for aerobic growth and the *spe2* mutant (unable to synthesize spermidine) was found to be hypersensitive to oxygen (Balasundaram *et al.,* 1993).

Ascorbic acid: Ascorbic acid is a hydrosoluble molecule with antioxidant properties known to be important in higher eukaryotes (Jamieson, 1998). Ascorbate, or vitamin C, the anion form of ascorbic acid, is not produced in yeast cells but a related compound, erythroascorbate, has been detected in *S. cerevisiae* at very low concentrations (Jamieson, 1998). Ascorbate has been demonstrated to promote protein

oxidation in the presence of metal ions, to induce apoptosis and also to enhance iron toxicity in hemochromatosis (Krzepiłko *et al.,* 2004). In *S. cerevisiae*, ascorbate is able to protect cells lacking Cu-Zn-dependent superoxide dismutase (SOD) against toxicity of pure oxygen atmosphere and against shortening of replicative life span, and also to rescue auxotrophy for lysine and methionine (Lewinska *et al.,* 2004).

Lipid-soluble antioxidants: Little is known about lipid-soluble antioxidant molecules in *S. cerevisiae*. However, it has been observed that the lipid membrane composition of yeast is important in giving resistance to oxidative stress. Cells containing membranes with a higher level of saturated fatty acids are more resistant to oxidative stress than those with a higher level of polyunsaturated fatty acids (Howlett & Avery, 1997).

Metallothioneins: Metallothioneins are a family of cysteine-rich low molecular weight proteins with antioxidant properties. They have the ability to bind a varying number of metal ions (such as iron or cupper). *CUP1* and *CRS5* are yeast genes for metallothioneins that participate in protecting cells against oxidants (Culotta *et al.,* 1994).

Flavohaemoglobin: Flavohaemoglobin is a metalloprotein that participates in the detection and protection against nitric oxide. Yeast flavohemoglobin, YHb1, has been implicated in both the oxidative and nitrosative stress responses in *S. cerevisiae*. Mutants deficient in Yhb1 are moderately sensitive to oxidants such as diamide, and expression of the gene *YHB1* is induced in the presence of oxygen (Zhao *et al.,* 1996).

Glutathione (GSH): This ϒ-L-glutamyl-L-cystinyl-glycine tripeptide (ca. 307 Da) is probably the best known example of non-enzymatic defence system. This is due to its presence at high concentration in most living cells from microorganisms to humans (Penninckx, 2000). As electron donor, GSH reduces protein disulfide bonds. In the process, GSH is converted to its oxidized form (GSSG). Once oxidized, GSH can be reduced back by glutathione reductase, using NADPH as an electron donor. The ratio of reduced glutathione to oxidized glutathione is often used as a measure of cellular toxicity. In *S. cerevisiae* two genes are involved in GSH biosynthesis, *GSH1* and *GSH2* (encoding for ϒ -glutamylcysteine synthetase and glutathione synthetase, respectively). Yeast *gsh1* mutants are absolutely dependent upon exogenous GSH for growth in minimal media, while *gsh2* mutants can grow in unsupplemented minimal media. Both mutants display a slower growth rate and a longer lag phase than wild-type cells. They also show a defect in sporulation (Suizu *et al.,* 1994). A number of studies show additional functional roles for

GSH, such as the participation in xenobiotic detoxification mediated by glutathione-S-transferases (GSTs), or as a substrate for phytochelatin biosynthesis (Deponte, 2013).

1.4.2. Enzymatic defence systems

This type of defences includes several enzymes which are capable of removing oxygen radicals and their products, and/or repair the damage caused by oxidative stress. Catalase, SOD, glutathione and thioredoxin peroxidases, or methionine reductase are some examples of these systems. The thioredoxin and glutathione reductases will be treated in more detail in following sections.

Catalase: Catalase is a homotetrameric iron-containing enzyme with the capacity to catalyse the breakdown of H_2O_2 to O_2 and H_2O. *S. cerevisiae* contains a peroxisomal and a cytosolic catalase, catalase A and T respectively, encoded by the *CTA1* and *CTT1* genes (Cohen *et al.,* 1988). The main physiological role of catalase A seems to be the removal of H_2O_2 produced by fatty acid β-oxidation, while the physiological role of catalase T is less clear. Yeast mutants in both genes are hypersensitive to H_2O_2 in stationary phase and are unable to assemble an adaptive stress response to H_2O_2 (Izawa *et al.,* 1996).

Superoxide dismutase: Practically all aerobic organisms possess SOD activity, which converts O_2^- into H_2O_2 and O_2. This reaction depends on metal co-factors, such as iron, copper, or manganese. *S. cerevisiae*, in common with other eukaryotes, possesses two intracellular SODs: a cytosolic Cu-Zn-SOD, encoded by the *SOD1* gene, and a Mn-SOD localized in the mitochondrial matrix, encoded by the *SOD2* gene (Toledano *et al.,* 2003). *SOD1* is essential for protection against O_2 toxicity as shown by the array of aerobic defects occurring in its absence, including reduced growth rate, poor respiratory growth, and lysine and methionine auxotrophy (Longo *et al.,* 1996). In the case of *SOD2*, this codes for the primary O_2^- scavenging enzyme for protecting against O_2^- generated during respiration, as suggested by the sensitivity to elevated O_2 concentrations of the s*od2* mutants and their inability to grow on a non-fermentable carbon source (van Loon *et al.,* 1986).

Glutathione peroxidase (GPX): Peroxidases in general reduce organic and inorganic peroxides into the corresponding alcohols using the cysteine thiols of their active site. GPXs catalyse the reduction of hydroperoxides, using GSH as a reductant. There are two types of GPXs. Classical GPXs are tetrameric, soluble and act on inorganic and organic hydroperoxides. On the contrary, phospholypid hydroperoxide GPXs (PHGPXs) are monomeric and partly membrane-associated. This second type of GPXs

reduces lipid hydroperoxides esterified to membranes, in addition to soluble peroxides. Initially three GPXs were described in *S. cerevisiae*, Gpx1, Gpx2 and Gpx3 (Inoue *et al.,* 1999). Later on, a careful alignment of the sequences of these three proteins with GPXs from higher eukaryotes showed higher sequence identities with PHGPXs than with GPXs, suggesting that all three *S. cerevisiae* GPXs are in fact PHGPXs (Avery & Avery, 2001). Gpx3 is the most functionally important of the three GPX isoforms based on the studies that demonstrated that the *gpx3* mutant is more sensitive to hydroperoxides compared to the other two ones (Inoue *et al.,* 1999; Avery & Avery, 2001). This is because, besides its protective role from peroxides during oxidative stress, Gpx3 also regulates and acts as a peroxide sensor of the major oxidative stress transcription factor Yap1 (Delaunay *et al.,* 2002).

Thioredoxin peroxidase (PRX): PRXs, also known as peroxiredoxins, constitute an evolutionary conserved family of antioxidants, using TRX as the physiological electron donor. They reduce both H_2O_2 and alkyl hydroperoxides to H_2O or the corresponding alcohols, in combination with thioredoxin reductase, TRX and NADPH. All PRXs have a conserved domain containing an active-site cysteine, and depending on the number of cysteine residues required for their activity, they are classified into 1-Cys and 2-Cys PRXs. *S. cerevisiae* possesses four 2-Cys PRX, and one 1-Cys PRX (Toledano *et al.,* 2003).

Methionine sulphoxide reductases (MSRs): Due to their importance as antioxidants, these reductases are conserved in almost all organisms from bacteria to humans. ROS can oxidize methionine to methionine sulfoxide (MetO) forming two enantiomers, *S*-MetO and *R*-MetO. These modifications can be repaired through the action of MSR, with the participation of TRX (as electron donor), thioredoxin reductase, and NADPH (Moskovitz, 2005). In *S. cerevisiae*, two genes have been described with MSR activities, *MSRA* that reduces the S stereoisomer of MetO, and *MSRB* that reduces the R stereoisomer of MetO. Mutants deficient for MSR activity are hypersensitive to H_2O_2 (Moskovitz *et al.,* 1997).

TRX system: A very comprehensive description related with the proteins which forms this system is given in the review by Hanschmann *et al.* (2013). TRX was first identified in 1964 as an hydrogen donor enzyme for ribonucleotide reductase (RNR) in *Escherichia coli* (Laurent *et al.,* 1964). These proteins are thiol oxidoreductases (ca. 12kDa) found in all living organisms, which contain two redox active cysteines within the conserved active site motif, WCGPC (Meyer *et al.,* 2009). The TRX system is completed by the flavoprotein TRX reductase, which reduces oxidised TRX to the active thiol form using

NADPH. TRXs participate in the reduction of enzymes that form a disulphide during their catalytic cycle, such as RNR [needed for maintaining deoxyribonucleotide triphosphates (dNTPs) pools for DNA synthesis], 3'-phosphoadenosine 5'-phosphosulphate reductase (PAPS reductase, required for sulphur assimilation) or PRX. In general, they may participate in modulating the redox state of cell protein sulphydryls and therefore in protein folding (Herrero *et al.,* 2008). Structurally the TRX-fold domain contains a four or five-stranded β-sheet flanked by three or more α-helices at either side of the β-sheet (Martin, 1995) (Fig. 2). This structural domain is shared with other protein families such as protein disulphide isomerases (Kamitani *et al.,* 1992), GPXs (Epp *et al.,* 1983), GSTs and GRXs. In spite of this common structure, there are no common biological or catalytic functions between these protein families. *S. cerevisiae* possesses two cytosolic (Trx1, Trx2) and one mitochondrial (Trx3) TRXs. Deletion of genes for both cytosolic proteins is not lethal in yeast cells, although the double mutant has longer cell cycle S-phase and is auxotrophic for sulphur amino acids. Cytosolic (Trr1) and mitochondrial (Trr2) TRX reductases are present in yeast cells, defining two separate cytosolic and mitochondrial systems. Hypersensitivity to hydroperoxides has been observed in a *trr2* mutant, pointing to a role of this redoxin system as antioxidant against ROS generated at mitochondria (Pedrajas *et al.,* 1999).

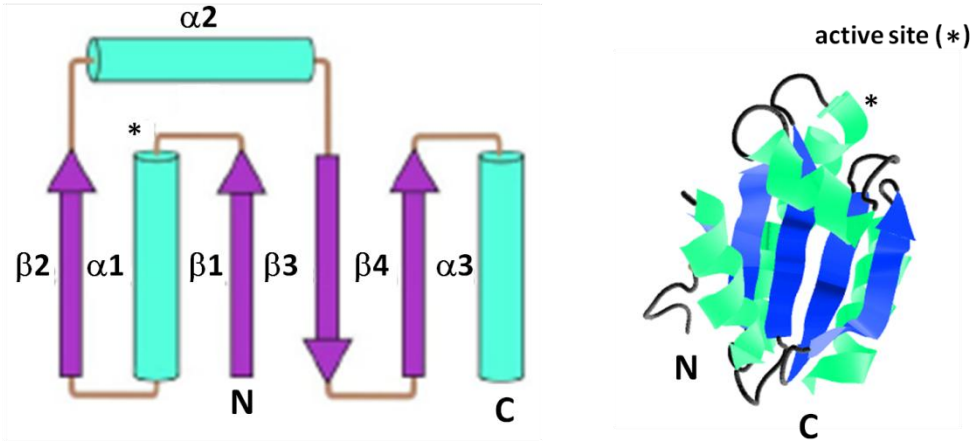

Fig. 2. TRX-fold domain. On the left it is represented the model scheme with the corresponding subregions nomenclature. On the right, the structure of oxidized *S. cerevisiae* Trx1. Adapted from Lillig *et al.* (2008).

2. GRX SYSTEM

2.1. General aspects

Almost four decades ago, GRXs were discovered as electron donors for the reduction of *E. coli* RNR, alternatively to TRXs (Holmgren, 1976). Since then, the role of TRXs and GRXs has been largely extended to the determination of their regulatory functions. In the present time, GRXs are described as thiol-disulfide oxidoreductases that regulate protein redox state, but in contrast to TRXs, they employ GSH as a reducing agent instead of the NADPH. The GRX system also includes NADPH and glutathione reductase, which is responsible for the reduction of GSSG (Fernandes & Holmgren, 2004) (Fig. 3). GRXs participates in a broad spectrum of biological processes such as activation of RNR and PAPS reductase, reduction of ascorbate, GSH-mediated reduction of dihydrolipoamide, regulation of the DNA binding activity of nuclear factors, neuronal protection against dopamine-induced apoptosis and excitotoxic mitochondrial damage, and regulation of signal cascades that protect against oxidative stress (Herrero *et al.,* 2010).

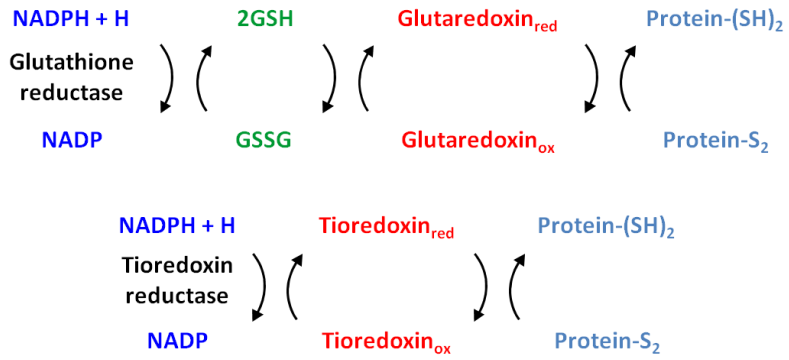

Fig. 3. Reaction mechanisms of the GRX and TRX systems. Adapted from Herrero & de la Torre-Ruiz (2007).

2.2. Structure of GRXs

Since their discovery, GRXs have been studied extensively by both X-ray crystallography and NMR spectroscopy. GRXs belong to the TRX-fold family of proteins. Structurally, this means that they possess a TRX-fold domain with a four stranded β-sheet flanked by three α-helices. On the other hand, GRXs share a common active site motif (CxxC/S) located at the loop connecting the first β-sheet strand and one of the α-helices. This region is important for the interactions with GSH.

2.3. Classification

Depending on the number of cysteine residues at the active site, a division has been established between dithiol and monothiol GRXs. The dithiol GRXs contain the active site consensus sequence CP/YFC, while the monothiol GRXs have a common active site motif (CXXS) with the presence of only one cysteine residue (Rodríguez-Manzaneque *et al.,* 1999; Herrero *et al.,* 2010). Monothiol GRXs can be further categorized into the single-domain monothiol GRXs, consisting of only one GRX domain, and the multidomain monothiol GRXs that contain an N-terminal TRX-like domain and one to three C-terminal monothiol GRX domains. Dithiol or/and monothiol GRXs are widely present in most living organisms.

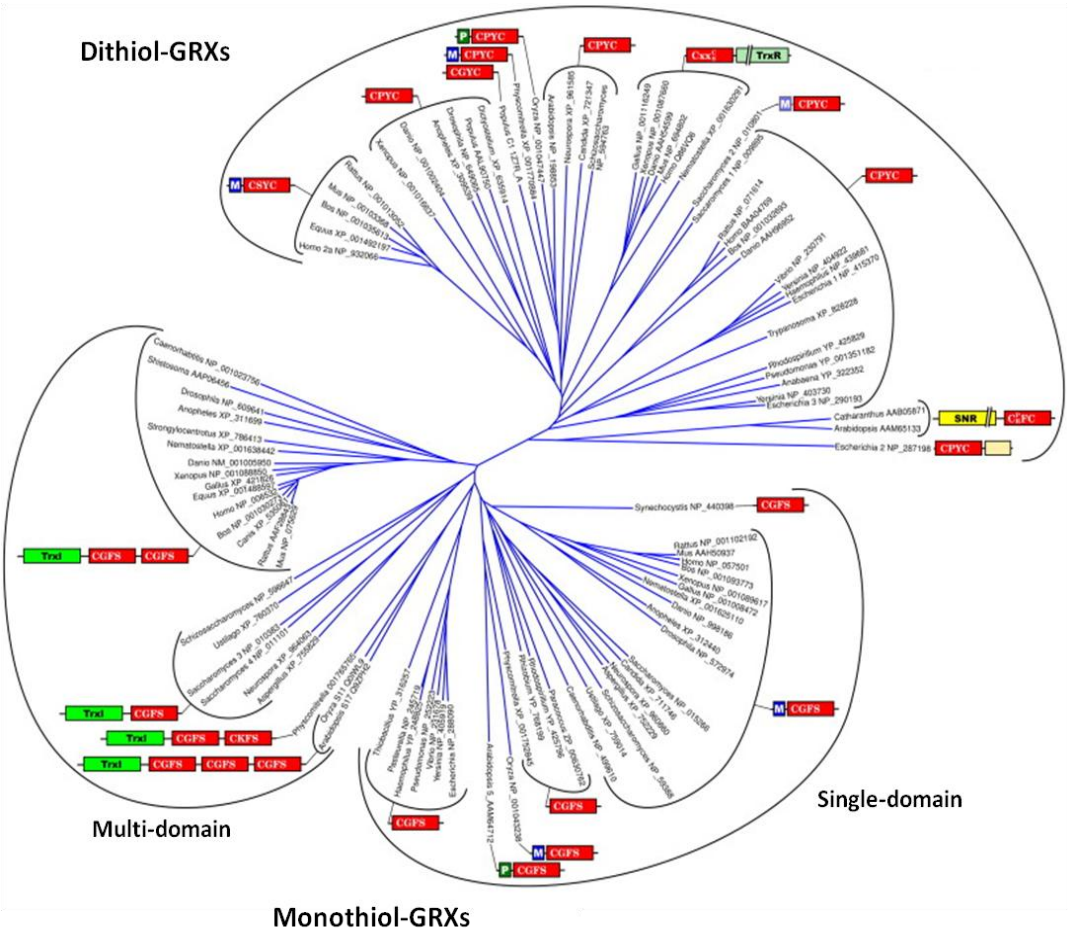

Fig. 4. Classification of GRXs based on phylogeny, active site and domain structure. Abbreviations used for non-GRX domains: M- mitochondrial signal peptide (blue boxes), P- plastid targeting sequence (dark green), SNR- sulfonucleotide reductase (yellow), Trxl- thioredoxin like (bright green), TrxR- thioredoxin reductase (green marine) (Lillig *et al.,* 2008).

While dithiol GRXs and single-domain monothiol GRXs are present in all kingdoms of life, multi-domain monothiol GRXs are only found in eukaryotic cells (Fig. 4). Besides differences at the active site, other subtle differences exist between the spatial structures

of dithiol and monothiol GRXs, affecting GSH binding (Lillig *et al.,* 2008). For instance, although the important GRX residues for the interaction with the C-terminal glycine of the GSH molecule are conserved between dithiol and monothiol GRXs, this conservation does not occur in the case of the charged residues of the dithiol GRXs, which are responsible for the interaction with the α-glutamyl residue of GSH. The small but significant differences in GSH binding between dithiol and monothiol GRXs may help to explain the biochemical differences between the two types of proteins. Monothiol GRXs are unable to deglutathionylate the small mixed disulfide between β-mercaptoethanol and a glutathione moiety (Herrero & de la Torre-Ruiz, 2007), an assay which is currently employed to determine the enzyme activity of dithiol GRXs, also named as hydroxyethyl disulfide (HED) assay. From an evolutionary point of view it is interesting to note that the monothiol GRXs show a higher degree of homology compared to the dithiol GRXs (Fig. 4). As an example of this conservation, mitochondrial monothiol GRXs represent a compact phylogenetic unit that evolved from a common bacterial origin. Mitochondrial dithiol GRXs, in contrast, seem to have evolved multiple times separately from each other, for instance, in mammals and fungi (Lillig *et al.,* 2008).

2.4. Dithiol GRXs

As above indicated, these low molecular weight proteins are present in all kingdoms of life. Dithiol GRXs were the first GRXs to be characterized at biochemical and structural levels. The first studies with these proteins were made in bacteria. *E. coli* contains two classical dithiol GRXs (Grx1 and Grx3) and one unusual dithiol GRX (Grx2) (Fernandes & Holmgren, 2004). Grx1 can serve as electron donor for metabolic enzymes like RNR and PAPS reductase. Grx3 cannot normally compensate the loss of Grx1 and its function *in vivo* is still unclear. Grx2 contains an N-terminal GRX domain followed by an α-helical domain and is structurally similar to the GST family of proteins (Lillig *et al.*, 2008; Alves *et al.*, 2009).

S. cerevisiae contains two classical dithiol GRXs (Grx1 and Grx2) (Luikenhuis *et al.,* 1998). While Grx1 is exclusively located in the cytosol, Grx2 is located in both, cytosol and mitochondria. Alternative translation initiation from two in-frame ATG sites explains the existence of the two isoforms (Porras *et al.,* 2006). Despite the high degree of homology between Grx1 and Grx2 (64% identity), studies with the respective mutants have demonstrated that the *grx1* mutant is sensitive to oxidative stress induced by O_2^-, whereas the *grx2* mutant is sensitive to H_2O_2 (Luikenhuis *et al.,* 1998). The same studies have demonstrated the participation of these two GRXs in the defence against the

superoxide generator menadione. Both yeast GRXs are also active as GPXs and GSTs (Collinson *et al.,* 2002; Collinson & Grant, 2003).

More recently, another dithiol GRX has been described in *S. cerevisiae*, Grx8 (Eckers *et al.,* 2009). The amino acid sequence of this molecule supports a TRX-fold structure, displaying more sequence homology with dithiol GRXs than with other GRXs. The mutant lacking Grx8 does not show sensitivity to oxidative stress and a fusion form with a green fluorescence protein (GFP) moiety displays a cytoplasmic location (Huh *et al.,* 2003). Further research is needed to understand better the function of this protein.

Human cells contain two dithiol GRXs. The cytosolic dithiol Grx1 is a functional homologue of *E. coli* and yeast Grx1 (Lillig *et al.,* 2008). Human Grx1 is an electron donor for RNR and it participates in many different cellular processes such as dehydroascorbate reduction, actin polymerization, protection against oxidative stress, apoptosis after acute cadmium exposure, and cellular differentiation (Johansson *et al.,* 2004). Human Grx2 was characterized as a Fe-S protein. Grx2 has two isoforms (nuclear and mitochondrial) derived from the same gene by alternative exon usage (Gladyshev *et al.,* 2001; Lundberg *et al.,* 2001). Grx2 has an unusual motif (CSYC) at the active site, while Grx1 has a CPYC consensus active site sequence. This subtle modification (Ser for Pro) enables the human Grx2 protein to receive electrons from TRX reductase and to complex an ISC (Fernandes *et al.,* 2005). It was proposed that this ISC serves as redox sensor for the activation of the protein in oxidative stress conditions (Johansson *et al.,* 2004).

2.5. Monothiol GRXs

These GRXs can be found in organisms from bacteria to multicellular eukaryotes (Fig. 5) (reviewed in Herrero & de la Torre-Ruiz, 2007). At first, it was thought that all monothiol GRXs contain a CGFS active site motif, but the discovery of two additional GRXs in *S. cerevisiae,* Grx6 and Grx7, with active site motifs CSYS and CPYS respectively (Mesecke *et al.,* 2008), led this concept to revision. As mentioned before, monothiol GRXs can be divided into two categories: those with a single GRX domain and those with a TRX-like region followed by one or more GRX domains. *E.coli* Grx4 is representative of bacterial CGFS-type monothiol GRXs. This molecule does not exhibit classical GRX activity, but it can be reduced by TRX reductase and seems to be involved in iron homeostasis (Fernandes *et al.,* 2005; Fladvad *et al.,* 2005).

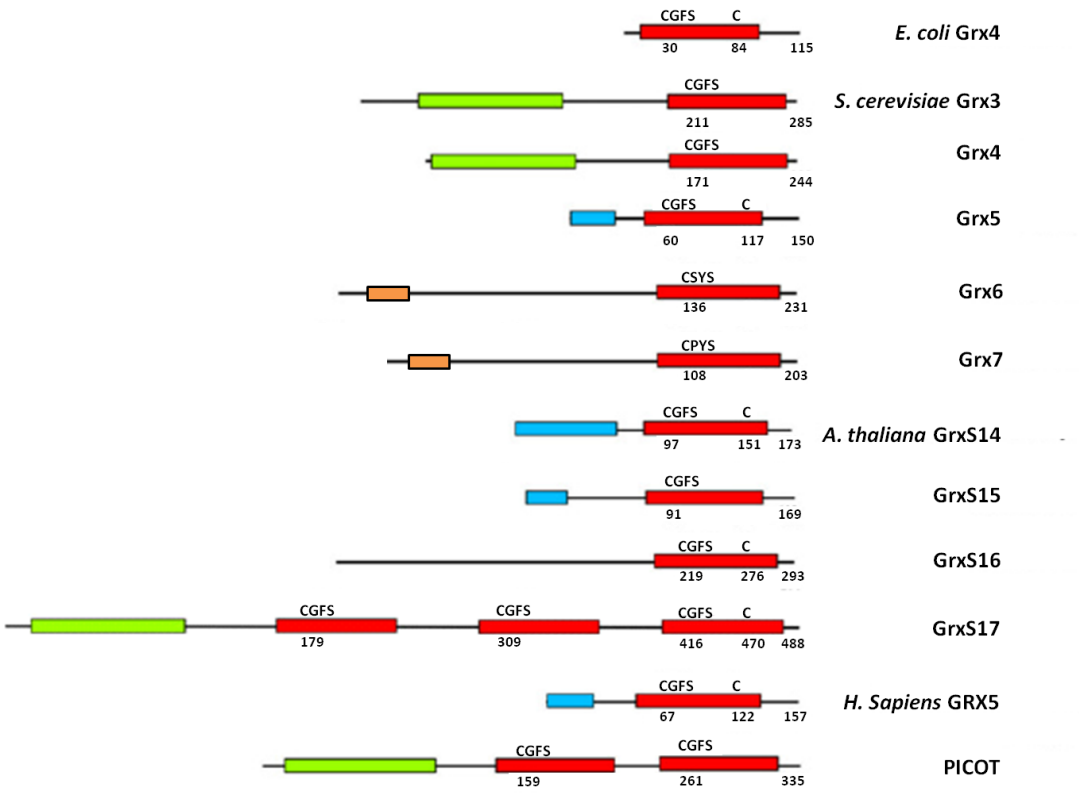

Fig. 5. Domain structure of monothiol GRXs from different organisms. The position and size of mitochondrial/plastid targeting sequences (blue boxes) and GRX (red), TRX-like domains (green) and the transmembrane domain (orange) is indicated. Numbers correspond to the position of the cysteine residue in the active site motif, the position of a partially conserved second C-terminal cysteine and the total length of the proteins. Adapted from Herrero & de la Torre-Ruiz (2007).

2.5.1. Monothiol GRXs in yeast

S. cerevisiae cells contain three monothiol GRXs with active site consensus sequence CGFS (Grx3, Grx4 and Grx5) (Rodríguez-Manzaneque *et al.,* 1999; Bellí *et al.,* 2002), and two monothiol GRXs with active site motifs CSYS and CPYS (Grx6 and Grx7 respectively) (Mesecke *et al.,* 2008) (Fig. 5). Grx3 and Grx4 molecules are larger than Grx5 because they contain a TRX-like domain as an N-terminal extension of the GRX domain, with a linking region between both domains (Bellí *et al.,* 2002; Vilella *et al.,* 2004) (Fig. 5). The nucleocytoplasmic location of Grx3 and Grx4 suggested a function as regulators of nuclear proteins and, consequently, gene expression. In accordance with this, it was demonstrated that both Grx3 and Grx4 regulate Aft1 nuclear localization, which implies that both GRXs share a function related to the regulation of cellular iron homeostasis (Ojeda *et al.,* 2006; Pujol-Carrion *et al.,* 2006). The Aft1 transcription factor, which regulates expression of the high-affinity iron-uptake regulon, translocates to the nucleus under conditions of iron depletion (Yamaguchi-Iwai *et al.,* 2002). Importantly, Aft1

transcriptional activity is precluded by its temporary cytosolic localization and not by iron availability. In this respect, the primary function of Grx3 and Grx4 appears to be the regulation of Aft1 nuclear localization, by interacting with the transcription factor (Ojeda *et al.,* 2006; Pujol-Carrion *et al.,* 2006).

S. cerevisiae Grx5 was first characterized as a GRX localized at the mitochondrial matrix, which participates in the synthesis of ISCs at this location through the ISC pathway (Rodríguez-Manzaneque *et al.,* 2002). This is one of the several pathways employed for the synthesis of the clusters in living cells (see Section 3.3. of this Introduction). Cells lacking Grx5 are not able to grow on minimal medium or in the presence of non-fermentable carbon sources (Rodríguez-Manzaneque *et al.,* 2002). The lack of this protein also leads to an iron accumulation inside the cells and defects in the activity of enzymes requiring ISCs as cofactors, like aconitase and succinate dehydrogenase (Rodríguez-Manzaneque *et al.,* 2002). Grx5 deficiency has also been related to increased protein oxidative damage in yeast cells (Rodríguez-Manzaneque *et al.,* 1999), maybe because the abnormal iron accumulation inside the cell as a result of the disturbance of ISC synthesis and consequent signalling of the intracellular iron state. In accordance with this, inhibition of Grx5 synthesis in human osteoblasts causes increased ROS formation and apoptosis (Linares *et al.,* 2009). Recently, significant progress on characterization of the role of Grx5 in yeast has been made, showing the interaction between this monothiol GRX and a specialized mitochondrial Hsp70 chaperone Ssq1 during the maturation of all cellular Fe-S proteins (Uzarska *et al.,* 2013). In that work it was shown that this chaperone binds the scaffold protein Isu1 (yeast nomenclature), facilitating dissociation of the newly synthesized ISC. Ssq1 also interacts with Grx5 at a binding site different from that of Isu1. Nevertheless, the detailed role of Grx5 in this synthesis is still not well known. Using the yeast *grx5* mutant, it has been shown that bacterial, parasite, plant and vertebrate homologues are able to substitute the function of yeast Grx5 (Cheng *et al.,* 2006; Molina-Navarro *et al.,* 2006; Bandyopadhyay *et al.,* 2008b), pointing to a functional conservation during evolution. Yeast Grx5 and some of its homologues in other organisms contain a second cysteine residue at the C-terminal end (Cys117 in *S. cerevisiae*) as observed in Fig. 5. On the contrary to the essential role of the cysteine residue at the active site motif, Cys117 is not essential for the biological activity of Grx5 (Bellí *et al.,* 2002).

The last two monothiol GRXs discovered in *S. cerevisiae* were Grx6 and Grx7 (Mesecke *et al.,* 2008). Curiously, sequence homology analyses led to group Grx6 and Grx7 close to the dithiol GRXs (Alves *et al.,* 2009). As previously mentioned they contain

CSYS and CPYS active site motifs, respectively. Detailed analysis of their primary sequences indicates that Grx6 and Grx7 contain a putative transmembrane domain at their N-terminal ends (Fig. 5), which is responsible for the insertion of the molecules at the membranes of the secretory vesicles, followed by a long linker domain and the GRX module. Consistent with this, it has been shown experimentally that Grx6 is localized at the endoplasmic reticulum and Golgi compartments, while Grx7 is mostly at Golgi (Izquierdo *et al.,* 2008).

2.5.2. Monothiol GRXs in human cells

In human cells two monothiol GRXs exist, one cytoplasmic and the other mitochondrial, Grx3 and Grx5 respectively. Grx3, also named protein kinase C (PKC) interacting cousin of TRX (PICOT), consists of a N-terminal TRX domain that lacks a redox active motif and two monothiol GRX domains each containing the active site motif CGFS (Fig. 5). Grx3 was first characterized as a PKC-θ-binding protein in human T lymphocytes that inhibits PKC-θ-dependent activation of JNK protein kinase and the AP-1 and NF-κB transcription factors (Witte *et al.,* 2000). Grx3 is an essential protein with suggested functions in a number of regulatory processes, as are embryonic development, immune response, and cardiac physiology. All of these functions are thought to be mediated by the direct and specific interaction with other proteins, through both the TRX and GRX domains, likely in response to redox signaling by ROS (Haunhorst *et al.,* 2010).

A *S. cerevisiae* Grx5 homolog protein is also present in human cells (referred as GLRX5). Deficiency of this GRX was previously identified as a cause of anaemia in a zebrafish model (Wingert *et al.,* 2005) and of sideroblastic anaemia in a human patient (Camaschella *et al.,* 2007). More recently, it has been demonstrated at cellular level that human GLRX5 is essential for ISC biosynthesis, for the maintenance of normal mitochondria and for cytosolic iron homeostasis in human cells (Ye *et al.,* 2010).

2.6. The GRX family in photosynthetic organisms

The latest phylogenomic analysis, performed on 58 sequenced photosynthetic organisms, has identified approximately 30 different GRX isoforms in higher plants, compared with four to eight found in other non-photosynthetic eukaryotic organisms (Lemaire, 2004; Morel *et al.,* 2008; Couturier *et al.,* 2009a). Initially, photosynthetic GRXs were divided in three distinct classes. More recently, this classification was extended into six, using as criteria both the active site sequence and the presence of amino acids potentially involved in GSH binding (Rouhier, 2010; Meyer *et al.,* 2012).

Classes I and II include GRXs with C[P/G/S][Y/F][C/S] and CGFS active sites, respectively, which are conserved from cyanobacteria to higher plants, suggesting that they might have fundamental functions for cellular life. The first class includes homologues to the classical dithiol GRXs such as *E. coli* Grx1 and Grx3, yeast Grx1 and Grx2, and mammalian Grx1 and Grx2. In the case of the second class this includes homologues to yeast Grx3, Grx4, and Grx5 and to *E. coli* Grx4. In land plants, gene duplication and fusion events have led to the extension of these two classes, which have been divided into five subclasses (GrxC1, C2, C3, C4 and C5 / S12) for class I and four subclasses (GrxS14, S15, S16 and S17) for class II (Meyer *et al.,* 2012). The nomenclatures of these GRXs are according to the presence of a cysteine or serine residue at the fourth position of the active site motif (CxxC or CxxS). GrxS14 and GrxS15 are small proteins (approximately 170 amino acids) with a single GRX module, therefore similar to yeast Grx5. GrxS16 is larger (around 290 amino acids) with the GRX module linked to an N-terminal extension, therefore similar to yeast Grx3 and Grx4. GrxS17 possesses a TRX-like module in the N-terminal part followed by two to three GRX domains depending on the organisms (Couturier *et al.,* 2009a).

The other four classes have been identified more recently, in particular because they are restricted to specific organisms, suggesting that they are involved in more specific processes. Class III (CC-type and recently named ROXY GRXs) is composed of 21 members in *Arabidopsis thaliana*; it includes proteins with CC [M/L][C/S/G/A/I] active sites. Class IV is restricted to land plants and eukaryotic photosynthetic organisms (including many algae), in which proteins with a GRX domain followed by four CxxC repeats that may form a zinc finger are present (Navrot *et al.,* 2006). The last two classes are majoritarily restricted to cyanobacteria. Members of class V are present in some other bacteria, whereas class VI appears to be restricted to cyanobacteria (Couturier *et al.,* 2009a; Meyer *et al.,* 2012).

2.6.1. Subcellular localization of plant GRXs

Three *A. thaliana* GRXs from two different classes (GrxS12, S14 and S16) confirmed experimentally the predicted chloroplastic localization (Cheng *et al.,* 2006; Bandyopadhyay *et al.,* 2008b; Couturier *et al.,* 2009b). Also the predicted mitochondrial localization of *A. thaliana* GrxS15 has been experimentally confirmed (Bandyopadhyay *et al.,* 2008b). On the other hand, GrxC1 has been confirmed experimentally to be localized at the cytosol (Rouhier *et al.,* 2007). Predictions on subcellular localizations suggest that most CC-type GRXs are cytosolic. This is also the case for several GRXs containing a CPYC

active site, although in plants two or three of these GRXs (GrxC2, GrxC3, or GrxC4) are predicted to be secreted and might correspond to highly abundant GRXs in the phloem sap (Szederkényi *et al.,* 1997). GrxS17 was predicted to be localized in the cytosol/nucleus. Later this co-localization was demonstrated (Rouhier *et al.,* 2008; Cheng *et al.,* 2011).

2.6.2. The roles of plant GRXs

Fig. 6 summarizes the established roles for plant GRXs and putative functions based on available data in other organisms. Several GRXs (GrxS14, S16, S17 and C1) have the possibility to oscillate between an apomonomer and a holodimer containing an ISC. They could have different and specific *in vivo* relevant functions. In plastids, the biochemical characterization of GrxS12 suggests that its function, using GSH as an electron donor, is to regulate the protein activity by deglutathionylation, to regenerate antioxidant enzymes, i.e. PRXs or MSR, or to sense the chloroplastic redox/glutathione status (Vieira Dos Santos *et al.,* 2007; Couturier *et al.,* 2009a). GRXs from the second class (GrxS14 and GrxS16) would primarily serve for ISC biogenesis or iron sensing (Couturier *et al.,* 2009a).

Alternatively, the apoforms could participate in plant arsenate tolerance (GrxS14) or, using presumably ferredoxin-thioredoxin reductase for their regeneration, could regulate many metabolic pathways by protein deglutathionylation (GrxS14 and GrxS16) (Sundaram *et al.,* 2008; Zaffagnini *et al.,* 2008). GrxS15 binds an ISC *in vivo*, and might be associated to iron-related processes, although it is unable to rescue the defects in ISC biogenesis observed in the yeast *grx5* mutant (Couturier *et al.,* 2009a). GrxS10 (also a member of the class II) can surprisingly support the activity of the mitochondrial PrxII (Finkemeier *et al.,* 2005). GrxC1 and GrxS17 might have functions related to iron homeostasis in the cytosol, as both enzymes have the capacity to bind a stable and liable ISC, respectively (Rouhier, 2010).

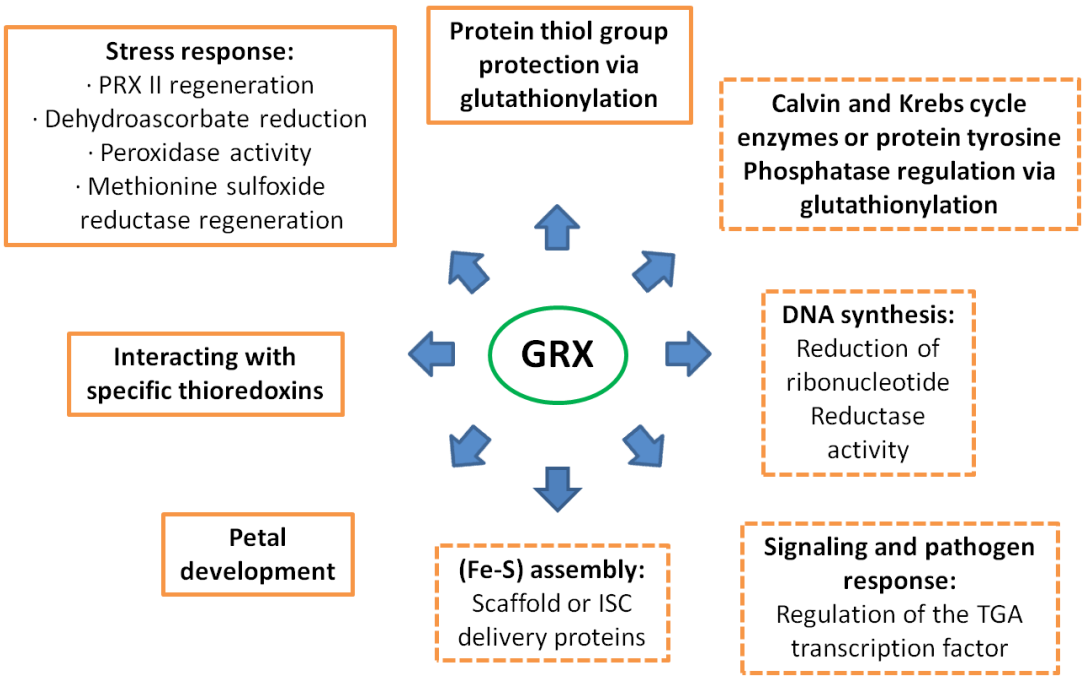

Fig. 6. Confirmed and proposed roles for plant GRXs. Established functions are on the left within plain frames. Putative functions are on the right and are represented in dashed frames (these functions are deduced from the known roles of GRXs in other organisms). Adapted from Rouhier *et al.*(2008).

2.7. Relation between TRX & GRX systems

In the middle 90's a work by Muller (1996) showed the first evidence about the relation between TRX and GRX systems, with the identification of Glr1 in a synthetic lethal genetic screen for mutations that confer a requirement for TRXs. It was demonstrated that cells lacking both Trr1 and Glr1 do not grow under aerobic and grow poorly in anaerobic conditions, and that glutathione reductase is required in the *trx1trx2* mutant cells. Later, other studies also observed similar relationships. Thus, yeast *trx1trx2grx1grx2* mutant cells are non-viable meaning that the cell requires at least one of the two TRX or GRX systems to survive (Draculic *et al.* 2000). Also, a mutation in *TRX1* and *TRX2* results in an increased concentration of glutathione in both reduced and oxidized forms (Garrido & Grant , 2002; Drakulic *et al.* 2005). Yeast cells lacking completely the cytoplasmic TRX (*trx1trx2trr1*) or GSH (*gsh1glr1*) systems are viable, but cells where components of both TRX and GRX systems were deleted, like the *gsh1trx1trx2* or *glr1trr1* mutants, did not grow (Trotter & Grant, 2003). Two years later it was shown that yeast cells lacking both TRX reductases (*trr1trr2*) or all three TRXs (*trx1trx2trx3*) are viable, giving the idea that cells can survive in the absence of both the cytoplasmic and mitochondrial TRX systems (Trotter & Grant, 2005). In the same work it was demonstrated that loss of both Trr2 and Glr1 accumulates the oxidized form of Trx3 in the mitochondria, indicating that the

mitochondrial Glr1 also participates in the maintenance of the redox status of Trx3. Fig. 7 summarizes the TRX and GRX systems present in the different compartments of *S. cerevisiae* and the respective connections between both.

Another example of the complexity of these systems is the GSSG reduction by the TRX system in some organisms such as *Drosophila melanogaster*, which lacks glutathione reductase (Kanzok *et al.,* 2001). In the same line, several studies on plant development have shown that the TRX and GRX systems play an important interrelated role in pollen development, meristem growth and auxin metabolism (reviewed in Meyer *et al.*, 2012).

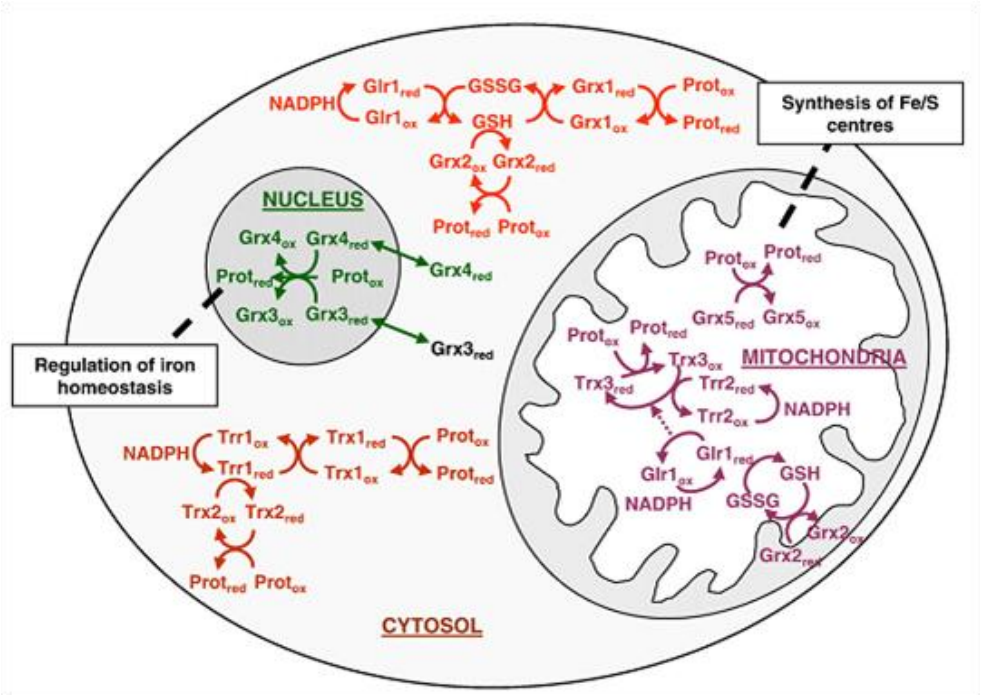

Fig. 7. Components of the *S. cerevisiae* TRX and GRX systems at the nucleus, mitochondria and cytosol. In the mitochondria, oxidised Trx3 can be either reduced by Trr (TRX reductase) or by Glr1. The dotted arrow indicates that action of Glr1 on Trx3 can be direct or through an unknown protein (Herrero *et al.,* 2008).

3. IRON-SULPHUR CLUSTERS

3.1. General overview

In the modern living world, ISCs are present in all kingdoms of life. Since the discovery of these small inorganic cofactors by Helmut Beinert in the early 60's, it was found that numerous important biological processes (such as respiration, photosynthesis and nitrogen fixation) require the participation of metalloproteins containing these cofactors. ISCs serve as catalysts in chemical reactions, electron carriers in redox reactions, regulatory sensors, and stabilizers of protein structure (reviewed in Lill, 2009). The most common and simplest of these clusters are the rhombic [2Fe-2S] and cubic [4Fe-4S] types, but also [3Fe-4S] can be found (Fig. 8). All of them contain ferrous (Fe^{2+}) and ferric (Fe^{3+}) iron cations, and inorganic sulphide (S^{2-}) anion (Beinert *et al.,* 1997), derived forms from two of the most versatile and abundant elements in our planet. In most Fe-S proteins, the iron atoms are bound by cysteine residues; however, histidine, serine and aspartic acid residues or backbone amides can also act as ligands (Meyer, 2008). Despite the large number of Fe-S proteins identified, there is no common consensus motif to predict whether a candidate protein can bind an ISC. However, some motifs have been recognized, including the $CX_4CX_2CX_{\approx 30}C$ motif in mammalian and plant [2Fe-2S] ferredoxins and the $CX_2CX_2CX_{20-40}C$ motif, which was originally defined in [4Fe-4S] ferredoxins but seems to be present in many other members of the [4Fe-4S] cluster type. Frequently, a proline (or sometimes a glycine) residue is located next to one of the cysteine residues (Lill *et al.,* 2006). Many ISCs are relatively unstable and can be destroyed under oxidative stress conditions, and this is the basis for their role as sensors of oxidant conditions (see next section).

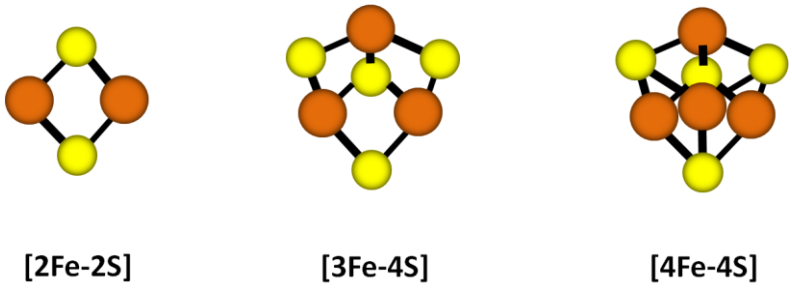

Fig. 8. Structures of the most commonly found ISCs. Iron is shown in orange balls, and sulphur in yellow balls. Adapted from Rouault & Tong (2005).

3.2. Biological functions of Fe-S proteins in eukaryotes

Eukaryotes contain Fe-S proteins in several cellular compartments: nucleus, cytosol, mitochondria, and chloroplasts. The biological functions of Fe-S proteins can be

assembled into three groups: electron transfer, catalysis of metabolic reactions and regulatory processes. The first biological function and the most common one is based on the fact that iron ions of the clusters can move between the reduced and oxidised state. For this reason, Fe-S proteins serve as excellent donors and acceptors of electrons in a multitude of biological reactions. Mitochondrial Fe-S proteins from complexes I, II and III of the respiratory chain, or plant ferredoxins, are some of the proteins involved in redox reactions [reviewed in Xu & Møller (2008), and Stehling *et al*. (2014)]. The most studied example in enzyme catalysis by Fe-S proteins is the mitochondrial protein aconitase of the citric acid cycle. In contrast to the previous proteins functioning as electron carriers, aconitase reacts directly with an enzyme substrate. In this case, aconitase isomerises citrate (substrate) and converts it into isocitrate.

Many of the known Fe-S proteins are located in mitochondria, but along the last decade the number of cytosolic and nuclear Fe-S proteins identified has been increasing. The cytosolic yeast protein isopropylmalate isomerase (Leu1) which participates in the biosynthesis of leucine is one of the well characterised Fe-S proteins. Another example of Fe-S protein located in the cytosol is the yeast sulfite reductase Met5 (also known as Ecm17) involved in the biosynthesis of methionine. The mammalian iron regulatory protein 1 (Irp1) involved in the post-transcriptional control of iron uptake, storage and use (which alternatively can act as cytosolic aconitase) is another example of cytosolic Fe-S protein [reviewed in Lill *et al.* (2006), and Lill (2009)]. Two yeast Fe-S proteins have cytoplasmic and nuclear co-localization, Rli1 and Nar1. This first one is required for the ribosome biogenesis, translation initiation and termination, and RNA assembling. Nar1 is involved on the maturation of cytosolic and nuclear Fe-S proteins and resistance to oxidative stress (reviewed in Lill *et al.*, 2006).

In the nucleus, most known Fe-S proteins are involved in DNA metabolism. DNA glycosylases, nucleases, helicases, DNA primase and DNA polymerases all of them have ISCs. Yeast DNA N-glycosylase Ntg2 participates in the base excision repair (BER), one of the several process of DNA repair (Lukianova & David, 2005). Yeast Dna2 nuclease and helicase is an ISC protein involved in DNA replication and recombinational repair (Pokharel & Campbell, 2012). The Pri2 primase of *S. cerevisiae* is required for the synthesis of short RNA primers for DNA replication, acting as a component of the system for repairing DSB in DNA (Klinge *et al.*, 2007). The yeast 5´ to 3´ helicase Rad3, the homolog of human XPD helicase (Rudolf *et al.,* 2006; Liu *et al.,* 2008), is involved in transcription (as a subunit of the transcription factor TFIIH) and in nucleotide excision repair (NER). More recently, it has been described that eukaryotic DNA polymerase

complexes include Fe-S proteins. Thus, the *S. cerevisiae* catalytic subunits of the DNA polymerases Polα, Polδ, Polε, and Polζ (Pol1, Pol2, Pol3 and Rev3, respectively) have ISCs (Netz *et al.*, 2011; Jain *et al.*, 2014).

3.3. Fe-S protein biogenesis pathways

At the end of 90's, several groups working with *S. cerevisiae* showed that the biogenesis of Fe-S proteins located at the mitochondria depended on a conserved number of several proteins (Strain *et al.*, 1998; Kispal *et al.*, 1999; Li *et al.*, 1999; Schilke *et al.*, 1999). These proteins were identified as the ISC assembly machinery. As the Fe-S biogenesis is essential for almost all forms of life it is not surprising that this process is conserved in prokaryotic and eukaryotic organisms. Our current knowledge about this biogenesis pathway came through studies carried out in the last two decades in bacteria and yeast [reviewed in Xu & Møller (2008), and Lill *et al.* (2012)]. One of the first works that contributed to this knowledge was made by Zheng and co-workers in *Azotobacter vinelandii*, where they identified the bacterial *isc* operon (Zheng *et al.*, 1998). Dean and colleagues, also in 1998, identified the first enzymes that promote the formation of ISC in the same bacterial species (Frazzon & Dean, 2003). Several studies have identified in *E. coli* three different bacterial Fe-S biogenesis systems: the nitrogen fixation (NIF) pathway, the ISC pathway, and the sulphur mobilization (SUF) pathway (Johnson *et al.*, 2005; Fontecave & Ollagnier-de-Choudens; 2008 Bandyopadhyay *et al.*, 2008a). The NIF system is responsible for the formation of ISCs for nitrogenase. Two components of this system, the cysteine desulfurase NifS and the scaffold protein NifU, participate in the preassembling of ISCs before insertion into nitrogenase. The second system, ISC, is required for the biogenesis of the Fe-S proteins. Two proteins of this system, IscS and IscU, are involved in the bacterial *isc* operon. Homologues for all the proteins of the *isc* operon are present in eukaryotes. The last bacterial Fe-S biogenesis system, SUF, functions only under oxidative stress conditions. This system contains a cysteine desulfurase SufS and an alternative scaffold protein named SufA. During evolution, the components of the two bacterial NIF and SUF systems were transferred by endosymbiosis to eukaryotes containing Fe-S proteins in mitochondria, cytosol and nucleus [reviewed in Xu & Møller (2011), and Lill *et al.* (2012)]. In all eukaryotic organisms except photosynthetic ones only the ISC system is located at the mitochondria. This Fe-S protein biogenesis pathway includes three stages: ISC assembly, ISC export and cytosolic Fe-S protein assembly by the cytosolic iron–sulphur protein assembly (CIA) machinery. The ISC assembly machinery is required for all cellular Fe-S proteins, while the functions of the ISC

export and the CIA machinery are restricted to the maturation of cytosolic and nuclear Fe-S proteins (Stehling & Lill, 2013). Fig. 9 summarizes the ISC biogenesis process in *S. cerevisiae*.

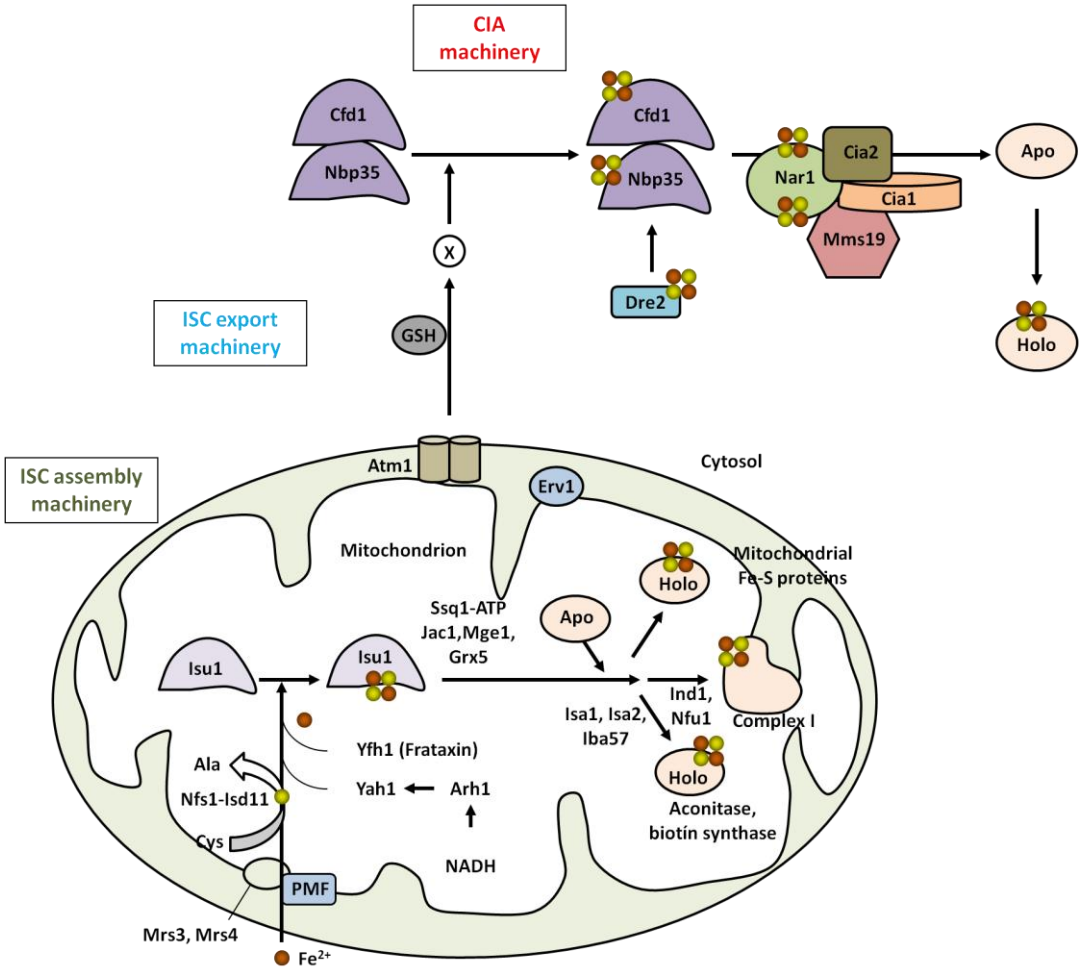

Fig. 9. ISC biogenesis in *S. cerevisiae*, including ISC assembly, ISC export, and CIA machinery. Adapted from Lill (2009), and Stehling & Lill (2013). See the text for details.

3.3.1. ISC assembly mechanism

This mechanism of Fe-S protein biogenesis is well conserved among eukaryotes (Lill & Mühlenhoff, 2005), although a significant amount of data regarding eukaryotic mitochondrial ISC assembly have come from studies performed using the yeast model system. The process of ISC assembly can be divided into two main steps. The first one is the *de novo* assembly of an ISC on a scaffold protein. The second is the transfer of the ISC from the scaffold to target apoproteins with the participation of intermediate proteins that bind the cluster, and further assembly into the polypeptide chain [reviewed in Stehling & Lill (2013)]. To achieve these objectives the yeast mitochondrial ISC assembly machinery requires the participation of at least 17 proteins. Because free iron and sulphur are toxic, it is important that the assembling of these two elements should be

very well regulated within the cell. The cytosolic ferrous iron (Fe^{2+}) is imported to the mitochondria through a membrane potential-dependent way, using a proton-motive force as an energy source. This import is facilitated by the inner membrane carriers Mrs3 and Mrs4. The cysteine desulfurase complex Nfs1–Isd11 releases sulphur from cysteine to produce alanine and persulfide. The sulphur is then transferred to the scaffold proteins Isu1 or Isu2. The ISC is assembled on Isu1 (or Isu2) with the participation of the iron-binding protein Yfh1 (frataxin) as the putative iron donor, and the electron-transport chain composed by NADH, ferredoxin reductase (Arh1) and ferredoxin (Yah1). Once assembled, the cluster needs to be transferred from the scaffold to target apoproteins and inserted into the polypeptide chain. To achieve this second objective at least ten different proteins are involved. The first part of this objective requires the participation of the ATP-dependent Hsp70 chaperone Ssq1, the co-chaperone Jac1, the nucleotide exchange factor Mge1 and Grx5. Co-chaperone Jac1 helps in the binding of Isu1 with Ssq1. Mge1 assists in the dissociation of Isu1 from Ssq1. The roles of Grx5 and Ssq1 in the ISC assembly will be described in more detail in section 3.3.3. The formed clusters are transferred to specific apoproteins with the participation of the ISC proteins Isa1, Isa2 and Iba57. Thus, these three proteins are involved in the ISC maturation of the aconitase family (Aco1, Lys4) and SAM-dependent proteins Bio2 and Lip5. The P-loop NTPase Ind1 is specifically required for the assembly of respiratory complex I. Nfu1 and Aim1 also participate in the maturation of respiratory complexes I and II, and lipoate synthase. The entire process has been recently reviewed by Lill *et al.* (2012), and Stehling & Lill (2013).

3.3.2. From ISC to CIA in *S. cerevisiae*

Cytosolic and nuclear Fe-S protein biogenesis requires both the mitochondrial ISC assembly and mitochondrial ISC export machinery proteins. The ATP binding cassette (ABC) transporter Atm1 of the inner membrane is supposed to export a sulphur-containing unknown compound (X) from the mitochondrial matrix to the cytosol. This process is supported by GSH and Erv1 (an intermembrane sulphydryl oxidase, which introduces disulphide bridges into substrates). In the cytosol, the proteins of the CIA machinery participate in the Fe-S protein maturation. Here ISCs are assembled on the scaffold P-loop NTPases Cfd1 and Nbp35, forming a heterotetrameric structure. This stage requires the involvement of the cysteine desulfurase Nfs1 serving as a sulphur donor, the electron transfer chain from NADPH (electron source) to the diflavin reductase Tah18, and the Fe-S protein Dre2. From the heterotetrameric complex Cfd1-Ndp35, the ISC is transferred to apoproteins, with the participation of the Nar1 protein, the CIA targeting

complex (Cia1, and Cia2), and Mms19. This last protein also known as Met18 was recently characterized as a late acting CIA component interacting with Fe-S proteins involved in DNA metabolism (Stehling *et al.*, 2012). In this study it was demonstrated that Mms19 interacts with several other Fe-S proteins including Rli1, Dna2, Rad3 and Ntg2 and its depletion results in a decrease of ISC in Rad3.

3.3.3. Role of Grx5 and Ssq1 in the ISC machinery

As mentioned before, ISCs are transferred from the scaffold protein Isu1 to target proteins with the help of, among others, Ssq1 and Grx5. Unlike other multifunctional Hsp70s that bind to several hydrophobic substrates, Ssq1 has preference for binding the LPPVK motif of Isu1. This binding interaction is regulated by Jac1 (Dutkiewicz *et al.*, 2004). The complex Isu1-Ssq1 is thought to induce a structural change in Isu1, facilitating cluster dissociation and transfer to apoproteins. The absence of Ssq1 and Jac1 results in the accumulation of ISCs on Isu1 because they are not transferred to the corresponding target apoproteins. As mentioned before (section 2.5.1 of this Introduction), among others phenotypes, yeast cells depleted of Grx5 display an accumulation of ISCs on Isu1, supporting that Grx5, as Ssq1 and Jac1, is also involved in ISC transfer from Isu1 to target apoproteins. Recently, Uzarska *et al.* (2013) demonstrated in *in vivo* experiments that Grx5 is an Fe-S protein that receives its clusters from the scaffold protein Isu1. This suggests that Grx5 has no function as a scaffold protein as previously thought (Bandyopadhyay *et al.,* 2008a; Rouhier *et al.,* 2010). Second, they identified an interaction between Grx5 and Ssq1, both *in vivo* and *in vitro*. This interaction appears to be crucial for the transfer of the ISC. In addition, they demonstrated that Grx5 and Isu1 bind simultaneously Ssq1 in independent binding sites. Fig. 10 shows a model with the putative roles of Grx5 and Ssq1 in the ISC assembly. This model integrates the new information brought by the work of Uzarska *et al.* (2013) and some others about the Hsp70 chaperone system in the ISC assembly pathway (Vickery & Cupp-Vickery, 2007; Kampinga & Craig, 2010). Initially, the ISC is assembled on the scaffold protein Isu1. Next, Jac1 participates in the binding process of the complex ISC-Isu1 and Ssq1. Grx5 binds to Ssq1 previously to the binding of the Hsp70 chaperone to Isu1. ATP hydrolysis induced by Jac1 and Isu1 provokes a conformational change in Ssq1, causing a tight binding of the Isu1 LPPVK motif and Grx5. This step facilitates an efficient transfer of the ISCs from Isu1 to Grx5. Mge1 (which mediates the exchange of ADP to ATP on Ssq1) assists in the dissociation of Isu1 from Ssq1. Finally, Grx5 would facilitate ISC integration into target apoproteins.

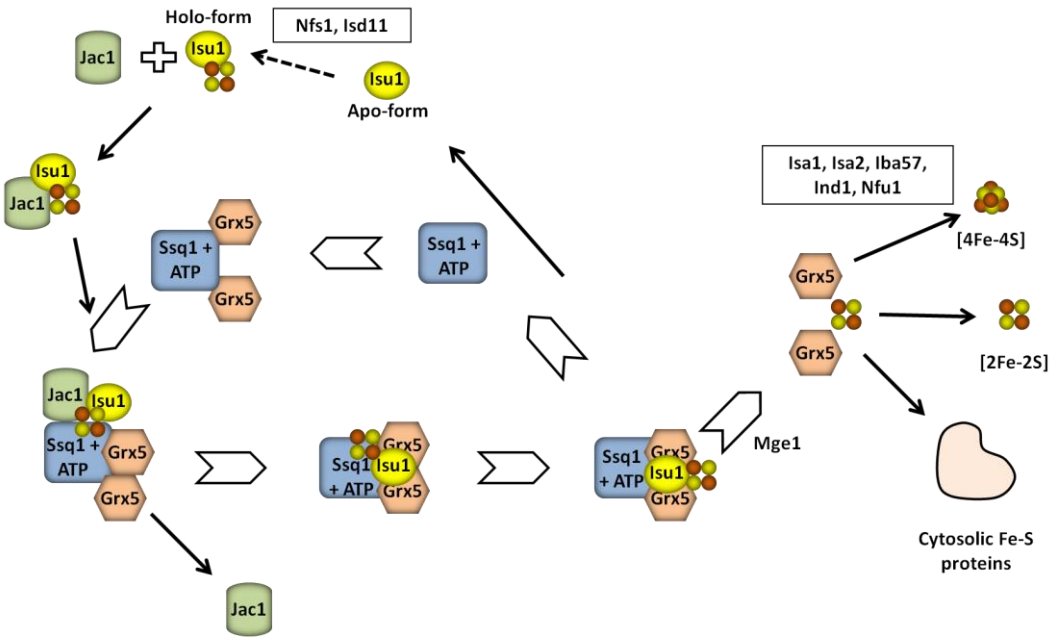

Fig. 10. Working model for the roles of the mitochondrial chaperone Ssq1-Jac1 and the glutaredoxin Grx5 in Fe-S protein maturation in eukaryotes. Adapted from Uzarska *et al.* (2013).

3.4. ISC and iron homeostasis

Several proteins of the ISC assembly and export machinery (such as Yfh1 and Atm1) were described primarily as participants in iron homeostasis (Babcock *et al.*, 1997; Kispal *et al.*, 1997). It is known that Fe-S proteins have important roles in mitochondrial iron homeostasis, since depletion of some proteins of the ISC system in the yeast cell (such as Nfs1, Isu1, Isu2, Grx5 or Atm1) causes an increase of iron accumulation in the mitochondria (Rouault, 2012; Stehling & Lill, 2013). In *S. cerevisiae*, iron homeostasis is achieved through the transcription factors Aft1 and Aft2 in an iron depletion condition, through another transcription factor, Yap5, in an iron overload condition, and at a post-transcriptional level by the mRNA-binding proteins Cth1 and Cth2. In response to iron depletion, yeast cells activate Aft1 and Aft2, inducing the expression of more than 20 genes that constitute the iron regulon [a comprehensive description of the yeast iron regulon is given in the reviews by Philpott & Protchenko (2008), and Kaplan & Kaplan (2009)]. Aft1 mostly controls the expression of the iron uptake genes, while Aft2 is more important for the expression of genes involved in intracellular iron distribution (Courel *et al.*, 2005). Aft1 changes its location between the nucleus in iron-deplete cells and the cytoplasm in iron-replete cells, depending on the activity of the mitochondrial ISC assembly and export machineries. This nucleus/cytosol movement by Aft1 requires the nuclear importin Pse1 and the nuclear exportin Msn5. This exportin is not required for the inhibition of the Aft1 activity, as *msn5* mutant cells are not affected in the normal

function of Aft1 despite its constitutive localization in the nucleus (Ueta *et al.,* 2012). In the same work, the interaction between Grx3, Grx4 and Aft1 was described in more detail. It was shown that both GRXs promote specifically the dissociation of Aft1 from its target promoters in an iron-replete situation. They also demonstrated that the mitochondrial transporter Atm1 is also needed for the iron binding to the two GRXs and the dissociation of the transcription factor from its target promoters. The interaction between the two GRXs and the transcription factor for its cellular localisation was already observed earlier by Pujol-Carrion *et al.* (2006), where yeast cells with deleted *GRX3* or *GRX4* had poor or no phenotypic consequence, while the *grx3grx4* double mutant was severely growth impaired or non-viable and exhibited intracellular iron over accumulation. Kumánovics *et al.* (2008) provided new information about the interaction between Grx3, Grx4 and Aft1, and about the involvement of two cytosolic proteins, Fra1 and Fra2. These two cytosolic proteins bind the two GRXs and this complex is involved in the regulation of Aft1. However, the molecular mechanism of how the complex Fra1-Fra2-Grx3-Grx4 affects Aft1 remains to be determined. Interestingly, only a defect in the ISC assembly machinery at mitochondria but not a defective cytosolic Fe-S protein assembly induces the iron regulon (Rutherford *et al.,* 2005; Mühlenhoff *et al.,* 2010).

The unknown sensor molecule exported by Atm1 is also involved in the response to high iron mediated by the transcription factor Yap5. Atm1 stimulates Yap5 activation consequently inducing its target genes including the vacuolar iron importer gene *CCC1*, the metallothionein gene *CUP1*, and the ISC binding protein genes *GRX4* and *TYW1*. The increased expression of *CCC1* stimulates iron import and retention in the vacuole, while the increased expression of *TYW1* promotes iron retention by binding of the Tyw1 protein to it (Li *et al.,* 2011; Li *et al.,* 2012; Pimentel *et al.,* 2012).

In addition to transcriptional activation of iron-related genes by Aft1, Aft2 and Yap5, *S. cerevisiae* also uses mRNA degradation mechanisms to control iron homeostasis. The transcriptional and post-transcriptional pathways are directly linked since the mRNA binding proteins Cth1 and Cth2 accumulate in an Aft1 and Aft2-dependent manner under iron depletion. *CTH1* and *CTH2* genes are both activated by Aft1 and Aft2 when iron is depleted. Cth1 is expressed early in iron depletion situation, while Cth2 expression continues during prolonged iron depletion (Vergara *et al.,* 2011). Both proteins destabilize mRNAs coding for proteins requiring iron.

3.5. Human diseases related to Fe-S proteins

Because of the importance of Fe-S proteins in numerous fundamental biochemical pathways, the number of human disease-related deficiencies in components of the Fe-S biogenesis pathway is relatively low since original mutations are lethal. Friedreich ataxia (FRDA), Iron-sulphur cluster scaffold homolog (ISCU) myopathy, GLRX5 deficiency, point mutation in Iba57, and mutations in the human P-loop NTPase Ind1 are some of well known reported human diseases and mutations concerning proteins involved in ISC biogenesis assembly [reviewed in Stehling & Lill (2013), and Beilschmidt & Puccio (2014)]. None of these human mutations is completely inactivating, which is not surprising because as it has been said, severe defects in ISC assembly can be lethal (Rouault & Tong, 2008). The most common recessive ataxia, FRDA, is an autosomal recessive neurodegenerative disorder caused by deficiency of the nuclear-encoded protein frataxin (Yfh1 in yeast). Expansion of the unstable GAA triplet repeat in the human frataxin gene is the most common causal mutation of FRDA. It is characterized by a progressive spinocerebellar neurodegeneration (including the dorsal root ganglia, which are responsible for sensory perception and maintenance of balance), dysarthria (a neuromuscular speech disorder) and muscle weakness, as well as cardiomyopathy and diabetes (Rouault, 2012).

A mutation in the *ISCU* gene (human homologue of the yeast *ISU1*) was found to be the cause of an inherited skeletal muscle disease, commonly known as myopathy, discovered among patients from northern Sweden (Mochel *et al.,* 2008). Patients develop muscle weakness, along with exercise-induced acidosis and myoglobinuria (reddish urine caused by muscle degeneration and excretion of myoglobin). Aconitase and succinate dehydrogenase activities are markedly reduced and mitochondrial iron overload is produced in patient muscle samples (Kollberg *et al.,* 2009).

A mutation in the *GLRX5* gene causes a sideroblastic anaemia which is a form of anemia where the bone marrow produces ringed sideroblasts (erythroblasts containing granules of ferritin) rather than healthy red blood cells. It is characterized by red blood cell precursors having iron accumulation in mitochondria. The only studied patient has a homozygous A294G mutation in the third nucleotide of the last codon of *GLRX5* exon 1. This substitution does not change the encoded amino acid glutamine, but it interferes with the correct splicing and removal of intron 1 and drastically reduces *GLRX5* mRNA (Camaschella *et al.,* 2007).

A homozygous mutation in human *IBA57* causes a metabolic syndrome before birth and is lethal in early infancy. The observed symptoms in two siblings were severe hypotonia, respiratory insufficiency, primitive reflexes absence, and congenital microcephaly. The syndrome was also characterized by hyperglycinemia and brain malformations (Ajit Bolar *et al.*, 2013).

Depletion of human *IND1*, also known as nucleotide binding protein-like (*NUBPL*), causes morphological changes in the mitochondria, with enlarged organelles that have lost their cristae membranes. Nubpl protein has recently been identified, in a high-throughput sequencing screen searching for mutations causing mitochondrial complex I deficiency, as important for the incorporation of ISCs into mitochondrial complex I subunits (Calvo *et al.*, 2010). Patients with this deficiency present mitochondrial encephalomyopathy.

4. DNA DAMAGE

It has been estimated that more than tens of thousands of DNA lesions occur in human cells every day (Jackson & Bartek, 2009). All cells require an intact genome to function properly. This includes the nuclear, mitochondrial and chloroplastic genomes in eukaryotic cells. There is a complex network of mechanisms tightly coordinated to ensure that eukaryotic genomes are protected from internal or external damage. Consequently, mutations and deletions in the mitochondrial genome, as well as instability of the nuclear genome, are involved in multiple human diseases.

4.1. Nuclear and mitochondrial genomes in *S. cerevisiae*

In eukaryotes, DNA molecules are present in the nucleus, mitochondria and in the case of plants also in chloroplasts (ctDNA). In *S. cerevisiae* cells the nucleus contains approximately 12.1 million base pairs of DNA and about 6,000 genes within 16 chromosomes (Yazgan & Krebs, 2012).

In most multicellular organisms, the mtDNA is organized as a circular, covalently closed, double-stranded DNA (dsDNA). Mitochondria convert chemical energy from nutrients into ATP, and carry out other cellular functions including iron homeostasis, amino acid metabolism and control of apoptosis (Valiathan & Weisman, 2008). Mitochondria provide the cell with specialized metabolic activities, some of which generate toxic products, making the mitochondria a challenging place to maintain a genome. mtDNA is much more vulnerable than nDNA because it is under much stronger oxidative conditions. *S. cerevisiae* mtDNA represents about 15% of the total DNA content, and measures 80 kb of circular genome, about 5 times larger than animal mitochondrial genomes due to extended regions of non-coding DNA (Bernardi, 2005). The yeast mitochondrial genome encodes several subunits of the respiratory chain and the ATPase complex, several mitochondria-specific tRNAs, one of the mitochondrial large ribosome subunit proteins and two mitochondrial rRNAs. The mitochondrial genome is thus critical for many of the mitochondrial functions (Yazgan & Krebs, 2012). Excessive damage in the mitochondria leads to the loss of parts or all of mtDNA, but unlike other organisms, yeast cells are able to survive without mtDNA or respiration when grown under fermentative conditions. Such strains are called “petite” due to the small size of the colonies they form (Bernardi, 2005). Numerous studies have shown that these “petite” strains have extensive deletions in mtDNA (rho^-) or even complete loss of mtDNA (rho^0) (Contamine & Picard, 2000). This capacity of yeast cells with damaged mitochondria for surviving under certain conditions allowed the performance of studies to check the role of mitochondria

in the maintenance of cellular integrity, since the lack of mtDNA frequently leads to genomic instability (Veatch *et al.,* 2009). Although the mtDNA is dispensable for growth in fermentative conditions, the mitochondria itself is essential for cell viability. When nDNA damage is too severe to be repaired, the cell undergoes apoptosis. In contrast, at least theoretically, the cell can abandon heavily damaged mtDNA molecules because they exist in multiple copies (Kang & Hamasaki, 2002).

4.2. DNA genome instability

All organisms are constantly exposed to exogenous and endogenous genotoxic attacks that put the integrity of their genome in danger. Genome instability is usually associated with pathological disorders, and in humans is often associated with premature aging, various cancer predispositions and hereditary diseases. The basis of genomic instability is the incorrect transmission of genetic information from a cell to its daughters (Schär, 2001). This happens, among other reasons, due to the accumulation of oxidative damage in DNA, to defects in mitochondrial function that promote oxidative stress and damage to DNA and other cellular constituents, to mutations in proteins required for efficient DNA replication, DNA repair and checkpoints, or to telomere erosion and epigenetic effects on DNA repair and other genome maintenance systems (Burhans & Weinberger, 2007; Aguilera & García-Muse, 2013). Although such events can be toxic for the cell and the organism, they also lead to evolution at the molecular level and generate genetic variation (Aguilera & Gómez-González, 2008). DNA plays a vital role in maintaining genetic stability. As a result, cells are normally prepared with various mechanisms to preserve genome integrity, including DNA replication, DNA repair and signalling pathways, which coordinate DNA metabolism with cell cycle progression. These mechanisms are well understood in *S. cerevisiae* and are mostly shared by higher organisms including humans (Pan *et al.,* 2006). Some of these mechanisms and common threats to genetic stability will be described in more detail in the next sections. Although the mitochondrial and nuclear genomes are physically distinct, there is a high degree of cross-talk and functional interdependence between both (Poyton & Mcewen, 1996).

Several studies in different organisms suggest that mitochondrial dysfunction leads to nuclear genome instability. Liu *et al.* (2002) showed that mitochondrial dysfunction causes telomere attrition and loss, and chromosome fusion and breakage, followed by apoptosis. Samper *et al.* (2003) were the first to demonstrate that endogenous mitochondrial oxidative stress in normal cell culture conditions results in nuclear genomic instability in primary mouse embryonic fibroblasts. Also in *S. cerevisiae*

cells, Rasmussen *et al.* (2003) demonstrated that mitochondrial activity plays an important role in maintaining the stability of the nuclear genome by measuring the frequency of nuclear mutations in cells in two distinct ways: after inhibiting mitochondrial activity by drugs, or by removing or deleting the mitochondrial genome. More recently, Veatch *et al.* (2009) reported that the loss of mtDNA leads to nuclear genome hyperecombination. These mitochondrial dysfunctions stimulate nuclear genome instability by inhibiting the production of ISC-containing proteins, which are required for maintenance of nuclear genome integrity. Another later work related mitochondrial ISC biosynthesis with nuclear genome stability (Díaz de la Loza *et al.,* 2011), by demonstrating that cells lacking the mitochondrial chaperone Zim17 (interacting with Ssq1 in the ISC biosynthesis machinery) display high recombination and mutation rates. These two recent studies therefore relate ISC biosynthesis at mitochondria with stability of the nuclear genome.

4.3. DNA damage repair systems

Due to the serious consequences that DNA damage accumulation may have on cellular function and survival, different DNA repair pathways exist. Because of their importance, DNA repair systems must have arisen early in evolution, explaining the high conservation of these systems among the different eukaryotic organisms (and some of them also in prokaryotes).

This section will focus only in the nuclear repair systems, however some of the known pathways have also been described in mitochondria. Fig. 11 summarizes the different nDNA repair pathways. These include BER for repairing damaged and/or lost bases, the NER active on ultraviolet (UV) light-induced DNA crosslinks and other bulky lesions, and the mismatch repair (MMR). Three other pathways with recombinatorial repair strategies are also explained. The homologous recombination (HR) and the nonhomologous end join (NHEJ), and interstrand cross-linked repair (ICL) systems are active in the repair of DNA DSBs. The section will be completed with the post-replication repair (PRR) pathway, involved in repairing DNA lesions bypassed by DNA polymerases.

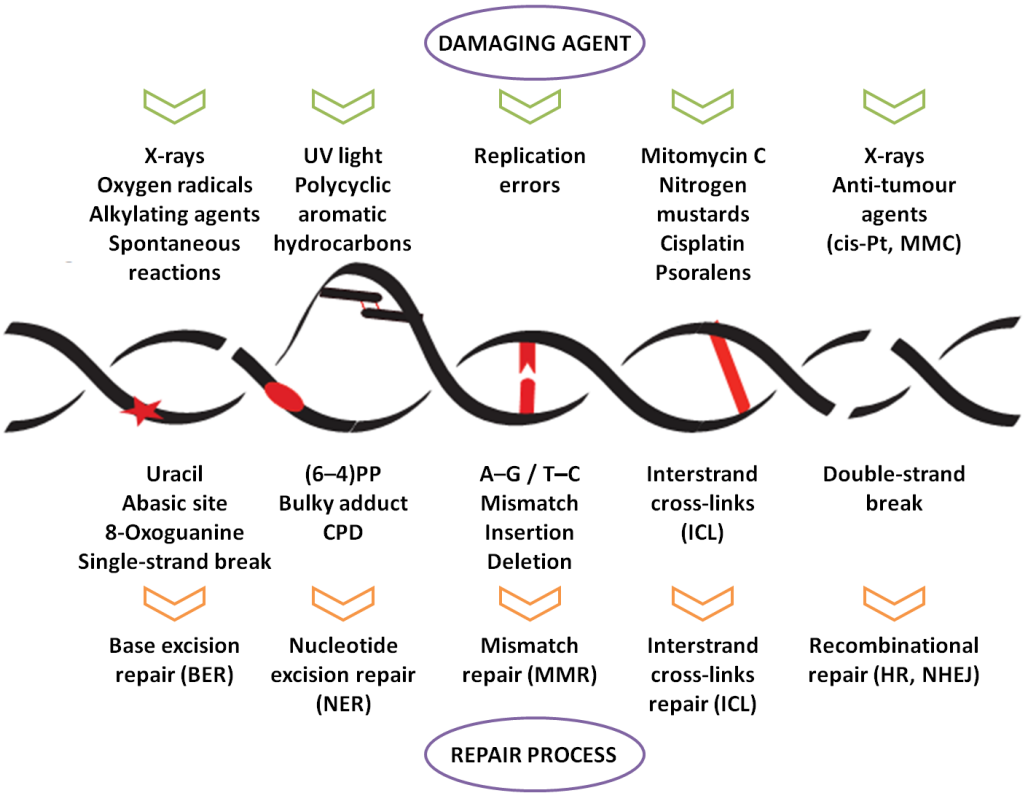

Fig. 11. nDNA repair mechanisms. Adapted from Gredilla *et al.* (2012).

4.3.1. Base Excision Repair

In yeast and mammalian cells, BER is the major DNA repair pathway for removal of endogenous DNA damage. This mechanism is activated when damaged DNA results from oxidative stress, hydrolysis or deamination. In BER, when an excision in a single DNA strand is generated, the complementary strand serves as a template to fill the resulting gap. As shown in Fig. 12, BER in *S. cerevisiae* is initiated by the action of uracil or 3-methyl-adenine DNA N-glycosylases (Ung1 and Mag1, respectively) that specifically recognize and excise damaged bases from DNA. Released damaged bases create an AP site that can be further processed by a DNA N-glycosylase/AP lyase (Ntg1, Ntg2, and Ogg1), or a separate, hydrolytic AP endonuclease (Apn1 and Apn2, with 95% of in vivo activity attributed to Apn1). AP sites are one of the most frequent spontaneous lesions in DNA. They are potentially mutagenic and provoke lethal lesions that can block DNA replication and transcription. Following appropriate 3' or 5' end processing steps, the DNA polymerase Pol2 inserts the correct base and the DNA ligase Cdc9 seals the nick, finishing the process for repairing the damage. These final steps have the participation of the Rad1-10 and Rad27 yeast endonucleases in the removal of 3' and/or 5' dirty ends respectively. This repair process is reviewed in Memisoglu & Samson (2000), Hoeijmakers (2001), Gredilla *et al.* (2012), and Boiteux & Jinks-Robertson (2013). The BER mechanism

also takes place in the mitochondria (Doudican *et al.,* 2005; Gredilla, 2010). Mitochondrial BER in *S. cerevisiae* presumably occurs via a similar mechanism as in the nucleus and is supported by the observation that several components of the yeast nuclear BER machinery colocalize into the mitochondria (Doudican *et al.,* 2005). As mentioned before, deletion of BER genes increases the mutation rate in a variety of organisms, predicting that loss of BER could contribute to the development of cancer.

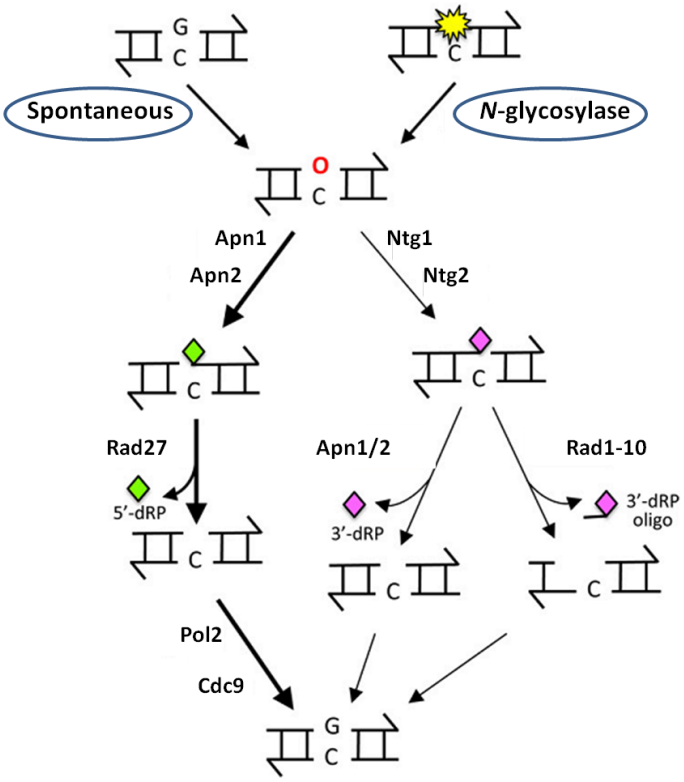

Fig. 12. The BER pathway. Adapted from Boiteux & Jinks-Robertson (2013).

4.3.2. Nucleotide Excision Repair

NER, together with BER, are the two known mechanisms involved in single strand DNA (ssDNA) damage. Both are differentiated by the extent of the ssDNA that is removed. Most of the NER lesions arise from exogenous sources (except for some oxidative lesions), whereas BER is mostly from endogenous origin. NER participates at a variety of DNA lesions such as the cyclobutane pyrimidine dimers (CPD), which are the most common induced DNA lesions caused by UV light or chemical compounds such as benzo[a]pyrene, aflatoxin and cisplatin [reviewed in Maeda *et al.* (2001)]. In both prokaryotes and eukaryotes, NER represents the most important repair system that is adapted to remove a large variety of DNA lesions, particularly those that distort the DNA

helix. As well, NER can provide an alternative mechanism to repair AP sites and oxidized bases.

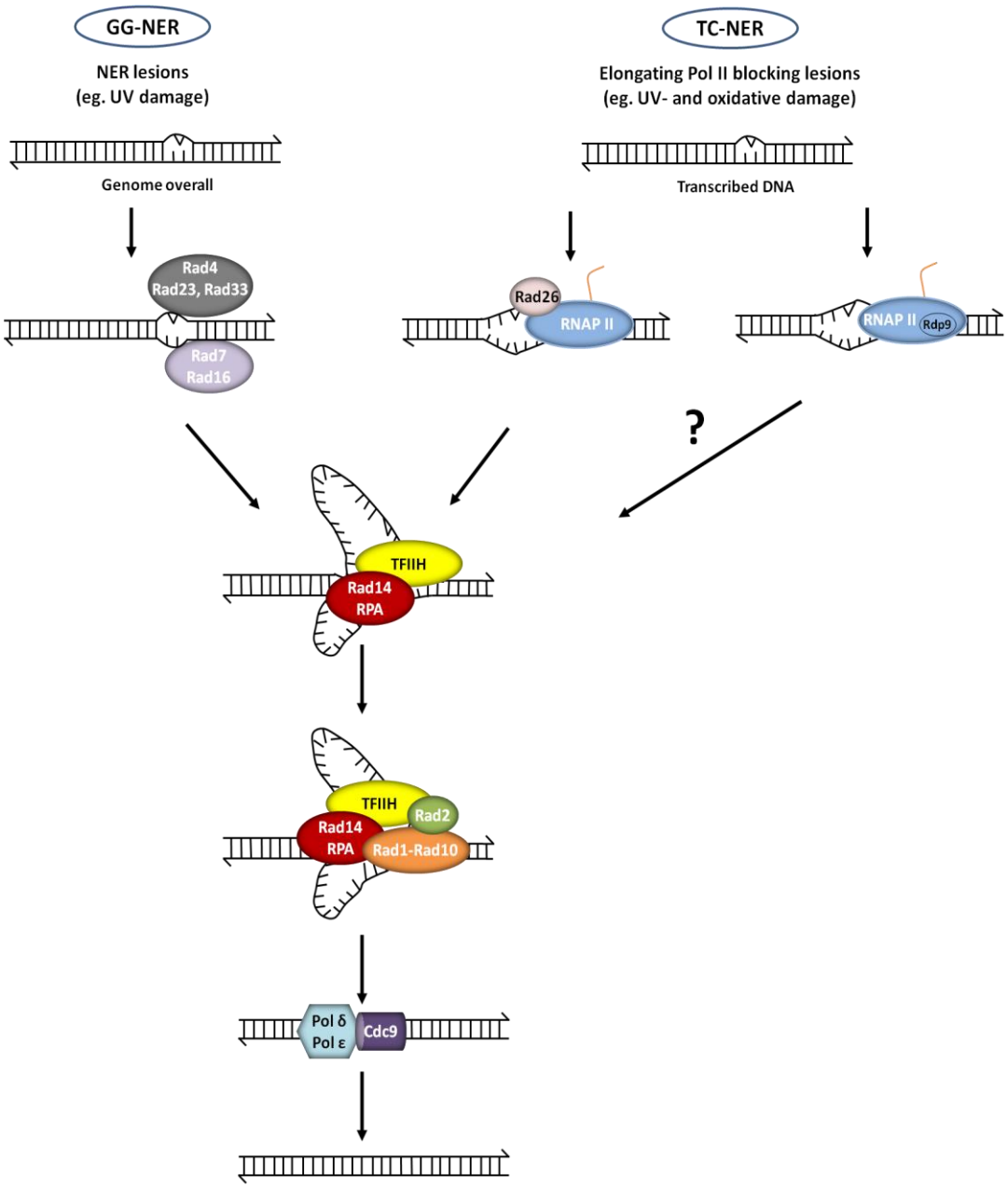

Fig. 13. The NER pathway including the corresponding subpathways, GG-NER and TC-NER. Adapted from Hoeijmakers (2001).

There are two NER subpathways, global genomic NER (GG-NER) and transcription coupled NER (TC-NER) as shown in Fig. 13. GG-NER repairs lesions in both transcribed and non-transcribed strands. In contrast, TC-NER repairs them only in the transcribed strand, leading to the faster removal of damage, and fewer mutations on the transcribed strand, compared to the non-transcribed one [(reviewed in Hanawalt (2002)]. Incision of UV-damaged DNA is a multiple-stages process involving damage recognition, DNA unwinding (which provides discrimination of the damaged strand from the non-damaged DNA

strand) and dual incision, which results in DNA fragments of approximately 25 to 30 nucleotides.

In yeast cells, the GG-NER pathway is initiated when the Rad4/Rad23/Rad33 complex senses a distortion on the DNA helix, and opens a 10 bp region around the lesion. The Rad7/Rad16 complex promotes the recruitment of Rad4 through its high affinity for DNA damage. The DNA structure generated by the Rad4/Rad23/Rad33 complex allows the recruitment of the TFIIH transcription factor, which extends the opening of the helix using the ATPase/helicase activities of Rad25 and Rad3 respectively. TFIIH is composed of 10 subunits that can be divided into two subcomplexes: a core TFIIH subcomplex with seven subunits (Rad25, Rad3, Tfb1, Tfb2, Ssl1, Tfb4, and Tfb5), and a CAK kinase complex composed of three subunits (Kin28, Ccl1, and Tfb3). After the release of the Rad4/Rad23/Rad33 complex, Rad14 and the Replication protein A, RPA (Rfa1, Rfa2 and Rfa3), are recruited to stabilize the pre-incision structure. With the intervention of Rad2 and the Rad1/Rad10 complex endonucleases the incision of damaged DNA takes place. Rad2 makes an incision about 2-8 nucleotides from the lesion on the 3' side, while the Rad1/Rad10 complex makes an incision 15-24 nucleotides away from the lesion on the 5' side. One important property of Rad2 and the Rad1/Rad10 complex, besides its endonuclease activity, is the capacity for recognizing the junction between ssDNA and dsDNA. Although poorly documented in yeast, it is suggested that either polymerase δ or polymerase ε can carry out the repair synthesis. The final ligation reaction is performed by the Cdc9 DNA ligase.

In the case of the TC-NER pathway in yeast, all proteins that are essential for GG-NER are required for TC-NER, with the exception of Rad7 and Rad16, which are required only for repairing the non-transcribed strand. The TC-NER pathway is initiated when a lesion on the transcribed strand blocks RNA polymerase II (RNAP II). TC-NER has two sub-pathways: a Rad26-dependent one and an Rpd9-dependent second one. Rdp9 is a nonessential subunit of RNAP II. At strong blocking lesions, RNAP II is permanently stalled, without the possibility of bypass, and TC-NER is triggered. Rad26 initiates chromatin remodelling to attract additional NER factors. These factors allow backtracking of RNAP II without dissociation from the template, which exposes the lesion to the NER machinery. After the fixation, the lesion transcription is rapidly resumed. Little is known about the Rpb9-mediated pathway, but it is thought to be similar as the Rad26 sub-pathway. All these mechanisms and sub-pathways are described with more detail in the reviews by Hoeijmakers (2001), Bernstein *et al.* (2002), Hanawalt (2002), Gredilla *et al.* (2012), and Boiteux & Jinks-Robertson (2013).

Loss of NER in humans is associated with the diseases xeroderma pigmentosum (XP), Cockayne syndrome and trichothiodystrophy (TTD), all of them characterized by extreme photosensitivity and predisposition to skin cancer. In the case of XP patients, they have a 1000-fold increased frequency of skin cancer (Hoeijmakers 2001; Boiteux & Jinks-Robertson, 2013).

4.3.3. Double strand breaks repair

DNA DSBs are cytotoxic lesions that can result in mutagenic events or cell death if left unrepaired or repaired inappropriately. DSBs can occur accidentally during normal cell metabolism and by exposure of cells to exogenous agents, such as ionizing radiation or some classes of chemotherapeutic drugs. Cells use two major pathways for DSB repair: HR and NHEJ, as shown in Fig. 14. HR requires an undamaged homologous sequence to serve as a template for the repair of both damaged strands whereas NHEJ involves direct ligation of the damage ends. The choice between these pathways depends on the phase of the cell cycle (HR is activated at S/G2 whereas NHEJ at G1 phase), and the nature of the DSB. The proteins that participate in the DSB repair pathways are highly conserved from yeast to humans.

HR: In *S. cerevisiae* this repair mechanism can be divided in five steps: i) recognition of DSBs, ii) resection of DNA ends, iii) checkpoint activation, iv) recombinational repair, and v) recovery from DNA damage. In the first step the Mrx complex (Mre11-Rad50-Xrs2) appears to be the earliest sensor of DNA DSBs by directly binding to DNA ends. These three proteins of the complex interact to form a heterohexameric DNA binding complex containing dimers of each subunit. Both Rad50 and Xrs2 increase the 3' to 5' nuclease activity of Mre11. Rad50 exhibits ATPase activity *in vitro*, which is required for DNA repair, and Xrs2 is important for targeting the Mrx complex to DNA ends. For the resection of DNA ends, the participation of the Mrx complex, Sae2 and the other two 5' to 3' nucleases, Exo1 and Rad27, is required. Once the ends are free of damage, the repair is compromised to HR and not to NHEJ. At this point, ssDNA-bound RPA recruits the checkpoint complexes Rad24/Rfc2-5, Ddc1/Mec3/Rad17 and Mec1/Ddc2. When DNA ends are absent of damage, Mre11, the Tel1 kinase and Sae2 dissociate from the DSB site suggesting that their primary role is the early processing of DSB ends and the decision between NHEJ and HR. DNA damage checkpoint activation (see section 4.4) results from a cascade of phosphorylation events initiated by the Mec1 and Tel1 kinases.Tel1 is recruited to sites of DNA damage by the Mrx complex.

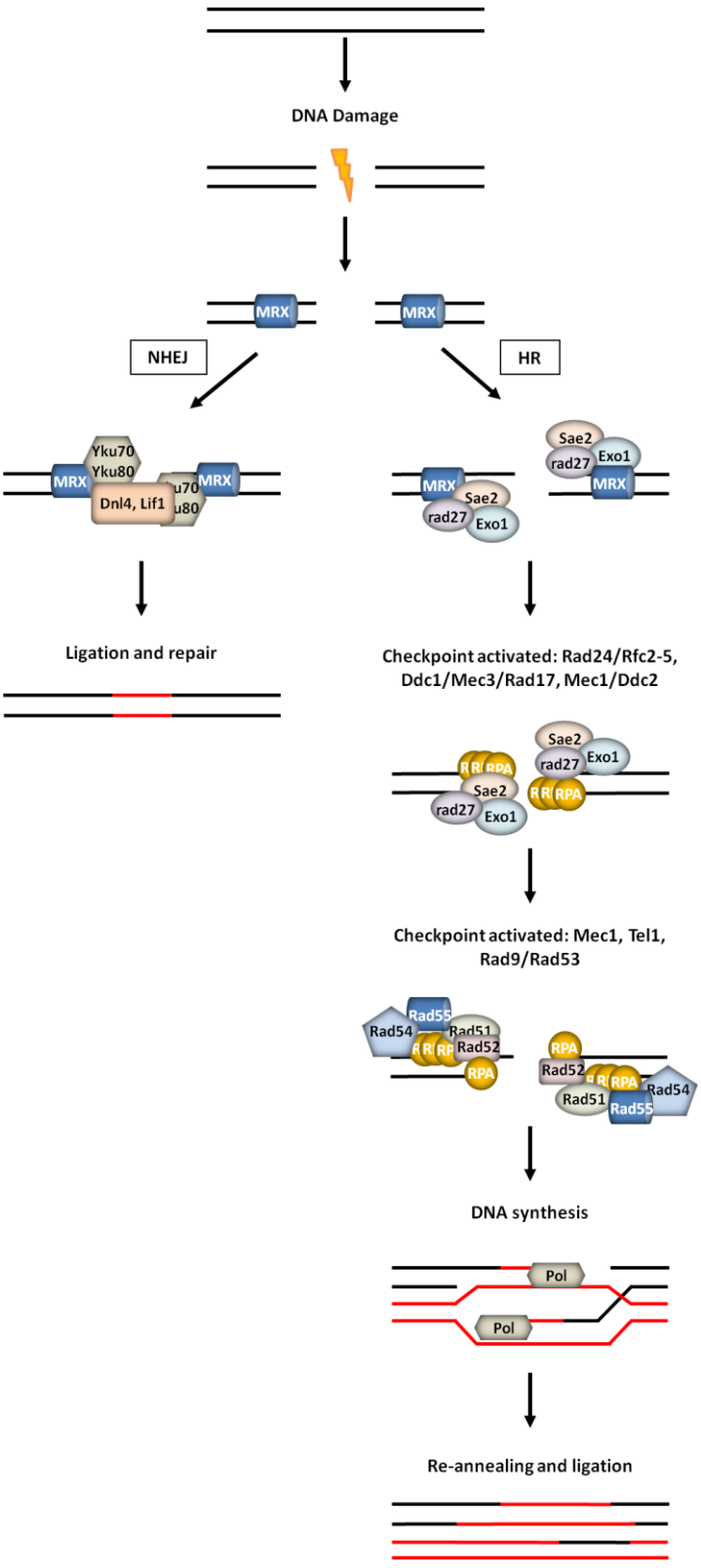

Fig. 14. The DNA DSB repair by NHEJ and HR. Adapted from San Filippo *et al.* (2008), and Finn *et al.* (2012).

Once Rad9 is recruited, it binds and activates Rad53 to form a checkpoint-active Rad9/Rad53 complex, which is responsible for Dun1 phosphorylation and subsequent upregulation of dNTP pools. Rad9 is also important for activation of the Chk1 kinase,

which acts in parallel to Rad53 in mediating DNA damage-induced cell cycle arrest. After dissociation of Tel1, the checkpoint continues being activated by Mec1. HR proteins of the Rad52 epistasis group (Rad50, Rad51, Rad52, Rad54, Rad55/57 complex, Rad59, Mre11, Xrs2, and Rfa1) are recruited to the sites of DNA damage only during S and G2 phase. This recruitment depends on the presence of RPA. Rad52 recruits Rad51, forming a nucleoprotein filament. During the DNA damage response, Rad52 and RPA are retained at Rad51 foci (DNA damage point), suggesting that these proteins have subsequent roles to Rad51 filament formation such as the strand-exchange and checkpoint maintenance. In addition to Rad52, the Rad55/Rad57 heterodimer, and the Swi2/Snf2-like factors, Rad54 and Rdh54, also stimulate Rad51 filament formation although in different degrees. After the DNA ends are resected and Rad51 filaments are formed, the cell is compromised to perform HR in order to repair the damaged DNA template. Rad51 mediates the search for the homologous DNA sequence and, once the homologous sequence is found, Rad51 filaments facilitate the invasion of the ssDNA through the homologous dsDNA. One strand of the dsDNA is moved leaving the complementary strand to serve as template. This recombination structure is referred to as a displacement loop or D-loop. The invading end of the D-loop can be extended by the DNA polymerase, which would then copy any information that might be missing at the break-site. Resolution of the D-loop structure can occur by two different mechanisms. In the first one, the invading strand of the DNA can be displaced and reannealed to the other broken chromosome end in a process called synthesis-dependent strand annealing, which leads to only on-crossover products. Alternatively, the second end of the DSB can be captured, giving rise to a structure called a double-Holliday junction. Resolution of the double-Holliday junction can result in a crossover or non-crossover product. This final step of recovery from DNA damage appears to involve disassembly of the cell cycle checkpoint and recombination apparatus. It has been shown that cells integrate repair and checkpoint functions so that they remain arrested until recombination foci have disassembled. More information can be found in the following reviews: Wu *et al.* (2008), San Filippo *et al.* (2008), Symington & Gautier (2011), and Karpenshif & Bernstein (2012).

NHEJ: This repair system represents the simplest mechanism to heal DSBs and restore chromosome integrity. Since NHEJ is often related to mutations and small deletions at the break-site, this pathway is generally considered as error-prone. In contrast, the genetic information of HR is preferentially copied from an intact sister chromatid, indicating that this pathway is generally error-free. *S. cerevisiae* does not have an end processing nuclease among its NHEJ proteins, so NHEJ only works efficiently and

with high accurancy at repairing DSBs with compatible ends, such as those generated by restriction endonucleases. In the yeast model, after DSB formation and the initiation of 5' resection, the Mrx complex binds the damaged site. The Ku complex (Yku70-Yku80) must also bind the DSB early, although it is unknown whether this precedes or follows Mrx. For the recruitment of the DNA ligase IV complex, Yku80 and Xrs2 bind to some components of the DNA ligase IV, Dnl4 and Lif1, respectively. This repair pathway has been reviewed in Hoeijmakers (2001), Lisby & Rothstein (2005), Daley *et al.* (2005), and Symington & Gautier (2011).

Recently, a third pathway of DSB repair has been suggested, the microhomology-mediated end joining (MMEJ). MMEJ utilizes annealing of short homologous sequences revealed by the end-resection machinery to align ends (Symington & Gautier, 2011).

Mutations in genes important for DSB repair have been implicated in cancer pre-disposition diseases such as ataxia telangiectasia, Nijmegen breakage syndrome, Fanconi anemia and Bloom syndrome (Karpenshif & Bernstein, 2012; San Filippo *et al.*, 2008).

4.3.4. Mismatch repair

MMR is activated when errors of DNA polymerase escape their proofreading activity or polymerase ineffectiveness occurs at repetitive sequences. This pathway was previously considered exclusively located in the nucleus, but several works have indicated some forms of mitochondrial MMR localization [(reviewed in Gredilla *et al.* (2010)]. The eukaryotic MMR system is well conserved during the evolution. The yeast nuclear MMR pathway can be divided in four main steps (Fig. 15).

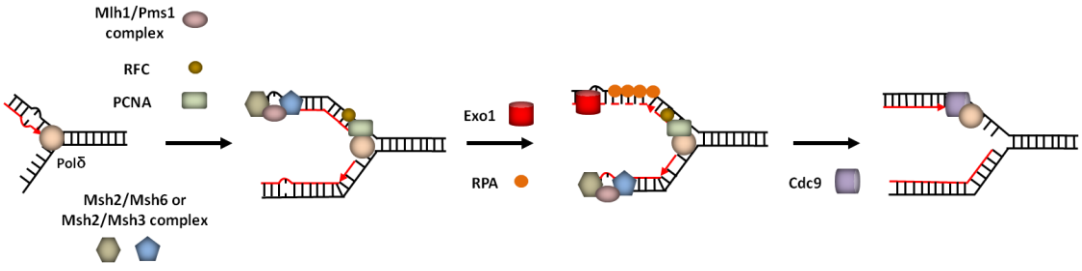

Fig. 15. Scheme of MMR. Adapted from Boiteux & Jinks-Robertson (2013).

The first one involves the recognition and binding of the mismatch. The Msh2/Msh6 or the Msh2/Msh3 heterodimeric ATPase complexes participate in this step. Msh2/Msh6 preferentially recognizes base/base mismatches and insertion/deletion loops of 1 and/or 2 nucleotides while Msh2/Msh3 has preference for larger insertion/deletion loops. The mismatch-bound Msh2/Msh6 or Msh2/Msh3 complex recruits the Mlh1/Pms1

complex in order to form a ternary complex. A proliferating cell nuclear antigen (PCNA) recruits MMR proteins to the replication fork while the replication factor C (RFC) loads PCNA. A strand-specific nick, which may reside either 5' or 3' to the mismatch, is sufficient to direct repair in 5' and 3' directed MMR, respectively. The second step concerns with the excision of the ssDNA. This event is conducted by Exo1, a 5' to 3' exonuclease. RPA binds to protect the ssDNA during the excision and to facilitate the following DNA repair synthesis. The third step includes DNA resynthesis performed accurately by Polδ. The remaining nick after DNA synthesis is then connected by DNA ligase Cdc9 [reviewed in Jun *et al.* (2006), and Gredilla *et al.* (2012)].

Defects in MMR are related to the hereditary nonpolyposis colorectal cancer (HNPCC) and also to a variety of sporadic cancers (Peltomaki, 2003).

4.3.5. Interstrand cross-links repair

DNA ICL lesions belong to those where both DNA strands are affected. They are extremely toxic because they can interfere with effectiveness of DNA repair, inhibition of DNA synthesis and transcription, cell-cycle checkpoint response and induction of cell death by apoptosis and other mechanisms.

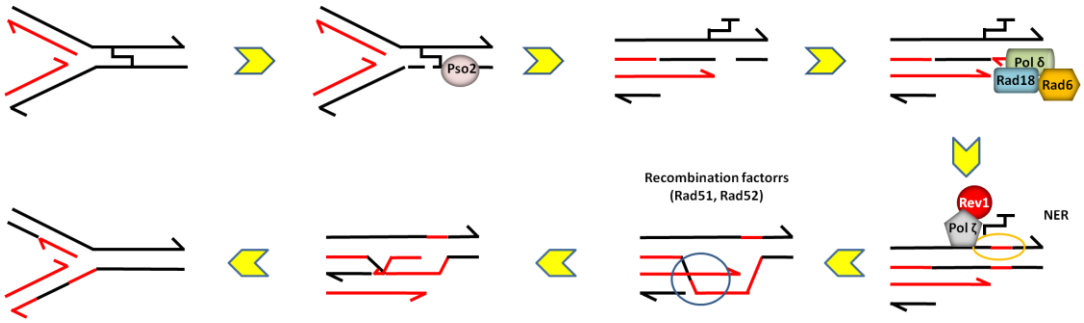

Fig. 16. Scheme of the ICL repair. 3' ends are indicated by the arrowheads. Parental and newly strands are shown in black and red, respectively. A replication fork is stalled at the crosslink structure. Adapted from Bergstralh & Sekelsky (2008).

UV light, 8-methoxy-psoralen (8-MOP), mitomycin C, cisplatin and mechlorethamine have been shown to induce ICL lesions. In this repair system there is a complex involvement of several other repair systems such as NER, HR and PRR. Fig. 16 shows a scheme of the ICLs repair system. Cell cycle regulating proteins participate in ICL repair, increasing the level of complexity and showing that certain pathway interactions are strongly influenced by the cell cycle.

NER is the first system to take control of the ICL lesion by recognizing the DNA damage strand, producing the incisions required up or downstream of the lesion, and moving the excised oligonucleotide. These steps have the participation of the NER factor

complexes 1-4 (NEF 1-4) with respective actions of Rad4, Rad23, Rad7, Rad16, Rad14, Rad1-Rad10 complex, Rad3, Rad25, Rad2, TFIIH and Pol ζ. In the case that both DNA strands are compromised, the HR repair system plays a role with the participation of Pso2 exonuclease and Rad52, among others. When a damaging agent affects replication, this process is re-established by HR repair and/or the participation of the PRR (see section 4.3.6 in this Introduction). The Rad6 and Rad18 proteins play a central role at PRR in addition to the participation of the polymerase Pol δ. ICL repair has been reviewed in Mchugh & Sarkar (2006), Lehoczký *et al.* (2007), and McVey (2010).

Patients with a deficient ICL repair system are susceptible to a wide variety of cancers, including Fanconi anemia (Huang & Li, 2013).

4.3.6. Post-replication repair

When the integrity of the DNA replication forks is compromised a cascade of events starts to occur. Thus, prolonged stalling of DNA replication is detected and instead of repairing these lesions, they are bypassed, allowing DNA replication to continue without removing the damage, through a mechanism called PRR. There are two PRR subpathways in eukaryotes, the translesion synthesis (TLS) and the damage avoidance pathway, as shown in Fig. 17. When the yeast cell undergoes to a DNA damage situation, the PCNA wraps the DNA in a doughnut shaped homotrimeric way and serves as a scafold for DNA polymerases and for binding many other proteins that participate in DNA replication and repair. In the first subpathway, PCNA is monoubiquitinated by the Rad6/Rad18 complex at the Lys64 residue. Rad6 is an E2 ubiquitin-conjugating enzyme and Rad18 is an E3 ubiquitin ligase. Polymerases Pol δ or Pol ε are replaced by one or more specialized TLS polymerases [Pol η (Rad30), Pol ι, Pol κ, Pol ζ (Rev3 and Rev7)], which catalyze DNA synthesis across the lesion that blocks the replicative DNA polymerases. These TLS polymerases have a low rate of accurancy and can incorporate incorrect nucleotides due to the absence of correcting exonuclease activity. Because of that this is also termed as error-prone subpathway. In the case of the second subpathway, the Rad6-dependent monoubiquitinated PCNA is further polyubiquitinated by the Ubc13/Mms2/Rad5 complex, which adds an ubiquitin chain onto the Lys164 residue of PCNA. This subpathway, termed as error-free, uses an undamaged sister chromatid as a template through HR. Although many details on PRR remain largely unknown its elimination results in a strong mutator phenotype, indicating that this mechanism acts as the major one for lesion bypass. More details can be found in the

reviews by Barbour (2003), Hochegger *et al.* (2004), Martin (2008), and Boiteux & Jinks-Robertson (2013).

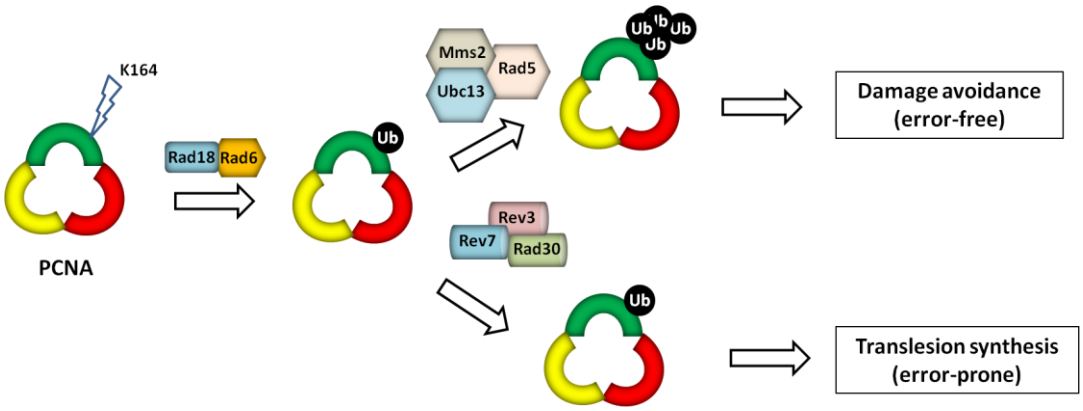

Fig. 17. Scheme of PRR. Adapted from Boiteux & Jinks-Robertson (2013).

4.4. Cell cycle and Mec1-Rad53-Dun1 dependent DNA damage checkpoint

Normal cells divide and grow in a controlled way. In cancer, cell proliferation becomes uncontrolled, forming malignant tumours which invade neighbour tissues and spread throughout the body. For controlling growth and division, cells have evolved surveillance mechanisms called cell cycle checkpoints. The main objective of these mechanisms is to monitor the cell cycle division and coordinate the cellular response when DNA damage or other cell cycle defects are detected. There are several responses coming from the DNA damage checkpoint such as cell cycle arrest and activation of different DNA repair pathways, but in the case that the damage is too severe for the cell, apoptotic mechanisms are activated. Eukaryotic cell cycle is divided into four phases: DNA synthesis (S), nuclear division (mitosis or M), and two gap phases (G1 and G2), as observed in Fig. 18. In the first phase, G1 cells grow until they reach a critical monitoring stage (where size and nutrient availability among other factors are taken into account) and pass through START (late G1 phase point where cells decide to continue for cell division or not), and enter into the second phase, S, followed by G2, where cells become prepared for the next phase, M, where chromosomes are segregated and the cell divides.

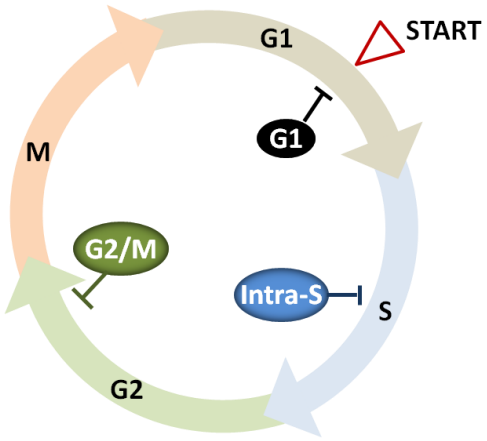

Fig. 18. Cell cycle and the DNA damage checkpoints in *S. cerevisiae*. Adapted from Finn *et al.* (2012).

The two critical phases of the cell cycle are the S-phase, when chromosomes must be accurately duplicated, and the M phase, when chromosomes must be correctly segregated. In *S. cerevisiae* the first DNA damage checkpoint (G1) arrests cells at the G1/S transition but before START. This arrest allows the repair of DNA lesions before its replication. Protein kinase Rad53 phosphorylates Swi6, a protein component of the MBF [MCB (Mlu1 cell cycle box) binding factor] transcriptional complex, which inhibits the transcription of the cyclins Cln1 and Cln2, and the formation of the cyclin-dependent kinase (CDK)-cyclin complexes Cdc28-Cln1/2 required for the G1/S transition. These facts stabilize the CDK inhibitor Sic1, which contributes to maintain the G1 arrest. There exists a relationship between Rad53 and mtDNA. Thus, yeast cells lacking mtDNA are defective in G1/S transition, and Rad53 phosphorylation is activated by loss of mtDNA (Crider *et al.,* 2012). The second cell cycle checkpoint (intra-S) is activated when the integrity of the DNA replication forks is compromised. When this situation occurs Rad53 and Mec1 kinases are activated to stabilise the replication forks. That occurs with the participation of the checkpoint proteins Mrc1, Rad9, Rad17 and Rad24. All of these proteins, besides the stabilization of the DNA replication forks, are also involved in the reduced rates of DNA replication, slowing the cell cycle progression, and preventing the cell entering into mitosis with any defect at the DNA. In the case of the third checkpoint (G2/M), it is relevant to mention that in budding yeast, the G2/M transition is not well defined and events normally considered as mitotic, such as spindle pole body duplication and mitotic spindle formation, are initiated during S-phase in order to facilitate bud formation and nuclear migration. So, it is the metaphase to anaphase transition rather than the G2 to M one which is regulated by the G2/M DNA damage checkpoint in *S. cerevisiae*. Rad53 and Chk1 kinases are responsible to stall cells to enter in anaphase and leaving mitotic phase

in the presence of DNA damage. This step is achieved, at least in part, by inhibiting the degradation of Pds1, the anaphase inhibitor. This subject is reviewed in more detail in Bähler (2005), Clémenson & Marsolier-Kergoat (2009), Cai & Tu (2012), and Finn *et al.* (2012).

As mentioned before, DNA damage events trigger DNA damage checkpoints answers that stall the cell cycle and activate several factors to repair the damage. Specifically, the Mec1-Rad53-Dun1 checkpoint kinase pathway regulates the dNTPs levels [reviewed in Andreson *et al.* (2010), and Sanvisens *et al.* (2011)].

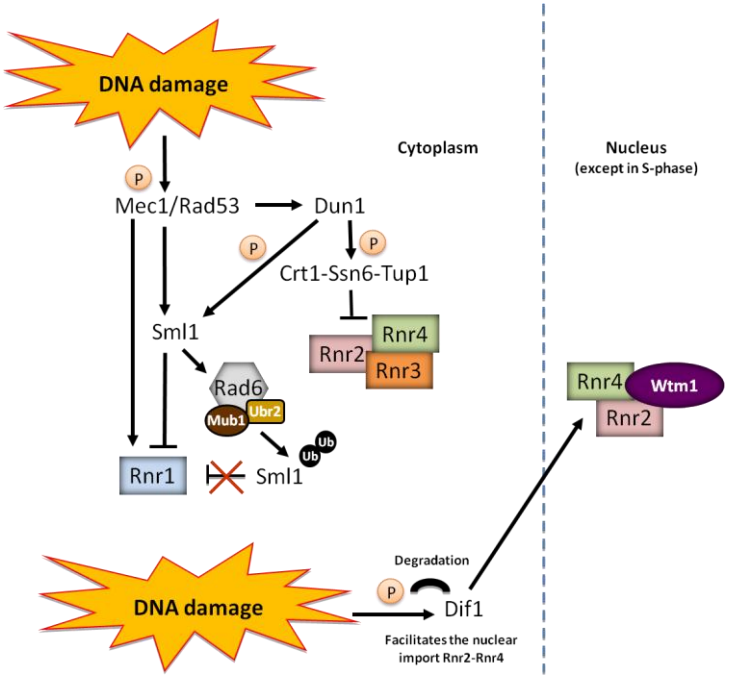

Fig. 19. Scheme of Mec1-Rad53-Dun1 checkpoint kinase pathway in *S. cerevisiae*.

When activated, an average of 6 to 8 fold increase in the dNTP levels occurs after a DNA damage event (Chabes *et al.,* 2003). High levels of dNTPs inhibit the cell entry into the S-phase cell cycle through the delay of the replication initiation (Chabes & Stillman, 2007). The production of dNTPs by RNR is tightly controlled throughout the cell cycle and in response to DNA damage. This control occurs at multiple levels. RNR is an essential enzyme that participates in the *de novo* synthesis of dNTPs, which are the precursors for DNA synthesis and repair. In *S. cerevisiae*, there are four genes (*RNR1-4*) that encode RNR polypeptides, but only the homodimeric Rnr1 subunit and the heterodimer formed by Rnr2-Rnr4 are essential for the proper function of the RNR. As observed in Fig. 19, the activity of RNR in yeast is regulated by the Mec1-Rad53-Dun1 checkpoint pathway. In a response to DNA damage and during S-phase, the complex Mec1-Rad53-Dun1 undergoes

a phosphorylation reaction cascade degrading the protein inhibitor Sml1, which binds Rnr1 and consequently inhibits the RNR activity. When Sml1 is phosphorylated it is also recognized by the Rad6–Ubr2–Mub1 complex, which ubiquitynates Sml1 promoting its degradation. At the end, the loss of Rnr1 inhibition after the degradation of Sml1 provides the activation of RNR, causing an increase in the levels of dNTPs and facilitating DNA damage repair, as observed with cells mutated in *SML1*, in which the respective levels of all four dNTPs are increased compared to wild type (Zhao *et al.,* 1998). The phosphorylated Mec1-Rad53-Dun1 complex induces the transcription of the *RNR2*, *RNR3*, and *RNR4* genes by releasing the repressor effect of the Crt1-Ssn6-Tup1 complex. In normal conditions, Rnr1 and Rnr3 are localized in the cytoplasm where the synthesis of dNTPs takes place. However, Rnr2 and Rnr4 are found in the nucleus during G1. The nuclear localization of Rnr2 and Rnr4 is regulated by two proteins: the nuclear WD40 protein Wtm1, which binds both Rnr2 and Rnr4 limiting their export, and the cytoplasmic protein Dif1, which is required for nuclear import of Rnr2 and Rnr4. In a DNA damage response Wtm1 releases both RNR subunits from the nucleus and together with the degradation of Dif1, Rnr2 and Rnr4 remain in the cytoplasm therefore increasing the levels of dNTPs (Zhang *et al.,* 2006; Wu & Huang, 2008).

In an iron depletion situation, degradation of the *WTM1* mRNA is promoted through both Cth1 and Cth2 proteins (members of the iron regulon), and the subsequent decrease of Wtm1 levels causes the displacement of Rnr2-Rnr4 to the cytosplasm increasing the levels of dNTPs (Sanvisens *et al.,* 2011). Therefore Cth1 and Cth2 are involved in the cytosolic distribution of Rnr2 and Rnr4 proteins when iron availability is limited, so indirectly are therefore related to DNA damage checkpoint events.

PART II

OBJECTIVES

The specific objectives are:

- To study recombination and mutation rates in cells lacking Grx5
- To determine the sensitivity of *Δgrx5* cells to DNA-damaging agents
- To determine whether phenotypic traits of *Δgrx5* cells related to DNA instability are influenced by oxidative stress
- To study the relationship between DNA lesion and repair pathways in *Δgrx5* cells
- To determine the state of the DNA damage checkpoint pathway in cells lacking Grx5

PART III

MATERIAL AND METHODS

1. YEAST STRAINS AND PLASMIDS

The yeast strains used in the work are described in Table 1, which includes the relevant phenotype and respective comments.

Table 1. Yeast strains employed in this thesis.

Strains	Relevant phenotype	Comments
W303-1A	*MAT**a** ura3-1 ade2-1 leu2-3,112 trp1-1 his3-11,15*	Wild type strain
W303-1B	As W303-1A but *MAT**α***	Wild type strain
CML235	*MAT**a** ura3-52 leu2Δ1 his3Δ200 GAL2+*	Wild type strain (Rodríguez-Manzaneque *et al.,* 1999)
CML236	As CML235 but *MATα*	Wild type strain
Cdc7-1	As W303-1A but *TRP1, cdc7-1*	Bousset & Diffley, 1998
MML19	CML235 *grx5::kanMX4*	Deletion of *GRX5* in CML235 (Rodríguez-Manzaneque *et al.,* 1999)
MML100	W303-1A *grx5::kanMX4*	Deletion of *GRX5* in W303-1A (Rodríguez-Manzaneque *et al.,* 2002)
MML102	W303-1A *cdc7-1 grx5::kanMX4 TRP1*	This work
MML281	W303-1B *yfh1::kanMX4 ade2 his3 ura3 trp1*	This work
MML289	W303-1B *grx5::kanMX4*	Rodríguez-Manzaneque *et al.* (2002)
MML298	W303-1A *yfh1::kanMX4*	Rodríguez-Manzaneque *et al.* (2002)
MML345	W303-1A *aft1::URA3 grx5::kanMX4*	Rodríguez-Manzaneque *et al.* (2002)
MML830	W303-1A [pCM244 (*tetR'-SSN6*)]*::LEU2*	Castells-Roca *et al.* (2011)
MML997	W303-1A *ssq1::kanMX4*	This work
MML1107	W303-1A *fet3::natMX4*	Castells-Roca *et al.* (2011)
MML1166	W303-1A *aif1::kanMX4*	Izquierdo *et al.* (2010)
MML1167	W303-1A *cox12::kanMX4*	Izquierdo *et al.* (2010)

Strains	Relevant phenotype	Comments
WFNL-5A	MAT**α** *ura3 leu2 leu2-k::URA3-ADE2::leu2-k*	W303 background (Díaz de la Loza *et al.*, 2011)
MML1343	WFNL-5A *grx5::kanMX4*	This work
MML1344	As MML1343 but *MAT***a**	This work
MML1345	WFNL-5A *yfh1::kanMX4*	This work
MML1346	As MML1345 but *MAT***a**	This work
MML1347	As MML1348 but *MAT***a**	This work
MML1348	WFNL-5A *ssq1::kanMX4*	This work
MML1349	As WFNL-5A but *MAT***a**	This work
MML1352	As MML1353 but *MAT***a**	This work
MML1353	WFNL-5A *cox12::kanMX4*	This work
MML1354	As MML1355 but *MAT***a**	This work
MML1355	WFNL-5A *aif1::kanMX4*	This work
MML1356	W303-1A *aft1::natMX4*	From the laboratory collection
MML1426	W303-1A *rad1::natMX4*	From the laboratory collection
MML1429	W303-1A *rad1::natMX4 grx5::kanMX4*	From the laboratory collection
MML1478	W303-1A *fet3::natMX4 grx5:: kanMX4*	This work
Scrad52-Δ	W303-1B *rad52::TRP1*	From Germán Larriba (Universidad de Badajoz)
MML1489	W303-1A *rad52::TRP1 grx5::kanMX4*	This work, from Scrad52-Δ
MML1490	W303-1B *rad52::TRP1 grx5::kanMX4*	This work, from Scrad52-Δ
MML1493	W303-1A *RAD52-YFP*	From R. Rothstein laboratory collection (Jordi Torres - Universitat de Lleida)
MML1495	W303-1A *RAD52-YFP grx5::kanMX4*	This work
MML1496	W303-1A *rev3::kanMX4*	This work
MML1497	CML235 *rev3::kanMX4*	This work
MML1498	W303-1A *rad5::kanMX4*	This work
MML1499	CML235 *rad5::kanMX4*	This work
MML1500	CML235 *grx5::natMX4*	This work
MML1520	W303-1A *rev3::kanMX4 grx5::natMX4*	This work

Strains	Relevant phenotype	Comments
MML1525	CML235 *rev3::kanMX4 grx5::natMX4*	This work
MML1545	CML235 *rad50::kanMX4*	This work
MML1556	W303-1A *RFA1-YFP*	From R. Rothstein laboratory collection (Jordi Torres - Universitat de Lleida)
MML1557	W303-1A *MRE11-YFP*	From R. Rothstein laboratory collection (Jordi Torres - Universitat de Lleida)
MML1559	W303-1A RFA1-YFP grx5::kanMX4	This work
MML1560	W303-1A *MRE11-YFP grx5::kanMX4*	This work
MML1562	W303-1A *DDC1-YFP*	From R. Rothstein laboratory collection (Jordi Torres - Universitat de Lleida)
MML1563	W303-1A *RAD53-YFP*	From R. Rothstein laboratory collection (Jordi Torres - Universitat de Lleida)
MML1565	W303-1A *DDC1-YFP grx5::kanMX4*	This work
MML1567	W303-1A *RAD53-YFP grx5::kanMX4*	This work
MML1583	CML235 *rad1::natMX4*	This work
MML1585	CML235 *rad52::kanMX4*	This work
MML1603	W303-1A *rad50::kanMX4 grx5::natMX4*	This work
MML1605	CML235 *rad50::kanMX4 grx5::natMX4*	This work
MML1607	CML235 *rad52::kanMX4 grx5::natMX4*	This work
MML1609	CML235 *rad1::natMX4 grx5::kanMX4*	This work
MML1620	CML235 *sml1::URA3*	This work
MML1621	CML235 *nej1::kanMX4*	This work
MML1633	CML236 *apn1::HIS3 grx5::natMX4*	This work
MML1643	CML235 *nej1::kanMX4 grx5::natMX4*	This work
MML1656	CML235 *apn1::HIS3 ntg1::kanMX4 ntg2::URA3 grx5::natMX4*	This work
MML1662	CML235 *apn1::HIS3*	This work
MML1666	CML235 *grx5::natMX4 sml1::URA3*	This work

Strains	Relevant phenotype	Comments
MML1677	CML235 *ssq1::kanMX4*	This work
MML1678	CML235 *iba57::natMX4*	This work
MML1681	CML235 *ssq1::kanMX4 grx5::natMX4*	This work
MML1694	CML235 *iba57::natMX4 grx5::natMX4*	This work

The plasmids employed and the respective characteristics are described in Table 2.

Table 2. Plasmids employed in this study.

Plasmids	Origin/Vector	Characteristics
YEplac181	Gietz & Sugino (1988)	Multicopy episomal vector with *LEU2* marker
pAG25	Goldstein & McCusker (1999)	Contains a *natMX4* module to disrupt genes
pMM70	Rodríguez-Manzaneque *et al.* (2002)	Contains *SSQ1* plus promoter and terminator regions, cloned in YEplac181*
pCM189	Garí *et al.* (1997)	Centromeric vector, $tet0_7$ promoter and *URA3* marker
pCM218	Bellí *et al.* (1998)	Integrative vector, CMV promoter, *tetR'-SSN6* repressor gene and *LEU2* marker
pCM244	Bellí *et al.* (1998)	Integrative vector, CMV promoter, *tetR'-SSN6* repressor gene and *LEU2* marker
pMM536	pFA6a-kanMX4	Contains a *kanMX4* module to disrupt genes
pMM1077	pCM189	Contains *NTG2* plus promoter and terminator regions cloned between *BamHI-PstI* sites of the pCM189 vector
pMM1078	pCM189	Contains *PRI2* plus promoter and terminator regions cloned between *BamHI-PstI* sites of the pCM189 vector
pMM1094	pCM189	Contains *RAD3* plus promoter and terminator regions cloned between *PmeI-NotI* sites of the pCM189 vector

*We considered promoter regions those ones located from 700 bp upstream the initiation codon, and terminator regions those that are located up to 250 bp downstream the stop codon.

2. CELL CULTURING

2.1. Growth conditions

S. cerevisiae and *E. coli* cells were respectively grown at 30°C and 37°C, unless otherwise indicated. The liquid cultures were incubated with rotation at 165 rpm. Growth was measured with a spectrophotometer by determining optical density at 600 nm. Yeast samples for further analyses were taken from cultures growing exponentially at a concentration between 1.5 to 2 x 10^7 cells·ml^{-1}, which is equivalent to 0.4-0.6 units of optical density (600 nm).

2.2. Growth media

2.2.1. Growth medium for *E. coli* cells

For cultures of *E. coli* cells **LB** medium was used with the following composition: triptone 1%, NaCl 1%, yeast extract 0.5%, at pH 7.5 ajusted with NaOH 1M. For the selection of transformed cells the medium was supplemented with ampicillin at 50 μg·ml^{-1} final concentration. The medium was solidified with 2% agar.

2.2.2. Growth medium for *S. cerevisiae* cells

YPD: glucose 2%, peptone 2%, yeast extract 1%. Depending on the required conditions, geneticin (selection with the *kanMX4* marker) or nourseothricin (selection with the *natMX4* marker) were added at a final concentration of 200 μg·ml^{-1}.

YPGly: glycerol 2%, peptone 2%, yeast extract 1%.

YPGal: galactose 2%, peptone 2%, yeast extract 1%.

SC (Sherman, 2002): yeast nitrogen base without amino acids (Difco™) 0.67%, glucose 2%, *Drop out* 0.2%. *Drop out* is the combination in dry of nitrogenated bases, amino acids and vitamins, except the adequate supplements for the required auxotrophies for each strain. Its composition is detailed in Table 3.

SC+5-FOA: as **SC** but supplemented with 0.5 mg·ml^{-1} of 5-fluororotic acid (5-FOA) (Fermentas). All aminoacids and nitrogenated bases were supplied at the usual concentrations, except in the case of uracil, which was added at a final concentration of 50 μg·ml^{-1}.

SC-Arg: as **SC** with supplements except that arginine was not added.

Sporulation medium: potassium acetate 1%, yeast extract 0.1%, glucose 0.05%, solidified with 2% agar.

Table 3. *Drop out* components and their respective quantities per liter of SC medium (Sherman, 2002). Final concentration of additional components (histidine, leucine, tryptophan and uracil) is also indicated.

Amino acid	(mg)	Amino acid	(mg)	Amino acid	(mg)
Adenine	20	Glycine	20	Serine	400
Alanine	20	Histidine	20	Threonine	200
Arginine	20	Isoleucine	30	Tryptophan	20
Asparagine	20	Leucine	30	Tyrosine	30
Aspartic acid	100	Lysine	30	Uracil	20
Cysteine	20	Methionine	20	Valine	150
Glutamine	20	Phenylalanine	50		
Glutamic acid	100	Proline	20		

2.3. Additional compounds

I. Methyl methane sulfonate (MMS): The adequate volume of a stock solution of MMS (Sigma) at 1% was added to obtain the desired final concentration.

II. Hydroxyurea (HU): The adequate volume of a stock solution of HU (Sigma) at 2 M was added to obtain the desired final concentration.

III. Diamide: The adequate volume of a stock solution of diamide (Sigma) at 100 mM was added to obtain the desired final concentration.

IV. *ter*-butyl hydroperoxide (*t*-BOOH): The adequate volume of a stock solution of *t*-BOOH (Sigma) at 1 M was added to obtain the desired final concentration.

V. N-acetyl cysteine (NAC): The adequate volume of a stock solution of NAC (Sigma) at 100 mM was added to obtain the desired final concentration.

VI. Camptothecin (CPT): A stock solution of CPT (Sigma) in chloroform/methanol (4:1) at 5 mg·ml^{-1} was added to obtain a final concentration of 8 µg·ml^{-1}.

VII. L-Canavanine: This compound (Sigma) was added directly to obtain a final concentration of 60 µg·ml^{-1}.

3. SENSITIVITY ANALYSES

Sensitivity to the different oxidative and DNA damaging agents was determined in YPD plates containing the indicated concentrations of the respective agents, by spotting on the medium 1:5 serial dilutions of exponential cultures from an initial concentration of 1.5 to 2 x 10^7 cells·ml^{-1}, which is equivalent to 0.4-0.6 units of optical density (600 nm). The growth was recorded after 2 and 3 days of incubation at 30°C. In the case of UV

sensitivity, plates were irradiated at the indicated doses after spotting the serial dilutions, followed by incubation at 30°C.

4. EXTRACTION OF *S. cerevisiae* GENOMIC DNA

The following solutions were used:

- **TNST**: Triton X-100 2%; SDS 1%; NaCl 0.1 M; EDTA 1 mM; Tris-HCl 10 mM, pH 8.
- **FC**: phenol/chloroform/isoamyl alcohol 25:24:1 with 8-hydroxyquinoline 0.1% and saturated with TE.
- **TE**: Tris-HCl 10 mM, pH 8; EDTA 1 mM, pH 8. Sterilized by autoclaving.
- **NaOAc**: sodium acetate 3 M, pH 8.

The extraction procedure was as follows:

- One colony of the desired strain was inoculated in 10 ml of liquid YPD medium and incubated for 16 hours at 30°C.
- Cells were recovered by centrifugation at 4000 rpm for 2 min and resuspended in 1 ml of sterile water.
- Cells were centrifuged again and resuspended in 200 µl of TNST and 200 µl of FC. A volume of glass beads (450-600 µm, Sigma) equivalent to about 200 µl was added.
- The mixture was shaken with a vortex at maximum speed for 4 min.
- Next, 200 µl of TE were added and mixed by inversion. The mixture was centrifuged at 12000 rpm for 5 min.
- The supernatant was transferred to a new tube, where 1 ml of ethanol 100% was added. After mixing by inversion, the suspension was centrifuged at 12000 rpm for 5 min.
- A volume of 400 µl of TE and 3 µl of RNAse (10 $mg \cdot ml^{-1}$) was added to the precipitate and let it incubate at 37°C for 5 min to recover the precipitate.
- Next, 50 µl of NaOAc and 500 µl of FC were added. This mixture was vortexed at maximum speed for 1 min. Then, the mixture was centrifuged at 12000 rpm for 5 min and the supernatant was removed.
- The precipitate was washed with 1 ml of ethanol at 70% and was centrifuged at 12000 rpm for 1 min.
- The supernatant was removed. The remaining precipitate was dried in a Speed Vacuum equipment (Eppendorf) for 2 min.
- The dried precipitate was resuspended in 50 µl of Milli-Q water and analysed by DNA electrophoresis in an agarose gel (Serva) at 0.8%.

5. RECOMBINANT DNA METHODS

5.1. Gene cloning

In order to clone the desired *S. cerevisiae* genes into a vector, the corresponding region was initially amplified by PCR from genomic DNA from CML235 strain.

I. Polymerase chain reaction (PCR)

The conditions for the PCR were: 30 sec at 98°C (followed by addition of the polymerase); 10 sec at 98°C; 30 cycles of 30 sec at 52°C, 150 sec at 72°C and 10 min at 72°C; finally 10 min at 72°C. Each reaction was carried out in a total volume of 50 µl that contained: 300-500 ng of DNA, Phusion HF buffer x1, $MgCl_2$ 50 mM, dNTPs 2.5 mM each, DMSO 3%, the primer oligonucleotides at a concentration of 0.5 µM each and 0.5 units of Phusion High-Fidelity DNA Polymerase (New England BioLabs). Oligonucleotides were designed to contain adequate restriction enzyme sites at the two ends of the PCR product for further cloning.

II. Enzyme digestions

The restriction enzymes employed were from Roche or Takara. The reactions with the PCR-amplified DNA (step I) were carried out during 2-4 hours at 37°C, with the respective recommended buffers.

III. Purification of the DNA fragments

The PCR-amplified and digested fragments were purified with the "High pure PCR Product Purification Kit" system from Roche. Final products were analysed by electrophoresis in 0.8% agarose gels. For checking the size of the fragments, the "1Kb DNA Ladder" from Invitrogen was used as a standard.

IV. Ligation reaction

For the insert-vector ligation reaction the T4 DNA ligase enzyme from Takara was used, following the manufacturer's instructions.

5.2. Plasmid purification from *E. coli* cultures

5.2.1. Miniprep technique

Plasmids were purified from *E. coli* cultures grown at 37°C for 16 hours in LB medium with ampicillin, using the NucleoSpin Plasmid QuickPure system (Macherey-Nagel) following the manufacturer's instructions. When higher quality of the plasmid DNA

was required (for instance for sequencing), the QIAprep Spin Miniprep kit (Qiagen) was used.

5.2.2. Jet-prep technique

A colony of transformed bacteria was inoculated in 500 µl of LB medium with ampicillin and incubated at 37°C for 16 hours. The cells were centrifuged at 12000 rpm for 1 min and the supernatant was removed. 50 µl of BT solution (Triton X-100 2%, pH adjusted at 12.4 with NaOH) was added without resuspension, followed by 50 µl of phenol/chloroform. Vigorous shaking of the samples was performed for 30 sec. Next, they were centrifuged at 14000 rpm for 5 min and 5 µl of each sample supernatant were loaded in an 0.8% agarose gel, after mixing with 5 µl of 5xFLB buffer (15% Ficoll, 0.1 M EDTA pH 8 and bromophenol blue) containing RNAse (10 $\mu g \cdot ml^{-1}$). The approximate relative size of the plasmids was determined by comparing with the "1kb DNA Ladder" used as standard.

5.3. Transformation methods for *E. coli* and *S. cerevisiae*

5.3.1. Transformation of *E. coli*

Obtention of *E. coli* competent cells and subsequent transformation was carried out according to standard laboratory protocols (Ausubel *et al.*, 1994). Basically, the transformation consists of a heat shock of 2 min at 42°C of the *E. coli* competent cells resuspended in a $CaCl_2$ solution and previously maintained at 0°C, followed by an incubation period of 1 hour at 37°C for ampicillin resistance expression, before plating in LB medium with ampicillin for selection.

5.3.2. Transformation of *S. cerevisiae*

For *S. cerevisiae* cells transformation, the lithium acetate (AcLi) method was employed (Gietz *et al.,*1992), as follows:

- Exponentially growing cells in YPD medium were centrifuged at 4000 rpm for 4 min at room temperature, washed with sterile water and centrifuged again in the same conditions.
- The precipitate was resuspended in 900 µl of AcLi/TE (TE 1x and AcLi 1M) solution and centrifuged at maximum speed for 5 sec. TE 1x consists of Tris-HCl 10 mM at pH 8,0 plus EDTA 1 mM
- The precipitate was resuspended in 100 µl of the same AcLi/TE solution with the following additions: 5 µl of denatured salmon sperm DNA (10 $mg \cdot ml^{-1}$), the transforming

DNA (in a volume not larger than 10 µl, about 800 ng for integrative plasmids and 100 ng for episomal and centromeric plasmids), and 300 µl of 40% polyethylene glycol (PEG) solution.

- The mixture was carefully homogenized and incubated at 30°C for 30 min.
- Next, the mixture was shifted to 42°C for 15 min to subject the cells to a heat shock.
- The mixture was centrifuged at maximum speed for 5 sec, the supernatant was removed and the cell pellet was resuspended in 100 µl of TE (1x). The cell suspension was spreaded on selective medium plates (according to the respective auxotrophies and selective marker), which were incubated at 30°C at least for 48 hours.
- When selection was based on antibiotic resistance, transformed cells were incubated in 4 ml of YPD medium at 30°C for 4 hours prior to plating on selective plates.

6. CONSTRUCTION OF NULL AND MULTIPLE MUTANTS IN *S. CEREVISIAE*

Null mutants for a single gene were obtained following the short-flanking homology approach (Wach *et al.,* 1994). The first step consisted of designing oligonucleotides pairs with a 5'-region of about 50 bp homologous to promoter (or terminator) sequences of the gene to be disrupted, plus a 3'-region of 18-20 bp respectively homologous to one or the other extreme of the disrupting module. The *kanMX4* module (which provides for resistance to geneticin) (Wach *et al.,* 1994) or the *natMX4* module (which provides for resistance to nourseothricin) (Goldstein & McCusker, 1999) were employed along this study. After PCR amplification of the disrupting modules, cells were transformed according to the protocol in previous section 5.3.2.

To confirm the incorporation of the module at the proper site of the genome, a colony PCR was performed. For this type of PCR, the selected geneticin or nourseothricin-resistant clones were previously incubated on YPD plates at 30°C overnight. Then, a small portion of the growing colonies was collected in PCR tubes and let them for 1 min in the microwave and then 5 min in ice. The conditions for the PCR were: 5 min at 94°C; 30 cycles of 1 min at 94°C, 45 sec at 50°C and 3 min at 72°C; finally 7 min at 72°C. Each PCR reaction was carried out in a total volume of 25 µl that contained: the treated cells (DNA sample), 10 X Standard Reaction Buffer, $MgCl_2$ 2 mM, dNTPs 2.5 mM each, tester oligonucleotides (a 18-20 bp oligonucleotide corresponding to the gene promoter region plus an oligonucleotide internal to the disrupting module or alternatively to the gene to be disrupted) at the concentration of 7 µM each and 0.25 µl of PCR DNA Polymerase (Biotools).

To obtain the multiple mutants, strains from opposite mating type containing the desired mutations were crossed by standard methods (Sherman, 2002). The resulting diploids were induced to sporulate, tetrads were dissected and the resulting haploid clones were selected for the desired phenotypes according to the genetic markers (Sherman, 2002).

7. GENETIC METHODS

7.1. Recombination rates

Yeast cells carrying the *leu2-k::URA3-ADE2::leu2-k* chromosomal recombination system (provided by Andrés Aguilera, University of Sevilla) were grown exponentially in YPD medium at 30°C up to $2x10^7$ cells·ml^{-1}, diluted (10^{-5}) and plated on YPD medium to achieve about 100 colonies per plate after 2 (wild type strain) or 3 (*Δgrx5* mutant) days of incubation at 30°C. Next, one colony (per duplicate) was resuspended in 100 µl of SC medium and dilutions were made (in the case of the wild type cells at 10^{-5} and in the case of the mutant cells at 10^{-4} and 10^{-5}). Aliquots of 100 µl of the diluted suspension samples were plated on solid SC medium plates containing all amino acids in order to determine the total number of cells after 2-3 days of incubation at 30°C, while the non-diluted suspension samples were plated on solid SC medium plates supplemented with 5-FOA (see section 2.3 in Material and Methods for final concentration) and incubated for 5 days at 30°C. The recombination rates were obtained based on the number of the 5-FOA resistant colonies and the number of colonies growing in SC medium without selection and considering the dilution fold. At least six independent experiments (two separate colonies for each one) were done for each strain.

7.2. Spontaneous mutation frequencies

Cells growing exponentially in YPD medium at 30°C (up to $2x10^7$ cells·ml^{-1}) were centrifuged at 2500 rpm for 2 min. They were then washed with sterile water and resuspended in 400 µl of water. The samples were diluted and 100 µl of the 10^{-4} dilution were plated on solid YPD medium and incubated for 3 days to determine total cell number. An additional volume of 300 µl of the cell suspension was divided in three aliquots and plated on SC-Arg plates that contained L-canavanine (60 µg·ml^{-1}) as selective agent. Plates were incubated for five days at 30°C. The spontaneous mutation frequencies were obtained by dividing the number of the colonies grows on the SC-Arg plus canavanine plates by the number of colonies growing on the YPD plates after correcting by the dilution fold. Eight independent experiments were done for each strain.

8. ANALYSIS OF GENE EXPRESSION BY NORTHERN BLOT

All the material used in Northern blot analyses was washed and rinsed with RNAse-free MiliQ water prior to use and manipulated with gloves.

8.1. Solutions

- **Anti-Digoxigenin-AP Fab fragments (Roche):** conjugated Fab fragments with alkaline phosphatase.
- **Buffer 1:** Tris-HCl 100mM pH 8. Sterilized by autoclaving.
- **Buffer 2:** Blocking Reagent 0.5% (Roche) in 100 ml of Buffer 1. Sterilized by autoclaving.
- **Buffer 3:** diethanolamine 1% (Applied Biosystems) and HCl 0.03% in 50 ml of water.
- CDP-Star™ (Roche).
- **FC:** phenol/chloroform/isoamilic alcohol 25:24:1 with 0.1% 8-hidroxiquinoline and saturated with TE.
- **Phenol-acid:** phenol:water 3.75:1 (Invitrogen).
- **MagycHyb:** Na_2HPO_4 250 mM at pH 7.2; EDTA 1 mM; SDS 20%; Blocking Reagent 0.5% (Roche) and water until 100 ml. Preserved at 4°C.
- Nylon+ membrane (Millipore).
- **NaOAc:** Sodium acetate 3 M at pH 5.2, sterilized by autoclaving.
- **10x NBC:** Boric acid 0.5 M, sodium citrate 10 mM, NaOH 50 mM, in water at pH 7.5. After the preparation of this solution, diethyl pyrocarbonate was added at 1%, mixed by inversion, incubated for 16 hours and sterilized by autoclaving.
- **Running buffer 10x:** Ficoll 15%; EDTA 0.1 M at pH 8.0; bromophenol blue 0.25%.
- **TE:** Tris-HCl 10 mM at pH 8.0 plus EDTA 1 mM. Sterilized by autoclaving.
- **TES:** TE buffer plus SDS 0.5%. Sterilized by autoclaving.
- **WB:** Na_2HPO_4 20 mM solution at pH 7.2; EDTA 1 mM; SDS 1% and water until 500 ml.

8.2. Sample collection

Cells were grown exponentially in YPD medium at 30°C until about $2x10^7$ cells·ml^{-1}. They were then collected by centrifugation at 3000 rpm for 5 min and washed with sterile water at 4°C. After washing, the cells were frozen with liquid nitrogen and conserved at -70°C.

8.3. Total RNA extraction

The following steps were done:

I. Cells were resuspended with 25 µl of TE, and 25 µl of phenol-acid were added.

II. This mixture was incubated at 60°C for 2 min, and glass beads (400-600 µm of diameter, Sigma) were added.

III. Cells were broken by vortexing at maximum speed for 7 min.

IV. 600 µl of TES buffer and 600 µl of phenol-acid were added. The mixture was homogenised by vortexing for 30 sec.

V. The mixture was incubated at 60°C for 15 min, and then it was cooled for 5 min in ice.

VI. Samples were centrifuged at 12000 rpm for 5 min, and 500 µl of the supernatant phase were collected and transferred to a new eppendorf tube, followed by addition of 500 µl of FC.

VII. The mixture was homogenised by vortexing for 30 sec, and then centrifuged for 7 min at 12000 rpm.

VIII. The supernatant was collected and transferred to a new eppendorf tube, followed by addition of 40 µl of NaOAc 3M pH 5.3 and 1 ml of ethanol 100%.

IX. To precipitate RNA, samples were incubated at -20°C for 1 to 2 hours, followed by centrifugation at 12000 rpm for 10 min at 4°C.

X. The pellet was washed with ethanol 70%, followed by centrifugation in the above conditions. The supernatant was eliminated and the pellet was dried with the Speed Vacuum system.

XI. The RNA pellet was resuspended in 50 µl of water.

XII. RNA was quantified with a spectrophotometer by measuring optical density at 260 and 280 nm wavelengths.

XIII. The RNA suspension was conserved at -20°C.

8.4. Labelling of DNA probes with Dioxigenin-dUDP (DIG-dUDP)

The synthesis and labelling of probes for mRNA detection was carried out using the product "DIG DNA Labeling Mix, 10x concentration" (Roche), following the manufacturer's instructions. As template for the synthesis of the labelled probe it was used an internal fragment of the gene of interest (between 300 and 500 bp), amplified by PCR from genomic DNA with appropriate primers for each case. The quality of the genomic DNA fragment amplified by PCR was tested by electrophoresis in a 0.8% agarose

gel. The quality of the probe was verified by the "dot-blot" technique. This technique consists of fixing 5 µl of 1:10 serial dilutions of the probe on a nylon membrane using the Stratalinker 1800 equipment (Stratagen), followed by irradiation with ultraviolet light (12000 $\mu J \cdot cm^{-2}$). Next, we proceeded to chemiluminescent detection (see section 8.8 below), by comparing the intensity of the signal given by the labelled probe with the signal of other known probes previously used. The relative signal intensity allowed determining the amount of probe to be used in subsequent hybridizations.

8.5. Formaldehyde-agarose gel electrophoresis

I. 0.8 g of agarose was boiled in 80 ml 1x of NBC buffer in a microwave oven until completely dissolved.

II. The solution was cooled down at 65°C for 5 min, then 2 ml of 37% formaldehyde were added and well mixed.

III. Next, the agarose solution was transferred into a tray under the hood, and a comb was placed and let stand for about 45 min until gel solidification. A 1x NBC solution was used as running buffer.

IV. In an eppendorf tube, 10-15 µg of RNA extract (in a 5 µl volume) were mixed with 2 µl of 10x NBC, 3 µl of formaldehide at 37% and 10 µl of formamide.

V. This mix was incubated at 65°C for 5 min and then 2 µl of 10x loading buffer and 0.5 µl of ethidium bromide solution (2 $mg \cdot ml^{-1}$) were added.

VI. Samples were loaded in the gel and ran at 100 V for about 90 min.

8.6. Transfer to Nylon+ membrane and UV crosslinking

I. A Nylon+ membrane (5 x 15 cm) was wetted in water for 5 min.

II. The membrane and the gel were assembled in the VacuBlot apparatus, and then a 50 mBar pressure was applied.

III. The gel was covered up with water for 15 min. Afterwards, water was removed.

IV. The gel was covered up with 0.1 M NaOH for 15 min, followed by solution removal. The step was repeated once.

V. The gel was covered up with 0.1 M Tris-HCl pH 7.5 for 15 min, followed by buffer removal.

VI. The chamber was flooded with water and a 50 mBar pressure was applied during 90 min for RNA transfer to the membrane.

VII. The water in the chamber was removed. Then, the membrane was removed from the VacuBlot system and placed over a filter paper wetted with water. Next, the

membrane was irradiated with UV light (12000 µJ/cm^2) in the Stratalinker 1800 equipment, in order to link the RNA to the membrane.

VIII. The positions of the rRNA bands were marked using a regular UV transilluminator.

IX. To remove formaldehyde, the membrane was washed twice with 100 ml WB for 15 min at 65°C.

8.7. Hybridization and washing steps

I. The MagicHyb solution was pre-heated at 65°C to dissolve the precipitates.

II. The washed membrane (from section 8.6) was pre-hybridized with 10 ml of MagicHyb for 1 hour at 65°C.

III. To denaturise the probe (2.5 ng·ml^{-1}), this was dissolved in 200 µl of TE and heated at 90°C for 4 min, then cooled down on ice for 5 min.

IV. The membrane was hybridized with freshly-denaturated probe in a cylindrical tube with 5 ml of MagicHyb solution for about 16 hours at 65°C.

V. To remove excess of probe, the membrane was washed three times with 100 ml of WB for 20 min at 65°C.

8.8. Chemiluminescent detection

I. The membrane was washed twice with 50 ml of Buffer 1 for 5 min.

II. Next, it was blocked in 50 ml of Buffer 2 for 60 min.

III. The Anti-DIG-AP was diluted in Buffer 2 at 1:15000 and incubated for 30 min.

IV. To wash the excess of antibody, the membrane was washed four times with 50 ml of Buffer 1 for 10 min each.

V. Next the membrane was incubated with 50 ml of Buffer 3 for 5 min, followed by an incubation during 5 min with 1 ml of Buffer 3 and CDP* diluted 1:100.

VI. In order to capture the chemiluminescency emission, the ChemiDoc™ MP Imaging System equipment (Bio-Rad) was used.

VII. The blocking and incubations steps were carried out with slow agitation (60 rpm), while the washes were made with more rapid agitation (100 rpm) on a "Shaker Unimax 1010" orbital platform (Heidolph).

9. MICROSCOPIC TECHNIQUES

- **Spontaneous and *t*-BOOH-induced foci formation**

Cells were grown at 30°C in SC liquid cultures to exponential phase (about 1.5x10^7 cells·ml^{-1}). Foci formation was observed with an OLYMPUS®BX51 microscope. These same

cells were stained with DAPI (4',6-Diamino-2-Phenylindole) as described in Silva *et al.* (2005). The fluorescence from the Yellow fluorescence protein (YFP) was detected by using 490-510 nm (excitation) and 535-565 nm (emission) wavelengths. For observation of nuclei in DAPI-stained cells an excitation filter (360-370 nm) and an emission filter (420-460 nm) was used. In the case of the *t*-BOOH treatment, this agent (at 0.5 mM) was added to the cultures 1 hour prior to observations. A minimum of 300 cells was counted per experiment, with the number of budded (S/G2-phase) and unbudded cells determined by visualization with Nomarski optics. At least three independent experiments were carried out for each strain and treatment.

10. CELL CYCLE SYNCHRONISATION AND FLOW CYTOMETRY ANALYSES

10.1. Sample collection

- 4 $\mu g \cdot ml^{-1}$ (final concentration) of α-factor mating pheromone (GenScript) were added into cultures of exponentially growing yeast cells (OD_{600}=0.3) in YPD medium at 30°C, in order to synchronize the cells at G1 phase. After 45 min, the same amount of α-factor was added again for an additional period of 45 min, before sample collection. In some experiments (as will be specifics) longer treatment times were employed.
- To remove the mating pheromone from the cultures, these were filtered and washed with YPD medium (ten-fold volume), followed by resuspension in fresh prewarmed (30°C) medium to continue the experiment as indicated in each case.
- Samples were taken at successive times for propidium iodide staining.

10.2. Propidium iodide staining

- A volume of 1 ml of sample (obtained as described in section 10.1 of Material and Methods) was added to 3 ml of ethanol.
- The mixtures were kept for 1 hour at 4°C. After this incubation time the cells were centrifuged at 2500 rpm for 5 min at room temperature and resuspended in 0.5 ml of 1x SSC (see section 11.1 of Material and Methods for composition).
- Next, 10 µl of RNase A solution (10 $mg \cdot ml^{-1}$) were added to each sample and incubated at 50°C overnight.
- 5 µl of proteinase K (Sigma) at 10 $mg \cdot ml^{-1}$ were added and incubated at 50°C for 1 hour.
- Following the above incubation, samples were sonicated for 5 sec at power 6.
- 1 ml of 1x SSC and 0.1ml of propidium iodide solution at 50 $\mu g \cdot ml^{-1}$ were added to each sample.

- Samples were kept at the dark for at least 30 min. DNA content was analyzed in a BD FACSCanto™ II flow cytometer (BD Biosciences).

11. THYMINE DIMERS DETECTION

11.1. Solutions

- **Lysis buffer (20 ml):** 1 ml of HEPES-KOH 1 M pH 7.5; 1.12 ml of NaCl 2.5 M; 40 µl of EDTA 0.5 M pH 8; 0.2 ml of Triton X-100; 200 µl of sodium deoxychlorate 0.1%; adjusted to 20 ml with Milli-Q water.
- **1 M HEPES-KOH pH 7.5 (100 ml):** 70 ml of Milli-Q water; 23.83 gr of HEPES; 0.55 gr of KOH (to adjust to pH 7.5); finally adjusted to 100 ml with additional Milli-Q water.
- **20x SSC (100 ml):** 17.53 gr of NaCl; 8.82 gr of sodium citrate; adjusted to pH 7 and to 100 ml with Milli-Q water.
- **TBST (1 L):** 10 ml of 2 M Tris-HCl pH 8; 50 ml of NaCl 2.5 M; 1 ml of Tween 20; adjusted to 1000 ml with Milli-Q water.
- **Buffer B (for one membrane):** 2.5 gr of milk powder in 50 ml of TBST.
- **Buffer I (for one membrane):** 2.5 ml of Buffer B in 50 ml of TBST.
- **Buffer 1 (500 ml):** 25 ml of 2 M Tris-HCl pH 8; 25 ml of NaCl 2.5 M; adjusted to 500 ml with Milli-Q water. Sterilized by autoclaving.
- **Buffer 2 (100 ml):** 1 gr of Blocking Reagent (Roche) in 100 ml of Buffer 1.
- **Buffer 3 (50 ml):** 0.5 ml of diethanolamine (Applied Biosystems); 40 µl of HCl at 37% to bring pH to 10; adjusted to 50 ml with Milli-Q water.

11.2. Protocol

For the detection of thymine dimers, the following steps were carried out:

- Cells were inoculated in 5 ml of SC medium with the corresponding amino acids and incubated overnight at 30°C.
- Each culture was diluted in 10 ml of SC medium and let it grow exponentially until about $2x10^7$ cells·ml^{-1}.
- Cultures were centrifuged at 35000 rpm for 5 min and then the cell pellet was resuspended in 60 ml of SC medium.
- The cell suspension was divided in 5 Petri plates with a volume of 12 ml each.
- At this point the cells were irradiated with UV at 100 J·cm^{-2} with a Stratalinker UV Crosslinker 2400 apparatus (Stratagen) and then all the cultures were mixed together for homogenization purposes.
- Samples of 10 ml were collected at 0, 45, 90 and 135 min after irradiation.

- After collection, each sample was centrifuged at 3500 rpm for 5 min and the cell pellet was kept at -80°C until processing.
- To obtain the DNA, 50 µl of lysis buffer and an equivalent volume of glass beads were added in the samples. Cells were broken by vortexing (two periods of 45 sec with force 5.5).
- 450 µl of lysis buffer were added and mixed in a vortex for 1 min.
- The samples were centrifuged at 12000 rpm for 2 min at 4°C, and 500 µl of the supernatant phase were collected and added to a new microcentrifuge tube, followed by sonication at force 6 for 10 sec.
- After centrifugation at 4°C (15 min at 12000 rpm) 450 µl of supernatant were transferred to a new tube and incubated with 5 µl of proteinase K (10 $mg \cdot ml^{-1}$) at 37°C for 1 hour, followed by the addition of 3 µl of RNase (10 $mg \cdot ml^{-1}$).
- For DNA extraction, 500 µl of phenol-chloroform were added, mixed in a vortex for 1 min and centrifuged at 12000 rpm for 7 min at room temperature.
- The resulting supernatant was transferred to a new microcentrifuge tube, and 40 µl of 3M NaOAc (pH 8) and 1ml of ethanol 100% were added to precipitate DNA.
- The samples were centrifuged at 12000 rpm for 10 min at 4°C.
- The supernatant was removed, and the pellet was washed with ethanol 70% and recovered again by centrifugation at 12000 rpm for 10 min at 4°C.
- The pellet was dried in the Speed Vacuum apparatus and resuspended in 100 µl of water. DNA concentration was determined in a Nanodrop apparatus.
- For DNA denaturation, an equal volume (100 µl) of a solution of 0.8 M NaOH and 20 mM EDTA was added. The samples were boiled for 10 min and DNA was neutralized by adding 200 µl of cold 2M ammonium acetate.
- Meantime, a Hybond N+ membrane (GE Healthcare) was wetted in 6x SSC buffer and the Bio-DotR SF Apparatus (Bio Rad) was washed with water and let it dry. Three filter papers were also wetted.
- Next, the Hybond N+ membrane and the papers were assembled in the Bio-DotR SF Apparatus and were rehydrated with 500 µl of TE. Then, the samples were transferred to the membrane following the manufacturer's instructions. At the end of this process, 500 µl of 2x SSC were added.
- Then, the membrane was removed, wetted with 2x SSC and let it dry. Next, it was placed in an oven at 80°C during 1 hour for DNA fixation.

- Following, a Western blot protocol for immunodetection of DNA thymine dimers was carried out:
  - The membrane was blocked in 40 ml of Buffer B for 1 hour at room temperature.
  - The membrane was then washed with 70 ml of TBST for 15 min and twice for 5 min periods.
  - Hybridization was carried out with 2 µl of primary mouse monoclonal Anti-Thymine Dimer antibody ab10347 (1 $\mu g \cdot ml^{-1}$) (Abcam) in 4 ml of Buffer I, overnight at room temperature.
  - The membrane was washed with 70 ml of TBST for 15 min once, again for 5 min and finally for 10 min with 25 ml of Buffer I.
  - Next, the membrane was incubated with the secondary antibody, which consisted of peroxidase-conjugated anti-mouse IgG (Sigma) (1:12500 dilution), in 25 ml of Buffer I for 30 min.
  - The membrane was washed with 70 ml of TBST for 15 min once, again for 10 min and three times for 5 min.
  - Next, the membrane was incubated with 1 ml of Super Signal West Pico Subtrate™ (Pierce) for 5 min.
  - Chemiluminescent detection was made with the ChemiDoc™ MP Imaging System equipment.
  - After detection of thymine dimers, the same membrane was employed to detect total DNA per sample, as follows:
  - The membrane was washed twice for 10 min at 65°C with 100 ml of 0.1x SSC plus 0.1% SDS solution. Then, it was prehybridized with 10 ml of MagicHyb solution (see section 8.1 of Material and Methods for composition) for 1 hour at 65°C.
  - Next, the membrane was hybridized with freshly denatured DIG-labelled DNA probe (1 µl in 5 ml of MagicHyb solution) for about 16 hours at 65°C.
  - The membrane was washed four times for 15 min at 65°C with 100 ml of 0.1x SSC plus 0.1% SDS solution.
  - For immunodetection the membrane was washed in 50 ml of Buffer 1 for 5 min and blocked in 50 ml of Buffer 2 for 30 min.
  - Next, the membrane was incubated for 30 min in 50 ml of Buffer 2 containing 2 µl of Anti-DIG-AP (1:10000) (see section 8.1 of Material and Methods for composition).

- The membrane was washed four times with 100 ml of Buffer 1 for 10 min.
- Next, it was incubated in 50 ml of Buffer 3 for 5 min and then for the adequate time in 2 ml of Buffer 3 containing 20 µl of CDP* substrate.
- In order to capture the chemiluminescence emission, the ChemiDoc™ MP Imaging System equipment was used.
- The blocking and incubations steps were carried out with slow agitation (60 rpm), while the washes were made with more rapid agitation (100 rpm) on a "Shaker Unimax 1010" orbital platform.
- The resulting image was quantified using the "ImageJ" program. The results were rationalized according to a unit value allocated to the reference, which is specified in each case. Five replicates were done for each sample, and the average signal was calculated.

12. DETERMINATION OF INTRACELLULAR IRON CONTENT

The protocol described by Tamarit *et al.* (2006) was employed, as follows:

- Samples containing a total of $2.5x10^7$ *S. cerevisiae* cells from exponential cultures in YPD medium at 30°C were collected and washed with iced Milli-Q water.
- Cell samples were digested in 285 µl of Milli-Q water and 214 µl of nitric acid at 7%. The mixture was homogenized by vortexing and incubated at 95-100°C at least 16 hours, followed by centrifugation at 10000 rpm for 5 min.
- Microcentrifuge tubes were prepared containing 300 µl of Milli-Q water, 160 µl of sodium ascorbate (38 $mg \cdot ml^{-1}$) and 126 µl of ammonium acetate (from a 1 ml solution of ammonium acetate saturated with 2 ml of water). As control, the following mixture was prepared: 528 µl of Milli-Q water, 172 µl of nitric acid, 160 µl of sodium ascorbate and 126 µl of ammonium acetate.
- To each of the problem mixtures 400 µl of the digested cell samples were added.
- For both the problem and control tubes, optical density at 425 nm was measured in a Shimadzu UV-2401 PC spectrophotometer. This measure value serves as control to normalize the number of cells of each sample.
- Optical density was then recorded at 535 nm after adding 16 µl of bathophenanthrolinedisulfonic acid (BPS) (34 $mg \cdot ml^{-1}$) to the same spectrophotometer cuvette. To eliminate the contribution of contaminant iron, absorbance was recorded against blanks containing all the reagents used, including BPS.
- The data obtained with the spectrophotometer were used to calculate the relative levels of intracellular iron, as described in Tamarit *et al.* (2006). A minimum of

three measurements from independent experiments was done for each biological condition.

PART IV

RESULTS

1. THE ABSENCE OF THE MITOCHONDRIAL PROTEIN Grx5 LEADS TO INCREASED GENETIC INSTABILITY

Cells lacking the mitochondrial chaperone Zim17 display increased recombination and mutation frequencies (Díaz de la Loza *et al.,* 2011). Based on the fact that Zim17 is functionally related to the Ssq1 chaperone, we asked if the same phenotype was observed in cells depleted of Grx5. To determine the recombination rate of the respective yeast strains, an intra-chromosomal *leu2-k::ADE2-URA3::leu2-k* recombination system was used (Fig. 20). When recombination occurs between the two flanking *leu2-k* repeats, it results consequently into the loss of the *ADE2* and *URA3* markers. Recombinants are selected by plating cells onto SC medium plates containing 5-FOA. This compound is toxic for all the cells containing the *URA3* marker (uracil prototrophs) and therefore selects positively for *ura3* mutants. As controls, mutants that do not express other mitochondrial proteins with different roles were also employed. Those proteins are: Yfh1 (more commonly known as frataxin, which supposedly participates as iron donor in the ISC assembly), Aif1 (which participates in the apoptotic response) and Cox12 (subunit of the cytochrome c oxidase complex).

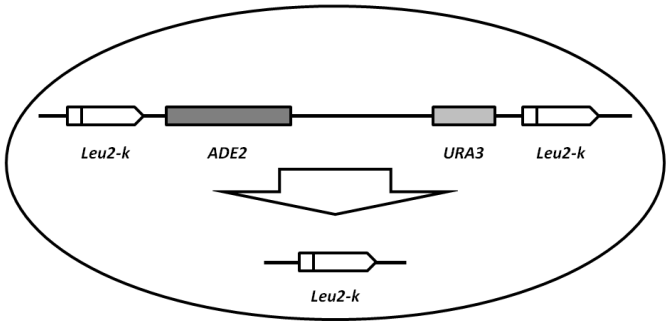

Fig. 20. Schematic representation of the *leu2-k::URA3-ADE2::leu-2K* chromosomal recombination system (Prado & Aguilera, 1995).

As it can be observed in Fig. 21, wild type cells show a low number of resistant cells in the presence of 5-FOA, which is indicative of the low spontaneous recombination

rate occurring in wild type cells. In contrast, *Δgrx5* mutant cells display a recombination rate that compared with wild type cells is approximately 17-fold higher. Concerning to the other mitochondrial mutants, they show a recombination rate slightly higher than wild type cells but in any case much lower that *Δgrx5* mutant cells.

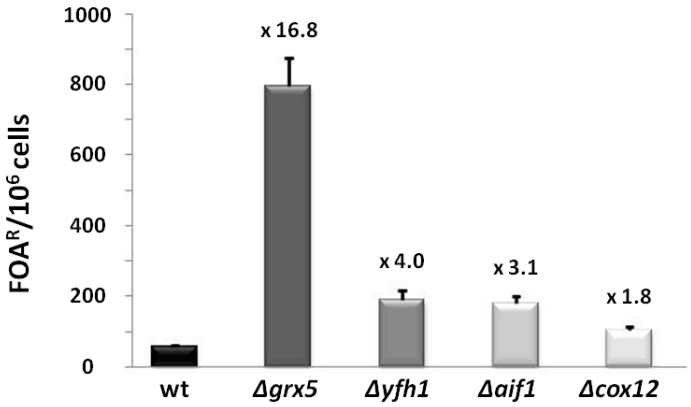

Fig. 21. *Δgrx5* mutant cells display increased recombination rate. Recombination frequencies in wild type (MML1349), *Δgrx5* (MML1344), *Δyfh1* (MML1346), *Δaif1* (MML1354) and *Δcox12* (MML1352) cells are shown, using the system described in Fig. 20. Recombinants were selected by plating cells onto 5-FOA-containing SC medium. Means and SD of a minimum of eight different independent experiments are shown.

A second parameter employed for checking the stability of the DNA was the spontaneous mutation rate in both, wild type and *Δgrx5* mutant cells. To study the mutation rates of both strains the resistance to L-canavanine was analyzed. With this objective, wild type and *Δgrx5* cells were incubated in SC plates without Arg plus L-canavanine as described in section 7.2 of Material and Methods. L-canavanine is a toxic analogue of the amino acid arginine and spontaneous resistance to L-canavanine appears because of mutations at the *CAN1* locus coding for the arginine permease. As observed in Fig. 22, *Δgrx5* mutant cells display an increase of 5.6-fold in canavanine-resistant cells in exponential cultures compared to wild type cells.

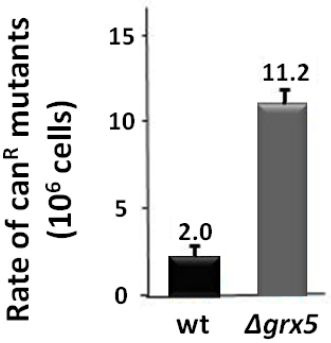

Fig. 22. *Δgrx5* mutant cells display high spontaneous mutation frequency. Spontaneous mutation frequencies in wild type (MML1349) and *Δgrx5* (MML1344) cells were analyzed by determining the frequency of L-canavanine-resistant cells in exponential cultures. Means and SD of a minimum of eight independent experiments are shown.

These results showing the high recombination and spontaneous mutation rates in *Δgrx5* mutant cells point to the fact that the lack of Grx5 function causes increased genetic instability compared to wild type cells.

2. THE HIGH RECOMBINATION AND SPONTANEOUS MUTATION RATES IN THE *Δgrx5* MUTANT CELLS ARE NOT PROVOKED BY IRON OVERLOADING

Intracellular iron accumulation is one of the phenotypes observed in *Δgrx5* mutant cells (section 2.5.1 of the Introduction). For this reason we asked if the genetic instability observed in the mutant was due to an effect of iron overloading, since an elevated amount of iron in the cell is related with an increase in the amount of ROS production through the Fenton reaction, and consequently these ROS could affect the structure and stability of the DNA.

In order to answer this question we first constructed *Δgrx5* mutant derivatives that do not accumulate iron, such as the *Δgrx5Δaft1* double mutant, as demonstrated in Fig. 23A. Aft1 is the major transcription factor involved in the high-affinity iron uptake process (Kaplan & Kaplan, 2009), so the entry of iron through the high-affinity system would be compromised in its absence. Nevertheless, synthetic lethal screens to identify mutants that cannot tolerate the deletion of *AFT1* showed that the Aft1 protein may affect numerous processes such as cell-cycle progression and chromosome stability, being this last one independent of iron homeostasis (Berthelet *et al*., 2010). In contrast, no interaction was found with another protein that also participates in the high-affinity iron uptake process, the multicopper ferroxidase Fet3 (Berthelet *et al*., 2010). For this reason the *Δgrx5Δfet3* double mutant was constructed. Our analysis showed that the *Δgrx5Δfet3*

double mutant does not accumulate iron at all (Fig. 23A), and therefore it was employed in subsequent experiments.

Next, a cell viability study was performed by comparing wild type, *Δgrx5* and *Δgrx5Δfet3* cells after being UV-irradiated for 30 sec. We also employed *Δfet3* cells as a control. As can be observed in Fig. 23B, only 30% of *Δgrx5* mutant cells kept alive after the UV irradiation relative to wild type cells. In the case of *Δfet3* mutant cells 87% of them remained viable, while in the case of *Δgrx5Δfet3* double mutant only 50% were rescued from the damage provoked by UV when compared with the wild type cells. These results demonstrated that the phenotypes concerning the genomic instability (and consequent sensitivity to DNA-damaging agents) observed previously were not dependent on the overloading of iron in the *Δgrx5* mutant.

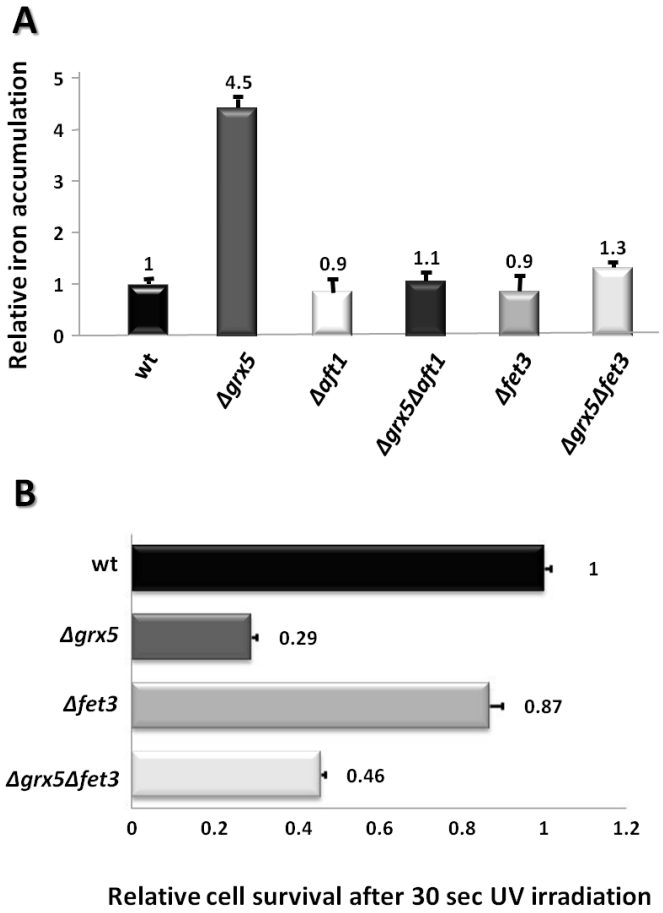

Fig. 23. The reduced survival of *Δgrx5* mutant cells upon UV radiation is independent of their iron content. A) Total cell iron content in exponentially growing cultures of the follow strains: wild type (W303-1A), *Δgrx5* (MML100), *Δaft1* (MML1356), *Δgrx5Δaft1* (MML345), *Δfet3* (MML1107) and *Δgrx5Δfet3* (MML1478). Values are made relative to wild type cells, which are given the unit value. B) Cell viability after 30 seconds of UV radiation in wild type (W303-1A), *Δgrx5* (MML100), *Δfet3* (MML1107) and *Δgrx5Δfet3* (MML1478) strains, relative to wild type cells (unit value). Means and SD of five different experiments are shown in both parts of the Figure.

3. FORMATION OF Rad52-ASSOCIATED FOCI IS INCREASED IN *Δgrx5* MUTANT CELLS

Based on the fact that cells depleted of *GRX5* have an increased genomic instability and that instability can promote, among other situations, an elevated damage in the DNA, we wanted to study if DNA was constitutively altered when Grx5 was absent. For this objective we used a construction version where the Rad52 protein was fused to YFP. Rad52 participates in the DSB repair pathway by binding to the free 3'-ends of the damaged ssDNA (as mentioned in section 4.3.3 of the Introduction) as well as in other spontaneous DNA lesions such as nicks and single-stranded gaps (Lisby *et al.,* 2001). This interaction between Rad52 and ssDNA results in formation of Rad52-containing foci. In that way, the Rad52-YFP protein became a good marker for visualizing foci formation by fluorescence microscopy, in order to report zones in the nucleus where ssDNA is accumulated and/or DSB are generated. When Rad52-YFP foci were visualized in wild type and *Δgrx5* cells, the latter ones apparently displayed higher number of them (Fig. 24).

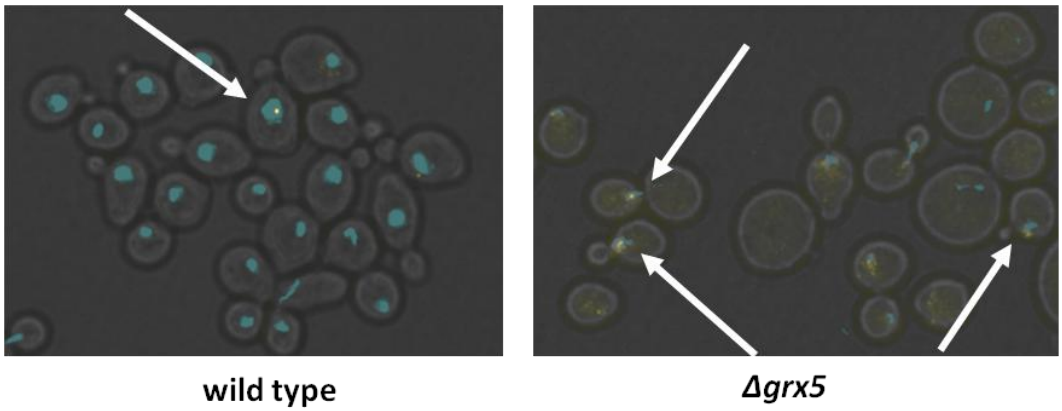

Fig. 24. Visualization of Rad52-YFP foci in wild type (MML1493) and *Δgrx5* (MML1495) mutant cells during exponential growth. DAPI was used for nuclear staining. Arrows indicate the foci localization.

The quantification of foci formation shows an increase of 5.2-fold in *Δgrx5* mutant cells with respect to wild type cells (Fig. 25). This increase in foci formation was only observed in budded cells, that is, in cells at the S/G2/M stages of the cell cycle where DNA synthesis was occurring or had been completed. Upon an oxidative stress condition, generated by addition of *t*-BOOH, *Δgrx5* mutant budded cells again presented an increase of 2.3-fold compared to the wild type (Fig. 25). Interestingly, upon oxidant treatment unbudded cells displayed foci formation, probably resulting from DNA damage generated by the oxidant. In this case, the number of foci was still about 50% higher in the mutant (Fig. 25).

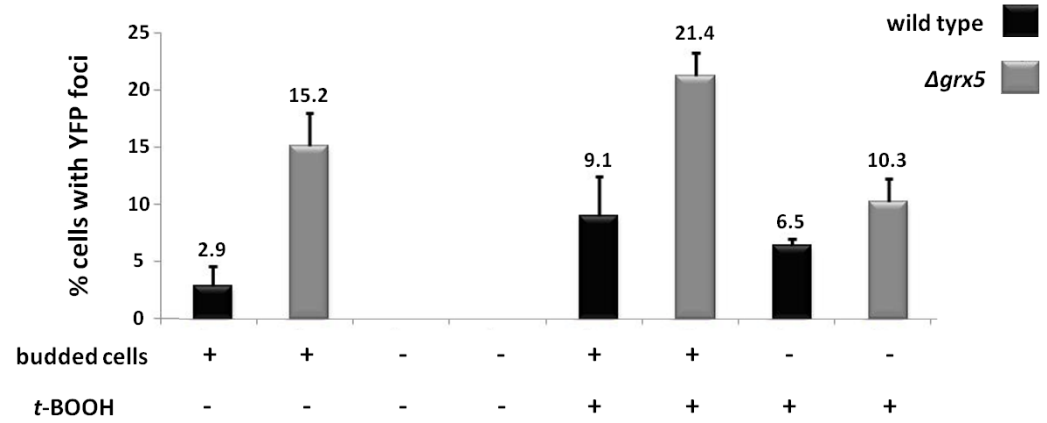

Fig. 25. Rad52-associated foci formation is increased in *Δgrx5* mutant cells. Quantification of Rad52-YFP foci formation in wild type (MML1493) and *Δgrx5* (MML1495) cells growing exponentially, treated (+) or not (-) with *t*-BOOH (0.3 mM) for 1 hour. The percentage of cells with one or more foci is indicated. Bars show the means and SD of three independent experiments.

In addition, foci formation was also determined by using another reporter protein involved in the HR repair system, Rfa1, which is a subunit of the heterotrimeric RPA that also binds the free 3'-ends of the damaged ssDNA. RPA acts previously in the DSB repair pathway, and then is replaced in the interaction with DNA by members of the Rad52 epistatic group. By using the Rfa1-YFP construction as a marker, we observed that foci were present in both, wt and *Δgrx5* cells (Fig. 26). In this case, in contrast to the results observed in Rad52-YFP marked cells, no significant differences were observed in the number of foci between wild type and *Δgrx5* cells for all the studied conditions (budded or unbudded cells, and with or without *t*-BOOH treatment).

The same experiment was also performed using other reporter proteins involved in the DNA damage repair system, Mre11, Ddc1 and Rad53, but no conclusive results were obtained (data not shown).

Taken together, these results suggest that first, cells lacking Grx5 have higher levels of constitutive DNA damage, and second, this DNA damage (compared to wild type cells) is specifically associated to Rad52, but not to Rfa1, binding to the lesions.

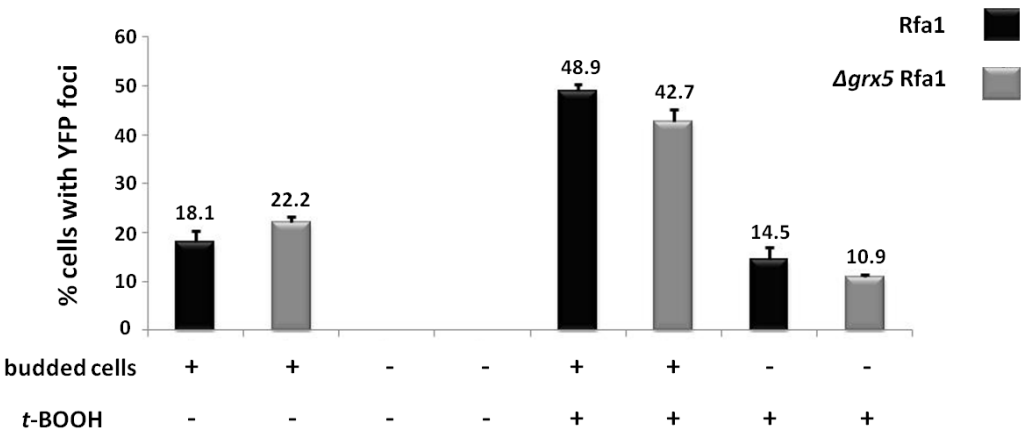

Fig. 26. Rfa1-associated foci formation is not increased in *Δgrx5* mutant cells. Quantification of Rfa1-YFP foci formation in wild type (MML1556) and *Δgrx5* (MML1559) cells growing exponentially, treated (+) or not (-) with *t*-BOOH (0.3 mM) for 1 hour. The percentage of cells with one or more foci is indicated. Bars show the means and SD of three independent experiments.

4. *Δgrx5* MUTANT CELLS ARE HYPERSENSITIVE TO DNA-DAMAGING AGENTS

Genomic instability affects DNA integrity and cell viability (section 4.2 of the Introduction). As demonstrated above, cells lacking *GRX5* show an increase in the genome instability as measured by different parameters. Therefore, we wanted to know if this constitutive instability could affect the viability of *Δgrx5* mutant cells after additional treatment with different DNA-damaging agents. Thus, we made sensitivity studies in wild type and *Δgrx5* mutant cells in YPD plates containing DNA-damaging agents, such as MMS (which alkylates DNA leading to ss/ds DNA breaks) and HU (which interferes with the activity of the RNR complex consequently inducing a decrease in the dNTPs levels and causing, therefore, DNA replication stress). Sensitivity studies to UV, which induces CPD formation (a target of the NER pathway), was also determined. As shown in Fig. 27, *Δgrx5* mutant cells are more sensitive than the wild type ones to both MMS and HU, as well as to UV irradiation. This latter experiment confirmed the hypersensitivity of *Δgrx5* cells to UV that had already been observed in liquid cell suspensions (Fig. 23B).

One of the many phenotypes observed in *Δgrx5* mutant cells is the increased protein oxidation (Rodríguez-Manzaneque *et al*., 1999). To verify if the hypersensitivity phenotype observed in *Δgrx5* cells upon treatment with the DNA damaging agents was or not associated to the constitutive oxidative environment in the mutant cells, we performed similar DNA damage sensitivity studies but now adding the anti-oxidant NAC to the YPD plates. NAC is a thiol-containing compound that interacts in a non-enzymatic way and detoxifies reactive electrophiles and free radicals (Kerksick & Willoughby, 2005).

As shown in Fig. 27, the addition of NAC did not rescue the sensitivity phenotypes provoked by the genotoxic agents, discarding the effect of *Δgrx5* endogenous oxidation as the main cause of the hypersensitivity. In addition, we used treatment with the *t*-BOOH peroxide compound as a control of the NAC ability to protect cells against oxidative stress. In this case, as expected, NAC partially rescued the hypersensitivity phenotype of *Δgrx5* cells to *t*-BOOH (Fig. 27).

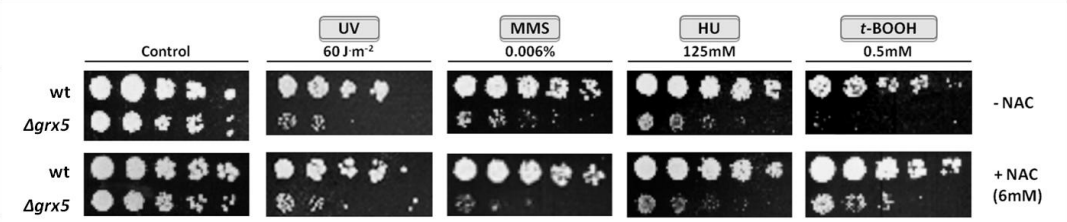

Fig. 27. *Δgrx5* mutant cells display hypersensitivity to DNA-damaging agents. Sensitivity studies to DNA-damaging agents (UV, HU, and MMS) in wild type (W303-1A) and *Δgrx5* (MML100) cells by serial dilutions of exponentially growing cultures in YPD plates containing the respective agents, or after irradiation with UV, with or without NAC. Sensitivity to *t*-BOOH is shown as a control.

We further wanted to confirm whether the hypersensitivity phenotype of *Δgrx5* cells could be extended to other mutants involved in the ISC biosynthetic machinery. Thus, we quantified the sensitivity of wild type, *Δyfh1*, *Δgrx5* and *Δssq1* cells to UV light by irradiating cells from exponential cultures after resuspending them in liquid, and measuring viability loss upon several irradiation periods. The absence of Ssq1 caused similar UV hypersensitivity phenotype as the absence of Grx5 (Fig. 28). Instead, the absence of Yfh1 did not lead to a different sensitivity phenotype compared to wild type cells, what seems surprising due of the primary role attributed to Yfh1 in ISC biogenesis. That *Δyfh1* cells are not significantly hypersensitive to UV radiation was also corroborated by cell irradiation on YPD plates (Fig. 29).

It has been described that the W303 background has a mutation in the *RAD5* gene, which produces a change of a glycine residue for arginine in the protein product that gives a weak DNA repair phenotype leading to a more sensitive phenotype when cells are treated with genotoxic agents (Fan *et al*., 1996). This mutation in *RAD5* and the consequent phenotype could interfere with our above results, obtained in W303 background strains.

To overcome this situation we changed the W303 genetic background by the FY1679 wild type strain one (CML235), where this mutation in *RAD5* is absent. Therefore, all subsequent experiments were done in this new background. As a general fact we observed that wild type and mutant cells were more resistant to the effects of the

genotoxic agents employed, so it was needed to increase the intensity for UV radiation, as well as the concentration of MMS and HU employed to observe sensitivity effects. Taking this into consideration, the *Δgrx5* mutant derived from the CML235 wild type strain was still significantly hypersensitive to UV and MMS and moderately hypersensitive to HU (Fig. 30). The hypersensitivity to these genotoxic agents was also not rescued by NAC addition to plates, confirming that it could not be explained by the highly oxidative intracellular environment of *Δgrx5* cells.

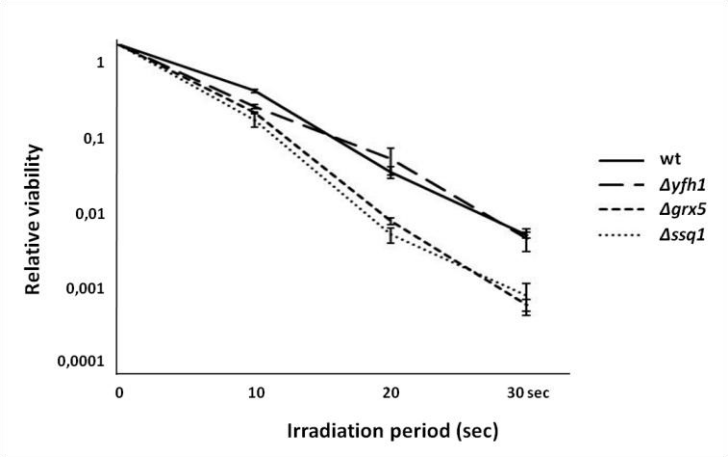

Fig. 28. *Δgrx5* and *Δssq1* mutant cells display hypersensitivity to DNA damage by UV radiation. Cell viability kinetics after 0, 10, 20 and 30 sec of UV irradiation were determined in liquid suspensions of wild type (W303-1A), *Δyfh1* (MML298), *Δgrx5* (MML100) and *Δssq1* (MML997) cells from exponentially growing cultures. Values are made relative to the viability (colony-forming units) in non-irradiated cell suspensions. The means and SD of three independent experiments is represented.

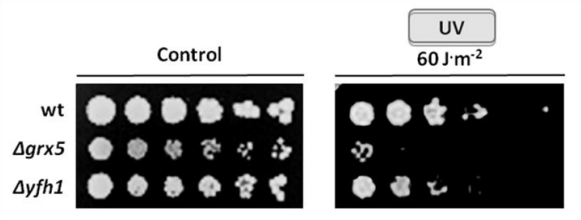

Fig. 29. Sensitivity of *Δyfh1* mutant cells to UV irradiation. Serial dilutions of wild type (W303-1A), *Δgrx5* (MML100) and *Δyfh1* (MML298) cells on YPD plates were irradiated with the indicated doses of UV.

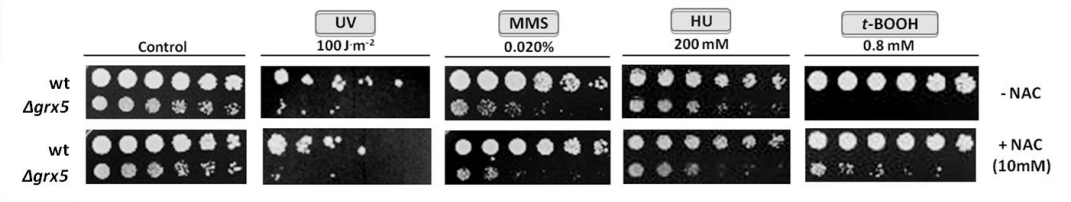

Fig. 30. *Δgrx5* mutant cells display hypersensitivity to DNA-damaging agents in different genetic backgrounds. Sensitivity studies to DNA-damaging agents (UV, HU, and MMS) in wild type (CML235) and *Δgrx5* (MML1500) cells by serial dilutions of exponentially growing cultures in YPD

onto plates containing the respective agents, or after irradiation with UV, with or without NAC. Sensitivity to *t*-BOOH is shown as a control.

It is known that oxygen environment generates ROS and these ROS at high levels conditions become toxic for the viability of the cells. We next performed a MMS sensitivity study in anaerobic conditions, where inoculated plates were placed in an anaerobic chamber. As shown in Fig. 31, *Δgrx5* mutant cells maintained the same hypersensitivity phenotype to MMS treatment, definitively confirming that this phenotype was independent of oxidant conditions.

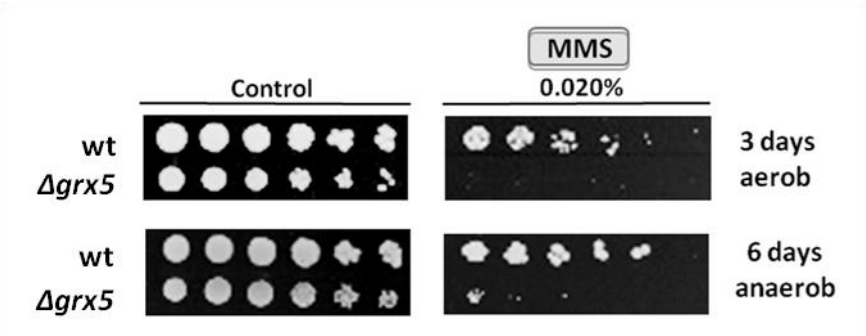

Fig. 31. *Δgrx5* mutant cells display hypersensitivity to MMS in anaerobic conditions. Inoculated YPD plates containing MMS were incubated in anaerobic conditions at 30°C during 6 days, or in aerobic conditions for 3 days as control.

5. A *GRX5* CONDITIONAL EXPRESSION MUTANT DISPLAYS THE SAME HYPERSENSITIVITY AS *Δgrx5* MUTANT CELLS TO MMS

Yeast cells with an impairment in the mtDNA are genetically unstable (Veatch *et al.,* 2009). Grx5 is a mitochondrial protein and the defects in mitochondrial metabolism occurring in its absence could cause deleterious effects in the stability of nDNA. To verify that the hypersensitivity phenotype displayed by *Δgrx5* mutant cells against DNA-damaging agents was directly provoked by the absence of Grx5 function and not due to some secondary effects or mutations, sensitivity studies to MMS were done using a *tetO$_7$-GRX5* conditional mutant. This construction results in *GRX5* regulatable expression by the addition of doxycicline to the media. In that way, in the absence of the antibiotic the transcription of *GRX5* occurs normally under control of the *tetO$_7$* promoter. When doxycicline is added, however, the expression of the gene is repressed so that Grx5 protein is progressively depleted (Rodriguez-Manzaneque *et al*. 2002). To perform the sensitivity studies, cells containing the *tetO$_7$-GRX5* construction were grown exponentially and half of the culture was treated with doxycicline whereas the other half was allowed to grow without the antibiotic. After 12 hours in these conditions both cultures were divided into two aliquots, one was treated with MMS (0.2%) for 1h whereas the other one

rested untreated. Sensitivity was determined by plating serially-diluted samples of the treated and non-treated cells from both conditions on YPD plates. In conditions were *GRX5* was expressed moderate sensitivity to MMS was observed (Fig. 32, upper part). Identical phenotype was observed when NAC was added into the YPD plates or when MMS-treated cells were grown in anaerobic conditions (Fig. 32, upper part). However, after 12 h of doxycycline treatment (that is, when no Grx5 protein was present), *tetO$_7$-GRX5* conditional mutant cells showed hypersensitivity when treated with MMS for 1 h. Similar phenotype was observed when NAC was added, and also in anaerobic conditions, as shown in the bottom part of Fig. 32.

These results show that the strain carrying the *tetO$_7$-GRX5* conditional expression system displays identical MMS-hypersensitivity phenotype as the *Δgrx5* mutant cells, and therefore indicate that the lack of Grx5 function is the primary cause of the MMS hypersensitivity.

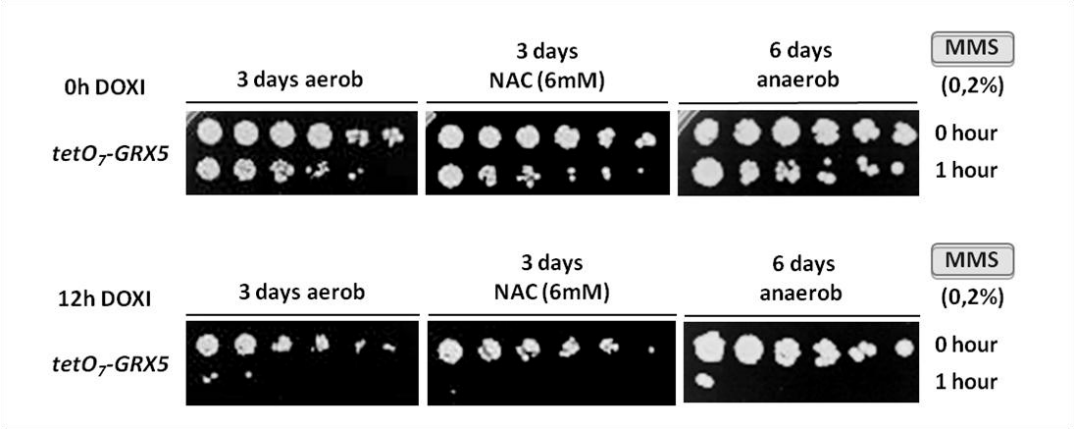

Fig. 32. A *tetO$_7$-GRX5* conditional mutant displays hypersensitivity to MMS. Sensitivity studies to MMS were carried out by using the *tet-GRX5* conditional mutant (MML1616). After 12 hours of doxycycline addition cell cultures were treated as indicated. See the text for additional experimental details.

6. *Δgrx5Δssq1* MUTANT CELLS SHOW AN ADDITIVE EFFECT OF HYPERSENSITIVITY TO DNA-DAMAGING AGENTS COMPARED TO THE SINGLE MUTANTS

Grx5 and Ssq1 participate in the same step of the mitochondrial ISC biogenesis pathway (section 3.3.3 of the Introduction), although both proteins have different roles in this pathway. The Ssq1 chaperone binds the scaffold protein Isu1 where ISCs are coupled, while Grx5 receives these clusters from the Isu1 complex and transfer them to the respective apoproteins. Based on the fact that *Δgrx5* mutant cells are hypersensitive to DNA-damaging agents (UV, HU and MMS) and that both proteins Grx5 and Ssq1 participate in the late steps of mitochondrial ISC synthesis, next we analyzed the

sensitivity of *Δssq1* mutant cells to DNA-damaging agents, in order to verify if the same hypersensitivity phenotype found in cells depleted of *GRX5* was observed in the absence of *SSQ1*. In fact, *Δssq1* mutant cells displayed slightly lower hypersensitive than *Δgrx5* mutant cells for all genotoxic agents studied (Fig. 33). On the other hand, the double mutant shows an additive hypersensitivity to all three DNA-damaging agents, compared to the single mutants. These results suggest overlapping roles for these two proteins in relation to cell survival in the presence of DNA-damaging agents.

Grx5-less cells are hypersensitive to oxidative damage (Rodríguez-Manzaneque *et al*., 1999). Therefore, we wanted to verify if the additive hypersensitivity phenotype presented by *Δgrx5Δssq1* double mutant cells in the presence of DNA-damaging agents still occurs in the presence of external oxidants. With this objective, we employed the hydrophilic oxidant *t*-BOOH and the sulfhydryl-oxidizing agent diamide on the wild type, *Δgrx5*, *Δssq1* single and *Δgrx5Δssq1* double mutant cells. As expected, *Δgrx5* and *Δssq1* mutant cells presented similar sensitivity phenotype to both oxidants (Fig. 34). Surprisingly, no additivity was observed in the double mutant, and even a moderate rescue phenotype was observed in the case of *t*-BOOH compared to the single mutants (Fig. 34A).

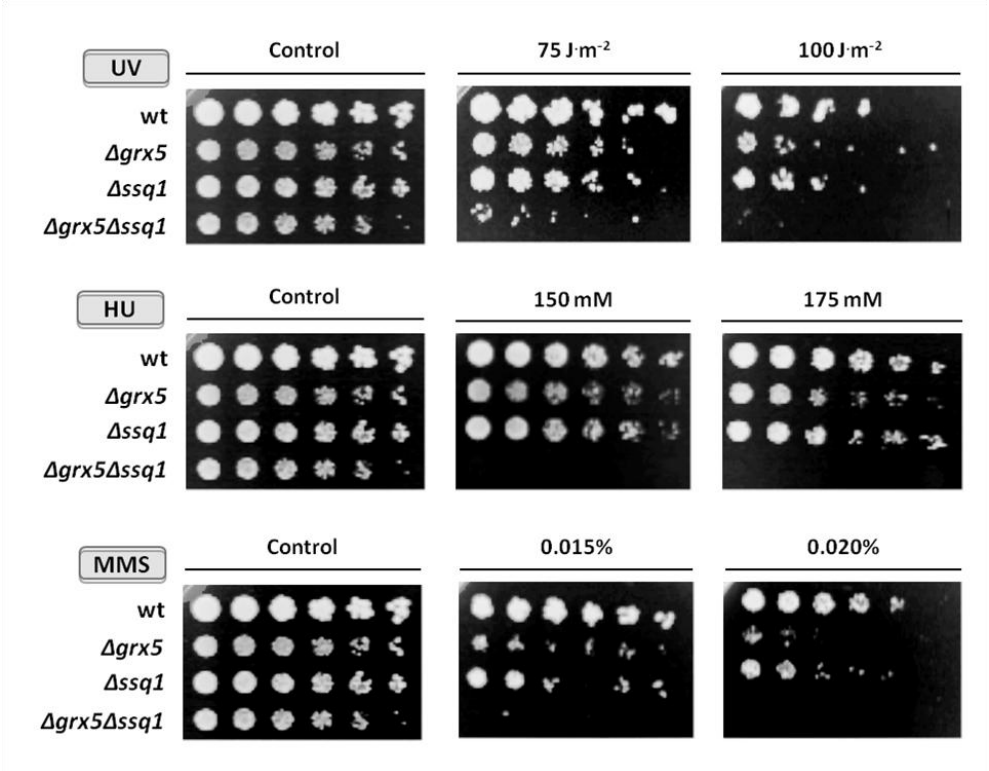

Fig. 33. *Δgrx5Δssq1* mutant cells show additive hypersensitivity to DNA damage by UV radiation, HU and MMS compared to single mutants. Sensitivity studies to DNA-damaging agents were done with wild type (CML235), *Δgrx5* (MML1500), *Δssq1* (MML1677) single mutants and *Δgrx5Δssq1*

(MML1681) double mutant cells by serial dilutions of exponentially growing cultures onto YPD plates containing the indicated agents or after UV irradiation. Plates were incubated at 30°C during 3 days.

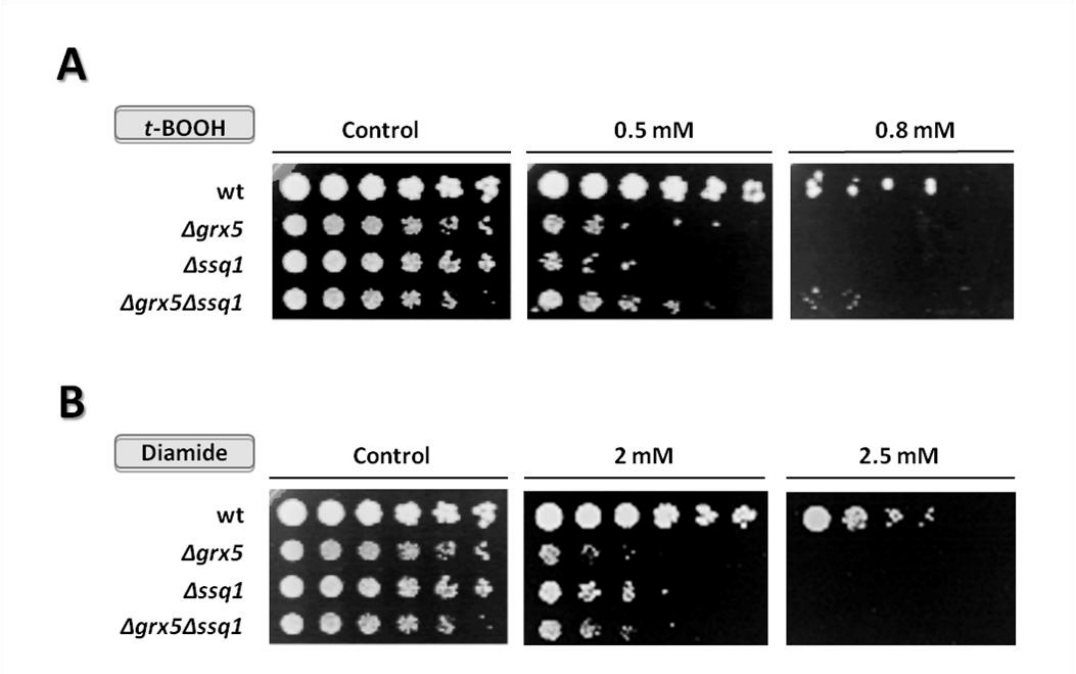

Fig. 34. *Δgrx5Δssq1* mutant cells display a hypersensitivity phenotype in the presence of diverse oxidants. Sensitivity studies to the oxidants *t*-BOOH (A) and diamide (B) were done in wild type (CML235), *Δgrx5* (MML1500), *Δssq1* (MML1677) single mutants and *Δgrx5Δssq1* (MML1681) double mutant cells by serial dilutions of exponentially growing cultures onto plates containing the indicated agents. Plates were incubated at 30°C during 3 days.

7. OVEREXPRESSION OF *SSQ1* RESCUES THE SENSITIVITY PHENOTYPE PRESENTED OF THE *Δgrx5* MUTANT AGAINST GENOTOXICS AGENTS

Years ago, our group showed in a work done by Rodríguez-Manzaneque *et al*. (2002) that the overexpression of the mitochondrial gene, *SSQ1*, suppresses the defects presented by cells lacking Grx5 as are the intracellular high iron content, the hypersensitivity to oxidant agents and the inability to grow in SD medium. To go further we studied the ability of rescuing the hypersensitivity to genotoxic agents (HU and UV) of the *Δgrx5* mutant carrying a multicopy plasmid containing *SSQ1*.

As observed in Fig. 35, the overexpression of *SSQ1* rescues the sensitivity defects of *Δgrx5* mutant cells against DNA damaging agents.

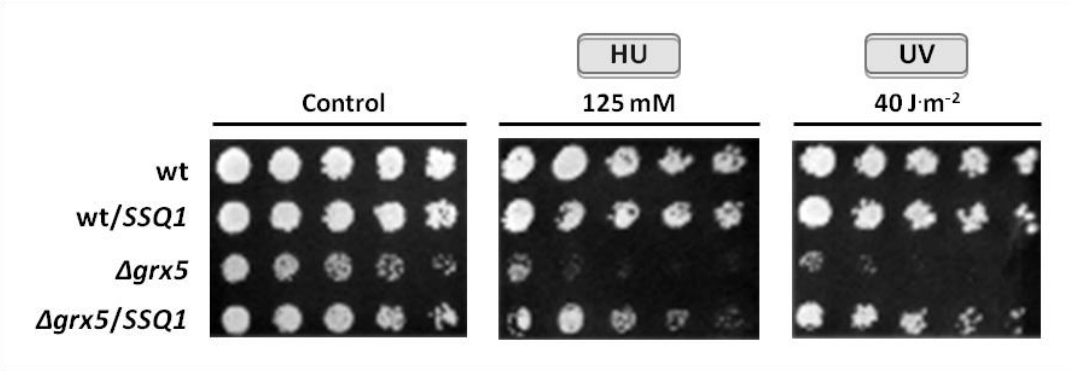

Fig. 35. Overexpression of *SSQ1* rescues the sensitivity defects of *Δgrx5* mutant cells. Sensitivity studies to DNA-damaging agents were done in wild type (W303-1A), wt/*SSQ1* (W303-1A/pMM70), *Δgrx5* (MML1448), *Δgrx5/SSQ1* (MML1448/pMM70) cells by serial dilutions of exponentially growing cultures onto YPD plates containing the indicated agent or after UV irradiation. Plates were incubated at 30°C during 3 days.

8. THE ABSENCE OF Grx5 AND Ssq1 PROTEINS CAUSES A DELAY IN THE CELL CYCLE S-PHASE PROGRESSION

In a DNA damage condition, cells activate a set of physiological responses to facilitate DNA repair processes. One of these responses is the cell cycle arrest in G1, S or G2 phases, which allows DNA replication to slow down and then to increase transcription of genes encoding for proteins that participate in DNA repair. Cell-cycle progression can be measured by flow cytometry, using the Flourescence-Activated Cell Sorting or FACS analysis. The genomic instability of Grx5-deficient cells and the hypersensitivity to DNA-damaging agents of both Grx5- and Ssq1-deficient cells could indicate that defects in the ISC machinery could affect somehow the cell cycle progression in a constitutive way and also upon treatment with DNA-damaging agents. Therefore, we made FACS analyses in wild type, *Δgrx5* and *Δssq1* mutant cells growing in YPD medium before and after treatment with a sublethal concentration of HU (Fig. 36). Thus, exponentially growing cells were arrested in G1 phase with α-factor pheromone. After releasing the cells from this arrest by filtration, cells were divided into two aliquots. In the first one, cells were allowed to grow in YPD medium (normal control condition), while in the second one they were grown in the presence of HU (stress condition), an inhibitor of RNR that cause replication forks to stall because of the depletion of dNTPs. Then, samples were taken every 20 min to follow the cell-cycle progression through FACS analysis (see section 10.2 of Material and Methods for further information). Samples were also collected from exponential cultures and at the final stage of the α-factor blockage to verify the correct arrest by the pheromone.

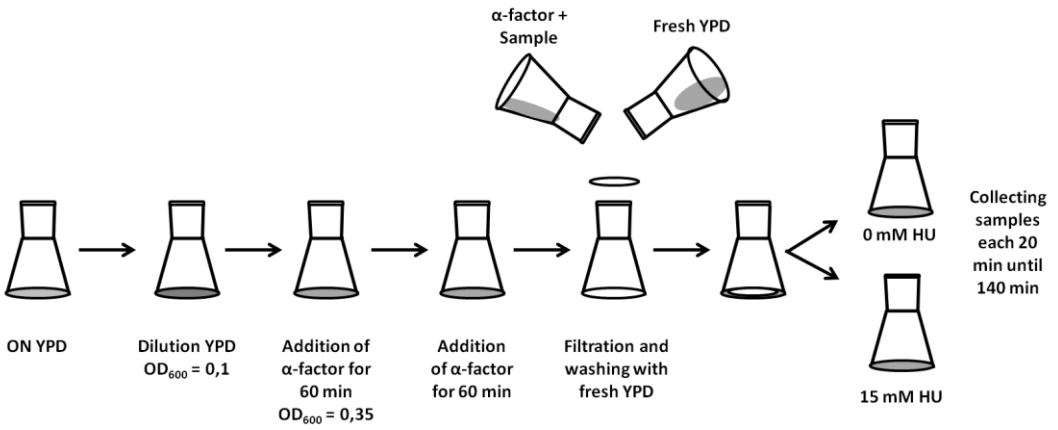

Fig. 36. Scheme of the experimental design for cell cycle synchronization, G1 release and sample collection (see text for details).

As shown in Fig. 37, we observed that in exponential phase the proportion of wild type cells with a 2N DNA content (G2 plus M cell cycle stages) was higher than those with a 1N content (G1 stage). On the contrary, in the case of the *Δgrx5* and *Δssq1* mutants, we observed the inverse result, that is, more cells with 1N content than with 2N. *A priori* this could be indicative of defects in cell cycle progression in the two ISC mutants. To narrow the study to the progression kinetics from G1 to G2/M, we followed this progression after α-factor synchronization and release from G1 arrest. In normal conditions (no HU treatment) wild type cells moved from 1N to 2N content in 30-40 min (Fig. 37A). However, both mutants took about 60 min to reach the 2N stage (Fig. 37B and C), that is a delay of 20 to 30 min when compared with wild type cells. When a sublethal concentration of HU (15 mM) was added to the cultures a delay in the transition from 1N to 2N was observed in all the strains. Thus, wild type cells took 60 to 80 min while mutant cells took 120 min to reach G2 phase. In other words, when HU is added a considerably larger increase (about two-fold) in the delay to reach the G2 stage was observed in mutant cells compared to wild type ones. In summary, the FACS analysis shows that both *Δgrx5* and *Δssq1* mutant cells have a delay in S-phase progression and that this delay is more pronounced upon HU addition, compared to wild type cells. These observations therefore confirm the hypersensitivity of the *Δgrx5* and *Δssq1* mutants to HU previously observed on YPD plates and indicate that this hypersensitivity reflects alterations in progression through the S-phase of the cell cycle.

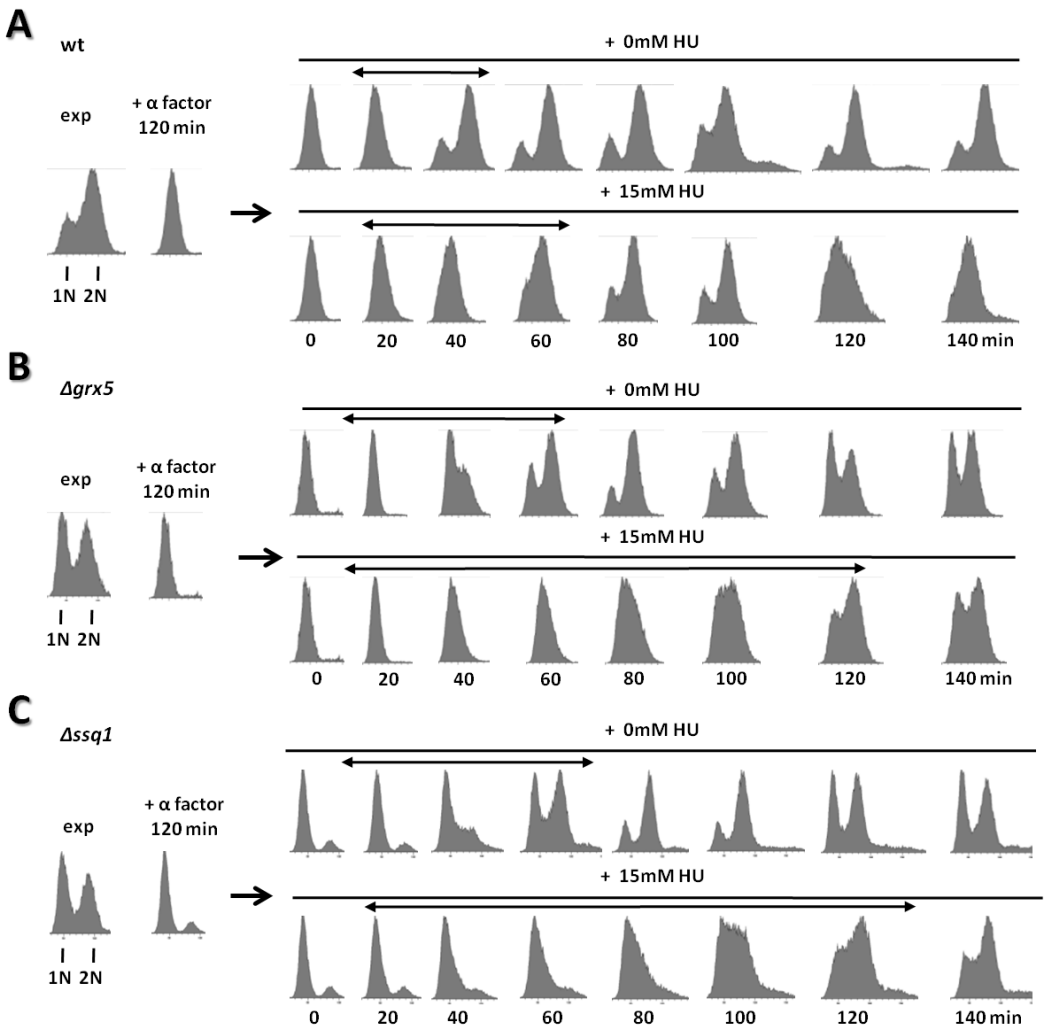

Fig. 37. Cell cycle progression from G1 to G2 is delayed in *Δgrx5* and *Δssq1* mutants. FACS analysis were done after release from α-factor mediated G1 synchronization, without or with HU treatment, in wild type (CML235, part A), *Δgrx5* (MML1500, part B) and *Δssq1* (MML1677, part C) cells.

Based on these results, we wanted to determine whether the defects in cell cycle progression were more accute in the *Δgrx5Δssq1* double mutant. For this purpose the experiment design was modified as shown in Fig. 38. First, the α-factor treatment was increased to 180 min (in two successive periods of 90 min) due to the slow exponential growth rate of the double mutant cells. Second, because of this slow cell cycle progression samples were collected each 45 min instead of each 20 min as before. As observed in Fig. 38, *Δgrx5Δssq1* double mutant cells took 135 min to reach the 2N phase after release from G1 arrest, twice the time observed in both single mutants. This is therefore indicative of an additive effect of both mutations on constitutive alterations in G1 to G2/M progression.

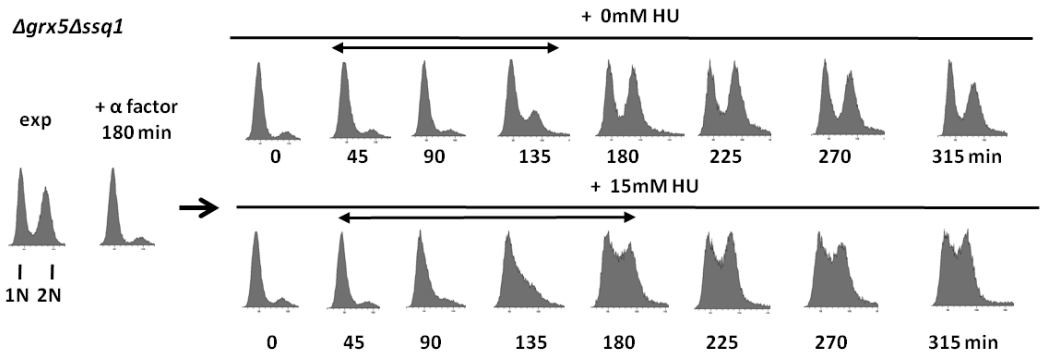

Fig. 38. Cell cycle progression from G1 to G2 is delayed in the *Δgrx5Δssq1* mutant. FACS analyses were done after release from α-factor mediated G1 synchronization, without or with HU treatment, in *Δgrx5Δssq1* (MML1681) cells.

8.1. The defects in cell cycle progression in *Δgrx5* mutant cells are specific of the S-phase

Cdc7 is an essential protein of *S. cerevisiae* that is required for the initiation of DNA replication, that is, for entry in the S-phase of the cell cycle (Schild & Byers, 1978). Therefore, a thermosensitive *cdc7^{ts}* mutant arrests at the beginning of S-phase at the non-permissive temperature (38°C), while at the permissive temperature (25°C) it grows normally (Fig. 39A). In order to localize more precisely in the cell cycle progression the defects observed in *Δgrx5* mutant cells (Fig. 38), we employed a *cdc7^{ts}* mutant carrying a wild type *GRX5* gene as well as a *cdc7^{ts}Δgrx5* double mutant. Both strains were grown at the permissive temperature in YPD medium, then arrested at G1 with α-factor for 180 min, released synchronously from this arrest and simultaneously shifted to 38°C for 45 min to arrest cells at the beginning of S-phase. After shifting cells again to the permissive temperature to allow resuming cell cycle progression (Fig. 39A), cells were divided into two aliquots. In the first one, cells were allowed to grow in YPD medium without additional treatment (control condition), and in the second one they were grown in the presence of a sublethal concentration of HU (15 mM). Meanwhile one sample of each mutant was kept at 38°C for 135 min as a control for checking the efficiency of the arrest at the restrictive temperature. After this time one more sample was collected. In the absence of HU treatment, after release from the early S-phase arrest, the *cdc7^{ts}* mutant cells took about 40 min to reach the 2N condition (G2), whereas *cdc7^{ts}Δgrx5* mutant cells took about 60 min, meaning that the *Δgrx5* mutation causes a 20 min delay specifically in moving along the S-phase (Fig. 39B). When a sublethal concentration of HU (15 mM) was added, *cdc7^{ts}* mutant cells took 60 min to reach G2 while the double mutant took 40 min more to reach the same phase.

We can therefore conclude that the cell cycle delay in the absence of Grx5 occurs in traversing the S-phase and that this delay is exacerbated by the addition of HU at higher magnitude in the mutant than in wild type cells.

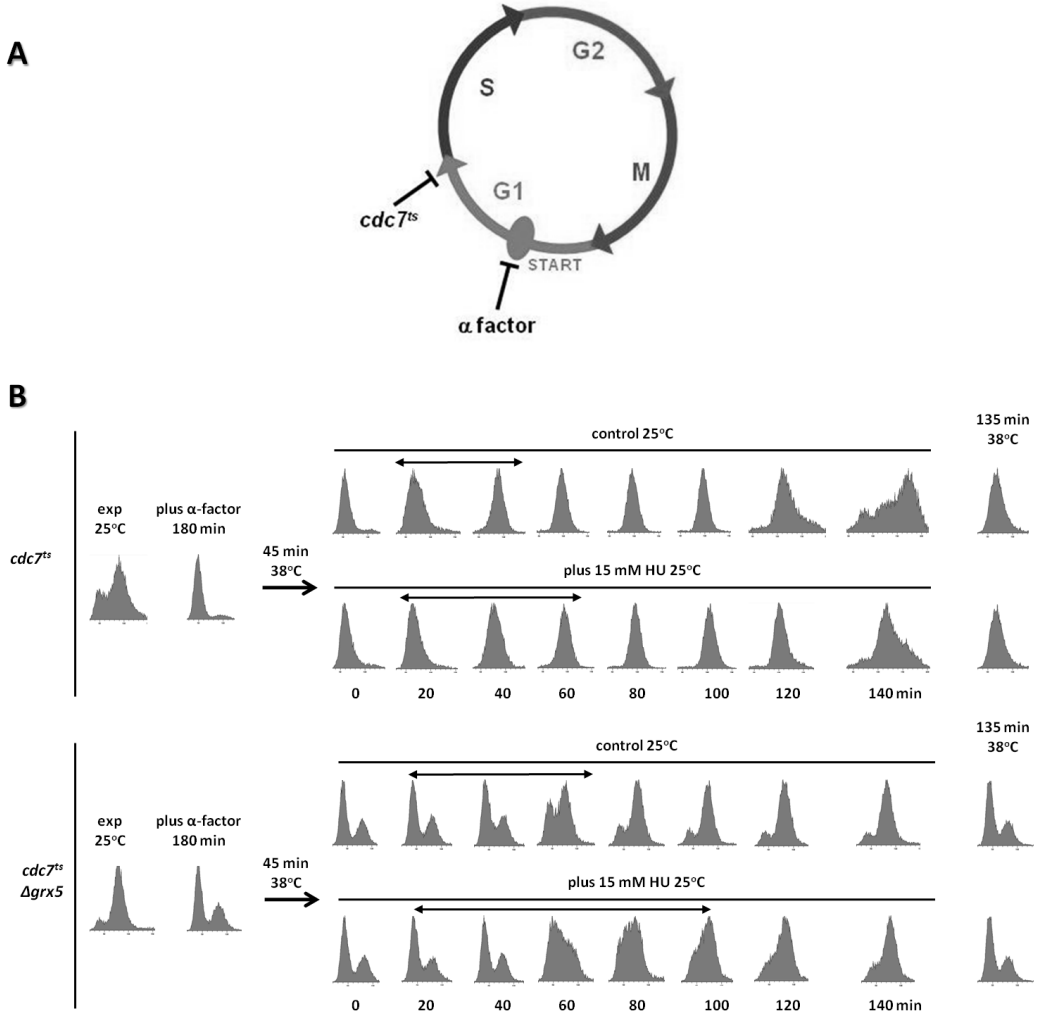

Fig. 39. HU-induced DNA damage causes an increased S-phase delay in the cell cycle progression in the absence of Grx5. Part A) shows a cell cycle diagram indicating the specific arrest after α-factor addition or after shifting *cdc7*^{ts} mutant cells to high temperature (37°C). B) FACS profiles after α-factor synchronization (180 min at 25°C) followed by release and subsequent S-phase entry arrest (45 min at 38°C) and release at 25°C, in cultures of *cdc7*^{ts} (Cdc7-1) and *cdc7*^{ts}*Δgrx5* (MML102) mutant cells. Samples for analysis were taken at the indicated times, in untreated and HU-treated cultures. Treatment with HU began at the time of release from S-phase entry arrest (time 0).

9. THE NER PATHWAY IS NOT SIGNIFICANTLY AFFECTED IN THE *Δgrx5* MUTANT CELLS

In the previous sections it was demonstrated that cells depleted of *GRX5* had elevated recombination and mutation rates, the foci formation was increased, cell cycle progression was delayed and the cells displayed hypersensitivity to DNA damage agents. Based on these phenotypes, it was postulated that the absence of *GRX5* could result in

defects in some DNA repair systems. To answer this question sensitivity studies with several DNA-damaging agents were done in cells carrying deletions in some of the genes that participate in DNA repair systems. The first gene studied was *RAD1*, which participates in the NER pathway. As mentioned is section 4.3.2 of the Introduction, *RAD1* encodes a ssDNA endonuclease that cleaves ssDNA in the NER pathway. It participates in the earliest steps of this repair system. As observed in Fig.40, *Δrad1* mutant cells are very sensitive to a low amount of UV radiation (25 J·m^{-2}), which are conditions in which the *Δgrx5* mutant does not show any sensitivity at all. In the case of HU, no significantly additive effect was shown in the *Δgrx5* mutant cells when *RAD1* was absent while a moderate additivity was observed with MMS (Fig. 40).

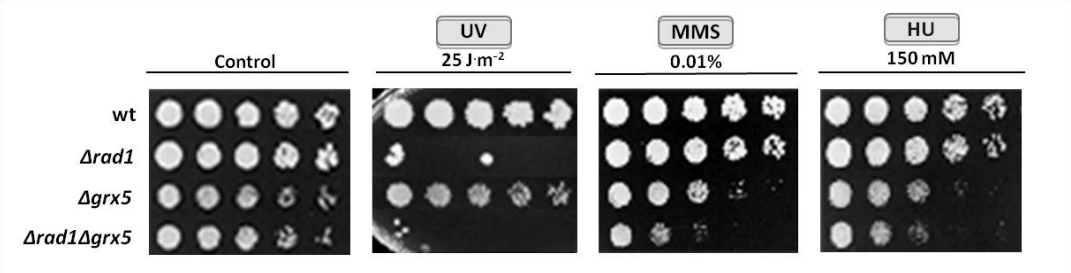

Fig. 40. The *Δgrx5* hypersensitivity to DNA damaging agents is not exacerbated when the NER pathway is compromised. Sensitivity studies to DNA-damaging agents were done with wild type (CML235), *Δrad1* (MML1583), *Δgrx5* (MML1500) single mutants and *Δgrx5Δrad1* (MML1609) double mutant cells by serial dilutions of exponentially growing cultures onto YPD plates containing the indicated agents or after UV irradiation. Plates were incubated at 30°C during 3 days.

As the previous results were not conclusive about the participation of *GRX5* in the NER system, another strategy was applied to detect DNA damage products reparable by the NER pathway (Moriel-Carretero & Aguilera, 2010). Thus, a slot blot assay was done to detect thymine dimers (TD) using a monoclonal antibody in DNA samples from wild type cells, *Δrad1*, *Δgrx5* and *Δssq1* mutant cells, once irradiated with 100 J·m^{-2} of UV and let stand for different periods of time to allow NER-mediated repair. This technique permits to quantify the number of DNA lesions, and this can be used to estimate the global genome repair rate. As the formation of TD is a photochemical reaction it can be expected a linear relationship between UV dose and the number of DNA lesions. As it can be observed in Fig. 41B, in wild type cells more than half of the TD had been repaired by 45 min after being irradiated, and after 135 min the repair was completed. In *Δrad1* mutant cells, TD repair was much slower, and by 135 min after irradiation only 40% of the TD had been repaired. *Δgrx5* mutant cells presented a TD recovery of 20% at 45 min, 50%

at 90 min and 80% at 135 min. This repair rate was very similar to that observed in *Δssq1* mutant cells (Fig. 41B).

From these experiments, we can conclude that NER pathway seems not to be significantly affected in *Δgrx5* mutant cells. Otherwise, this mutant would have been much more sensitive to UV radiation and would have shown a slower rate of TD repair.

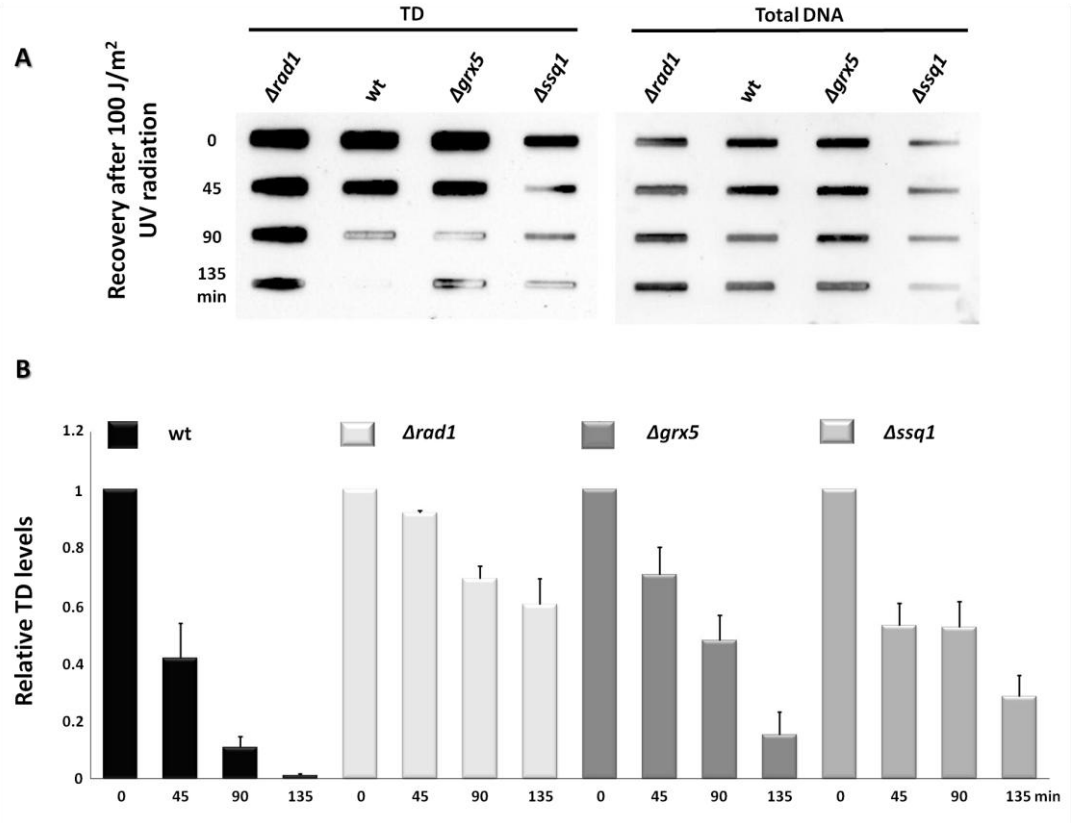

Fig. 41. TD repair kinetics in wild type, *Δgrx5* and *Δssq1* mutant cells. A) A slot blot assay of TD in extracts from wild type (CML235), *Δrad1* (MML1583), *Δgrx5* (MML1500) and *Δssq1* (MML1677) cells growing exponentially in SC medium, resuspended in 60 ml of the same medium and divided in 5 Petri plates with a volume of 12 ml each, then irradiated with 100 J/m^2 of UV. After irradiation all the cultures were mixed together and 10 ml for TD detection were taken at the indicated times. Total DNA was measured in parallel (see section 11 of the Material and Methods). B) Relative levels quantified from blots shown in part A). Bars correspond to means and SD of five different experiments.

10. HR DNA REPAIR PATHWAY COULD PLAY AN IMPORTANT ROLE IN REPAIRING DNA DAMAGE IN *Δgrx5* MUTANT CELLS

DSBs are repaired mainly through the HR pathway, in which Rad52 participates. The fact that cells lacking Grx5 have increased number of Rad52 foci, as observed in Fig. 24, could be indicative of the upregulation of this pathway in Grx5-deficient cells as a consequence of constitutive DNA damage. We therefore analyzed survival of HR mutants to DNA-damaging agents, both in the presence and in the absence of *GRX5*. For this

purpose, we focused on *RAD50* and *RAD52*, both members of the so-called *RAD52* epistasis group. As mentioned in section 4.3.3 of the Introduction, all members of the *RAD52* epistasis group are involved in the DSBs repair through HR. Rad50 with Mre11 and Xrs2 form the MRX complex which appears to be the earliest sensor of DNA DSBs by directly binding to DNA ends. Rad52 participates at a later step of the HR process, where it stimulates Rad51 recombinase activity.

As shown in Fig.42, *Δrad50* mutant cells are more sensitive than *Δgrx5* mutant cells to 50 $J \cdot m^{-2}$ of UV radiation, while *Δrad50Δgrx5* mutant cells display an added hypersensitivity. The same result is observed regarding *Δrad52* mutant cells and the *Δrad52Δgrx5* strain also shows added hypersensitivity compared to the respective single mutants.

In the presence of MMS, the sensitivity of the *Δgrx5* mutant is similar to that of the *Δrad52* mutant, although lower than that of *Δrad50* mutant cells. However, an added hypersensitivity to MMS is observed in both *Δrad50Δgrx5* and *Δrad52Δgrx5* double mutants. Finally, with respect to sensitivity to HU, both *Δrad50Δgrx5* and *Δrad52Δgrx5* mutant cells show an additive hypersensitivity phenotype but, unlike the previous cases, the single mutants *Δrad50* and *Δrad52* show similar sensitivity compared to the *Δgrx5* mutant.

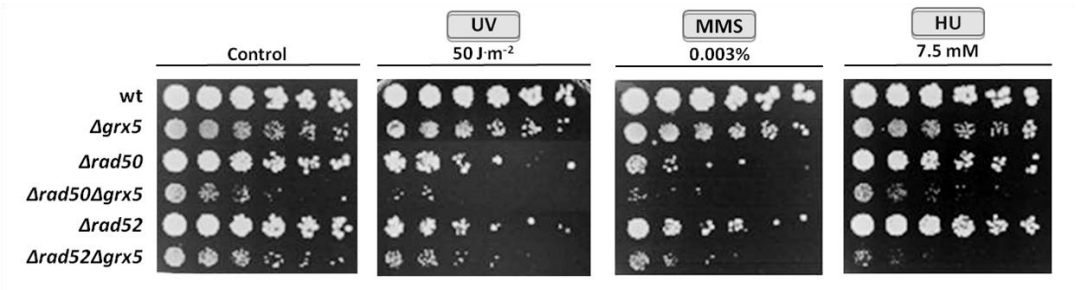

Fig. 42. The *Δgrx5* mutant cells display increased hypersensitivity to DNA damaging agents when *RAD50* or *RAD52* are deleted. Sensitivity studies to DNA-damaging agents were done in wild type (CML235), *Δgrx5* (MML1500), *Δrad50* (MML1545), and *Δrad52* (MML1585) single mutants, and in *Δrad50Δgrx5* (MML1605) and *Δrad52Δgrx5* (MML1607) double mutants cells by serial dilutions of exponentially growing cultures onto YPD plates containing the indicated agents or after UV irradiation. Plates were incubated at 30°C during 3 days.

These results suggest that the function of repair proteins such as Rad50 and Rad52 involved in HR is important for survival of Grx5-deficient cells, probably because of the participation of HR in repairing the DNA lesions raised in *Δgrx5* mutant cells.

11. THE *Δgrx5* MUTANT DISPLAYS ADDED SENSITIVITY TO CPT WHEN COMBINED WITH MUTATIONS IN HR

Since the previous results indicated that the HR DNA repair pathway could play an important role in repairing DNA damage in *Δgrx5* mutant cells, we employed another strategy to verify the interaction between HR and *GRX5*, involving the use of the antitumor drug CPT. This alkaloid was first identified in a screen of plant extracts for antineoplastic drugs (reviewed in Saleem *et al*., 2000). It is known that CPT upregulates the HR repair pathway to cope with the lesions provoked by the drug (Nitiss & Wang, 1988). CPT binds irreversibly to the DNA topoisomerase I (Top1) complex, inhibiting the re-ligation of DNA after cleavage by the enzyme, which results in DSB during DNA replication and subsequent arrest of the cell cycle at S-phase (Fiorani & Bjornsti, 2006).

Sensitivity studies to CPT were done in cells mutated in genes of the ISC assembly mechanism and/or in different DNA repair pathways such as NER, BER, NHEJ, HR and PPR. As shown in Fig. 43, at the sublethal CPT concentration employed no sensitivity effect was observed in the single mutants analyzed (*Δgrx5*, *Δssq1*, *Δiba57*, *Δrad1*, *Δapn1*, *Δnej1*, *Δrad52*, *Δrad50* and *Δrev3*). In the case of the BER mutants neither the double *Δapn1Δgrx5* nor the multiple *Δapn1Δntg1Δntg2Δgrx5* displayed a differential sensitivity phenotype to CPT compared to wild type cells. By analyzing the multiple mutant, we could conclude that none of the two subpathways of BER (Fig.12) is related to repairing CPT-induced DNA damage in *Δgrx5* cells at higher levels than in wild type cells. With respect to other DNA repair systems only the cells with a mutation in one of the HR genes *RAD50* or *RAD52* combining the *Δgrx5* mutation demonstrated an additive hypersensitivity phenotype.

This additive hypersensitivity in the presence of CPT shown by the *Δrad50Δgrx5* and *Δrad52Δgrx5* double mutant cells confirms the possible role of HR in maintaining the viability of *Δgrx5* cells by repairing constitutive and CPT-induced DSB damage.

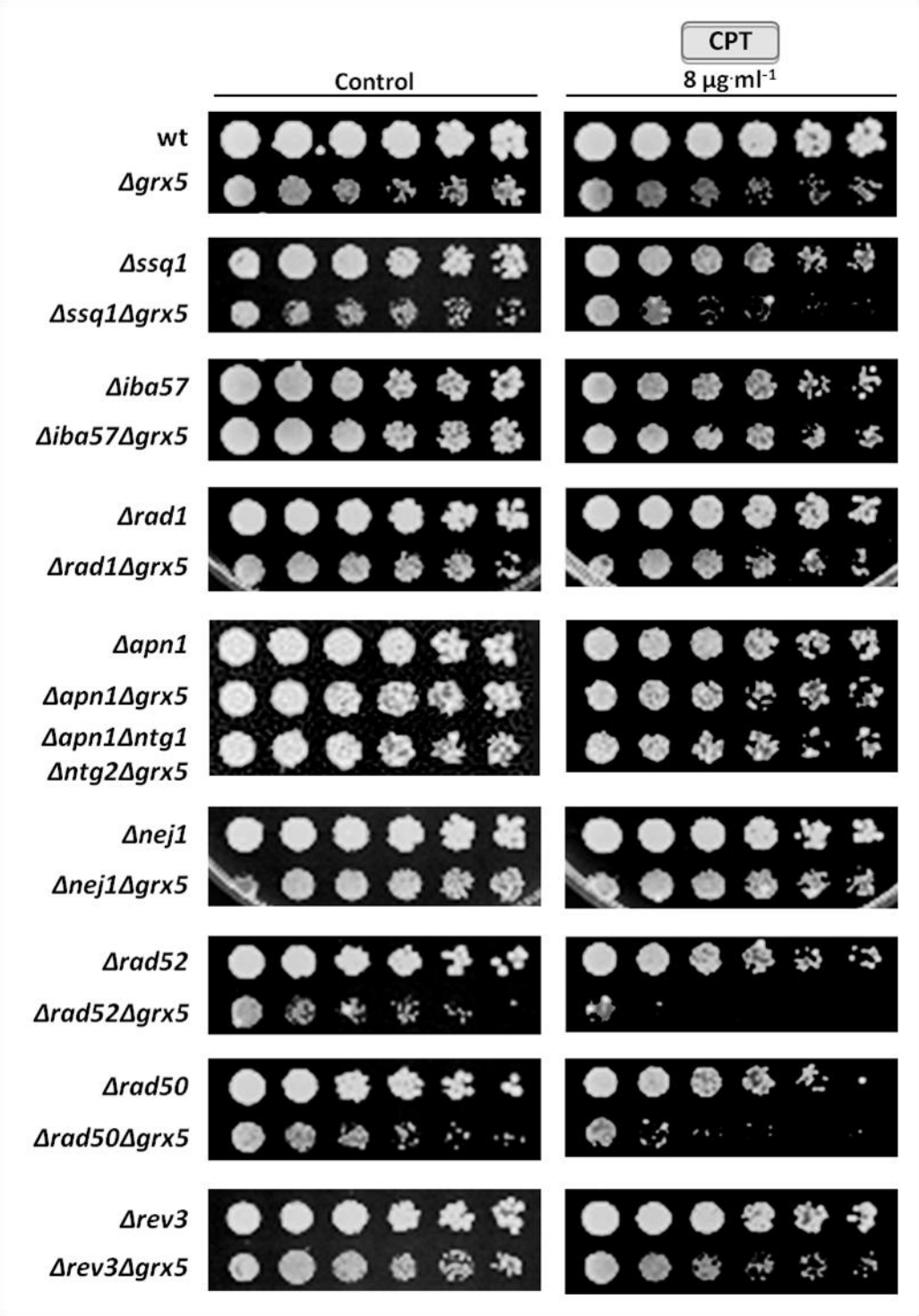

Fig. 43. Both *Δrad52Δgrx5* and *Δrad50Δgrx5* mutant cells display increased hypersensitivity to the antitumor drug CPT. Sensitivity studies to CPT were done in wild type (CML235), *Δgrx5* (MML1500), *Δssq1* (MML1677), *Δiba57* (MML1678), *Δrad1* (MML1583), *Δapn1* (MML1662), *Δnej1* (MML1621), *Δrad52* (MML1585), *Δrad50* (MML1545) and *Δrev3* (MML1497) single mutants, in *Δssq1Δgrx5* (MML1681), *Δiba57Δgrx5* (MML1694), *Δrad1Δgrx5* (MML1609), *Δapn1Δgrx5* (MML1633), *Δnej1Δgrx5* (MML1643), *Δrad52Δgrx5* (MML1608), *Δrad50Δgrx5* (MML1605), *Δrev3Δgrx5* (MML1524) double mutants and in *Δapn1Δntg1Δntg2Δgrx5* (MML1656) multiple mutant cells by serial dilutions of exponentially growing cultures onto YPD plates containing the antitumor agent (8 µg·ml^{-1}). Plates were incubated at 30°C during 3 days.

12. EXPRESSION OF THE *RNR1-4* GENES IS NOT AFFECTED IN THE *Δgrx5* MUTANT

When a DNA damage event occurs, it triggers several checkpoint responses to repair the damage. One of these is the Mec1-Rad53-Dun1-mediated checkpoint pathway, which regulates the dNTPs levels, as detailed in section 4.4 of the Introduction.

It is known that when this DNA damage checkpoint pathway is activated, transcription of the genes (*RNR2-4*) for the components of the RNR complex becomes strongly induced because of the Crt1-Ssn6-Tup1 complex repressor inactivation (see in section 4.4 of the Introduction). To verify if this branch of the Mec1-Rad53-Dun1 checkpoint was affected by the absence of Grx5 the expression levels of *RNR1-4* in wild type and *Δgrx5* cells were analyzed by northern blot, in untreated and treated cells with HU (dNTPs depletor). As shown in Fig. 44, the four *RNR* genes increased their levels over the basal ones when HU was added, in both wild type and mutant cells.

The mRNA quantification from two independent experiments is shown in Fig. 45. For the four *RNR* genes, the maximum expression levels were reached at 60 min. However, for none of them significant differences were detected between both.

These results indicate therefore that at least the Crt1-Ssn6-Tup1 control branch of the DNA damage Mec1-Rad53-Dun1 checkpoint pathway is not activated in *Δgrx5* mutant cells.

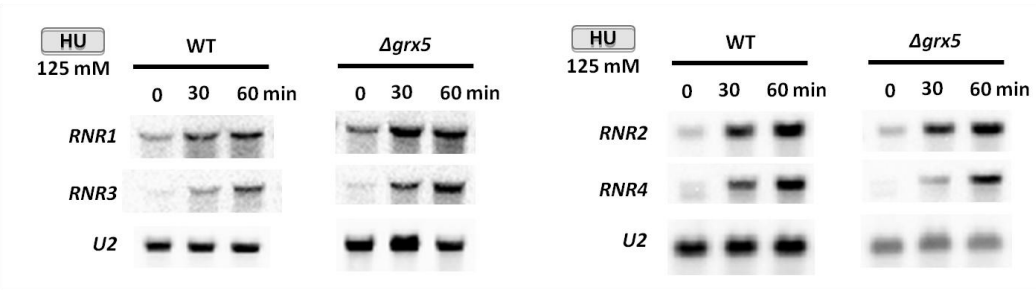

Fig. 44. In the absence of Grx5, transcription levels of the RNR genes (*RNR1-4*) do not change. mRNA levels of *RNR1*, *RNR2*, *RNR3* and *RNR4* in wild type (W303-1A) and *Δgrx5* (MML100) in cultures in YPD medium treated with HU. The samples were collected at times 0 (untreated), 30 and 60 min (treated). *U2* probe was used as a loading control.

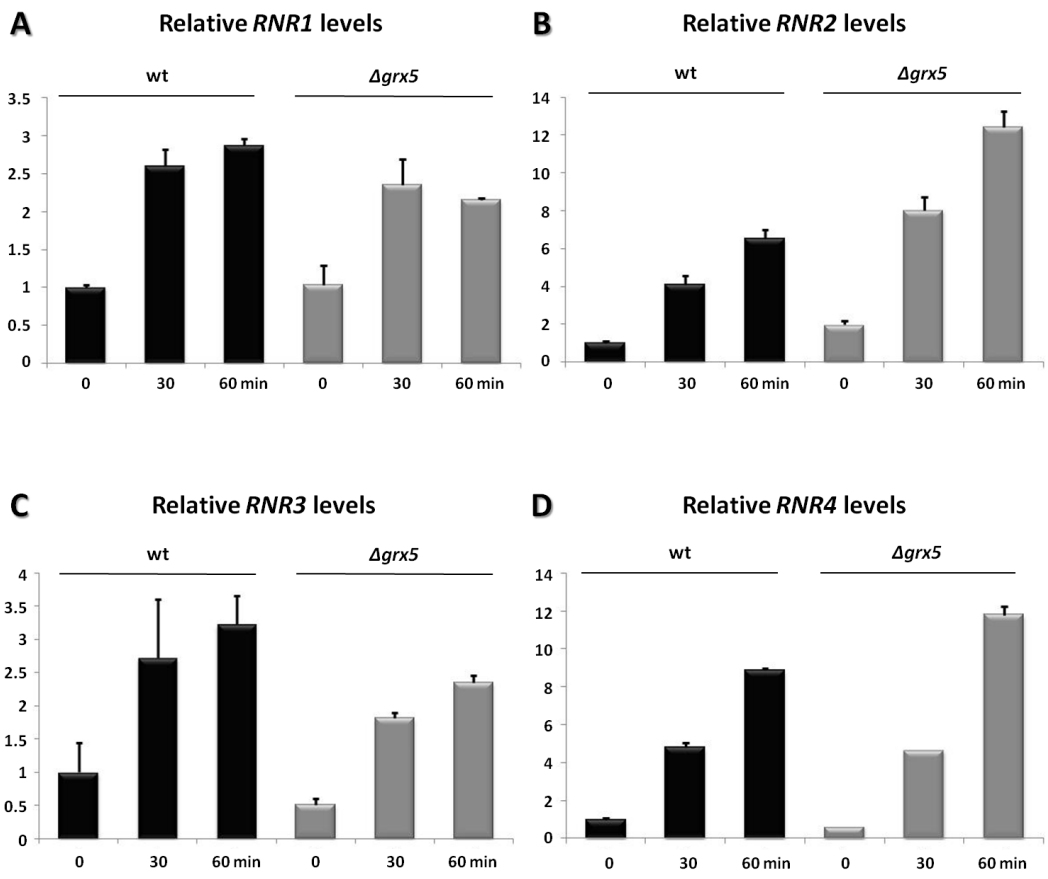

Fig. 45. Quantification of mRNA relative levels shows no significant differences for any of *RNR1-4* mRNAs between wild type and *Δgrx5* cells. Values were made relative to the unit value attributed to untreated wild type cells. Bars show the means plus SD from two independent experiments.

13. OVEREXPRESSION OF *PRI2, RAD3* OR *NTG2* CANNOT RESCUE THE SENSITIVITY DEFECTS OF CELLS LACKING *GRX5* TO DNA DAMAGING AGENTS

Stehling *et al.* (2013) showed that depletion of Mms19 (involved in the CIA machinery for cytosolic synthesis of ISC, see in section 3.3.2 of the Introduction) resulted in a decrease of the ISC binding to various ISC proteins involved in DNA metabolism, which included the DNA helicase Rad3, among others. Earlier, Kou *et al.* (2008), had demonstrated that increase of the Rad3 protein levels by overexpressing the corresponding gene under a *GAL1* promoter rescued the UV sensitivity of *Δmms19* mutants. Both works suggest therefore that Mms19 is necessary for the stabilization of Rad3 but not for its helicase activity. Other nuclear proteins involved in DNA metabolism that have been suggested to contain ISCs are the DNA N-glycosylase, Ntg2 (Alseth *et al*., 1999) and the DNA primase, Pri2 (Foiani *et al*., 1989). Accordingly, we constructed different plasmids in which *RAD3*, *NTG2* and *PRI2* were overexpressed under control of a

tetO$_7$ promoter, and these plasmids were transformed in wild type and *Δgrx5* mutant cells.

Fig. 46 shows the results of sensitivity studies with the corresponding transformants onto plates containing the DNA damaging and oxidative stress agents are shown. As it can be observed with the several DNA damage agents (UV, MMS and HU), the overexpression of *PRI2*, *RAD3* or *NTG2* did not rescue the sensitivity defects of the *Δgrx5* mutant cells. The same result was observed when *t*-BOOH was added into the plates. These results suggest that the hypersensitivity of *Δgrx5* cells to the agents is not due to deffects of ISC assembly and/or maturation of Pri2, Rad3 or Ntg2.

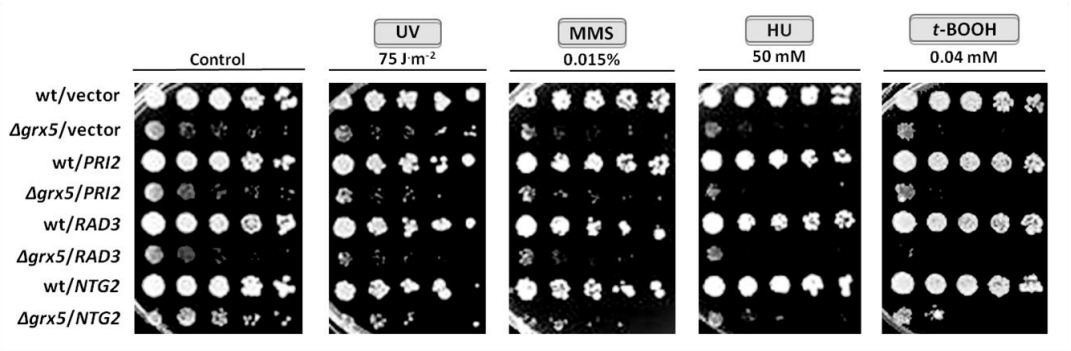

Fig. 46. Overexpression of *PRI2, RAD3* or *NTG2* cannot rescue the sensitivity defects of *Δgrx5* mutant cells to genotoxic agents or peroxide. Sensitivity studies to the indicated DNA-damaging agents and to the oxidant *t*-BOOH were done in wild type/vector (CML235/pCM189), *Δgrx5*/vector (MML1500/pCM189), wild type/*PRI2* (CML235/pMM1078), *Δgrx5*/*PRI2* (MML1500/pMM1078), wild type/*RAD3* (CML235/pMM1094), *Δgrx5*/*RAD3* (MML1500/pMM1094), wild type/*NTG2* (CML235/pMM1077) and *Δgrx5*/*NTG2* (MML1500/pMM1077) cells by serial dilutions of exponentially growing cultures onto SC plates containing the indicated agents or after UV irradiation. Plates were incubated at 30°C during 7 days.

PART V

DISCUSSION

Tens of thousands of DNA lesions occur in a single cell of the human body per day, consequently interfering with the genome replication (Jackson & Bartek, 2009). If these lesions are not repaired or are repaired in an incorrect way, they may lead to mutations that compromise cell and/or organism viability. To fight against these threats, cells have evolved systems (commonly named DNA damage response or DDR) to detect DNA lesions and promote their repair. Cells defective in these systems generally display an increased sensitivity in the presence of DNA damaging agents and as a consequence, defects in the genetic material are produced causing many human diseases.

In the past three decades, an increase has occurred in understanding how cells detect and employ several DDR mechanisms in the response to DNA damage. At the same time, a relationship has been established between DNA damage and oxidative stress. Since the first article by Biaglow *et al.* (1986) until now with the joined terms "oxidative stress" and "DNA damage", a large number of articles have been published relating both fields, demonstrating the importance of the relation between them. The findings from these studies had important implications for knowing more about cancer (Hoeijmakers, 2001), neurodegenerative disorders (Kulkarni & Wilson, 2008), immune deficiencies and infertility (Matzuk & Lamb, 2008), ageing (Breitenbach *et al.,* 2013), stem-cell dysfunction (Sharpless & DePinho, 2007), cardiovascular disease (Vousden & Lane, 2007), metabolic syndrome (Kastan, 2008) and genome instability in other heritable human diseases (Veatch *et al.,* 2009).

As mentioned in section 1 of the Introduction, cells generate ROS as a consequence of aerobic metabolism. In fact, the major source of ROS generation is the loss of electrons from the mitochondrial electron transport chain. These electrons react with molecular oxygen forming $O_2^{\cdot-}$, which is quickly converted to H_2O_2 by the mitochondrial protein Sod2 and then to water through the participation of peroxidases and/or catalases. It is known that DNA and proteins are not very reactive to H_2O_2. However, in the presence of metals (iron or copper), H_2O_2 is converted to $OH\cdot$, a reactive species causing diverse forms of DNA damage.

This thesis has been focused in studying the relationship between genomic instability and Grxs, a family of enzymes initially related to oxidative stress responses. For this purpose the budding yeast *S. cerevisiae* was chosen as model of study. Many reasons were taken into account for this election. To start, *S. cerevisiae* was the first eukaryote to have its genome fully sequenced (reviewed in Ingalls *et al.,* 2007). It has also been used as an efficient tool to study DNA repair, cell cycle, aging, gene expression and the molecular and cellular basis of several human diseases (Kurtz *et al.,* 2004; Karathia *et al.,* 2011). This budding yeast has a small genome (approximately 200 times smaller than the human genome) and fast doubling time (approximately 2 h), it can be easily genetically manipulated, it is easily grown in the lab and less susceptible to be contaminated in relation to most other eukaryotic cell cultures, and the cell cycle progression can be monitored by cellular and nuclear morphology. It also presents a haploid and diploid phase in its life cycle, which allows the study of recessive mutations that can be masked in the diploid state by the wild type allele. Approximately 30% of the genes known to be involved in human diseases have yeast orthologs and hundreds of yeast genes exhibit a relation to disease-related human genes (Karathia *et al.,* 2011). Screening based on phenotypic trades in a marker stability strategy provide a singular approach to identify genes that act to preserve genomic structures (Yuen *et al.,* 2007). Since yeast cells are viable under fermentative conditions even after losing its mtDNA, this allows the study of mitochondrial processes, which are involved in DNA damage and genome maintenance. Finally, the six main DNA repair systems BER, NER, HR, NHEJ, MMR and TLS are deeply understood (see section 4.3 of the Introduction) and are well conserved from yeast to higher eukaryotes. These advantageous aspects have been considered in the present study.

As said previously, DNA damage has an important participation in the aging process. The increased sensibility to cellular and functional loss observed during the process of aging has been related with mtDNA integrity (Wang *et al*., 2013). The stability of mtDNA is constantly under attack for its proximity with the mitochondrial ROS generation site (Muller *et al*., 2004). Indeed, it was observed that the oxidative levels of induced lesions in mtDNA were several-fold higher compared with those in nDNA (Hamilton *et al.,* 2001). It was thought that the higher amount of oxidative lesions detected in mtDNA compared to nDNA was, in part, due to the possible absence of DNA repair mechanisms in mitochondria. However, several studies done over the last decade discovered the existence of new mtDNA repair systems, and also new DNA repair proteins

have been detected. This is, for example, the case of the MMR (de Souza-Pinto *et al.,* 2010) and BER (Liu *et al*., 2008) DNA repair pathways.

It is known that most human cancers are consequence of genome instability (Aguilera & Gómez-González, 2008), and an increased body of data relate this instability to functional dysfunctions at mitochondria. Thus, Liu *et* al. (2002) demonstrated that mitochondrial dysfunction generates ROS leading to telomere attrition and loss, chromosome fusion and breakage, resulting at the end in an apoptosis situation. More recently, Veatch *et al.* (2009) proposed a model to explain the relationship between mtDNA damage in yeast cells and genomic instability. In this study they reported that defects in ISC metabolism at mitochondria resulted in nuclear genome instability through changes in the mitochondrial membrane potential. In a situation where mtDNA loss occurred (for instance by treatment with propidium iodide), the mitochondrial membrane potential became reduced compromising the normal assembly of ISCs and the respective export to the cytosol. These events resulted in an induction of the iron regulon and nuclear genome instability. Another evidence connecting genomic instability and ISC biosynthesis at mitochondria came through the work by Díaz de la Loza *et al.* (2011). In this study they found that *S. cerevisiae* cells depleted of Zim17 (which interacts with other chaperones such as the mtHsp70 homologs Ssc1 and Ssq1) display an extreme hyper recombination phenotype, increased mutation rates and spontaneous DSB formation affecting the stability of the genome. The study therefore directly related alterations of the ISC machinery (through downregulation of Ssq1 activity) with alterations in the stability of the nuclear genome. In another work by Rudolf *et al.* (2006) they identified Fe-S domains in the DNA repair human helicase XPD (homologue of *S. cerevisiae* Rad3), which is involved in the NER repair system, and demonstrated that the cells lacking the corresponding ISC binding domain could no longer maintain their function as DNA helicase. Thus, this work directly implicated for the first time an ISC protein in DNA repair functions.

Considering all this previous experimental background, in this thesis we intended to gain further insight on the relationship between ISC biosynthesis and genome instability by studying genomic instability in a *S. cerevisiae Δgrx5* mutant. We chose this mutant because cells lacking the mitochondrial Grx5 protein (which participates at the late stages of the ISC assembly mechanism in the mitochondrial matrix) have diverse phenotypes, such as inability to grow in minimal medium or in the presence of non-fermentable carbon sources, hypersensitivity to external oxidants, iron accumulation inside the cell, increase in the protein oxidative damage and defects in the activity of

enzymes requiring ISCs as cofactors, such as aconitase or succinate dehydrogenase. These phenotypes are found as well in cell lacking other proteins involved in the ISC biosynthetic machinery.

Taking into account the work by Díaz de la Loza *et al.* (2011), we observed in this thesis that the absence of Grx5 leads to a raised genetic instability due to increased recombination and mutation frequencies. As a control, we also determined the recombination rate of other mutants in mitochondrial functions not directly related to ISC biosynthesis (*Δyfh1, Δaif1* and *Δcox12*). These mutants showed a recombination frequency slightly higher than wild type cells but in any case much lower than *Δgrx5* mutant cells, indicating that the nuclear genome instability generated in the absence of Grx5 function was specifically due to the lack of this function (in the context of ISC biogenesis) and not to a more general and undefined effect caused by disruption to any mitochondrial process. Interestingly, the increase of the chromosomal mutation frequency in the *Δgrx5* mutant compared to wild type cells in our work (5.6-fold) was similar to that observed in the *Δzim17* mutant (5.9-fold) by Díaz de la Loza *et al.* (2011).

Evidence that the hyperrecombination phenotype shown by *Δgrx5* mutant cells could be partially caused by an increase in DSB formation came through the increased foci formation observed with the Rad52-YFP marker in cells depleted of Grx5 with respect to the wild type cells. In fact, the Rad52 protein associates with ssDNA ends. Interestingly, this constitutive increase in foci formation in the absence of Grx5 was only detected in budded cells, that is, in cells actively replicating chromosomal DNA or during chromosomal segregation prior to the next cell division cycle. On the other hand, an external oxidant such as *t*-BOOH could indiscriminately damage DNA (with consequent Rad52 foci formation) of both budded and unbudded cells, that is, at any stage of the cell division cycle. Foci formation was also determined with another reporter protein involved in the HR repair system, Rfa1, but in this case no significant differences were observed in the number of foci between wild type and *Δgrx5* cells with any of both morphologies, and with or without oxidant treatment. We cannot discriminate whether this is due to the fact that no differences exist between wild type and Grx5-minus cells at the DNA repair stage reported by Rfa1, or whether this reporter protein is not enough sensitive to differentiate between subtle differences among strains. Overall, the results provide evidence on the relationship between the absence of Grx5 and constitutive DSB formation, and point to the participation of the Rad52-mediated HR pathway in counteracting this damage.

After demonstrating that cells lacking Grx5 have an increased genetic instability we wanted to know if this constitutive instability could affect the viability of *Δgrx5*

mutant cells after additional treatment with different DNA-damaging agents. Three agents were initially considered: UV radiation (inducing formation of TD), MMS (which alkylates DNA bases) and HU (which compromises DNA replication by depleting the cell of deoxynucleotides). In fact, the *Δgrx5* mutant cells were more sensitive than the wild type ones to both MMS and HU, as well as to UV irradiation. In the case of HU, however, the hypersensitivity phenotype of the *Δgrx5* mutant cells was milder than in the case of the other two genotoxic agents. Also, this hypersensitivity to the DNA-damaging agents was not a result of the endogenous hyperoxidation state of the *Δgrx5* mutant as demonstrated by the addition of the anti-oxidant agent (NAC) or by carrying out treatments with genotoxics in anaerobic conditions. In fact, in these two conditions the hypersensitivity phenotype was still observed.

We also demonstrated that the hypersensitivity to genotoxics observed in *Δgrx5* mutant cells was not a consequence of the iron accumulation observed in cells depleted of *GRX5* [described in Rodríguez-Manzaneque *et al.* (2002)]. We initially hypothesized that this iron accumulation in the mutant could mislead the interpretation of the above results due to the relationship existing between elevated iron amount and increased ROS production, which could affect the structure and the stability of the DNA, and consequently the sensitivity to external DNA damaging agents. As shown in this thesis, a *Δgrx5Δfet3* double mutant does not accumulate intracellular iron (due to inhibition of the plasma membrane-associated high affinity system for iron uptake) but still displays the same sensitivity phenotype to UV light as that observed in cells depleted of Grx5, which keep intact the iron uptake system. The sensitivity of the cells lacking Grx5 therefore seems to be independent of the intracellular iron content.

To verify if the hypersensitivity phenotype presented by *Δgrx5* mutant cells was directly provoked by the absence of Grx5 and not due to the possible secondary unspecific defects created through instability of nDNA in the absence of this mitochondrial protein, sensitivity studies to MMS were also carried out in a strain expressing *GRX5* conditionally under a doxycycline-regulable $tetO_7$ promoter (Garí *et al*., 1997; Bellí *et al*, 1998). In this way we could conclude that it is the depletion of the Grx5 protein which is directly causing the hypersensitivity phenotype to the DNA-damaging agents and not possible secondary effects. Overall, these experiments are indicating that Grx5 is directly required for maintenance of nDNA stability in parallel to other possible roles of this protein.

Next, we wanted to determine whether the genetic instability and hypersensitivity to genotoxics of the *Δgrx5* mutant could be extended to mutants in other

components directly participating in the mitochondrial ISC biosynthetic machinery, and we focused our attention on the Ssq1 protein, which participates at a similar stage of the ISC pathway as the Grx5 protein (Rodríguez-Manzaneque *et al*., 2002). Although cells lacking Ssq1 displayed slightly lower hypersensitivity than cells lacking Grx5 for all genotoxic agents earlier mentioned, they still were more sensitive than wild type cells, indicating that the requirement of the integrity of the ISC biosynthesis machinery for the cells to survive in the presence of DNA-damaging agents can be generalized. As demonstrated in this work, *Δgrx5Δssq1* double mutant cells show an added hypersensitivity to the DNA-damaging agents studied previously. These results may suggest different participation for these two proteins in relation to cell survival in the presence of DNA-damaging agents, otherwise if there was a overlapping of roles we could not observe any addition in the hypersensitivity in the case of the double mutant. Curiously, in the presence of the thiol oxidant diamide the same additive sensitivity phenotype was observed in either *Δgrx5*, *Δssq1* and *Δgrx5Δssq1* mutant cells. On the contrary, in the case of *t*-BOOH a moderate rescuing phenotype in the *Δgrx5Δssq1* double mutant cells with respect to both single mutants was observed. This last result is beyond our comprehension.

Overexpression of Ssq1 rescued the sensitivity phenotype to the DNA damaging agents of the *Δgrx5* mutant cells. The same result was observed previously by Rodríguez-Manzaneque *et al.* (2002) when a multicopy plasmid containing *SSQ1* allowed cells depleted of Grx5 to grow in SD medium and in YPD plates with the oxidant menadione. In the same work the authors also put in evidence that two other monothiol Grxs, Grx3 and Grx4, when overexpressed in mitochondria only rescued in a very slight manner the sensitivity phenotype to menadione of cells lacking Grx5. Overall, these experiments show that higher than normal Ssq1 levels can substitute for the absence of Grx5 with respect to different functions, including those related to DNA metabolism.

When DNA damage occurs cells initiate diverse responses to facilitate DNA repair processes. One of these responses is the activation of a serial of checkpoints in the cell cycle, which monitor and control the order and the timing of cell cycle transitions ensuring that critical steps such as DNA replication and chromosome segregation are carried out with high fidelity. Defects in these checkpoints result in genomic instability and have been associated with the evolution of normal cells into cancer cells. The DNA damage checkpoint is a mechanism which detects abnormal DNA and sends a signal that arrests cells in G1 and G2, slows down the S-phase and induces the transcription of some genes that participate in DNA damage repair. The position of the arrest within the cell

cycle varies according the respective phase in which the damage is detected (reviewed in Branzei & Foiani, 2008). Once repair is achieved, the DNA damage checkpoint response is down-regulated and cells turn to re-enter the cell cycle progression (Clémenson & Marsolier-Kergoat, 2009). One way to follow cell cycle progression is by flow cytometry through FACS analyses, which allow the observation of the cell movement from 1N stage to 2N stage. To verify if the cell cycle progression was affected in some way in genetically-instable cells depleted of Grx5 we carried out such FACS analyses. We observed that cells depleted of Grx5 or Ssq1 presented a cell cycle delay phenotype due to a slow-down movement through the S-phase. This situation is similar to that in cells lacking Zim17 (Díaz de la Loza *et al.*, 2011). Through studies of cell synchronization at the S-phase entry point, in the case of the *Δgrx5* mutant we could show precisely that the delay affected S-phase progression and that it was exacerbated by the addition of HU at higher magnitude in the mutant than in wild type cells. Another work by Crider *et al*. (2012) also observed a defective progression through S-phase in *S. cerevisiae* cells lacking mtDNA (rho^0 cells). Our observations with the mutant lacking Grx5 could indicate that the absence of this protein directly compromises DNA replication but also that in these conditions the DNA damage checkpoint is activated further slowing-down progression through S-phase.

After observing that cells lacking Grx5 display an elevated recombination and mutation rates, increased foci formation, hypersensitivity to DNA-damaging agents and a delay in cell cycle progression (which all of them are threats to the genome stability) we wanted to analyse the relationship of Grx5 with some DNA repair mechanisms. The first repair system that we studied was the NER mechanism. Sensitivity studies to DNA-damaging agents were done with cells depleted of *RAD1*. Rad1 participate in the earliest steps of this repair system (as mentioned in section 4.3.2 of the Introduction). This function was first discovered by Siede *et al*. (1993) where reported that cells lacking *RAD1* presented a UV-sensitive phenotype. We confirmed the same sensitive phenotype by serial dilutions of exponentially growing cultures followed by UV irradiation on plates. The sensitivity of the *Δrad1* mutant was much higher than that of *Δgrx5* cells, indicating that the latter were not severely compromised for the NER pathway. In the case of HU and MMS, cells depleted of *RAD1* did not show an hypersensitivity phenotype compared to cells lacking *GRX5*. Also, no significant additive effect was observed in the *Δgrx5* mutant cells when *RAD1* was also absent, while only a moderate additivity was observed with MMS. The NER system removes helix-distorting lesions from DNA, repairing UV-induced pyrimidine dimers (reviewed in Boiteux & Jinks-Robertson, 2013). For this reason we checked TD formation and subsequent repair in wild type, *Δrad1*, *Δgrx5* and *Δssq1*

mutant cells, after been irradiated with UV light. We observed that cells lacking both mitochondrial proteins, Grx5 and Ssq1, presented an intermediate rate of TD repair compared to wild type cells, although at the end all of the three strains completed TD repair in the experimental conditions employed. On the contrary, *Δrad1* mutant cells proved to be unable to remove the TD lesions. Overall, we could conclude that the NER pathway seems not to be significantly affected in cells depleted of Grx5, nor participate in repairing DNA damage in these same cells.

We next moved to another DNA repair system, the HR pathway, where DSB lesions are repaired whenever an undamaged homologous sequence is present to serve as a template. We selected two genes that participate in different step in this repair mechanism: *RAD50* (participates at the first step of the pathway by sensing the damage in DNA) and *RAD52* (participates at a later step by stimulating Rad51 recombinase activity), being both members of the *RAD52* epistasis group. Cells depleted of *RAD50* or *RAD52* were more sensitive to the DNA-damaging agents UV and MMS compared to the cells lacking *GRX5*, but this was not the case of HU, for which all three single mutants displayed similar sensitivity. However, when *GRX5* was deleted in cells already depleted of *RAD50* or *RAD52* an additive sensitivity phenotype was observed in the respective double mutants in the presence of any of these three DNA-damaging agents. This suggests that the repair function of these HR proteins is important for the survival of cells deficient of Grx5, pointing to a role of HR in repairing DNA lesions occurring in *Δgrx5* cells.

Another way to induce DSBs lesions is to interfere with the proper function of DNA topoisomerase Top1. The incorrect function of Top1 has been demonstrated to be the cause of the origin of ssDNA breaks. It is known that during the replication process the continuous formation of this type of breaks leads to the appearance of DSBs, reviewed in Caldecott (2001). The addition of the anticancer drug CPT to cell cultures inhibits Top1 to re-ligate the DNA after the cleavage by binding the topoisomerase, therefore blocking DNA religation after the cleavage and generating DSBs. We did studies of sensitivity to concentrations of CPT which are sublethal in wild type cells on strains lacking some proteins of the ISC pathway (Grx5, Ssq1 and Iba57), or the NER (Rad1), BER (Apn1, Ntg1 and Ntg2), NHEJ (Nej1), HR (Rad50 and Rad52) and PPR (Rev3) repair systems. We verified an added hypersensitivity phenotype only in cells lacking *GRX5* in combination with a deletion in one of the genes that participate in the HR pathway, *RAD50* or *RAD52*. These results indicate that in cells deficient of Grx5 only HR is necessary to repair the damage provoked by CPT, and therefore confirm the need for the integrity of the HR pathway in the absence of Grx5. Lettier *et al.* (2006) suggested that *Δrad52*

mutant strains are not efficient in the repair of single-ended DSBs originated by the progression of the replication fork. We can suggest that the absence of Grx5 amplifies this effect. It is important to note that the ISC mutants tested in this work (*Δgrx5, Δssq1, Δiba57, Δssq1Δgrx5, Δiba57Δgrx5*) require high concentrations of CPT to observe growth inhibitory effects, in the same line as reported in Díaz de la Loza & Wellinger (2009). In this work the authors concluded that the absence of the sensitive phenotype when CPT is added is due to the fact that CPT is excluded from mitochondria through specific transporters or that the drug is unable to cross the mitochondrial membranes.

In a DNA damage event several checkpoints are triggered to repair the damage. One of these is the Mec1-Rad53-Dun1-mediated checkpoint pathway. One consequence of the activation of this pathway is the increase of dNTP production (Chabes & Stillman, 2007). This is accomplished by the regulation of the enzyme RNR, which controls the rate of dNTPs synthesis. Moreover, high dNTPs levels inhibit the cells to entry into S-phase by blocking replication initiation, which permits the Mec1-Rad53-Dun1 checkpoint pathway to induce the transcription of a number of DNA repair genes. *MEC1* and *RAD3* genes are well conserved among eukaryotes at evolutionarily level: Mec1 is the homolog of the human ATR and Rad53 is the homolog of the human Chk2 (reviewed in Rotman & Shiloh, 1999). Since cells lacking *GRX5* have a delay in the cell cycle S-phase progression, this could reflect activation of the above mentioned pathway. Therefore, we analyzed the expression levels of the mRNAs for the four RNR components (*RNR1-4*) in wild type and *Δgrx5* mutant cells. As a control, we also determined *RNR1-4* mRNA levels in cells treated with HU, conditions in which the checkpoint pathway is activated. As mentioned in Chabes *et al.* (2003), where the authors observed an increase of 6 to 8-fold in the dNTPs levels after a DNA damage event, we also verified an increase in the mRNAs levels for all four *RNR* genes when HU was added, with a minimum of 2-fold for *RNR3* mRNA levels in *Δgrx5* mutant cells and a maximum of 12-fold with *RNR2* and *RNR4* mRNA levels in *Δgrx5* mutant cells. However, no significant differences were observed between both strains in basal and stress conditions. These results show that in cells lacking *GRX5* the Mec1-Rad53-Dun1 checkpoint pathway is not activated, and therefore discard the explanation that the S-phase delay in those cells were due to such activation.

Overexpressing the Fe-S DNA helicase Rad3 rescues the UV sensitive phenotype shown by the *Δmms19* mutant cells (Kou *et al.*, 2008). It is known that Mms19 is a component in the CIA machinery acting at a late step of ISC assembly at the cytosol. Also, Stehling *et al.* (2012) demonstrated that the maturation of Rad3 was dependent on the levels of Mms19 but the function of the helicase in the DNA damage repair was

independent of the CIA proteins. We overexpressed three genes that encode for Fe-S proteins (or suggested to be Fe-S proteins) which participate in different DNA repair systems, *RAD3, NTG2* and *PRI2*, under the control of a $tet0_7$ promoter, and these plasmids were transformed in wild type and *Δgrx5* mutant cells. The sensitivity studies with the corresponding transformants in the presence of DNA-damaging agents did not report rescuing of the *Δgrx5* mutant phenotype when overexpressing any of the three genes. The same result was observed for oxidative stress conditions. These results suggest that the hypersensitivity of *Δgrx5* mutant cells to the agents is not due to deffects of ISC assembly and maturation of any of the three DNA metabolism proteins Pri2, Rad3 or Ntg2.

Overall, this study indicates that Grx5 (and in a more general way the mitochondrial machinery for ISC biogenesis) is required for maintaining the integrity of the nuclear genome, and that dysfunction of Grx5 causes constitutive DNA damage that requires DNA repair pathways (in particular HR) for cell survival, especially when additional DNA damage is induced by external genotoxic agents. Further research is needed to fully understand the intricate mechanism of DNA repair in the yeast model and through this model to level-up to humans, and the importance of mitochondrial functions for the stability of genetic information.

PART VI

CONCLUSIONS

The development of this thesis led to the following conclusions:

1. The *Δgrx5* mutant cells display high recombination and spontaneous mutation rates, which affects the stability of the chromosomal genome.

2. Genome instability is not dependent on the overloading of iron that occurs in cells lacking Grx5.

3. Cells not expressing Grx5 have higher levels of constitutive DNA damage that is specifically associated to Rad52-containig foci, but not to Rfa1-containing ones. This may be indicative of double strand breaks in DNA.

4. Cells lacking Grx5 and Ssq1 are hypersensitive to DNA-damaging agents (UV light, methyl methanesulfonate and hydroxyurea) in an additive way, and this sensitivity is independent of the constitutive oxidative stress state occurring in Grx5-minus cells. In addition, the overexpression of *SSQ1* rescues the hypersensitivity to the genotoxic agents in *Δgrx5* mutant cells.

5. The absence of Grx5 and Ssq1 proteins causes a delay in cell cycle progression through the S-phase. This delay, compared to wild type cells, is exacerbated by the addition of hydroxyurea.

6. The *Δgrx5* hypersensitivity to DNA-damaging agents is not exacerbated when the Nucleotide Excision Repair pathway (NER) is compromised, although the repair of thymine dimers is delayed in both, the *Δgrx5* and *Δssq1* mutants.

7. The repair functions of the Rad50 and Rad52 proteins, which are involved in the Homologous Recombination DNA repair pathway, are important for the survival of Grx5-deficient cells, as shown by the additional sensitivity to UV radiation, methyl methanesulfonate or hydroxyurea displayed by cells lacking both Grx5 and one of the above two proteins.

8. The additive hypersensitivity shown by the *Δrad50Δgrx5* and *Δrad52Δgrx5* double mutant cells in the presence of camptothecin confirms the possible role of homologous recombination in maintaining the viability of *Δgrx5* cells by repairing constitutive and camptothecin-induced double strand breaks damage.

9. The DNA damage checkpoint pathway, mediated by Mec1-Rad53-Dun1 is not activated in *Δgrx5* mutant cells, as the expression of the *RNR1-4* genes is not upregulated in these cells.

10. The hypersensitivity phenotype shown by the *Δgrx5* cells to the DNA-damaging agents is not due to deffects of ISC assembly and maturation of the Pri2, Rad3 or Ntg2 proteins, involved in DNA metabolism processes.

CONCLUSIONES

La realización de esta tesis ha dado lugar a las siguientes conclusiones:

1. Las células mutantes *Δgrx5* presentan unas altas frecuencias de recombinación y de mutación espontánea que afectan la estabilidad del genoma cromosómico.

2. La inestabilidad del genoma no depende de la acumulación de hierro que se produce en las células que carecen de Grx5.

3. Las células que no expresan Grx5 tienen mayores niveles de daño constitutivo en el ADN, que se asocia específicamente a la formación de "focis" asociados a Rad52, pero no asociados a Rfa1. Esto puede ser indicativo de roturas de doble cadena en el ADN.

4. Las células que carecen Grx5 y Ssq1 son hipersensibles a agentes que dañan el ADN (luz UV, metanosulfonato de metilo y hidroxiurea) de forma aditiva. Esta sensibilidad es independiente del estado de estrés oxidativo constitutivo que se produce en las células que carecen de Grx5. Por otro lado, la sobreexpresión de *SSQ1* rescata la hipersensibilidad a los agentes genotóxicos en células mutantes *Δgrx5*.

5. La ausencia de las proteínas Grx5 y Ssq1 provoca un retraso en la progresión del ciclo celular a través de la fase S. Este retraso, en comparación con el de las células de tipo salvaje, se ve agravado por la adición de hidroxiurea.

6. La hipersensibilidad del mutante *Δgrx5* a agentes que dañan el ADN no se agrava cuando se ve comprometida la vía de reparación de excisión de nucleótidos (NER), aunque la reparación de los dímeros de timina se retrasa en los mutantes *Δgrx5* y *Δssq1*.

7. Las funciones de reparación de las proteínas Rad50 y Rad52, implicadas en la vía de reparación del ADN por recombinación homóloga, son importantes para la supervivencia de las células deficientes en Grx5, como se demuestra por la sensibilidad adicional a la radiación UV, metanosulfonato de metilo o hidroxiurea mostrada por las células que carecen de Grx5 junto con una de las dos proteínas anteriores.

8. La hipersensibilidad aditiva que presentan las células mutantes dobles *Δrad50Δgrx5* y *Δrad52Δgrx5* en presencia de camptotecina confirma el posible papel de la recombinación homóloga en el mantenimiento de la viabilidad de las células,

posiblemente mediante la reparación de cortes de doble cadena de ADN del mutante *Δgrx5*, tanto a nivel constitutivo, como los producidos por la camptotecina.

9. La vía de punto de control de daño en el ADN mediada por Mec1-Rad53-Dun1 no se activa en las células mutantes *Δgrx5*, como se demuestra por la falta de inducción de los niveles de los genes *RNR1-4* en estas células.

10. El fenotipo de hipersensibilidad mostrado por las células *Δgrx5* a los agentes que dañan el ADN no es debido a defectos en el ensamblaje/maduración de las proteínas Pri2, Rad3 o Ntg2, involucradas en diversos procesos de metabolismo del ADN.

PART VII

REFERENCES

Aguilera, A., García-Muse, T. (2013). Causes of genome instability. *Annual Review of Genetics* 47, 1-32

Aguilera, A., Gómez-González, B. (2008). Genome instability: a mechanistic view of its causes and consequences. *Nature Reviews. Genetics* 9(3), 204–17

Ajit Bolar, N., Vanlander, A. V., Wilbrecht, C., Van der Aa, N., Smet, J., De Paepe, B., Vandeweyer, G., Kooy, F., Eyskens, F., De Latter, E., Delanghe, G., Govaert, P., Leroy, J.G., Loeys, B., Lill, R., Van Laer, L., Van Coster, R. (2013). Mutation of the iron-sulfur cluster assembly gene IBA57 causes severe myopathy and encephalopathy. *Human Molecular Genetics* 22(13), 2590–602

Alves, R., Vilaprinyo, E., Sorribas, A., Herrero, E. (2009). Evolution based on domain combinations: the case of glutaredoxins. *BioMed Central Evolutionary Biology* 9, 66

Alseth, I., Eide, L., Pirovano, M., Rognes, T., Seeberg, E., Bjoras, M. (1999). The Saccharomyces cerevisiae homologues of endonuclease III from Escherichia coli, Ntg1 and Ntg2, are both required for efficient repair of spontaneous and induced oxidative DNA damage in yeast. *Molecular and cellular biology* 19(5), 3779-87

Ames, B. N., Shigenaga, M. K., Hagen, T. M. (1993). Oxidants, antioxidants, and the degenerative diseases of aging. *Proceedings of the National Academy of Sciences of the United States of America* 90(17), 7915–22

Andreson, B. L., Gupta, A., Georgieva, B. P., Rothstein, R. (2010). The ribonucleotide reductase inhibitor, Sml1, is sequentially phosphorylated, ubiquitylated and degraded in response to DNA damage. *Nucleic Acids Research* 38(19), 6490–501

Ausubel, F. M., Brent, R., Kingston, R. E., Moore, D. D., Seidman, J. G., Smith, J. A., Struhl, K. (1994). *Current Protocols in Molecular Biology*. New York: John Wiley and Sons

Avery, A. M., Avery, S. V. (2001). Saccharomyces cerevisiae expresses three phospholipid hydroperoxide glutathione peroxidases. *The Journal of Biological Chemistry* 276(36), 33730–5

Babcock, M., de Silva D., Oaks, R., Davis-Kaplan, S., Jiralerspong, S., Monterimini, L., Pandolfo, M., Kaplan, J. (1997). Regulation of mitochondrial iron accumulation by Yfh1p, a putative homolog of frataxin. *Science* 276(5319), 1709–12

Bähler, J. (2005). Cell-cycle control of gene expression in budding and fission yeast. *Annual Review of Genetics* 39, 69–94

Balasundaram, D., Tabor, C. W., Tabor, H. (1993). Oxygen toxicity in a polyamine-depleted spe2 delta mutant of Saccharomyces cerevisiae. *Proceedings of the National Academy of Sciences of the United States of America* 90(10), 4693–7

Bandyopadhyay, S., Chandramouli, K., Johnson, M. K. (2008a). Iron-sulfur cluster biosynthesis. *Biochemestry Society Transactions* 36(Pt 6), 1112–9

Bandyopadhyay, S., Gama, F., Molina-Navarro, M. M., Gualberto, J. M., Claxton, R., Naik, S. G., Huynh, B. H., Herrero, E., Jacquot, J. P., Johnson M. K., Rouhier, N. (2008b). Chloroplast monothiol glutaredoxins as scaffold proteins for the assembly and delivery of [2Fe-2S] clusters. *The EMBO Journal* 27(7), 1122–33

Barbour, L., Xiao, W. (2003). Regulation of alternative replication bypass pathways at stalled replication forks and its effects on genome stability: a yeast model. *Mutation Research/Fundamental and Molecular Mechanisms of Mutagenesis* 532(1-2), 137–55

Beilschmidt, L. K, Puccio, H. M. (2014). Mammalian Fe-S cluster biogenesis and its implication in disease. *Biochimie* 100C, 48-60

Beinert, H., Holm, R. H., Münck, E. (1997). Iron-sulfur clusters: nature's modular, multipurpose structures. *Science* 277(5326), 653–9

Bellí, G., Garí, E., Piedrafita, L., Aldea, M., Herrero, E. (1998). An activator/repressor dual system allows tight tetracycline-regulated gene expression in budding yeast. *Nucleic Acids Research* 26(4), 942–7

Bellí, G., Polaina, J., Tamarit, J., De La Torre, M. A., Rodríguez-Manzaneque, M. T., Ros, J., Herrero, E. (2002). Structure-function analysis of yeast Grx5 monothiol glutaredoxin defines essential amino acids for the function of the protein. *The Journal of Biological Chemistry* 277(40), 37590–6

Bergstralh, D. T., Sekelsky, J. (2008). Interstrand crosslink repair: can XPF-ERCC1 be let off the hook? *Trends in Genetics* 24(2), 70–6

Bernardi, G. (2005). Lessons from a small, dispensable genome: the mitochondrial genome of yeast. *Gene* 354, 189–200

Bernstein, C., Bernstein, H., Payne, C. M., Garewal, H. (2002). DNA repair/pro-apoptotic dual-role proteins in five major DNA repair pathways: fail-safe protection against carcinogenesis. *Mutation Research* 511(2), 145–78

Berthelet, S., Usher, J., Shulist, K., Hamza, A., Maltez, N., Johnston, A., Fong, Y., Harris, L. J., Baetz, K. (2010). Functional genomics analysis of the Saccharomyces cerevisiae iron responsive transcription factor Aft1 reveals iron-independent functions. *Genetics* 185(3), 1111–28

Biaglow, J. E., Varnes, M. E., Roizen-Towle, L., Clark, E. P., Epp, E. R., Astor, M. B., Hall, E. J.(1986). Biochemistry of reduction of nitro heterocycles. *Biochemical pharmacology* 35(1), 77-90

Boiteux, S., Jinks-Robertson, S. (2013). DNA repair mechanisms and the bypass of DNA damage in Saccharomyces cerevisiae. *Genetics* 193(4), 1025–64

Bousset, K., Diffley, J. F. (1998). The Cdc7 protein kinase is required for origin firing during S-phase. *Genes & Development* 12(4), 480–90

Branzei, D., Foiani, M. (2008). Regulation of DNA repair throughout the cell cycle. *Nature Reviews. Molecular Cell Biology* 9(4), 297–308

Breitenbach, M., Rinnerthaler, M., Hartl, J., Stincone, A., Vowinckel, J., Breitenbach-Koller, H., Ralser, M. (2013). Mitochondria in ageing: there is metabolism beyond the ROS. *FEMS Yeast Research* 14, 198–212

Burhans, W. C., Weinberger, M. (2007). DNA replication stress, genome instability and aging. *Nucleic Acids Research* 35(22), 7545–56

Cabiscol, E., Piulats, E., Echave, P., Herrero, E., Ros, J. (2000). Oxidative stress promotes specific protein damage in Saccharomyces cerevisiae. *The Journal of Biological Chemistry* 275(35), 27393–8

Cai, L., Tu, B. P. (2012). Driving the cell cycle through metabolism. *Annual Review of Cell and Developmental Biology* 28, 59–87

Caldecott, K. W. (2001). Mammalian DNA single-strand break repair: an X-ra(y)ted affair. *BioEssays : News and Reviews in Molecular, Cellular and Developmental Biology* 23(5), 447–55

Calvo, S. E., Tucker, E. J., Compton, A. G., Kirby, D. M., Crawford, G., Burtt, N. P., Rivas, M., Guiducci, C., Bruno, D. L., Goldberger, O. A., Redman, M. C., Wiltshire, E., Wilson, C. J., Altshuler, D., Gabriel, S. B., Daly, M. J., Thorburn, D. R., Mootha, V. K. (2010). High-throughput, pooled sequencing identifies mutations in NUBPL and FOXRED1 in human complex I deficiency. *Nature Genetics* 42(10), 851–8

Camaschella, C., Campanella, A., De Falco, L., Boschetto, L., Merlini, R., Silvestri, L., Levi, S., Iolascon, A. (2007). The human counterpart of zebrafish shiraz shows sideroblastic-like microcytic anemia and iron overload. *Blood* 110(4), 1353–8

Castells-Roca, L., Mühlenhoff, U., Lill, R., Herrero, E., Bellí, G. (2011). The oxidative stress response in yeast cells involves changes in the stability of Aft1 regulon mRNAs. *Molecular Microbiology* 81(1), 232–48

Chabes, A., Georgieva, B., Domkin, V., Zhao, X., Rothstein, R., Thelander, L. (2003). Survival of DNA damage in yeast directly depends on increased dNTP levels allowed by relaxed feedback inhibition of ribonucleotide reductase. *Cell* 112(3), 391–401

Chabes, A., Stillman, B. (2007). Constitutively high dNTP concentration inhibits cell cycle progression and the DNA damage checkpoint in yeast Saccharomyces cerevisiae. *Proceedings of the National Academy of Sciences of the United States of America* 104(4), 1183–8

Cheng, N. H., Liu, J. Z., Brock, A., Nelson, R. S., Hirschi, K. D. (2006). AtGRXcp, an Arabidopsis chloroplastic glutaredoxin, is critical for protection against protein oxidative damage. *The Journal of Biological Chemistry* 281(36), 26280–8

Cheng, N. H., Liu, J. Z., Liu, X., Wu, Q., Thompson, S. M., Lin, J., Chang, J., Whitmham, S. A., Park, S., Cohen, J. D., Hirschi, K. D. (2011). Arabidopsis monothiol glutaredoxin, AtGRXS17, is critical for temperature-dependent postembryonic growth and development via modulating auxin response. *The Journal of Biological Chemistry* 286(23), 20398–406

Clémenson, C., Marsolier-Kergoat, M. C. (2009). DNA damage checkpoint inactivation: adaptation and recovery. *DNA Repair* 8(9), 1101–9

Cohen, G., Rapatz, W., Ruis, H. (1988). Sequence of the Saccharomyces cerevisiae CTA1 gene and amino acid sequence of catalase A derived from it. *European Journal of Biochemistry/FEBS* 176(1), 159–63

Collinson, E. J., Grant, C. M. (2003). Role of yeast glutaredoxins as glutathione S-transferases. *The Journal of Biological Chemistry* 278(25), 22492–7

Collinson, E. J., Wheeler, G. L., Garrido, E. O., Avery, A. M., Avery, S. V, Grant, C. M. (2002). The yeast glutaredoxins are active as glutathione peroxidases. *The Journal of Biological Chemistry* 277(19), 16712–7

Contamine, V., Picard, M. (2000). Maintenance and integrity of the mitochondrial genome: a plethora of nuclear genes in the budding yeast. *Microbiology and Molecular Biology Reviews* 64(2), 281–315

Costa, N. J., Dahm, C. C., Hurrell, F., Taylor, E. R., Murphy, M. P. (2003). Interactions of mitochondrial thiols with nitric oxide. *Antioxidants & Redox Signaling* 5(3), 291-305

Courel, M., Lallet, S., Camadro, J. M., Blaiseau, P. L. (2005). Direct activation of genes involved in intracellular iron use by the yeast iron-responsive transcription factor Aft2 without its paralog Aft1. *Molecular and Cellular Biology* 25(15), 6760–71

Couturier, J., Jacquot, J. P., Rouhier, N. (2009a). Evolution and diversity of glutaredoxins in photosynthetic organisms. *Cellular and Molecular Life Sciences* 66(15), 2539–57

Couturier, J., Koh, C. S., Zaffagnini, M., Winger, A. M., Gualberto, J. M., Corbier, C., Decottignies, P., Jacquot, J. P., Lemaire, S. D., Didjerjean, C., Rouhier, N. (2009b). Structure-function relationship of the chloroplastic glutaredoxin S12 with an atypical WCSYS active site. *The Journal of Biological Chemistry* 284(14), 9299–310

Crider, D. G., García-Rodríguez, L. J., Srivastava, P., Peraza-Reyes, L., Upadhyaya, K., Boldogh, I. R., Pon, L. A. (2012). Rad53 is essential for a mitochondrial DNA inheritance checkpoint regulating G1 to S progression. *The Journal of Cell Biology* 198(5), 793–8

Culotta, V. C., Howard, W. R., Liu, X. F. (1994). CRS5 encodes a metallothionein-like protein in Saccharomyces cerevisiae. *Journal of Biological Chemistry* 269(41), 25295–302

Daley, J. M., Palmbos, P. L., Wu, D., Wilson, T. E. (2005). Nonhomologous end joining in yeast. *Annual Review of Genetics* 39, 431–51

Dalle-Donne, I., Aldini, G., Carini, M., Colombo, R., Rossi, R., Milzani, A. (2006). Protein carbonylation, cellular dysfunction, and disease progression. *Journal of Cellular and Molecular Medicine* 10(2), 389–406

de Souza-Pinto, N. C., Mason, P. A., Hashiguchi, K., Weissman, L., Tian, J., Guay, D., Lebel, M., Stevnsner, T. V., Rasmussen, L. J., Bohr, V. A. (2009). Novel DNA mismatch-repair activity involving YB-1 in human mitochondria. *DNA Repair* 8(6), 704–19

Delaunay, A., Pflieger, D., Barrault, M. B., Vinh, J., Toledano, M. B. (2002). A thiol peroxidase is an H_2O_2 receptor and redox-transducer in gene activation. *Cell* 111(4), 471–81

Deponte, M. (2013). Glutathione catalysis and the reaction mechanisms of glutathione-dependent enzymes. *Biochimica et Biophysica Acta* 1830(5), 3217–66

Díaz de la Loza, M. del C., Gallardo, M., García-Rubio, M. L., Izquierdo, A., Herrero, E., Aguilera, A., Wellinger, R. E. (2011). Zim17/Tim15 links mitochondrial iron-sulfur cluster biosynthesis to nuclear genome stability. *Nucleic Acids Research* 39(14), 6002–15

Díaz de la Loza, M. del C., Wellinger, R. E. (2009). A novel approach for organelle-specific DNA damage targeting reveals different susceptibility of mitochondrial DNA to the anticancer drugs camptothecin and topotecan. *Nucleic Acids Research* 37(4), e26

Doudican, N. A., Song, B., Shadel, G. S., Doetsch, P. W. (2005). Oxidative DNA damage causes mitochondrial genomic instability in Saccharomyces cerevisiae. *Molecular and Cellular Biology* 25(12), 5196–204

Draculic, T., Dawes, I. W., Grant, C. M. (2000). A single glutaredoxin or thioredoxin gene is essential for viability in the yeast Saccharomyces cerevisiae. *Molecular Microbiology* 36(5), 1167–74

Drakulic, T., Temple, M. D., Guido, R., Jarolim, S., Breitenbach, M., Attfield, P. V, Dawes, I. W. (2005). Involvement of oxidative stress response genes in redox homeostasis, the level of reactive oxygen species, and ageing in Saccharomyces cerevisiae. *FEMS Yeast Research* 5(12), 1215–28

Dutkiewicz, R., Schilke, B., Cheng, S., Knieszner, H., Craig, E. A., Marszalek, J. (2004). Sequence-specific interaction between mitochondrial Fe-S scaffold protein Isu and Hsp70 Ssq1 is essential for their in vivo function. *The Journal of Biological Chemistry* 279(28), 29167–74

Eckers, E., Bien, M., Stroobant, V., Herrmann, J. M., Deponte, M. (2009). Biochemical characterization of dithiol glutaredoxin 8 from Saccharomyces cerevisiae : the catalytic redox mechanism redux. *Biochemistry* 48(6), 1410–23

Epp, O., Ladenstein, R., Wendel, A. (1983). The refined structure of the selenoenzyme glutathione peroxidase at 0.2nm resolution. *European Journal of Biochemistry / FEBS* 133(1), 51–69

Fan, H. Y., Cheng, K. K., Klein, H. L. (1996). Mutations in the RNA polymerase II transcription machinery suppress the hyperrecombination mutant hpr1 delta of Saccharomyces cerevisiae. *Genetics* 142(3), 749–59

Fernandes, A. P., Fladvad, M., Berndt, C., Andrésen, C., Lillig, C. H., Neubauer, P., Sunnerhagen, M., Holmgren, A., Vlamis-Gardikas, A. (2005). A novel monothiol glutaredoxin (Grx4) from Escherichia coli can serve as a substrate for thioredoxin reductase. *The Journal of Biological Chemistry* 280(26), 24544–52

Fernandes, A. P., Holmgren, A. (2004). Glutaredoxins: glutathione-dependent redox enzymes with functions far beyond a simple thioredoxin backup system. *Antioxidants & Redox Signaling* 6(1), 63-74

Finkemeier, I., Goodman, M., Lamkemeyer, P., Kandlbinder, A., Sweetlove, L. J., Dietz, K. J. (2005). The mitochondrial type II peroxiredoxin F is essential for redox homeostasis and root growth of Arabidopsis thaliana under stress. *The Journal of Biological Chemistry* 280(13), 12168–80

Finn, K., Lowndes, N. F., Grenon, M. (2012). Eukaryotic DNA damage checkpoint activation in response to double-strand breaks. *Cellular and Molecular Life Sciences* 69(9), 1447–73

Fiorani, P., Bjornsti, M. A. (2000). Mechanisms of DNA Topoisomerase I-Induced Cell Killing in the Yeast: Saccharomyces cerevisiae. *Annals of the New York Academy of Sciences* 922, 65–75

Fladvad, M., Bellanda, M., Fernandes, A. P., Mammi, S., Vlamis-Gardikas, A., Holmgren, A., Sunnerhagen, M. (2005). Molecular mapping of functionalities in the solution structure of reduced Grx4, a monothiol glutaredoxin from Escherichia coli. *The Journal of Biological Chemistry* 280(26), 24553–61

Flattery-O'Brien, J. A., Dawes, I. W. (1998). Hydrogen peroxide causes RAD9-dependent cell cycle arrest in G2 in Saccharomyces cerevisiae whereas menadione causes G1 arrest independent of RAD9 function. *The Journal of Biological Chemistry* 273(15), 8564–71

Flattery-O'Brien, J. A., Collinson, L. P., Dawes, I. W. (1993). Saccharomyces cerevisiae has an inducible response to menadione which differs from that to hydrogen peroxide. *Journal of General Microbiology* 139(3), 501–7

Foiani, M., Snatocanale, C., Plevani, P., Lucchini, G.(1989). A single essential gene, PRI2, encodes the large subunit of DNA primase in Saccharomyces cerevisiae. *Molecular and cellular biology* 9(7), 3081-7

Fontecave, M., Ollagnier-de-Choudens, S. (2008). Iron-sulfur cluster biosynthesis in bacteria: Mechanisms of cluster assembly and transfer. *Archives of Biochemistry and Biophysics* 474(2), 226–37

Frazzon, J., Dean, D. R. (2003). Formation of iron–sulfur clusters in bacteria: an emerging field in bioinorganic chemistry. *Current Opinion in Chemical Biology* 7(2), 166–73

Garí, E., Piedrafita, L., Aldea, M., Herrero, E. (1997). A set of vectors with a tetracycline-regulatable promoter system for modulated gene expression in Saccharomyces cerevisiae. *Yeast* 13(9), 837–48

Garrido, E. O., Grant, C. M. (2002). Role of thioredoxins in the response of Saccharomyces cerevisiae to oxidative stress induced by hydroperoxides. *Molecular Microbiology* 43(4), 993–1003

Ghezzi, P., Bonetto, V. (2003). Redox proteomics: identification of oxidatively modified proteins. *Proteomics* 3(7), 1145–53

Gietz, R. D., St Jean, A., Woods, R. A., Schiestl, R. H. (1992). Improved method for high efficiency transformation of intact yeast cells. *Nucleic Acids Research* 20(6), 1425

Gietz, R. D., Sugino, A. (1988). New yeast-Escherichia coli shuttle vectors constructed with in vitro mutagenized yeast genes lacking six-base pair restriction sites. *Gene* 74(2), 527–34

Gilbert, H. F. (1995). Thiol/disulfide exchange equilibria and disulfide bond stability. *Methods in Enzymology* 251, 8-28

Girard, P. M., Boiteux, S. (1997). Repair of oxidized DNA bases in the yeast Saccharomyces cerevisiae. *Biochimie* 79(9-10), 559–66

Gladyshev, V. N., Liu, A., Novoselov, S. V., Krysan, K., Sun, Q. A., Kryukov, V. M., Kryukov, G. V., Lou, M. F. (2001). Identification and characterization of a new mammalian glutaredoxin (thioltransferase), Grx2. *The Journal of Biological Chemistry* 276(32), 30374–80

Goldstein, A. L., McCusker, J. H. (1999). Three new dominant drug resistance cassettes for gene disruption in Saccharomyces cerevisiae. *Yeast* 15(14), 1541–53

Gredilla, R. (2010). DNA damage and base excision repair in mitochondria and their role in aging. *Journal of Aging Research* 2011, 257093

Gredilla, R., Bohr, V. A., Stevnsner, T. (2010). Mitochondrial DNA repair and association with aging--an update. *Experimental Gerontology* 45(7-8), 478–88

Gredilla, R., Garm, C., Stevnsner, T. (2012). Nuclear and mitochondrial DNA repair in selected eukaryotic aging model systems. *Oxidative Medicine and Cellular Longevity* 2012, 282438

Hamilton, M. L., Guo, Z., Fuller, C. D., Van Remmen, H., Ward, W. F., Austad, S. N., Troyer, D. A., Thompson, I., Richardson, A. (2001). A reliable assessment of 8-oxo-2-deoxyguanosine levels in nuclear and mitochondrial DNA using the sodium iodide method to isolate DNA. *Nucleic Acids Research* 29(10), 2117–26

Hanawalt, P. C. (2002). Subpathways of nucleotide excision repair and their regulation. *Oncogene* 21(58), 8949–56

Hanschmann, E. M., Godoy, J. R., Berndt, C., Hudemann, C., Lillig, C. H. (2013). Thioredoxins, glutaredoxins, and peroxiredoxins--molecular mechanisms and health significance: from cofactors to antioxidants to redox signaling. *Antioxidants & Redox Signaling* 19(13), 1539–605

Haunhorst, P., Berndt, C., Eitner, S., Godoy, J. R., Lillig, C. H. (2010). Characterization of the human monothiol glutaredoxin 3 (PICOT) as iron-sulfur protein. *Biochemical and Biophysical Research Communications* 394(2), 372–6

Herrero, E., Bellí, G., Casas, C. (2010). Structural and functional diversity of glutaredoxins in yeast. *Current Protein & Peptide Science* 11(8), 659–68.

Herrero, E., de la Torre-Ruiz, M. A. (2007). Monothiol glutaredoxins: a common domain for multiple functions. *Cellular and Molecular Life Sciences* 64(12), 1518–30

Herrero, E., Ros, J., Bellí, G., Cabiscol, E. (2008). Redox control and oxidative stress in yeast cells. *Biochimica et Biophysica Acta* 1780(11), 1217–35

Hochegger, H., Sonoda, E., Takeda, S. (2004). Post-replication repair in DT40 cells: translesion polymerases versus recombinases. *BioEssays : News and Reviews in Molecular, Cellular and Developmental Biology* 26(2), 151–8

Hoeijmakers, J. H. (2001). Genome maintenance mechanisms for preventing cancer. *Nature* 411(6835), 366–74

Holmgren, A. (1976). Hydrogen donor system for Escherichia coli ribonucleoside-diphosphate reductase dependent upon glutathione. *Proceedings of the National Academy of Sciences of the United States of America* 73(7), 2275–9

Howlett, N. G., Avery, S. V. (1997). Induction of lipid peroxidation during heavy metal stress in Saccharomyces cerevisiae and influence of plasma membrane fatty acid unsaturation. *Applied and Environmental Microbiology* 63(8), 2971–6

Huang, Y., Li, L. (2013). DNA crosslinking damage and cancer - a tale of friend and foe. *Translational Cancer Research* 2(3), 144–54

Huh, W. K., Falvo, J. V., Gerke, L. C., Carroll, A. S., Howson, R. W., Weissman, J. S., O'Shea, E. K. (2003). Global analysis of protein localization in budding yeast. *Nature* 425(6959), 686–91

Ingalls, B. P., Duncker, B. P., Kim, D. R., McConkey, B. J. (2007). Systems level modeling of the cell cycle using budding yeast. *Cancer Informatics* 3, 357–70

Inoue, Y., Matsuda, T., Sugiyama, K., Izawa, S., Kimura, A. (1999). Genetic analysis of glutathione peroxidase in oxidative stress response of Saccharomyces cerevisiae. *Journal of Biological Chemistry* 274(38), 27002–9

Izawa, S., Inoue, Y., Kimura, A. (1996). Importance of catalase in the adaptive response to hydrogen peroxide: analysis of acatalasaemic Saccharomyces cerevisiae. *The Biochemical Journal* 320(Pt 1), 61–7

Izquierdo, A., Casas, C., Herrero, E. (2010). Selenite-induced cell death in Saccharomyces cerevisiae: protective role of glutaredoxins. *Microbiology* 156(Pt 9), 2608–20

Izquierdo, A., Casas, C., Mühlenhoff, U., Lillig, C. H., Herrero, E. (2008). Saccharomyces cerevisiae Grx6 and Grx7 are monothiol glutaredoxins associated with the early secretory pathway. *Eukaryotic Cell* 7(8), 1415–26

Jackson, S. P., Bartek, J. (2009). The DNA-damage response in human biology and disease. *Nature* 461(7267), 1071–8

Jaffrey, S. R., Erdjument-Bromage, H., Ferris, C. D., Tempst, P., Snyder, S. H. (2001). Protein S-nitrosylation: a physiological signal for neuronal nitric oxide. *Nature Cell Biology* 3(2), 193–7

Jain, R., Vanamee, E. S., Dzikovski, B. G., Buku, A., Johnson, R. E., Prakash, L., Prakash, S., Aggarwal, A. K. (2014). An iron-sulfur cluster in the polymerase domain of yeast DNA polymerase ε. *Journal of Molecular Biology* 426(2), 301–8

Jamieson, D. J. (1998). Oxidative stress responses of the yeast Saccharomyces cerevisiae. *Yeast* 14(16), 1511–27

Johansson, C., Lillig, C. H., Holmgren, A. (2004). Human mitochondrial glutaredoxin reduces S-glutathionylated proteins with high affinity accepting electrons from either glutathione or thioredoxin reductase. *The Journal of Biological Chemistry* 279(9), 7537–43

Johnson, D. C., Dean, D. R., Smith, A. D., Johnson, M. K. (2005). Structure, function, and formation of biological iron-sulfur clusters. *Annual Review of Biochemistry*, 74, 247–81

Jun, S. H., Kim, T. G., Ban, C. (2006). DNA mismatch repair system. Classical and fresh roles. *The FEBS Journal* 273(8), 1609–19

Kamitani, S., Akiyama, Y., Ito, K. (1992). Identification and characterization of an Escherichia coli gene required for the formation of correctly folded alkaline phosphatase, a periplasmic enzyme. *The EMBO Journal* 11(1), 57–62

Kampinga, H. H., Craig, E. A. (2010). The Hsp70 chaperone machinery: J proteins as drivers of functional specificity. *Nature Reviews. Molecular Cell Biology* 11(8), 579–92

Kang, D., Hamasaki, N. (2002). Maintenance of mitochondrial DNA integrity: repair and degradation. *Current Genetics* 41(5), 311–22

Kanzok, S. M., Fechner, A., Bauer, H., Ulschmid, J. K., Müller, H. M., Botella-Munoz, J., Schneuwly, S., Schirmer, R., Becker, K. (2001). Substitution of the thioredoxin system for glutathione reductase in Drosophila melanogaster. *Science* 291(5504), 643–6

Kaplan, C. D., Kaplan, J. (2009). Iron acquisition and transcriptional regulation. *Chemical Reviews* 109(10), 4536–52

Karathia, H., Vilaprinyo, E., Sorribas, A., Alves, R. (2011). Saccharomyces cerevisiae as a model organism: a comparative study. *PLoS One* 6(2), e16015

Karpenshif, Y., Bernstein, K. A. (2012). From yeast to mammals: Recent advances in genetic control of homologous recombination. *DNA Repair* 11(10), 781–8

Kastan, M. B. (2008). DNA damage responses: mechanisms and roles in human disease: 2007 G.H.A. Clowes Memorial Award Lecture. *Molecular Cancer Research* 6(4), 517–24

Kerksick, C., Willoughby, D. (2005). The antioxidant role of glutathione and N-acetyl-cysteine supplements and exercise-induced oxidative stress. *Journal of the International Society of Sports Nutrition* 2, 38–44

Kispal, G., Csere, P., Guiard, B., Lill, R. (1997). The ABC transporter Atm1p is required for mitochondrial iron homeostasis. *FEBS Letters* 418(3), 346–50

Kispal, G., Csere, P., Prohl, C., Lill, R. (1999). The mitochondrial proteins Atm1p and Nfs1p are essential for biogenesis of cytosolic Fe/S proteins. *The EMBO Journal* 18(14), 3981–9

Klinge, S., Hirst, J., Maman, J. D., Krude, T., Pellegrini, L. (2007). An iron-sulfur domain of the eukaryotic primase is essential for RNA primer synthesis. *Natural Structure & Molecular Biology*, 14(9), 875–7

Kollberg, G., Tulinius, M., Melberg, A., Darin, N., Andersen, O., Holmgren, D., Oldfors, A., Holme, E. (2009). Clinical manifestation and a new ISCU mutation in iron-sulphur cluster deficiency myopathy. *Brain : A Journal of Neurology* 132(Pt 8), 2170–9

Kou, H., Zhou, Y., Gorospe, R. M. , Wang, Z. (2008). Mms19 protein functions in nucleotide excision repair by sustaining an adequate cellular concentration of the TFIIH component Rad3. *Proceedings of the National Academy of Sciences of the United States of America* 105(41), 15714-9

Krzepiłko, A., Swieciło, A., Wawryn, J., Zadrag, R., Kozioł, S., Bartosz, G., Biliński, T. (2004). Ascorbate restores lifespan of superoxide-dismutase deficient yeast. *Free Radical Research* 38(9), 1019–24

Kulkarni, A., Wilson, D. M. 3rd. (2008). The involvement of DNA-damage and repair defects in neurological dysfunction. *The American Journal of Human Genetics* 82(3), 539–66

Kumánovics, A., Chen, O. S., Li, L., Bagley, D., Adkins, E. M., Lin, H., Dingra, N. N., Outten C. E., Keller, G., Winge, D., Ward, D. M., Kaplan, J. (2008). Identification of FRA1 and FRA2 as genes involved in regulating the yeast iron regulon in response to decreased mitochondrial iron-sulfur cluster synthesis. *The Journal of Biological Chemistry* 283(16), 10276–86

Kurtz, J. E., Dufour, P., Duclos, B., Bergerat, J. P., Exinger, F.(2004). Saccharomyces cerevisiae: an efficient tool and model system for anticancer research. *Bulletin du cancer* 91(2), 133-9

Laurent, T. C., Moore, E. C., Reichard, P. (1964). Enzymatic synthesis of Deoxyribonucleotides* IV. Isolation and characterization of thioredoxin, the hydrogen donor from Escherichia coli b. *The Journal of Biological Chemistry* 239, 3436–44

Lehoczký, P., McHugh, P. J., Chovanec, M. (2007). DNA interstrand cross-link repair in Saccharomyces cerevisiae. *FEMS Microbiology Reviews* 31(2), 109–33

Lemaire, S. D. (2004). The glutaredoxin family in oxygenic photosynthetic organisms. *Photosynthesis Research* 79(3), 305–18

Lettier, G., Feng, Q., de Mayolo, A. A., Erdeniz, N., Reid, R. J. , Lisby, M., Mortensen, U. H., Rothstein, R. (2006). The role of DNA double-strand breaks in spontaneous homologous recombination in S. cerevisiae. *PLoS Genetics* 2(11), e194

Lewinska, A., Bilinski, T., Bartosz, G. (2004). Limited effectiveness of antioxidants in the protection of yeast defective in antioxidant proteins. *Free Radical Research* 38(11), 1159–65

Li, J., Kogan, M., Knight, S. A., Pain, D., Dancis, A. (1999). Yeast mitochondrial protein, Nfs1p, coordinately regulates iron-sulfur custer proteins, cellular iron uptake, and iron dstribution. *The Journal of Biological Chemistry* 274(46), 33025–34

Li, L., Jia, X., Ward, D. M., Kaplan, J. (2011). Yap5 protein-regulated transcription of the TYW1 gene protects yeast from high iron toxicity. *The Journal of Biological Chemistry* 286(44), 38488–97

Li, L., Miao, R., Bertram, S., Jia, X., Ward, D. M., Kaplan, J. (2012). A role for iron-sulfur clusters in the regulation of transcription factor Yap5-dependent high iron transcriptional responses in yeast. *The Journal of Biological Chemistry* 287(42), 35709–21

Lill, R. (2009). Function and biogenesis of iron-sulphur proteins. *Nature* 460(7257), 831–8

Lill, R., Dutkiewicz, R., Elsässer, H. P., Hausmann, A., Netz, D. J., Pierik, A. J., Stehling, O., Urzica, E., Muhlenhoff, U. (2006). Mechanisms of iron-sulfur protein maturation in mitochondria, cytosol and nucleus of eukaryotes. *Biochimica et Biophysica Acta* 1763(7), 652–67

Lill, R., Hoffmann, B., Molik, S., Pierik, A. J., Rietzschel, N., Stehling, O., Uzarska, M. A., Webert, H., Wilbrecht, C., Mühlenhoff, U. (2012). The role of mitochondria in cellular iron-sulfur protein biogenesis and iron metabolism. *Biochimica et Biophysica Acta* 1823(9), 1491–508

Lill, R., Mühlenhoff, U. (2005). Iron-sulfur-protein biogenesis in eukaryotes. *Trends in Biochemical Sciences* 30(3), 133–41

Lillig, C. H., Berndt, C., Holmgren, A. (2008). Glutaredoxin systems. *Biochimica et Biophysica Acta* 1780(11), 1304–17

Linares, G. R., Xing, W., Govoni, K. E., Chen, S. T., Mohan, S. (2009). Glutaredoxin 5 regulates osteoblast apoptosis by protecting against oxidative stress. *Bone* 44(5), 795–804

Lisby, M., Barlow, J. H., Burgess, R. C., Rothstein, R. (2004). Choreography of the DNA damage response: spatiotemporal relationships among checkpoint and repair proteins. *Cell* 118(6), 699–13

Lisby, M., Rothstein, R. (2005). Localization of checkpoint and repair proteins in eukaryotes. *Biochimie* 87(7), 579–89

Lisby, M., Rothstein, R., Mortensen, U. H. (2001). Rad52 forms DNA repair and recombination centers during S-phase. *Proceedings of the National Academy of Sciences of the United States of America* 98(15), 8276-82

Liu, H., Rudolf, J., Johnson, K. A., Mcmahon, S. A., Oke, M., Carter, L., Mcrobbie, A. M., Brown, S. E., Naismith, J. H., White, M. F. (2008). Structure of the DNA repair helicase XPD. *Cell* 133(5), 801–12

Liu, L., Trimarchi, J. R., Smith, P. J., Keefe, D. L. (2002). Mitochondrial dysfunction leads to telomere attrition and genomic instability. *Aging Cell* 1(1), 40–6

Liu, P., Qian, L., Sung, J. S., de Souza-Pinto, N. C., Zheng, L., Bogenhagen, D. F., Bohr, V. A., Wilson, D. M. 3rd, Shen, B., Demple, B. (2008). Removal of oxidative DNA damage via FEN1-dependent long-patch base excision repair in human cell mitochondria. *Molecular and Cellular Biology* 28(16), 4975–87

Longo, V. D., Gralla, E. B., Valentine, J. S. (1996). Superoxide dismutase activity is essential for stationary phase survival in Saccharomyces cerevisiae: Mitochondrial production of toxic oxygen species in vivo. *Journal of Biological Chemistry* 271(21), 12275–80

Luikenhuis, S., Perrone, G., Dawes, I. W., Grant, C. M. (1998). The yeast Saccharomyces cerevisiae contains two glutaredoxin genes that are required for protection against reactive oxygen species. *Molecular Biology of the Cell* 9(5), 1081–91

Lukianova, O. A., David, S. S. (2005). A role for iron-sulfur clusters in DNA repair. *Current Opinion in Chemical Biology* 9(2), 145–51

Lundberg, M., Johansson, C., Chandra, J., Enoksson, M., Jacobsson, G., Ljung, J., Johansson, M., Holmgren, A. (2001). Cloning and expression of a novel human glutaredoxin (Grx2) with mitochondrial and nuclear isoforms. *The Journal of Biological Chemistry* 276(28), 26269–75

Madeo, F., Fröhlich, E., Ligr, M., Grey, M., Sigrist, S. J., Wolf, D. H., Fröhlich, K. U. (1999). Oxygen stress: a regulator of apoptosis in yeast. *The Journal of Cell Biology* 145(4), 757–67

Maeda, T., Chua, P. P., Chong, M. T., Sim, A. B., Nikaido, O., Tron, V. A. (2001). Nucleotide excision repair genes are upregulated by low-dose artificial ultraviolet B: evidence of a photoprotective SOS response? *The Journal of Investigative Dermatology* 117(6), 1490–7

Martin, J. L. (1995). Thioredoxin--a fold for all reasons. *Structure* 3(3), 245–50

Martin, L. J. (2008). DNA damage and repair: relevance to mechanisms of neurodegeneration. *Journal of Neuropathology and Experimental Neurobiology* 67(5), 377–87

Matzuk, M. M., Lamb, D. J. (2008). The biology of infertility: research advances and clinical challenges. *Nature Medicine* 14(11), 1197–213

Mchugh, P. J., Sarkar, S. (2006). DNA interstrand cross-link repair in the cell cycle: a critical role for polymerase zeta in G1 phase. *Cell Cycle* 5(10), 1044–7

McVey, M. (2010). Strategies for DNA interstrand crosslink repair: insights from worms, flies, frogs, and slime molds. *Environmental and Molecular Mutagenesis* 51(6), 646–58

Memisoglu, A., Samson, L. (2000). Base excision repair in yeast and mammals. *Mutation Research*, 451(1-2), 39–51

Mesecke, N., Mittler, S., Eckers, E., Herrmann, J. M., Deponte, M. (2008). Two novel monothiol glutaredoxins from Saccharomyces cerevisiae provide further insight into iron-Sulfur cluster binding, oligomerization, and enzymatic activity of glutaredoxins. *Biochemistry* 47(5), 1452–63

Meyer, J. (2008). Iron-sulfur protein folds, iron-sulfur chemistry, and evolution. *Journal of Biological Inorganic Chemistry* 13(2), 157–70

Meyer, Y., Belin, C., Delorme-Hinoux, V., Reichheld, J. P., Riondet, C. (2012). Thioredoxin and glutaredoxin systems in plants: molecular mechanisms, crosstalks, and functional significance. *Antioxidants & Redox Signaling* 17(8), 1124–60

Meyer, Y., Buchanan, B. B., Vignols, F., Reichheld, J. P. (2009). Thioredoxins and glutaredoxins: unifying elements in redox biology. *Annual Review of Genetics* 43, 335–67

Michelet, L., Zaffagnini, M., Massot, V., Keryer, E., Vanacker, H., Miginiac-Maslow, M., Issakidis-Bourquet, E., Lemaire, S. D. (2006). Thioredoxins, glutaredoxins, and glutathionylation: new crosstalks to explore. *Photosynthesis Research* 89(2-3), 225–45

Mochel, F., Knight, M. A., Tong, W. H., Hernandez, D., Ayyad, K., Taivassalo, T., Andersen, P. M., Singleton, A., Rouault, T. A., Fischbeck, K. H., Haller, R. G. (2008). Splice mutation in the iron-sulfur cluster scaffold protein ISCU causes myopathy with exercise intolerance. *American Journal of Human Genetics* 82(3), 652–60

Molina-Navarro, M. M., Casas, C., Piedrafita, L., Bellí, G., Herrero, E. (2006). Prokaryotic and eukaryotic monothiol glutaredoxins are able to perform the functions of Grx5 in the biogenesis of Fe/S clusters in yeast mitochondria. *FEBS Letters* 580(9), 2273–80

Møller, I. M., Jensen, P. E., Hansson, A. (2007). Oxidative modifications to cellular components in plants. *Annual Review of Plant Biology* 58, 459–81

Morel, M., Kohler, A., Martin, F., Gelhaye, E., Rouhier, N. (2008). Comparison of the thiol-dependent antioxidant systems in the ectomycorrhizal Laccaria bicolor and the saprotrophic Phanerochaete chrysosporium. *The New Phytologist* 180(2), 391–407

Moriel-Carretero, M., Aguilera, A. (2010). A postincision-deficient TFIIH causes replication fork breakage and uncovers alternative Rad51-or Pol32-mediated restart mechanisms. *Molecular Cell* 37(5), 690–701

Moskovitz, J. (2005). Methionine sulfoxide reductases: ubiquitous enzymes involved in antioxidant defense, protein regulation, and prevention of aging-associated diseases. *Biochimica et Biophysica Acta* 1703(2), 213–9

Moskovitz, J., Berlett, B. S., Poston, J. M., Stadtman, E. R. (1997). The yeast peptide-methionine sulfoxide reductase functions as an antioxidant in vivo. *Proceedings of the National Academy of Sciences of the United States of America* 94(18), 9585–9

Mühlenhoff, U., Molik, S., Godoy, J. R., Uzarska, M. A., Richter, N., Seubert, A., Zhang, Y., Stubbe, J., Pierrel, F., Herrero, E., Lillig, C. H., Lill, R. (2010). Cytosolic monothiol glutaredoxins function in intracellular iron sensing and trafficking via their bound iron-sulfur cluster. *Cell Metabolism* 12(4), 373–85

Muller, E. G. (1996). A glutathione reductase mutant of yeast accumulates high levels of oxidized glutathione and requires thioredoxin for growth. *Molecular Biology of the Cell* 7(11), 1805–13

Muller, F. L., Liu, Y., Van Remmen, H. (2004). Complex III releases superoxide to both sides of the inner mitochondrial membrane. *The Journal of Biological Chemistry* 279(47), 49064–73

Navrot, N., Gelhaye, E., Jacquot, J. P., Rouhier, N. (2006). Identification of a new family of plant proteins loosely related to glutaredoxins with four CxxC motives. *Photosynthesis Research 89*(2-3), 71–9

Netz, D. J., Stith, C. M., Stümpfig, M., Köpf, G., Vogel, D., Genau, H. M., Stodola, J. L., Lill, R., Burgers, P. M., Pierik, A. J. (2011). Eukaryotic DNA polymerases require an iron-sulfur cluster for the formation of active complexes. *Nature Chemical Biology* 8(1), 125–32

Nitiss, J., Wang, J. C. (1988). DNA topoisomerase-targeting antitumor drugs can be studied in yeast. *Proceedings of the National Academy of Sciences of the United States of America* 85(20), 7501–5

Ojeda, L., Keller, G., Muhlenhoff, U., Rutherford, J. C., Lill, R., Winge, D. R. (2006). Role of glutaredoxin-3 and glutaredoxin-4 in the iron regulation of the Aft1 transcriptional activator in Saccharomyces cerevisiae. *The Journal of Biological Chemistry* 281(26), 17661–9

Pan, X., Ye, P., Yuan, D. S., Wang, X., Bader, J. S., Boeke, J. D. (2006). A DNA integrity network in the yeast Saccharomyces cerevisiae. *Cell* 124(5), 1069–81

Pedrajas, J. R., Kosmidou, E., Miranda-Vizuete, A., Gustafsson, J., A., Wright, A., P., Spyrou, G. (1999). Identification and functional characterization of a novel mitochondrial thioredoxin system in Saccharomyces cerevisiae. *The Journal of Biological Chemistry* 274(10), 6366–73

Peltomäki, P. (2003). Role of DNA mismatch repair defects in the pathogenesis of human cancer. *Journal of Clinical Oncology* 21(6), 1174–9

Penninckx, M. (2000). A short review on the role of glutathione in the response of yeasts to nutritional, environmental, and oxidative stresses. *Enzyme and Microbial Technology* 26(9-10), 737–42

Philpott, C. C., Protchenko, O. (2008). Response to iron deprivation in Saccharomyces cerevisiae. *Eukaryotic Cell* 7(1), 20–7

Pimentel, C., Vicente, C., Menezes, R. A., Caetano, S., Carreto, L., Rodrigues-Pousada, C. (2012). The role of the Yap5 transcription factor in remodeling gene expression in response to Fe bioavailability. *PLoS One* 7(5), e37434

Pokharel, S., Campbell, J. L. (2012). Cross talk between the nuclease and helicase activities of Dna2: role of an essential iron-sulfur cluster domain. *Nucleic Acids Research* 40(16), 7821–30

Porras, P., Padilla, C. A., Krayl, M., Voos, W., Bárcena, J. A. (2006). One single in-frame AUG codon is responsible for a diversity of subcellular localizations of glutaredoxin 2 in Saccharomyces cerevisiae. *The Journal of Biological Chemistry* 281(24), 16551–62

Poyton, R. O., Mcewen, J. E. (1996). Crosstalk between nuclear and mitochondrial genomes. *Annual Review of Biochemistry* 65, 563–607

Prado, F., Aguilera, A. (1995). Role of reciprocal exchange, one-ended invasion crossover and single-strand annealing on inverted and direct repeat recombination in yeast: different requirements for the RAD1, RAD10 and RAD52 genes. *Genetics* 139(1), 109-23

Pujol-Carrion, N., Belli, G., Herrero, E., Nogues, A., de la Torre-Ruiz, M. A. (2006). Glutaredoxins Grx3 and Grx4 regulate nuclear localisation of Aft1 and the oxidative stress response in Saccharomyces cerevisiae. *Journal of Cell Science* 119(Pt 21), 4554–64

Rasmussen, A. K., Chatterjee, A., Rasmussen, L. J., Singh, K. K. (2003). Mitochondria-mediated nuclear mutator phenotype in Saccharomyces cerevisiae. *Nucleic Acids Research* 31(14), 3909–17

Raspor, P., Plesnicar, S., Gazdag, Z., Pesti, M., Miklavcic, M., Lah, B., Logar-Marinsek, R., Poljsak, B. (2005). Prevention of intracellular oxidation in yeast: the role of vitamin E analogue, Trolox (6-hydroxy-2,5,7,8-tetramethylkroman-2-carboxyl acid). *Cell Biology International* 29(1), 57–63

Rodríguez-Manzaneque, M. T., Ros, J., Cabiscol, E., Sorribas, A., Herrero, E. (1999). Grx5 glutaredoxin plays a central role in protection against protein oxidative damage in Saccharomyces cerevisiae. *Molecular and Cellular Biology* 19(12), 8180–90

Rodríguez-Manzaneque, M. T., Tamarit, J., Bellí, G., Ros, J., Herrero, E. (2002). Grx5 is a mitochondrial glutaredoxin required for the activity of iron/sulfur enzymes. *Molecular Biology of the Cell* 13(4), 1109–21

Rotman, G., Shiloh, Y. (1999). ATM: a mediator of multiple responses to genotoxic stress. *Oncogene* 18(45), 6135–44

Rouault, T. A. (2012). Biogenesis of iron-sulfur clusters in mammalian cells: new insights and relevance to human disease. *Disease Models & Mechanisms* 5(2), 155–64

Rouault, T. A, Tong, W. H. (2005). Iron-sulphur cluster biogenesis and mitochondrial iron homeostasis. *Nature Reviews. Molecular Cell Biology* 6(4), 345–51

Rouault, T. A, Tong, W. H. (2008). Iron-sulfur cluster biogenesis and human disease. *Trends in Genetics* 24(8), 398–407

Rouhier, N. (2010). Plant glutaredoxins : pivotal players in redox biology and iron- sulphur centre assembly. *The New Phytologist* 186(2), 365–72

Rouhier, N., Couturier, J., Johnson, M. K., Jacquot, J. P. (2010). Glutaredoxins: roles in iron homeostasis. *Trends in Biochemical Sciences* 35(1), 43–52

Rouhier, N., Lemaire, S. D., Jacquot, J. P. (2008). The role of glutathione in photosynthetic organisms: emerging functions for glutaredoxins and glutathionylation. *Annual Review of Plant Biology* 59, 143–66

Rouhier, N., Unno, H., Bandyopadhyay, S., Masip, L., Kim, S. K., Hirasawa, M., Gualberto, J. M., Lattard, V., Kusunoki, M., Knaff, D. B., Georgiou, G., Hase, T., Johnson, M. K., Jacquot, J. P. (2007). Functional, structural, and spectroscopic characterization of a glutathione-ligated [2Fe-2S] cluster in poplar glutaredoxin C1. *Proceedings of the National Academy of Sciences of the United States of America* 104(18), 7379–84

Rudolf, J., Makrantoni, V., Ingledew, W. J., Stark, M. J., White, M. F. (2006). The DNA repair helicases XPD and FancJ have essential iron-sulfur domains. *Molecular Cell* 23(6), 801–8

Rutherford, J. C., Ojeda, L., Balk, J., Mühlenhoff, U., Lill, R., Winge, D. R. (2005). Activation of the iron regulon by the yeast Aft1/Aft2 transcription factors depends on mitochondrial but not cytosolic iron-sulfur protein biogenesis. *The Journal of Biological Chemistry* 280(11), 10135–40

Saleem, A., Edwards, T. K., Rasheed, Z., Rubin, E. H. (2000). Mechanisms of resistance to camptothecins. *Annals of the New York Academy of Sciences* 922, 46–55

Samper, E., Nicholls, D. G., Melov, S. (2003). Mitochondrial oxidative stress causes chromosomal instability of mouse embryonic fibroblasts. *Aging Cell* 2(5), 277–85

San Filippo, J., Sung, P., Klein, H. (2008). Mechanism of eukaryotic homologous recombination. *Annual Review of Biochemistry* 77, 229–57

Sanvisens, N., Bañó, M. C., Huang, M., Puig, S. (2011). Regulation of ribonucleotide reductase in response to iron deficiency. *Molecular Cell* 44(5), 759–69

Schär, P. (2001). Spontaneous DNA damage, genome instability, and cancer--when DNA replication escapes control. *Cell* 104(3), 329–32

Schild, D., Byers, B. (1978). Meiotic effects of DNA-defective cell division cycle mutations of Saccharomyces cerevisiae. *Chromosoma* 70(1), 109–30

Schilke, B., Voisine, C., Beinert, H., Craig, E. (1999). Evidence for a conserved system for iron metabolism in the mitochondria of Saccharomyces cerevisiae. *Proceedings of the National Academy of Sciences of the United States of America* 96(18), 10206–11

Sharpless, N. E., DePinho, R. A. (2007). How stem cells age and why this makes us grow old. *Nature Reviews. Molecular Cell Biology* 8(9), 703–13

Sherman, F. (2002). Getting Started with Yeast. *Methods of Enzymology* 350, 3–41

Siede, W., Friedberg, A. S., Friedberg, E. C. (1993). Evidence that the Rad1 and Rad10 proteins of Saccharomyces cerevisiae participate as a complex in nucleotide excision repair of UV radiation damage. *Journal of Bacteriology* 175(19), 6345–7

Silva, R. D., Sotoca, R., Johansson, B., Ludovico, P., Sansonetty, F., Silva, M. T., Peinado, J. M., Côrte-Real, M. (2005). Hyperosmotic stress induces metacaspase- and mitochondria-dependent apoptosis in Saccharomyces cerevisiae. *Molecular Microbiology* 58(3), 824–34

Stehling, O., Lill, R. (2013). The role of mitochondria in cellular iron–sulfur protein biogenesis: mechanisms, connected processes, and diseases. *Cold Spring Harbor Perspectives in Medicine* 3(7), 1–17

Stehling, O., Vashisht, A. A., Mascarenhas, J., Jonsson, Z. O., Sharma, T., Netz, D. J., Pierik, A. J., Wohlschegel, J. A.,Lill, R. (2012). MMS19 assembles iron-sulfur proteins required for DNA metabolism and genomic integrity. *Science* 337(6091), 195–9

Stehling, O.,Wilbrecht, C., Lill, R. (2014). Mitochondrial iron-sulfur protein biogenesis and human disease. *Biochimie* 100C, 61-77

Strain, J., Lorenz, C. R., Bode, J., Garland, S., Smolen, G. A., Ta, D. T, Vickery, L. E., Culotta, V. C. (1998). Suppressors of superoxide dismutase (SOD1) deficiency in Saccharomyces cerevisiae. Identification of proteins predicted to mediate iron-sulfur cluster assembly. *The Journal of Biological Chemistry* 273(47), 31138–44

Suizu, T., Tsutsumi, H., Ohtake, Y., Kawado, A., Imayasu, S., Kimura, A., Murata, K. (1994). Absolute glutathione requirement for sporulation of a yeast Saccharomyces cerevisiae. *Biochemical and Biophysical Research Communications* 205(2), 1151-4

Sundaram, S., Rathinasabapathi, B., Ma, L. Q., Rosen, B. P. (2008). An arsenate-activated glutaredoxin from the arsenic hyperaccumulator fern Pteris vittata L. regulates intracellular arsenite. *The Journal of Biological Chemistry* 283(10), 6095–101

Symington, L. S., Gautier, J. (2011). Double-strand break end resection and repair pathway choice. *Annual Review of Genetics* 45, 247–71

Szczesny, B., Hazra, T. K., Papaconstantinou, J., Mitra, S., Boldogh, I. (2003). Age-dependent deficiency in import of mitochondrial DNA glycosylases required for repair of oxidatively damaged bases. *Proceedings of the National Academy of Sciences of the United States of America* 100(19), 10670–5

Szederkényi, J., Komor, E., Schobert, C. (1997). Cloning of the cDNA for glutaredoxin, an abundant sieve-tube exudate protein from Ricinus communis L. and characterisation of the glutathione-dependent thiol-reduction system in sieve tubes. *Planta* 202(3), 349–56

Tamarit, J., Irazusta, V., Moreno-Cermeño, A., Ros, J. (2006). Colorimetric assay for the quantitation of iron in yeast. *Analytical Biochemistry* 351(1), 149–51

Toledano, M. B., Delaunay, A., Biteau, B., Spector, D., Azevedo, D. (2003). Oxidative stress responses in yeast. *Topics in Current Genetics*, 242–87

Trotter, E. W., Grant, C. M. (2003). Non-reciprocal regulation of the redox state of the glutathione-glutaredoxin and thioredoxin systems. *EMBO Reports* 4(2), 184–8

Trotter, E. W., Grant, C. M. (2005). Overlapping roles of the cytoplasmic and mitochondrial redox regulatory systems in the yeast Saccharomyces cerevisiae. *Eukaryotic Cell* 4(2), 392–400

Ueta, R., Fujiwara, N., Iwai, K., Yamaguchi-Iwai, Y. (2012). Iron-induced dissociation of the Aft1p transcriptional regulator from target gene promoters is an initial event in iron-dependent gene suppression. *Molecular and Cellular Biology* 32(24), 4998–5008

Uzarska, M. A., Dutkiewicz, R., Freibert, S. A., Lill, R., Mühlenhoff, U. (2013). The mitochondrial Hsp70 chaperone Ssq1 facilitates Fe/S cluster transfer from Isu1 to Grx5 by complex formation. *Molecular Biology of the Cell* 24(12), 1830–41

Valiathan, R. R., Weisman, L. S. (2008). Pushing for answers: is myosin V directly involved in moving mitochondria? *The Journal of Cell Biology* 181(1), 15–8

van Loon, A. P., Pesold-Hurt, B., Schatz, G. (1986). A yeast mutant lacking mitochondrial manganese-superoxide dismutase is hypersensitive to oxygen. *Proceedings of the National Academy of Sciences of the United States of America* 83(11), 3820–4

Veatch, J. R., Mcmurray, M. A., Nelson, Z. W., Gottschling, D. E. (2009). Mitochondrial dysfunction leads to nuclear genome instability via an iron-sulfur cluster defect. *Cell* 137(7), 1247–58

Vergara, S. V, Puig, S., Thiele, D. J. (2011). Early recruitment of AU-rich element-containing mRNAs determines their cytosolic fate during iron deficiency. *Molecular and Cellular Biology* 31(3), 417–29

Vickery, L. E., Cupp-Vickery, J. R. (2007). Molecular chaperones HscA/Ssq1 and HscB/Jac1 and their roles in iron-sulfur protein maturation. *Critical Reviews in Biochemistry and Molecular Biology* 42(2), 95–111

Vieira Dos Santos, C., Laugier, E., Tarrago, L., Massot, V., Issakidis-Bourguet, E., Rouhier, N., Rey, P. (2007). Specificity of thioredoxins and glutaredoxins as electron donors to two distinct classes of Arabidopsis plastidial methionine sulfoxide reductases B. *FEBS Letters* 581(23), 4371–6

Vilella, F., Alves, R., Rodríguez-Manzaneque, M. T., Bellí, G., Swaminathan, S., Sunnerhagen, P., Herrero, E. (2004). Evolution and cellular function of monothiol glutaredoxins: involvement in iron-sulphur cluster assembly. *Comparative and Functional Genomics* 5(4), 328–41

Vousden, K. H., Lane, D. P. (2007). P53 in health and disease. *Nature Reviews. Molecular Cell Biology* 8(4), 275–83

Wach, A., Brachat, A., Pöhlmann, R., Philippsen, P. (1994). New heterologous modules for classical or PCR-based gene disruptions in Saccharomyces cerevisiae. *Yeast* 10(13), 1793–808

Wang, C. H., Wu, S. B., Wu, Y. T., Wei, Y. H. (2013). Oxidative stress response elicited by mitochondrial dysfunction: implication in the pathophysiology of aging. *Experimental Biology and Medicine* 238(5), 450–60

Wingert R. A., Galloway J. L., Barut B., Foott H., Fraenkel P., Axe J. L., Weber G. J., Dooley K., Davidson A. J., Schmid B., Paw B. H., Shaw G. C., Kingsley P., Palis J., Schubert H., Chen, O., Kaplan J., Zon, L. I. (2005). Deficiency of glutaredoxin 5 reveals Fe-S clusters are required for vertebrate haem synthesis. *Nature* 436(7053), 1035–39

Witte, S., Villalba, M., Bi, K., Liu, Y., Isakov, N., Altman, A. (2000). Inhibition of the c-Jun N-terminal Kinase/AP-1 and NF-kappaB pathways by PICOT, a novel protein kinase C-interacting protein with a thioredoxin homology domain. *Journal of Biological Chemistry* 275(3), 1902–9

Wu, X., Huang, M. (2008). Dif1 controls subcellular localization of ribonucleotide reductase by mediating nuclear import of the R2 subunit. *Molecular and Cellular Biology* 28(23), 7156–67

Wu, Y., Kantake, N., Sugiyama, T., Kowalczykowski, S. C. (2008). Rad51 protein controls Rad52-mediated DNA annealing. *The Journal of Biological Chemistry* 283(21), 14883–92

Xu, X. M., Møller, S. G. (2008). Iron-sulfur cluster biogenesis systems and their crosstalk. *Chembiochem* 9(15), 2355–62

Xu, X. M., Møller, S. G. (2011). Iron-sulfur clusters: biogenesis, molecular mechanisms, and their functional significance. *Antioxidants & Redox Signaling* 15(1), 271–307

Yamaguchi-Iwai, Y., Ueta, R., Fukunaka, A., Sasaki, R. (2002). Subcellular localization of Aft1 transcription factor responds to iron status in Saccharomyces cerevisiae. *The Journal of Biological Chemistry* 277(21), 18914–8

Yazgan, O., Krebs, J. E. (2012). Mitochondrial and nuclear genomic integrity after oxidative damage in Saccharomyces cerevisiae. *Frontiers in Bioscience* 17, 1079–93

Ye, H., Jeong, S. Y., Ghosh, M. C., Kovtunovych, G., Silvestri, L., Ortillo, D., Uchida, N., Tisdale, J., Camaschella, C., Rouault, T. A. (2010). Glutaredoxin 5 deficiency causes sideroblastic anemia by specifically impairing heme biosynthesis and depleting cytosolic iron in human erythroblasts. *Journal of Clinical Investigation*, 120(5), 1749–61

Yuen, K. W., Warren, C. D., Chen, O., Kwok, T., Hieter, P., Spencer, F. A. (2007). Systematic genome instability screens in yeast and their potential relevance to cancer. *Proceedings of the National Academy of Sciences of the United States of America* 104(10), 3925–30

Zaffagnini, M., Michelet, L., Massot, V., Trost, P., Lemaire, S. D. (2008). Biochemical characterization of glutaredoxins from Chlamydomonas reinhardtii reveals the unique properties of a chloroplastic CGFS-type glutaredoxin. *The Journal of Biological Chemistry* 283(14), 8868–76

Zhang, Z., An, X., Yang, K., Perlstein, D. L., Hicks, L., Kelleher, N., Stubbe, J., Huang, M. (2006). Nuclear localization of the Saccharomyces cerevisiae ribonucleotide reductase small subunit requires a karyopherin and a WD40 repeat protein. *Proceedings of the National Academy of Sciences of the United States of America* 103(5), 1422–7

Zhao, X. J., Muller, E. G., Rothstein, R. (1998). A suppressor of two essential checkpoint genes identifies a novel protein that negatively affects dNTP pools. *Molecular Cell* 2(3), 329–40

Zhao, X. J., Raitt, D., V Burke, P., Clewell, A. S., Kwast, K. E., Poyton, R. O. (1996). Function and expression of flavohemoglobin in Saccharomyces cerevisiae. Evidence for a role in the oxidative stress response. *Journal of Biological Chemistry* 271(41), 25131–8

Zheng, L., Cash, V. L., Flint, D. H., Dean, D. R. (1998). Assembly of iron-sulfur clusters. Identification of an iscSUA-hscBA-fdx gene cluster from Azotobacter vinelandii. *Journal of Biological Chemistry* 273(21), 13264–72

APPENDIX

In the following chapter we presented the paper submitted to "The Plant Journal" entitled "The nucleo-cytoplasmic *Arabidopsis thaliana* glutaredoxin S17 integrates environmental signals for proper meristem differentiation". It is posted as an Appendix because it has no direct connexion to the main theme of this thesis.

The nucleo-cytoplasmic *Arabidopsis thaliana* glutaredoxin S17 integrates environmental signals for proper meristem differentiation

Nicolas König[1,†], Christophe Riondet[2,†], **Carlos Maria[3]**, Inga Kruse[4], Noëlle Bécuwe[5,6,7], Johannes Knuesting[1], Carsten Berndt[8,9], Sébastien Tourrette[5,6,7], Jocelyne Guilleminot-Montoya[2], Enrique Herrero[3], Frédéric Gaymard[10], Janneke Balk[4], Gemma Belli[3], Renate Scheibe[1], Jean-Philippe Reichheld[2], Nicolas Rouhier[11,12] and Pascal Rey[5,6,7*]

[1] Department of Plant Physiology, FB5, University of Osnabrueck, D-49069 Osnabrueck, Germany

[2] Laboratoire Génome et Développement des Plantes, UMR 5096 CNRS-UPVD, 58 Avenue de Villeneuve - Bat T, 66860 Perpignan Cedex, France

[3] Departament de Ciències Mèdiques Bàsiques, IRBLleida, Universitat de Lleida, Montserrat Roig 2, 25008 Lleida, Spain

[4] Department of Biological Chemistry, John Innes Centre, Norwich NR4 7UH, United Kingdom

[5] CEA, DSV, IBEB, Laboratoire d'Ecophysiologie Moléculaire des Plantes, Saint-Paul-lez-Durance, F-13108, France

[6] CNRS, UMR 7265 Biologie Végétale & Microbiologie Environnementale, Saint-Paul-lez-Durance, F-13108, France

[7] Aix-Marseille Université, Saint-Paul-lez-Durance, F-13108, France

[8] Division for Biochemistry, Department for Medical Biochemistry and Biophysics, Karolinska Institutet, 17177 Stockholm, Sweden

[9] Heinrich-Heine-University, Department of Neurology, Medical Faculty, Merowinger Platz 1a, 40225 Düsseldorf, Germany

[10] Biochimie et Physiologie Moléculaire des Plantes, Centre National de la Recherche Scientifique, Institut National de la Recherche Agronomique, Université Montpellier 2, Montpellier Cedex 1, France

[11] Université de Lorraine, Interactions Arbres - Microorganismes, UMR1136, F-54500 Vandoeuvre-lès-Nancy, France

[12] INRA, Interactions Arbres - Microorganismes, UMR1136, F-54280 Champenoux, France

[†] The authors have equally contributed to the work

[*] Corresponding author

Pascal Rey

CEA, DSV, IBEB, Laboratoire d'Ecophysiologie Moléculaire des Plantes, Saint-Paul-lez-Durance, F-13108, France

Phone: ++33 442254776

E-mail: pascal.rey@cea.fr

Running head*:* Temperature and photoperiod signaling via GrxS17

Keywords: Glutaredoxin, development, meristem, *Arabidopsis thaliana*, photoperiod, temperature, nucleus, redox regulation, iron-sulfer cluster.

Word count : ca. 7050 (13-03-2014)

Summary: 192
Introduction: 687
Results: 2675
Discussion: 1499
Experimental procedures; 1091
Acknowledgements; 75
Figure and table legends: 829

Summary

Glutaredoxins (Grxs) are involved in redox regulation through the reduction of protein disulphide bonds but they are also associated to iron sensing and iron-sulphur (Fe-S) cluster trafficking owing to their capacity to bind Fe-S clusters. The role of Arabidopsis nucleo-cytoplasmic GrxS17 was investigated by combining genetic, biochemical and physiological approaches. The recombinant protein can bind three [2Fe-2S] clusters into a dimer, a property that likely contributes to its capacity to complement the defects in Fe-S cluster assembly of a yeast strain null for the mitochondrial Grx5. However, an Arabidopsis mutant knock-out for GrxS17 expression did not show alteration in the activity of two cytosolic Fe-S proteins, aconitase and aldehyde oxidase. In conditions of long day or high temperature, *grxS17* plants exhibit a severely altered phenotype, having abnormal apical meristem, elongated leaves and impaired flowering. When both environmental conditions are combined, GrxS17 deficient plants display complete growth arrest. Using affinity chromatography and split-YFP methods, a nuclear factor termed NF-YC11/NC2α and involved in regulation of transcription was identified as interacting with GrxS17. We propose that GrxS17 relays redox signals in response to environmental variations for the proper expression of genes involved in meristem activity.

INTRODUCTION

Glutaredoxins (Grxs) are small oxidoreductases structurally related to thioredoxins (Trxs) and present in most living organisms (Rouhier et al., 2008; Meyer et al., 2009). Their capacity to reduce disulphide bonds is usually dependent on glutathione and relies on a 4-residue active-site motif comprising at least one redox-active cysteine (Rouhier et al., 2006). In higher plants, glutaredoxins are encoded by multigene families and subdivided into four classes (Couturier et al., 2009). Grxs from classes I and II are present in all photosynthetic organisms and possess mostly CPXC and CGFS active sites, respectively. Grxs from class III are restricted to terrestrial plants and display a CCXX motif. Those from class IV are present both in algae and in terrestrial plants and are composed of three domains, one N-terminal Grx module carrying a CXXC/S motif followed by two domains of unknown function

The recognized biochemical function of Grxs is the reduction of disulphide bonds mostly in glutathionylated target proteins (Rouhier et al., 2008), through which they likely regulate the activity of metabolic enzymes and transcriptional regulators (Michelet et al., 2005; Li et al., 2009; Murmu et al., 2010, Couturier et al., 2014). They also participate in the regeneration of thiol-dependent antioxidant enzymes (Rouhier et al., 2001; Gama et al., 2007; Tarrago et al., 2009; Couturier et al., 2011). Besides, novel functions have been proposed for class I and II Grxs owing to their capacity to bind iron-sulphur (Fe-S) clusters (Rouhier et al., 2007; Bandyopadhyay et al., 2008; Rouhier et al., 2010). As oxidized glutathione promotes Fe-S cluster disassembly from human Grx2 and restores its disulphide reductase activity, class I Grxs might constitute redox sensors (Lillig et al., 2005). Grxs belonging to class II, also called monothiol Grxs, seem intimately linked

to iron metabolism. Those present in organelles participate in Fe-S cluster assembly machineries likely as Fe-S carriers from scaffold proteins to acceptor proteins (Rodriguez-Manzaneque et al., 2002; Mühlenhoff et al., 2003; Bandyopadhyay et al., 2008) whereas nucleo-cytoplasmic monothiol Grxs participate in iron sensing and trafficking in yeast and animals (Ojeda et al., 2006; Pujol-Carrion et al., 2006; Kumanovics et al., 2008; Mühlenhoff et al., 2010; Haunhorst et al., 2013).

Recently, essential roles of plant Grxs have been unveiled in developmental processes and in stress responses. Several Arabidopsis Grxs from class III participate in the tolerance to photooxidative stress (Laporte et al., 2012) and in the defense against pathogens (Ndamukong et al., 2007; La Camera et al., 2011). Others, like GrxC7 and C8, are required for proper reproductive development through an interaction with TGA transcription factors (Xing and Zachgo, 2008; Li et al., 2009; Murmu et al., 2010). Concerning class I Grxs, an Arabidopsis mutant deficient in both GrxC1 and C2 has a lethal phenotype due to impaired embryo development (Riondet et al., 2012). Among the four class II Grxs (S14, S15, S16 and S17), the plastidial S14 isoform participates in arsenic tolerance in a hyperaccumulating fern (Sundaram et al., 2008) and in response to high temperature in *A. thaliana* (Sundaram and Rathinasabapathi, 2010). Tomato plants silenced for the expression of GrxS16, also located in plastids, display increased sentivity to osmotic stress (Guo et al., 2010). Organellar GrxS14 and GrxS15 seem also to participate in the maturation of Fe-S clusters and responses to oxidative stress (Cheng et al., 2006; Bandyopadhyay et al., 2008; Cheng, 2008). Concerning GrxS17, Arabidopsis knockdown lines C exhibit at 28° inhibition of primary root growth, impaired flowering and altered sensitivity to auxin compared to Wt (Cheng et al., 2011). Accordingly, expression of Arabidopsis GrxS17 in tomato plants results in enhanced thermo-tolerance (Wu et al., 2012).

In this work, we further examined the physiological role of Arabidopsis GrxS17 in relation with its possible biochemical functions. Although recombinant GrxS17 incorporates [2Fe-2S] clusters and complements the yeast *grx5* mutant, the activity of two cytosolic Fe-S cluster enzymes is not modified in *grxS17* plants. These plants exhibit defects in the meristematic area and delayed flowering depending on photoperiod conditions. We show that GrxS17 interacts with NF-YC11 a nuclear factor involved in regulating transcription, suggesting a fundamental role in the control of meristem functioning through redox-based mechanisms related to environmental signals.

RESULTS

Protein architecture

The *A. thaliana* GrxS17 possesses an N-terminal thioredoxin-like domain deprived of the canonical CGPC active site, followed by three Grx domains containing CGFS motifs (Fig. 1A). This architecture is unique to land plants, since mammalian, fungal and algal homologs are constituted by one Trx and maximally two Grx domains (Couturier et al., 2009). From secondary structure prediction and 3D-structure modeling, the four domains of plant GrxS17 all adopt a classical Trx fold and are connected by quite long linker

sequences, which might provide flexibility to the protein (Fig. S1). The Grx GrxS17modules share 62 to 65% identity and are subsequently referred to as M2**,** M3 and M4.

A recombinant *A. thaliana* GrxS17 binds Fe-S clusters

GrxS17 and variants carrying Cys substitutions were produced in *E. coli* to analyze their capacity to incorporate Fe-S clusters *in vitro*. First, the GrxS17 oligomeric state was estimated using exclusion chromatography. Both Wt and triple Cys mutant eluted as a single peak whose estimated molecular mass, 104 kDa, corresponds to a dimeric form (Fig. S2). *E. coli* cells expressing Wt GrxS17 displayed a brown pellet, revealing the protein ability to bind Fe-S clusters like other Arabidopsis CGFS Grxs (Bandyopadhyay et al., 2008). Since Fe-S clusters proved to be oxygen sensitive, the nature of the Fe-S clusters was assessed by anaerobic IscS-mediated *in vitro* reconstitution from apo-GrxS17. The UV-visible spectrum of reconstituted protein is typical of the presence of [2Fe-2S] clusters, which display a major absorption band at 420 nm (Fig. 1B). Estimation of the iron content in a freshly reconstituted Wt protein indicated the presence of 2.48 ±0.58 Fe atoms/monomer. Assuming that the holoprotein is dimeric and that each Grx domain contributes to the binding of one Fe-S cluster, as found for animal orthologs, it indicated the presence of ~2.5 [2Fe-2S] cluster/dimer (Haunhorst et al., 2010). Then, to investigate the contribution of each domain, the active site cysteines were replaced by serines in each domain or in all three. Whereas the triple-Cys mutant did not incorporate any Fe-S cluster upon *in vitro* reconstitution, variants carrying one single Cys substitution all incorporated between 40 to 60% of clusters as assessed by relative absorbance measurements at 420 nm (Fig. 1C). Altogether, these data indicate that GrxS17 incorporates up to three $[2Fe\text{-}2S]^{2+}$ clusters in a dimer and that all Grx domains contribute to the binding.

***A. thaliana* GrxS17 rescues most yeast *grx5* mutant phenotypes**

13.1. To gain insight into a possible role of GrxS17 as an Fe-S cluster carrier, its capacity to rescue the defects of a yeast *grx5* mutant was examined. The entire protein and the three Grx domains were fused to the targeting sequence of Grx5 to allow mitochondrial compartmentalization. Phenotype studies indicate that only the entire protein, and the M3 module to a lesser extent, rescued the sensitivity to *t*-BOOH and diamide oxidants (Fig. 2A). Both also fully rescued the ability to express active aconitase holoenzyme (Fig. 2C) and nearly totally the cytosolic isopropylmalate isomerase activity (Leu1) activity, a marker of the Fe-S sensing and signalling between mitochondria and cytoplasm (Fig. 2D). Concerning growth in respiratory conditions, both M3 and M4 modules, in addition to the entire GrxS17 molecule, totally or partially rescued the *S. cerevisiae grx5* phenotype (Fig. 2B).

We then checked the expression of iron uptake genes by determining the transcript levels of two reporter genes of the Aft1 regulon, *FTR1* and *FIT3*. Of the three modules, only M3 allowed down-regulation of both genes when expressed in the *grx5* mutant as observed in Wt cells, while the entire GrxS17 molecule was totally

unable to rescue the mutant phenotype (Fig. 2E). Accordingly, the M3 domain suppressed the increased iron content in *grx5* mutant, like strikingly the entire GrxS17 protein (Fig. 2F).

To summarize, the entire GrxS17 rescued all the *grx5* mutant phenotypes but the deregulation of the Aft1 transcriptional factor, indicating that one component participating in iron status signalling is still deficient. This could be due to steric incompatibility linked to the modular architecture of GrxS17 compared to yeast Grx5. Surprisingly, considering that all Grx domains are very close and able to incorporate an Fe-S cluster, they do not have equivalent capacities to complement the *grx5* mutant.

Expression of GrxS17 in plant organs and subcellular localization

In *A. thaliana*, quantitative RT-PCR and promoter-GUS fusion data revealed high levels of *GrxS17* expression in growing leaves and anthers (Cheng et al., 2011). To further delineate *GrxS17* expression territories, we achieved *in situ* hybridization experiments on shoot apical meristem (SAM) and flowers of Wt plants grown under standard conditions. A strong digoxigenin staining was found in all meristematic cells, particularly in stem cells. Strong staining was also found in flower tissues (Fig. 3A). We then investigated GrxS17 abundance using a serum raised against the whole recombinant protein. The serum specifically recognized a protein at *ca.* 50 kDa in all organs analysed, the abundance being substantially high in stems, young leaves and flowers. Note that the band position varies in leaf samples due to high RubisCO abundance (Fig. 3B). Altogether, these data indicate that *GrxS17* is expressed in very different cell types in meristematic, reproductive and vascular tissues.

We then investigated the GrxS17 subcellular localization in Arabidopsis cells. Transient expression in protoplasts (Fig. 4A) and stable expression (Fig. 4B) of Pr_{35S}*:GrxS17:GFP* fusion indicated that the protein is targeted to both cytoplasm and nucleus. The nuclear localization is surprising considering the size of the fusion protein, which should be too big to freely diffuse through nuclear pores, and the absence of recognizable nuclear localization signal in GrxS17 sequence. Therefore we prepared nuclear and cytosolic fractions from Arabidopsis inflorescences. Their relative purity was verified using sera raised against Trxh5 (Marchal et al., 2013) and Nuc 1, used respectively as cytosolic and nuclear markers (Pontvianne et al., 2010). The latter specifically revealed one 100-kDa band in the nuclei-enriched fraction, and the former one 15-kDa band in the cytosolic fraction (Fig. 4C). Concerning GrxS17, the protein was detected in both fractions in agreement with fusion protein data.

Using bimolecular fluorescence complementation (BiFC) *i.e.*, by transiently expressing two *GrxS17* constructs fused to half YFPs in *Arabidopsis* protoplasts, the observed YFP signal first confirmed the nucleocytoplasmic localization but also indicated that GrxS17 forms dimers also *in vivo* (Fig. 4E). The GrxS17 dimerization capacity was further investigated from crude leaf extracts incubated with a cross-linker compound, dimethyl pimelimidate•2 HCl (DMP), and analyzed by Western blots after non-reducing SDS-PAGE. A single band at 50 kDa was

apparent in untreated proteins, whereas a strong additional 100-kDa band, very likely corresponding to a GrxS17 dimer, was revealed in the same extract incubated with DMP (Fig. 4D).

Activity of cytosolic Fe-S cluster enzymes in Arabidopsis lines modified for *GrxS17* expression

Homozygous Arabidopsis mutant plants (SALK_021301) knockout for *GrxS17* expression were selected (Fig. S3). The mutant line was transformed to restore *GrxS17* expression under the control of the CaMV-35S promoter. In two independent $S17^{-}/S17^{+}$ lines, termed 3.3 and 17.8, the presence of *GrxS17* cDNA and a high GrxS17 protein level, particularly in the line 17.8, were observed (Fig. S3).

Based on the ability of recombinant *A. thaliana* GrxS17 to bind Fe-S clusters and the rescue by GrxS17 of Fe-S enzymes in the yeast *grx5* mutant, its contribution to the maturation of Fe-S proteins was investigated in *Arabidopsis* plants. The activities of cytosolic aconitase and aldehyde oxidase, two Fe-S enzymes possessing respectively a [4Fe-4S] cluster or a FAD, molybdenum (MoCo) and two [2Fe-2S] clusters as cofactors, were measured relatively to xanthine dehydrogenase, a MoCo-containing enzyme (Fig. S4). All measurements were performed using 2-week old plants grown under conditions where no macroscopic phenotype is visible (22°C for 14 days) or leading to impaired growth (22°C for 7 days followed by 28°C for 7 days) (see below). An *A. thaliana* mutant for the ABC transporter ATM1 (M29), in which cytosolic aconitase and aldehyde oxidase activities are affected, was used for comparison. Overall, we did not detect significant differences for aconitase and aldehyde oxidase activities in plants modified for *GrxS17* expression indicating no defect in the Fe-S cluster assembly of these proteins

Vegetative development of the *grxS17* mutant as a function of photoperiod

The phenotype characteristics of *GrxS17* mutant and complemented lines were then investigated under various light and temperature conditions. When cultivated under standard conditions *e.g.*, a 22°C/18°C regime, an 8-h photoperiod and moderate light (200 µmoles photons.m^{-2}.s^{-1}), all lines showed similar development (Fig. 5A). We then transferred 2-week old seedlings grown under standard conditions at 28°C (night and day) and the same light conditions. After a few days, we observed that high temperature strongly impaired the development of all genotypes, which displayed thin and elongated leaves. In *grxS17* plants, the absence of very young leaves was clearly visible after two weeks at high temperature (Fig. 5B, arrow). In the complemented line 3.3, some small leaflets developed, whereas in the line 17.8, leaf development was not affected. These data, consistent with the known thermo-sensitivity of *grxS17* plants (Cheng et al., 2011), reveal that the functioning of the shoot apical meristem is impaired in this mutant at high temperature. Then, plants were grown at standard temperature and light intensity, but under long photoperiod (16 h). Most interestingly, we observed that 4-week old *grxS17* plants displayed thickened-lamina and elongated leaves. Furthermore, the development of the main floral spike was strongly delayed compared to Wt (Fig. 5E). This observation achieved at 22°C raised the question of a light-related effect on

mutant development. To gain further insight, 3-week old plants grown under standard conditions were transferred to continuous light (200 µmoles photons.m^{-2}.s^{-1}) at 22°C. *GrxS17* plants rapidly exhibited a strong phenotype, their leaves turning thick and curved (Fig. 5F). Moreover, the floral spike development was completely abolished in the mutant, but not or slightly altered in complemented lines (Fig. 5F).

To analyse whether the effect of day length could be related to the amount of received light energy, plants grown for 3 weeks under standard conditions were transferred to high light (500 µmoles photons.m^{-2}.s^{-1}) at 22°C and short photoperiod. There was no change in the development of mutant plants in this light regime (Fig. S5), clearly revealing that photoperiod length is the primary determinant underlying the light-related phenotype. When plants were grown under the same high light intensity under long day, mutant plants exhibited strongly impaired development (Figs. S5B and S6G). It is worth mentioning that the temperature measured at the plant level is elevated by 2°C (24°C) in high-light conditions, thus possibly explaining the more severe mutant phenotype in long day at high light compared to moderate light.

When combining high temperature and long day, we observed that the growth of *grxS17* plants was entirely stopped after a few days, as illustrated by the much smaller leaf size and the absence of newly formed leaves (Fig. 5C). Noteworthy, the growth and reproductive development of *grxS17* plants grown in standard conditions and then transferred for 3 weeks to long-day conditions, but at 15°C, was not altered (Fig. 5D). Similarly, when young plants were transferred to long-day conditions at 15°C and high light (500 µmoles photons.m^{-2}.s^{-1}), no alteration was noticed in mutant plants (Fig. S5C). Altogether, these data reveal that plants deficient in GrxS17 display sensitivity to long day in a temperature-dependent manner.

Reproductive development of the *grxS17* mutant as a function of photoperiod

The reproductive development of the mutant was thus thoroughly examined in relation with photoperiod. In short day conditions, where no obvious phenotype regarding the vegetative growth of *grxS17* plants, we noticed that the floral development was accelerated, their floral spike being significantly longer compared to Wt at the same age (Fig. S6). Consistently, their leaf number at flowering is significantly lower (Fig. S6). Mutant plants complemented for GrxS17 expression exhibited contrasting phenotypes under short day, one line (3.3) flowering like the mutant and the other (17.8) like Wt. The difference is likely related to the higher GrxS17 amount in the latter (Fig. S3).

When grown from sowing under long day and high light conditions, *grxS17* plants exhibited a severe phenotype and no development of the primary floral spike in contrast to Wt and complemented lines (Fig. S6). In mutant plants, only secondary floral spikes developed. As a consequence, the leaf number at flowering was significantly higher in *grxS17* than in other lines (Fig. S6). Taken collectively, these data reveal that GrxS17 fulfils a complex, but central role in the development of reproductive organs, since mutant plants display opposite

characteristics depending on photoperiod, *i.e.*, early and delayed flowering under short and long day, respectively.

Histological studies of the *grxS17* mutant

To gain further insight into *grxS17* mutant phenotype, the histology of the shoot apical meristem (SAM) was analysed. The SAM overall structure was apparently not altered in the mutant grown in short-day conditions compared to Wt (Fig. 6A). On the contrary, when grown under long day, the meristem appeared smaller in the mutant compared to Wt. The number of stem cells in the L1, L2 and L3 layers was estimated from cross-sections. The numbers of L1 and L2+L3 cells were 45% lower in the mutant than in Wt, revealing impairment in the pool of stem cells (Fig 6B). Moreover, the size of meristematic cells was noticeably increased in the mutant, suggesting compensation of lower cell division by increased cell elongation (Fig. 6A). The strong alteration in meristematic cells in the mutant appears consistent with the high *GrxS17* expression level in these cells (Fig. 3A) and with the absence of young leaves under conditions of long day and/or high temperature (Fig. 5; Fig. S5). We also carried out a histological analysis of mesophyll cells in Wt and *grxS17* plants grown under long day and high light conditions leading to severely altered leaf development. In mutant plants, the cell density (362 ±53 cells.mm^{-2}) was reduced compared to Wt (810 ± 72 cells.mm^{-2}) and their size much larger (Fig 6C-D). Taken together, histological data indicate that cell division, and likely differentiation, are affected in *grxS17* plants grown under environmental conditions leading to impaired development.

Identification of a nuclear factor as GrxS17-interacting partner

A Ni-matrix loaded with a recombinant His-tagged apo-GrxS17 was prepared to identify possible redox-interacting partners. After applying a crude leaf extract and washing, bound proteins were eluted first with a reductant, dithiothreitol (DTT), and then with imidazole and identified by mass-spectrometry. A consolidated list of 28 partners repeatedly isolated was dressed (Table 1). Interestingly, the predicted or experimentally determined localization of most proteins, *e.g.* cytosol or nucleus, is comparable to that of GrxS17. Moreover, in accordance with a central regulatory role of GrxS17 in signaling pathways and with the known interaction of Grx3/PICOT with protein kinase C in animal cells, two transcription factors and two kinases were isolated. The product of the At3g12480 gene, named NF-YC11, appeared relatively abundant and particularly interesting, taking into consideration the phenotype of *grxS17* plants. Indeed, proteins of the NF-Y family are nuclear factors regulating developmental processes (Kumimoto et al., 2010). Transient expression of NF-YC11-GFP in *A. thaliana* protoplasts indicated that the protein is localized both in cytosol and nucleus (Fig. 7A), like GrxS17 (Fig. 4). Using BiFC, the reconstituted YFP signal was exclusively observed in the nucleus, indicating interaction between GrxS17 and NF-YC11 in this compartment (Fig. 7B). Hence, we finally sought to characterize the phenotype of Arabidopsis plants from the GABI-Kat 043E02 line (Kleinboelting et al., 2012) knockout for NF-YC11 expression (Fig.

8A-B). When grown in short day and moderate light, *nf-yc11* plants showed a very slow and impaired development with a compact rosette and small leaves (Fig. 8C-D). In these conditions, the development of the main floral spike was altered (Fig. 8E). We transferred 35-day old mutant plants grown in short day to long day conditions and observed that these plants developed no main floral spike, but several secondary inflorescences (Fig. 8F). When sown directly in long day conditions at moderate light, mutant plants remained very small and developed reproductive organs earlier than Wt (data not shown). Taken together, these data indicate that NF-YC11 controls plant development and that photoperiod length alters the phenotype of plants deficient in this nuclear factor.

DISCUSSION

Biochemical function of GrxS17: Fe/Fe-S sensing or redox regulation?

GrxS17 appears as a central element for proper plant development in relation to environmental factors, but the precise biochemical function underlying its physiological role remains unknown. Previous studies indicated that multi-domain Grx orthologs from yeast and vertebrates regulate iron-responsive transcriptional regulators (Mercier and Labbé 2009; Ojeda et al., 2006; Pujol-Carron et al., 2006; Kumanovics et al., 2008; Jbel et al., 2011) and intracellular iron distribution through the maturation of most iron-containing proteins (Mühlenhoff et al., 2010; Haunhorst et al., 2013). We thus expected that the functions of this multi-domain monothiol Grx are similar in plants. Accordingly, we showed that Arabidopsis GrxS17 is able to bind Fe-S clusters by *in vitro* reconstitution experiments and to complement the defects in Fe-S cluster maturation of the *S. cerevisiae grx5* strain. However, no noticeable change in the activity of two major cytosolic Fe-S enzymes was observed in plants modified for *GrxS17* expression, indicating no general impairment in Fe-S clusters biogenesis. Overall, these findings indicate that GrxS17 can incorporate labile Fe-S clusters *in vitro* like their non-plant counterparts, but unlike them, the *in vivo* relevance of this property has yet to be determined. As a consequence, we presumed that the physiological role of GrxS17 is rather related to the redox control of partner proteins.

GrxS17: a hub integrating hormonal and redox signals?

Consistent with the pleiotropic phenotype of *grxS17* plants, Western data revealed the presence of GrxS17 protein in all organs, particularly in those containing actively dividing or elongating cells. In addition, *in situ* hybridization showed a high transcript level in apical meristem and histological analyses of plants grown in long day specifically revealed a larger cell size in both meristems and leaves of *grxS17* plants. All these data suggest a crucial role of GrxS17 in meristem activity and cell division. Several studies provided evidence for a tight relationship between intracellular redox status, auxin homeostasis and cell cycle. For instance, the development of root meristems is influenced by changes in the overall redox status and auxin content/distribution (Vernoux et al., 2000; Jiang et al., 2003). Another example is the *A. thaliana ntra ntrb cad2* mutant, which is defective in thioredoxin reduction and GSH synthesis and exhibits strongly impaired reproductive

development in relation to altered auxin metabolism (Bashandy et al., 2010). With regard to disulfide reductases, the plastidial Trx m3 is essential for meristem maintenance in Arabidopsis through a role in the redox regulation of symplastic permeability (Benitez-Alfonso et al., 2009). Focusing on nuclear redoxins, ROXY1 and 2, belonging to class III Grxs, are required for proper development of floral organs likely through the interaction with TGA transcription factors (Xing and Zachgo, 2008; Li et al., 2009; Hong et al., 2012) and nucleoredoxins, NRX1 and NRX2, participate in the establishment of pollen fertility (Marchal et al., 2014). Altogether, these reports support the view that disulfide reductases, particularly in the nucleocytoplasmic compartment, finely control plant development.

Arabidopsis lines knockdown for *GrxS17* expression display hypersensitivity to high temperature and altered auxin-mediated signalling pathways in roots (Cheng et al., 2011). The present work unveils a novel function for GrxS17 in integrating photoperiod signals for proper development. Temperature appears however, as a primary determinant, since the phenotype appears in long-day conditions at 22°C and 28°C, but not a 15°C. In this study, we mainly investigated the phenotype of aerial parts of plants grown on soil and we first observed a modification in the shape of leaves which turned thick and elongated and displayed a reduced number of large cells. Looking for mutants with a similar phenotype (Bensmihen et al., 2008), we noticed that *drl1* and *elo* mutants exhibit elongated leaves and a strongly reduced number of larger palisade cells compared to Wt (Nelissen et al., 2003; 2005). Interestingly, by investigating the genes co-expressed with *GrxS17* using Genevestigator (Hruz et al., 2008), a high correlation was found with *ELO2* (At5g13680). Importantly, the floral development of *drl1* plants is delayed and the root development of both *elo* and *drl1* mutants is substantially reduced (Nelissen et al., 2003). DRL1 regulates RNA polymerase II-mediated transcription through the elongator complex, which is composed of several ELO proteins, displays histone acetyltransferase activity and preferentially acetylates regions in auxin-regulated genes (Nelissen et al., 2010). We may thus hypothesize that the *grxS17* phenotype results from defects in transcription of genes regulated by auxin, a major actor in primordia differentiation and growth (Scarpella et al., 2010).

Possible roles of GrxS17 in interaction with the NF-YC11/Nc2α nuclear factor

The nature of the signal(s) controlling GrxS17 function is unclear, but the regulation could occur at several levels. The changes in the cellular redox status occurring in response to environmental variations or in specific physiological states, like dividing cells, might affect either the protein subcellular localization and/or modify the set of interacting partners through redox post-translational modifications. Concerning the first point, our experiments (GFP-fusion and cellular fractionation) indicate that GrxS17 is localized in both nucleus and cytoplasm (Fig. 4), whereas a former study indicated that high-temperature induced translocation of GrxS17 from cytoplasm to nucleus (Wu et al., 2012). Thus it is

tempting to speculate that, in response to environmental signals or to a specific physiological state, the function(s) of GrxS17 are regulated either by a nucleocytoplasmic shuttling or by a change in the ratio of nucleus *vs* cytoplasm proteins.

A strategy based on affinity chromatography allowed identifying 28 GrxS17 partners, the localization of most of them being consistent with a possible *in vivo* interaction. Note that BolA2, a possible transcriptional regulator whose interaction with GrxS17 was recently characterized by binary yeast-two hybrid and BiFc experiments (Couturier et al., 2014), was not isolated using this procedure. Among identified partners, we focused on the *NF-YC11* gene, which encodes a nuclear factor. Importantly, the interaction was confirmed by BiFC experiments in Arabidopsis protoplasts, further arguing for a physiologically relevant interaction. The *A. thaliana* NF-Y family comprises three main types (A, B and C) represented by 10, 13 and 13 members, respectively, and involved in multiple processes (Laloum et al., 2013). They were initially named CCAAT-binding factor (CBF) or Heme Activator protein (HAP) and usually form trimeric complexes binding to CCAAT-promoter sequences and transcriptionally regulating plant development and stress responses (Dolfini et al., 2012; Laloum et al., 2013). In animal cells, they are central to cell cycle progression (Benatti et al., 2011) and in fungi, the corresponding trimeric complex formed by HAP2, 3 and 5 includes a fourth HAP4 subunit. Interestingly, in *S. pombe*, the function and subcellular localization of HAP4, which participates in iron homeostasis regulation, is regulated by the multidomain Grx4 (Mercier and Labbé 2009). In relation to the flowering phenotype observed in this work, it is worth mentioning that AtNF-YC11 specifically interacts with AtNF-YB3, an isoform controlling flowering time (Kumimoto et al., 2008). To date, the only evidence for a redox control was obtained for a mammalian NF-YB whose association to NF-YC is dependent on the reduction of an intermolecular disulfide (Nakshatri et al., 1996). Most interestingly, all plant NF-YC11 orthologs have a unique N-terminal sequence which clearly distinguishes them from other NF-YCs. On this basis, they have been recently reclassified as homologs to NC2α factors from yeast and mammals (Petroni et al., 2012). NC2α also termed DrAp1, forms with another nuclear factor called NC2β or Dr1, a tight heterodimer able to associate with the TATA-binding complex and thus acting as a transcription repressor as shown in *S. cerevisiae* and in rice (Kim et al., 1997; Song et al., 2002). Two cysteine residues, strictly conserved in plant orthologs, are present in the NC2α/NF-YC11 N-terminal extension. Unfortunately, all attempts to produce recombinant NC2α/NF-YC11 in *E. coli* failed which precluded investigations on a possible redox interaction with GrxS17. In other respects, we observed that the development of a mutant knockout for NC2α/NF-YC11 expression is impaired in a much more pronounced manner compared to *grxS17*, revealing a critical role of this nuclear factor. We might thus hypothesize that GrxS17 regulates the NC2α/NF-YC11 function by controlling its redox state. In the working model inferred from the resemblance of *grxS17* and *elo* mutants and proposing the participation of GrxS17 in the transcriptional regulation

of auxin-related genes, it is conceivable that GrxS17-mediated redox changes modify the capacity of AtNC2α to bind to an NC2β subunit (AtNF-YB11 to 13). This would ultimately result in modification in the transcription level of genes involved in developmental programmes. Consistently with this hypothesis of redox-regulated transcription, it was recently demonstrated that the mammalian H3 histone is glutathionylated and that this modification affects nucleosome stability leading to a more open chromatin structure in response to a redox signal (García-Giménez et al., 2013).

In conclusion, *A. thaliana* GrxS17 appears as a key actor in the control of developmental processes in relation with environment signals and seems to be intimately linked to the regulation of gene expression. It might relay subtle changes in the cellular/nuclear GSH redox state to initiate essential developmental steps, entering this information into the control of gene transcription to regulate meristem activity.

EXPERIMENTAL PROCEDURES

Plant material and growth conditions

Arabidopsis thaliana ecotype Col-0 plants were grown in standard conditions under an 8 h photoperiod and a photon flux density of 200 µmol photons.m^{-2}.s^{-1} at 22°C. Other conditions of light (500 µmol photons.m^{-2}.s^{-1}), temperature (15°C or 28°C) and photoperiod (16 h or continuous light) were applied in controlled growth chambers either from sowing or on 2- to 3-week old plants grown under standard conditions.

Transformation of *A. thaliana* plants

The full-length cDNA encoding GrxS17 (At4g04950) was cloned in the sense direction into the pB2GW7 vector (GATEWAY system, Invitrogen, Carlsbad, CA, USA). Following transformation using *Agrobacterium tumefaciens* C58 strain (Clough and Bent, 1998), homozygous lines (T2) were obtained from resistance segregation assays.

Leaf genomic DNA was extracted using the DNeasy Plant Mini Kit (Qiagen) to perform PCR using the 5'-ATGAGCGGTACGGTGAAG-3' and 5'-CTTACTCGGATAGAGTTGC-3' primers to amplify the *GrxS17* gene and 5'AAAATGGCCGATGGTGAGGATAT-3 and 5'CAATACCGGTTGTACGACCACT-3' for the *actin* gene (Atxx). The PCR program was 95°C for 5 min; 30 cycles (denaturation at 95°C for 50 s, annealing at 55°C for 50 s, extension at 72°C for 2 min) and finally 72°C for 7 min (GeneAmp, PCRSystem 2700, Applied Biosystems).

Expression of recombinant Wt and Cys-mutant proteins and antibody production

The full-length sequence was amplified from *A. thaliana* leaf cDNA, using the 5`-GGGAATTCCATATGAGCGGTACGGTGAAG G-3` and reverse 5`-CGGGATCCTTACTCGGATAGAGTTGCTTTG -3` primers, and cloned into the pET-16b vector (Novagen, Merck Biosciences, Germany) for expression in *E. coli* BL21(DE3)pLysS. The protein was purified by nickel-chelate chromatography (GE Healthcare). The For Mutagenesis was performed using the QuikChange II Site-directed Mutagenesis protocol as recommended by the manufacturer (Stratagene, Germany)and using the following

primers: C33S-sense-CTTCTGGGCTTCTTGGAGTGATGCTTCGAAGCA, C33S-anti-sense TGCTTCGAAGCATCACTCCAAGAAGCCCAGAAG, C179S sense CCTGAAGAGCCTAGGAGTGGGTTTAGCAGGA, C179S anti-sense TCCTGCTAAACCCACTCCTAGGCTCTTCAGG, C309S sense GACCAGAAGAACCAAAGAGTGGGTTCAGTGGGAAA, C309S anti-sense TTTCCCACTGAACCCACTCTTTGGTTCTTCTGGTC C416S sense GGTTCACCAGATGAACCGAAAAGCGGATTTAGCT C416S anti-sense AGCTAAATCCGCTTTTCGGTTCATCTGGTGAACC.

***In vitro* reconstitution assay of Fe-S clusters and analytical measurements**

GrxS17 was reconstituted *in vitro* by incubation with $Fe(NH_4)2(SO_4)2$, cysteine, GSH, pyridoxal phosphate, and *E. coli* IscS in the molar ratio of 1Grx : 6 : 9 : 10 : 0.04 : 0.02 in 50 mM sodium phosphate, 300 mM NaCl, pH 8.0, 5 mM DTT under argon atmosphere for 2 h. After centrifugation for 4 min at 4°C and 13,000 rpm, UV/visible spectra were recorded.

Transient transformation of protoplasts with GFP and split-YFP constructs

Protoplasts were isolated from leaves of 6-week-old wild-type *A. thaliana* plants and used for transient expression of fusion proteins (Wojtera-Kwiczor et al., 2013). cDNAs encoding GrxS17 and NF-YC11 were cloned in sense direction into the pGFP2-vector for C-terminal GFP fusion. For BiFC, pUC SPYNE and pUC SPICE obtained from Jörg Kudla (University of Muenster), were used to insert the sequences of GrxS17 and NF-YC11//NC2α in frame with the N- and C-terminal parts of YFP (pUC-SPINE N-terminal and pUC-SPICE C-terminal). Observations were performed using the cLSM 510 META (Carl Zeiss, Göttingen, Germany). GFP and autofluorescence of chlorophyll were visualized with excitation at 488 nm and emission at 500-530 nm and 650-710 nm, respectively. YFP and autofluorescence of chlorophyll were visualized with excitation at 514 nm and emission at 535-590 nm and 650-704 nm, respectively.

Affinity chromatography and electrospray ionization (ESI) mass spectrometry

His-tagged GrxS17 protein bound to a Ni-NTA-column was used as affinity matrix to purify interaction partners from leaves of 5-week old plants ground in 20 ml extraction buffer (50 mM Bicine, pH 7.8, 100 mM sucrose, 50 mM NaCl). After filtration through Miracloth and centrifugations (10 min, 6,000 *x g*, 4°C and 50 min, 4°C, 100,000 *x g*), the supernatant (30 mg proteins) was directly applied onto the column and incubated for 2 h at 4°C. Then four washing steps with 10 ml containing 20 mM Bicine, pH 7.8 were applied and followed by one washing with 4 ml of the same buffer including 150 mM DTT, another washing without DTT and the final elution with 1 M imidazole. The fractions recovered with DTT and imidazole were analyzed by ESI-MS using 50 µg of proteins per analysis. After tryptic digestion, the protein fragments were separated by reverse-phase HPLC and analyzed by ESI-MS (Holtgrefe et al., 2008). Results were analyzed using the Brucker Daltronics software.

Protein extraction, SDS-PAGE, Western blotting, crosslinking and immunodetection

Plant soluble proteins were prepared as in Rey et al. (2005), separated by SDS-PAGE and electro-transferred onto a nitrocellulose membrane (Pall Corporation, Ann Arbor, MI, USA). Protein crosslinking was achieved using dimethyl pimelimidate•2 HCl (DMP) (Thermo Fisher Scientific, Illkirch, France), as described previously (Riondet et al., 2012). Immunodetection was carried out using primary antibodies diluted 1:1000 and the goat anti-rabbit "Alexa Fluor® 680" IgG (1:10,000) from Invitrogen. Bound antibodies were revealed at 680 nm using the "Odyssey Infrared Imager" from LiCor. Polyclonal antibodies were raised in rabbit against His-tagged AtGrxS17 according to the protocol of the Genecust company.

Yeast plasmids and strains

The GrxS17 entire sequence and each of Grx module, M2 ($S17_{167-252}$), M3 ($S17_{297–383}$) and M4 ($S17_{404-488}$) were cloned in-frame in the yeast plasmid pMM221. pMM221 contains the *S. cerevisiae* mitochondrial targeting sequence of Grx5 plus a C-terminal 3HA/His6 tag, under the control of the doxycycline-regulatory tetO2 promoter (Table S1 and S3) (Molina et al., 2004). pMM54 contains a yeast *GRX5*-3HA construction under its endogenous promoter (Rodriguez-Manzaneque et al., 2002). *S. cerevisiae* strains are described in Table S2. Plasmids were linearized by *Cla*I digestion previous to chromosomal integration.

Growth conditions for *S. cerevisiae* cells

S. cerevisiae cultures were grown as described (Molina et al., 2004). Samples were taken from cultures grown exponentially for at least 10 generations at 30˚C. Sensitivity to oxidants was determined on YPD plates, by spotting 1:5 serial dilutions of exponential cultures and recording growth after 2 days of incubation at 30˚C.

Other methods

Aconitase and malate dehydrogenase were assayed in extracts prepared from cells growing exponentially in YPGalactose medium as described in Robinson et al. (1987).

Isopropylmalate isomerase (Leu1) activity was determined in extracts prepared from cells growing exponentially in SC medium supplemented with the specific auxotrophy requirement (Pierik et al., 2009). In the case of leucine, only 1/3 of the standard concentration was added into the medium to allow growth.

For northern blot analyses, RNA isolation and electrophoresis, probe labelling with digoxigenin, hybridization and signal detection were done as described by Belli et al. (1998). Gene probes were generated by PCR from genomic DNA, using oligonucleotides designed to amplify internal open reading frame sequences.

Total iron cell content was determined under reducing conditions, after acid digestion of cells using 3% nitric acid (Fish, 1988). Mean cell volumes were determined in non-fixed cells using a Coulter Z2 counter to calculate cell iron concentration.

ACKNOWLEDGMENTS

We are very grateful to the Groupe de Recherche Appliquée en Phytotechnologie (CEA, IBEB, SBVME) for technical assistance with controlled growth chambers, P. Henri for valuable technical assistance and D. Cerveau for helpful assistance in phenotype characterization.

This work was funded by ANR JC07_204825 to N.R. and P.R.; ANR 2010 BLAN 1616 to N.R., P.R., N.B., S.T., F.G., C.R., J-P.R., J.G-M.;

LITERATURE CITED

Balasubramanian, S., Sureshkumar, S., Lempe, J. and Weigel, D. (2006) Potent induction of *Arabidopsis thaliana* flowering by elevated growth temperature. *PLoS Genet*., **7,** e106.

Bandyopadhyay, S., Gama, F., Molina-Navarro, M.M., Gualberto, J.M., Claxton, R., Naik, S.G., Huynh, B.H., Herrero, E., Jacquot, J.P., Johnson, M.K. and Rouhier, N. (2008) Chloroplast monothiol glutaredoxins as scaffold proteins for the assembly and delivery of [2Fe-2S] clusters. *EMBO J*., 27, 1122-1133.

Bashandy, T., Guilleminot, J., Vernoux, T., Caparros-Ruiz, D., Ljung, K., Meyer, Y. and Reichheld, J.P. (2010) Interplay between the NADP-linked thioredoxin and glutathione systems in Arabidopsis auxin signalling. *Plant Cell*, 22**,** 376-391.

Belli, G., Gari, E., Piedrafita, L., Aldea, M. and Herrero, E. (1998) An activator/repressor dual system allows tight tetracycline-regulated gene expression in budding yeast. *Nucl. Acids Res*., 26, 942-947.

Benatti, P., Dolfini, D., Vigano, A., Ravo, M., Weisz, A. and Imbriano, C**.** (2011) Specific inhibition of NF-Y subunits triggers different cell proliferation defects. *Nucl. Acids Res.*, 39**,** 5356–5368.

Benitez-Alfonso, Y., Cilia, M., San Roman, A., Thomas, C., Maule, A., Hearn, S. and Jackson, D. (2009) Control of Arabidopsis meristem development by thioredoxin-dependent regulation of intercellular transport. *Proc. Natl. Acad. Sci. USA*, 106, 3615–3620.

Ben-Naim, O., Eshed, R., Parnis, A., Teper-Bamnolker, P., Shalit, A., Coupland, G, Samach, A., and Lifschitz, E. (2006) The CCAAT binding factor can mediate interactions between CONSTANS-like proteins and DNA. *Plant J*., 46, 462–476.

Bensmihen, S., Hanna, A.I., Langlade, N.B., Micol, J.L., Bangham, A. and Coen, E.S. (2008) Mutational spaces for leaf shape and size. *HFSP J*., 2, 110-120.

Cheng, N.H. (2008) AtGRX4, an Arabidopsis chloroplastic monothiol glutaredoxin, is able to suppress yeast grx5 mutant phenotypes and respond to oxidative stress. *FEBS Lett*., 582, 848-854.

Cheng, N.H., Liu, J.Z., Brock, A., Nelson, R.S. and Hirschi, K.D. (2006) AtGRXcp, an Arabidopsis chloroplastic glutaredoxin, is critical for protection against protein oxidative damage. *J. Biol. Chem*., 281, 26280-26288.

Cheng, N.H., Liu, J.Z., Liu, X., Wu, Q., Thompson, S.M., Lin, J., Chang, J., Whitham, S.A., Park, S., Cohen, J.D. and Hirschi, K.D. (2011) Arabidopsis monothiol glutaredoxin, AtGRXS17, is critical for temperature-dependent postembryonic growth and development via modulating auxin response. *J. Biol. Chem.,*286, 20398-20406.

Cheng, N.H., Zhang, W., Chen, W.Q., Jin, J., Cui, X., Butte, N.F., Chan, L. and Hirschi, K.D. (2011) A mammalian monothiol glutaredoxin, Grx3, is critical for cell cycle progression during embryogenesis. *FEBS J*., 278**,** 2525-2539.

Clough, S.J. and Bent, A.F. (1998) Floral dip: a simplified method for Agrobacterium-mediated transformation of *Arabidopsis thaliana*. *Plant J*., 16, 735-43.

Couturier, J., Jacquot J.P. and Rouhier, N. (2009) Evolution and diversity of glutaredoxins in photosynthetic organisms. *Cell. Mol.Life Sci*., 66, 2539-2557.

Couturier, J., Koh, C.S., Zaffagnini, M., Winger, A.M., Gualberto, J.M., Corbier, C., Decottignies, P., Jacquot, J.P., Lemaire, S.D., Didierjean, C. and Rouhier, N. (2009) Structure-function relationship of the chloroplastic glutaredoxin S12 with an atypical WCSYS active site. *J. Biol. Chem.,* 284, 9299-9310.

Couturier, J., Stroher, E., Albetel, A.N., Roret, T., Muthuramalingam, M., Tarrago, L., Seidel, T., Tsan, P., Jacquot, J.P., Johnson, M.K., Dietz, K.J., Didierjean, C., and Rouhier, N. (2011) Arabidopsis chloroplastic glutaredoxin C5 as a model to explore molecular determinants for iron-sulfur cluster binding into glutaredoxins. *J. Biol. Chem.,* 286, 27515-27527.

Couturier, J., Wu, H.C., Dhalleine, T., Pégeot, H., Sudre, D., Gualberto, J.M., Jacquot, J.P., Gaymard, F., Vignols, F. And Rouhier, N. (2014) Monothiol glutaredoxin-BolA interactions: redox control of *Arabidopsis thaliana* BolA2 and SufE1. *Mol. Plant*, **7,** 187-205.

Dolfini, D., Gatta, R. and Mantovani, R. (2012) NF-Y and the transcriptional activation of CCAAT promoters. *Critical Rev.Biochem. Mol. Biol*., 47, 29–49.

Fish, W.W. (1988) Rapid colorimetric micromethod for the quantitation of complexed iron in biological samples. *Method. Enzymol*., 158, 357-364.

Gama, F, Keech, O., Eymery, F., Finkemeier, I., Gelhaye, E., Gardestrom, P., Dietz, K.J., Rey, P., Jacquot, J.P. and Rouhier, N. (2007) The mitochondrial type II peroxiredoxin from poplar. *Physiol. Plant*., 129, 196-206.

García-Giménez, J.L., Òlaso, G., Hake, S.B., Bönisch, C., Wiedemann, S.M., Markovic, J., Dasí, F., Gimeno, A., Pérez-Quilis, C., Palacios, O., Capdevila, M., Viña, J. and Pallardó, F.V. (2013) Histone h3 glutathionylation in proliferating mammalian cells destabilizes nucleosomal structure. *Antioxid. Redox Signaling*, 19, 1305-1320.

Guo, Y., Huang, C., Xie, Y., Song, F. and Zhou, X. (2010) A tomato glutaredoxin gene SlGRX1 regulates plant responses to oxidative, drought and salt stresses. *Planta,* 232, 1499-1509.

Haunhorst, P., Berndt, C., Eitner, S., Godoy, J.R. and Lillig, C.H. (2010) Characterization of the human monothiol glutaredoxin 3 (PICOT) as iron-sulfur protein.

Biochem. Biophys Res. Co., 394, 372-376.

Haunhorst, P., Hanschmann, E.M., Brautigam, L., Stehling, O., Hoffmann, B., Muhlenhoff, U., Lill, R., Berndt, C. and Lillig, C.H. (2013) Crucial function of vertebrate glutaredoxin 3 (PICOT) in iron homeostasis and hemoglobin maturation. *Mol. Biol Cell*, 24, 1895-1903.

Hoffmann, B., Uzarska, M.A., Berndtn C., Godoy, J.R., Haunhorstn P., Lillig, C.H., Lill, R. and Mühlenhoff, U. (2011) The multidomain thioredoxin-monothiol glutaredoxins represent a distinct functional group. *Antioxid. Redox Signaling*, 15, 19-30.

Holtgrefe, S., Gohlke, J., Starmann, J., Druce, S., Klocke, S., Altmann, B., Wojtera, J., Lindermayr, C. and Scheibe, R. (2008) Regulation of plant cytosolic glyceraldehyde 3-phosphate dehydrogenase isoforms by thiol modifications. *Physiol Plant*, 133, 211-228.

Hong, L., Tang, D., Zhu, K., Wang, K., Li, M. and Cheng, Z. (2012) Somatic and reproductive cell development in rice anther is regulated by a putative glutaredoxin. *Plant Cell*, 24, 577-588.

Hruz, T., Laule, O., Szabo, G., Wessendorp, F., Bleuler, S., Oertle, L., Widmayer, P., Gruissem, W. and Zimmermann, P. (2008). Genevestigator v3: a reference expression database for the meta-analysis of transcriptomes. *Ad. Bioinformatics,* 2008, 420747.

Jbel, M., Mercier, A. and Labbé, S. (2011) Grx4 monothiol glutaredoxin is required for iron limitation-dependent inhibition of Fep1. *Eukaryotic Cell,* 10, 629-645.

Jiang, K., Meng, YL. and Feldman, L.J. (2003) Quiescent center formation in maize roots is associated with an auxin-regulated oxidizing environment. *Development*, 130, 1429-1438.

Kim, S., Na, J.G., Hampsey, M. And Reinberg, D. (1997) The Dr1/DRAP1 heterodimer is a global repressor of transcription in vivo. *Proc. Natl. Acad. Sci. USA*, 94, 820-825.

Kleinboelting, N., Huep, G., Kloetgen, A., Viehoever, P. and Weisshaar, B.. (2012) GABI-Kat SimpleSearch: new features of the *Arabidopsis thaliana* T-DNA mutant database. *Nucl. Acids Res*., 40(D1), D1211–D1215.

Kumanovics, A., Chen, O.S., Li, L., Bagley, D., Adkins, E.M., Lin, H., Dingra, N.N., Outten, C.E., Keller, G., Winge, D., Ward, D.M. and Kaplan, J. (2008) Identification of FRA1 and FRA2 as genes involved in regulating the yeast iron regulon in response to decreased mitochondrial iron-sulfur cluster synthesis. *J. Biol. Chem.,* 283, 10276-10286.

Kumimoto, R.W., Adam, L., Hymus, G.J., Repetti, P.P., Reuber, T.L., Marion, C.M., Hempel, F.D. and Ratcliffe, O.J. (2008) The Nuclear Factor Y subunits NF-YB2 and NF-YB3 play additive roles in the promotion of

flowering by inductive long-day photoperiods in Arabidopsis. *Planta*, 228, 709-723.

Kumimoto, R.W., Zhang, Y., Siefers, N., Holt III, B.F. (2010) NF–YC3, NF–YC4 and NF–YC9 are required for CONSTANS-mediated, photoperiod-dependent flowering in *Arabidopsis thaliana*. *Plant J.*, 63, 379–391.

Lai, A.G., Doherty, C.J., Mueller-Roeber, B., Kay, S.A., Schippers, J.H. and Dijkwel, P.P. (2012) CIRCADIAN CLOCK-ASSOCIATED 1 regulates ROS homeostasis and oxidative stress responses. *Proc. Natl. Acad. Sci. USA*, 109, 17129-17134.

La Camera, S., L'Haridon, F., Astier, J., Zander, M., Abou-Mansour, E., Page, G., Thurow, C., Wendehenne, D., Gatz, C., Metraux, J.P. and Lamotte, O. (2011) The glutaredoxin ATGRXS13 is required to facilitate *Botrytis cinerea* infection of *Arabidopsis thaliana* plants. *Plant J.*, 68, 507-519.

Laloum, T., De Mita, S., Gamas, P., Baudin, M. and Niebel, A. (2013) CCAAT-box binding transcription factors in plants: Y so many? *Trends Plant Sci.*, 18, 157-166.

Laporte, D., Olate, E., Salinas, P., Salazar, M., Jordana, X. and Holuigue, L. (2012) Glutaredoxin GRXS13 plays a key role in protection against photooxidative stress in Arabidopsis. J. *Exp. Bot*., 63, 503-515.

Lepistö, A., Kangasjärvi, S., Luomala, E.M., Brader, G., Sipari, N., Keränen, M., Keinänen, M., and Rintamäki, E. (2009). Chloroplast NADPH-thioredoxin reductase interacts with photoperiodic development in Arabidopsis. *Plant Physiol*., 149, 1261-1276.

Li, S., Lauri, A., Ziemann, M., Busch, A., Bhave, M. and Zachgo, S. (2009) Nuclear activity of ROXY1, a glutaredoxin interacting with TGA factors, is required for petal development in *Arabidopsis thaliana*. *Plant Cell*, 21, 429-441.

Lillig CH, Berndt C, Vergnolle O, Lonn ME, Hudemann C, Bill E, Holmgren A (2005) Characterization of human glutaredoxin 2 as iron-sulfur protein: a possible role as redox sensor. *Proc. Natl. Acad. Sci. USA*, 102, 8168-8173.

Liu, Y.J., Nunes-Nesi, A., Wallström, S.V., Lager, I., Michalecka, A.M., Norberg, F.E.B., Widell, S., Fredlund, K.M., Fernie, A.R. and Rasmusson, A.G. (2009) A Redox-Mediated Modulation of Stem Bolting in Transgenic *Nicotiana sylvestris* Differentially Expressing the External Mitochondrial NADPH Dehydrogenase. *Plant Physiol.*, 150, 1248–1259.

Marchal, C., Delorme-Hinoux, V., Bariat, L., Siala, W., Belin, C., Saez-Vasquez, J., Riondet, C., and Reichheld, J.P. (2014) NTR/NRX define a new thioredoxin system in the nucleus of *Arabidopsis thaliana* cells. *Mol. Plant*, 7, 30-44.

Mercier, A. and Labbé, S. (2009) Both Php4 function and subcellular localization are regulated by iron via a multistep mechanism

involving the glutaredoxin Grx4 and the exportin Crm1. *J. Biol. Chem*., 284, 20249-20262.

Meyer, Y., Buchanan, B.B., Vignols, F. and Reichheld, J.P. (2009) Thioredoxins and glutaredoxins: unifying elements in redox biology. *Ann. Rev. Genet*., 43, 335-367.

Michelet, L., Zaffagnini, M., Marchand, C., Collin, V., Decottignies, P., Tsan, P., Lancelin, J.M., Trost, P., Miginiac-Maslow, M., Noctor, G., and Lemaire, S.D. (2005) Glutathionylation of chloroplast thioredoxin f is a redox signaling mechanism in plants. *Proc. Natl. Acad. Sci. USA*, 102, 16478-16483.

Molina, M.M., Belli, G., de la Torre, M.A., Rodriguez-Manzaneque, M.T., and Herrero E. (2004) Nuclear monothiol glutaredoxins of Saccharomyces cerevisiae can function as mitochondrial glutaredoxins. *J. Biol. Chem*., 279, 51923-51930.

Mühlenhoff, U., Gerber, J., Richhardt, N. and Lill, R. (2003) Components involved in assembly and dislocation of iron-sulfur clusters on the scaffold protein Isu1p. *EMBO J*., 22, 4815-4825.

Mühlenhoff, U., Molik, S., Godoy, J.R., Uzarska, M.A., Richter, N., Seubert, A., Zhang, Y., Stubbe, J., Pierrel, F., Herrero, E., Lillig, C.H. and Lill, R. (2010) Cytosolic monothiol glutaredoxins function in intracellular iron sensing and trafficking via their bound iron-sulfur cluster. *Cell Metab*., 12, 373-385.

Murmu, J., Bush, M.J., DeLong, C., Li, S., Xu, M., Khan, M., Malcolmson, C., Fobert, P.R., Zachgo, S. and Hepworth, S.R. (2010) Arabidopsis basic leucine-zipper transcription factors TGA9 and TGA10 interact with floral glutaredoxins ROXY1 and ROXY2 and are redundantly required for anther development. *Plant Physiol.,* 154, 1492-1504.

Nakshatri, H., Bhat-Nakshatri, P. and Currie, R.A. (1996) Subunit association and DNA binding activity of the heterotrimeric transcription factor NF-Y is regulated by cellular redox. *J. Biol. Chem*., 271, 28784-28791.

Ndamukong, I., Abdallat, A.A., Thurow, C., Fode, B., Zander, M., Weigel, R. and Gatz, C. (2007) SA-inducible Arabidopsis glutaredoxin interacts with TGA factors and suppresses JA-responsive PDF1.2 transcription. *Plant J*., 50, 128-139.

Nelissen, H., Clarke, J.H., De Block, M., De Block, S., Vanderhaeghen, R., Zielinski, R.E., Dyer, T., Lust, S., Inzé, D. and Van Lijsebettens, M. (2003) DRL1, a homolog of the yeast TOT4/KTI12 protein, has a function in meristem activity and organ growth in plants. *Plant Cell*, 15, 639-654.

Nelissen, H., De Groeve, S., Fleury, D., Neyt, P., Bruno, L., Bitonti, M.B., Vandenbussche, F., Van der Straeten, D., Yamaguchi, T., Tsukaya, H., Witters, E., De Jaeger, G., Houben, A. and Van Lijsebettens, M. (2010) Plant Elongator regulates auxin-related genes during RNA

polymerase II transcription elongation. *Proc. Natl. Acad. Sci. USA*, 107, 1678-1683.

Nelissen, H., Fleury, D., Bruno, L., Robles, P., De Veylder, L., Traas, J., Micol, J.L., Van Montagu, M., Inzé, D. and Van Lijsebettens, M. (2005) The elongata mutants identify a functional Elongator complex in plants with a role in cell proliferation during organ growth. *Proc. Natl. Acad. Sci. USA,* 102, 7754-7759.

Ojeda, L., Keller, G., Muhlenhoff, U., Rutherford, J.C., Lill, R. and Winge, D.R. (2006) Role of glutaredoxin-3 and glutaredoxin-4 in the iron regulation of the Aft1 transcriptional activator in *Saccharomyces cerevisiae*. *J. Biol. Chem*., 281, 17661-17669.

Petroni, K., Kumimoto, R.W., Gnesutta, N., Calvenzani, V., Fornari, M., Tonelli, C., Holt, BF 3rd. and Mantovani, R.. (2012) The promiscuous life of plant NUCLEAR FACTOR Y transcription factors. *Plant Cell*, 24, 4777-4792.

Pierik, A.J., Netz, D.J. and Lill, R. (2009) Analysis of iron-sulfur protein maturation in eukaryotes. *Nature Protocols*, 4, 753-766.

Pontvianne, F., Abou-Ellail, M., Douet, J., Comella, P., Matia, I., Chandrasekhara, C., Debures, A., Blevins, T., Cooke, R., Medina, F.J., Tourmente, S., Pikaard, C.S. and Sáez-Vásquez J. (2010) Nucleolin is required for DNA methylation state and the expression of rRNA gene variants in *Arabidopsis thaliana*. *PLoS Genet*., 6, e1001225.

Pujol-Carrion, N., Belli, G., Herrero, E., Nogues, A. and de la Torre-Ruiz, M.A. (2006) Glutaredoxins Grx3 and Grx4 regulate nuclear localisation of Aft1 and the oxidative stress response in *Saccharomyces cerevisiae*. *J. Cell Sci*., 119, 4554-4564.

Rey, P., Cuine, S., Eymery, F., Garin, J., Court, M., Jacquot, J.P., Rouhier, N. and Broin, M. (2005) Analysis of the proteins targeted by CDSP32, a plastidic thioredoxin participating in oxidative stress responses. *Plant J*., 41, 31-42.

Riondet, C., Desourisn J.P., Montoyan J.G., Chartier, Y., Meyer, Y. and Reichheld, J.P. (2012) A dicotyledon-specific glutaredoxin GRXC1 family with dimer-dependent redox regulation is functionally redundant with GRXC2. *Plant Cell Environ*., 35, 360-373.

Robinson, J.B. Jr., Inman, L., Sumegi, B. and Srere, P.A. (1987) Further characterization of the Krebs tricarboxylic acid cycle metabolon. *J. Biol. Chem*., 262, 1786-1790.

Rodriguez-Manzaneque, M.T., Tamarit, J., Belli, G., Ros, J. and Herrero, E. (2002) Grx5 is a mitochondrial glutaredoxin required for the activity of iron/sulfur enzymes. *Mol. Biol. Cell*, 13, 1109-1121.

Rouhier, N., Couturier, J. and Jacquot, J.P. (2006) Genome-wide analysis of plant glutaredoxin systems. *J. Exp. Bot.*, 57, 1685-1696.

Rouhier, N., Couturier, J., Johnson, M.K. and Jacquot, J.P. (2010) Glutaredoxins: roles in iron

homeostasis. *Trends Bochem. Sci*., 35, 43-52.

Rouhier, N., Gelhaye, E., Sautiere, P.E., Brun, A., Laurent, P., Tagu, D., Gerard, J., de Fay, E., Meyer, Y. and Jacquot, J.P. (2001) Isolation and characterization of a new peroxiredoxin from poplar sieve tubes that uses either glutaredoxin or thioredoxin as a proton donor. *Plant physiol*., 127, 1299-1309.

Rouhier, N., Lemaire, S.D. and Jacquot, J.P. (2008) The role of glutathione in photosynthetic organisms: emerging functions for glutaredoxins and glutathionylation. *Annual Rev. Plant Biol.*, 59, 143-166.

Rouhier, N., Unno, H., Bandyopadhyay, S., Masip, L., Kim, S.K., Hirasawa, M., Gualberto, J.M., Lattard, V., Kusunoki, M., Knaff, D.B., Georgiou, G., Hase, T., Johnson, M.K. and Jacquot, J.P. (2007) Functional, structural, and spectroscopic characterization of a glutathione-ligated [2Fe-2S] cluster in poplar glutaredoxin C1. *Proc. Natl. Acad. Sci. USA*, 104, 7379-7384.

Scarpella E, Barkoulas M, Tsiantis M. (2010) Control of leaf and vein development by auxin. *Cold Spring Harb. Perspect. Biol*., 2, a001511.

Siefers, N., Dang, K.K., Kumimoto, R.W., Bynum IV, W.E., Tayrose, G., Holt III, B.F. (2009) Tissue-specific expression patterns of Arabidopsis NF-Y transcription factors suggest potential for extensive combinatorial complexity. *Plant Physiol.,* 149, 625–641.

Song, W., Solimeo, H., Rupert, R.A., Yadav, N.S. and Zhu, Q. (2002) Functional dissection of a rice Dr1/DrAp1 transcriptional repression complex. *Plant Cell.*, 14, 181-195.

Sundaram, S. and Rathinasabapathi, B. (2010) Transgenic expression of fern *Pteris vittata* glutaredoxin PvGrx5 in *Arabidopsis thaliana* increases plant tolerance to high temperature stress and reduces oxidative damage to proteins. *Planta*, 231, 361-369.

Sundaram, S., Wu, S., Ma, L.Q. and Rathinasabapathi, B. (2009) Expression of a *Pteris vittata* glutaredoxin PvGRX5 in transgenic Arabidopsis thaliana increases plant arsenic tolerance and decreases arsenic accumulation in the leaves. *Plant Cell Environ.*, 32, 851-858.

Tarrago, L., Laugier, E., Zaffagnini, M., Marchand, C., Le Marechal, P., Rouhier, N., Lemaire, S.D. and Rey, P. (2009) Regeneration mechanisms of *Arabidopsis thaliana* methionine sulfoxide reductases B by glutaredoxins and thioredoxins. *J. Biol. Chem*., 284, 18963-18971.

Vernoux, T., Wilson, R.C., Seeley, K.A., Reichheld, J.P., Muroy, S., Brown, S., Maughan, S.C., Cobbett, C.S., Van Montagu, M., Inzé, D., May, M.J. and Sung, Z.R. (2000) The ROOT MERISTEMLESS1/CADMIUM SENSITIVE2 gene defines a glutathione-dependent pathway involved in initiation and maintenance of cell division

during postembryonic root development. *Plant Cell*, 12, 97-110.

Wojtera-Kwiczor J, Groß F, Leffers HM, Kang M, Schneider M, Scheibe R. (2013). Transfer of a redox-Signal through the cytosol by redox-dependent microcompartmentation of glycolytic enzymes at mitochondria and actin cytoskeleton. *Front. Plant Sci.*, 3, 284.

Wu, Q., Lin, J., Liu, J.Z., Wang, X., Lim, W., Oh, M., Park, J., Rajashekar, C.B., Whitham, S.A., Cheng, N.H., Hirschi, K.D. and Park, S. (2012) Ectopic expression of Arabidopsis glutaredoxin AtGRXS17 enhances thermotolerance in tomato. *Plant Biotechnol. J.*, 10, 945-955.

Xing, S. and Zachgo, S. (2008) ROXY1 and ROXY2, two Arabidopsis glutaredoxin genes, are required for anther development. *Plant J.*, 53, 790-801.

Table 1: List of putative interaction partners of GrxS17.

These proteins have been found repeatedly in affinity chromatography with His-tagged GrxS17 bound to Ni^{2+}-NTA matrix.

Accession number	Protein name	Function	Sequence length (AA)	Sequence coverage [%]
At4g04950	GrxS17		488	90 %
At1g50570	Calcium-dependent lipid-binding family protein	Unknown	388	68 %
At3g12480	NF-YC11	Transcription factor	293	59 %
At4g25860	Oxysterol-binding protein-related protein 4A	Sterol transport	386	56 %
At3g13460	CIPK1 interacting protein ECT2	Unknown	667	52 %
At2g39960	Microsomal signal peptidase 25 kDa subunit	Peptidase activity	192	45 %
At1g13440	GapC2	Glycolysis	338	41 %
At5g46570	BR-signaling kinase 2	Protein phosphorylation	492	41 %
At4g32450	MEF8 similar	Unknown	537	37 %
At4g38710	Glycine-rich protein	Translation initiation factor	465	36 %
At5g26110	Protein kinase family protein	Protein phosphorylation	226	34 %
At1g24510	T-complex protein 1 subunit epsilon	Chaperone activity	535	33 %
At4g31180	Aspartate-tRNA ligase-like protein	Aspartyl-tRNA synthetase activity	270	31 %
At5g11870	Alkaline phytoceramidase	Hydrolase activity	270	28 %
At2g30110	ATUBA1	Ubiquitin activating enzyme activity	1080	26 %
At1g78780	Pathogenesis-related protein	Unknown	238	21 %
At5g54050	Cysteine/histidine-rich C1 domain-containing protein	Protein-disulfide reductase activity	580	21 %
At5g20830	Sucrose synthase 1	UDP-glycosyltransferase activity	808	19 %
At3g61950	Transcription factor bHLH67	Transcription factor	358	16 %
At1g04730	Chromosome transmission fidelity protein 18	ATPase activity	943	14 %
At3g10340	Phenylalanine ammonia-lyase 4	Ammonia-lyase activity	707	12 %
At4g22030	Probable F-box protein At4g22030	Unknown	626	12 %
At1g12900	GapA2	Glycolysis	238	11 %
At4g03350	Eternally vegetative phase 1	Unknown	263	11 %
At3g15730	Phospholipase d alpha 1	Phospholipase D activity	810	8 %
At1g30750	Unknown protein	Unknown	212	7 %
At1g31230	AK-HSDH	Bifunctional aspartate kinase/ homoserine dehydrogenase	911	6 %
At1g79280	Nuclear-pore anchor	Nuclear transport	2115	4 %

FIGURE LEGENDS

Figure 1. Incorporation of Fe-S clusters into recombinant Wt and mutated GrxS17 protein.

(A) Domain structure of GrxS17. Trx-HD: Trx-like domain; M2-Grx, M3-Grx and M4-Grx: three monothiol Grx domains). The positions of the cysteines are indicated by triangles.

(B) Absorption spectra of GrxS17 and cysteine mutants. UV-visible absorption spectra were recorded immediately after *in vitro* reconstitution in anaerobic conditions. The active site cysteines of each Grx domain were individually or all substituted by serines (M2:C179S; M3: C309; M4: C416S; C179/309/416S).

(C) Relative absorption at 420 nm of GrxS17 mutants.

Figure 2. Rescue of the *S. cerevisiae grx5* mutant defects by *A. thaliana* GrxS17.

(A) Sensitivity to *t*-BOOH or diamide after 3 days at 30˚C on YPD plates.

(B) Growth on glucose (YPD plates) or glycerol (YPGly plates) after 3 days at 30˚C.

(C) Ratio between aconitase and malate dehydrogenase activities in exponential cultures at 30˚C in YPGalactose medium.

(D) Relative specific Leu1 activity.

(E) Northern blot analysis of *FIT3* and *FTR1* mRNA levels from exponential cultures at 30˚C. Loading control: *SNR19* mRNA.

(F) Relative iron content from exponential cultures at 30˚C in YPD medium. Mean ± SD (n: 3).

Figure 3. Expression of *A. thaliana* GrxS17.

(A-D) RNA *in situ* hybridization. (A-D) Longitudinal sections of wild-type meristem inflorescences (A, B) and flower buds (C, D). Hybridizations were performed with antisense (A, C) or sense (B, D) GrxS17 cDNA probes. (E). Western analysis of GrxS17 abundance in organs of Arabidopsis Wt plants grown under standard conditions R, root; S, stem; YL: young leaf; ML, mature leaf; OL, old leaf; B, floral bud; F, flower.

Figure 4. Subcellular localization and dimerization of GrxS17.

(A) Transient expression of a GrxS17:GFP fusion in *A. thaliana* mesophyll protoplasts. Autofluorescence of chlorophyll indicates chloroplasts.

(B) Stable expression of a GrxS17:GFP fusion in *A. thaliana* leaves.

(C) Detection of GrxS17 protein in cytosolic (C) and nuclear (N) extracts of Arabidopsis flower buds. Immunodetections of cytosolic thioredoxins TRXh5, and nuclear nucleolin Nuc1 were used to evaluate fraction purity.

(D) Western blot detection of GrxS17 in Wt extracts cross-linked (C) or not (NC) with DMP.

(E) Bimolecular fluorescence complementation assay of GrxS17. Vectors encoding C- and N-terminal split-YFP fusions with GrxS17 were co-transformed into *A. thaliana* mesophyll protoplasts.

Figure 5. Growth and development of plants modified in GrxS17 expression as a function of photoperiod and temperature.

(A) Five-week old plants grown in standard conditions (8 h photoperiod, 200 µmol photons.m^{-2}.s^{-1} at 22°C). (B) Plants grown for 2.5 weeks in standard conditions and transferred to 28°C (8 h photoperiod, 200 µmol photons.m^{-2}.s^{-1}) for 2.5 weeks. (C) Plants grown for 2 weeks in standard conditions and transferred to 28°C and long photoperiod (16 h) (200 µmol photons.m^{-2}.s^{-1}) for 2.5 weeks. (D) Plants grown for 3 weeks in standard conditions and transferred to 15°C and long photoperiod (16 h) (200 µmol photons.m^{-2}.s^{-1}) for 4 weeks. (E) Plants grown in long photoperiod conditions (16 h) (200 µmol photons.m^{-2}.s^{-1} at 22°C). (F) Plants grown for 2 weeks in standard conditions and transferred to continuous light (200 µmol photons.m^{-2}.s^{-1}, 22°C) for 3 weeks. Wt; Wild-type plants; KO: SALK_021301 plants; KO-S17^{+} 3.3 and 17.8: two independent KO lines expressing GrxS17. SD and LD, short day (8 h) and long day (16 h).

Figure 6. Structure of the shoot apical meristem and leaves in the *grxS17* mutant.

(A) Histological structure of the SAM in wild-type, *grxS17* mutant and KO-S17+ 3.3 stained by toluidine blue. Upper-panel (LD, HL): Seven-day old plants grown in long day (16 h) and high light (500 µmol photons.m^{-2}.s^{-1}). Lower panel (SD, LL): Eleven-day old plants grown in short day (8 h) and low light (200 µmol photons.m^{-2}.s^{-1}). Bars = 10 µm.

(B) Number of L1, L2 and L3 layer stem cells in cross-sections of SAM shown in (A). Ten sections per genotype were analyzed

(C) Observation of mesophyll cells in leaves of wild-type (top) and *grxS17* (bottom) plants grown under long day/high light conditions. Bars = 50 µm.

(D) Density of mesophyll cells in the samples shown in (C) (n: 12).

*, value significantly different from Wt value with $p < 0.05$ (*t*-test).

Figure 7. Localization of NF-YC11/NC2α and interaction with GrxS17.

Isolated *A. thaliana* mesophyll protoplasts were transiently transformed with a NF-YC11/NC2α:GFP fusion (A) or with split-YFP constructs containing either GrxS17 or NF-YC11/NC2α (B).

Figure 8. Characterization of a NF-YC11/NC2α T-DNA mutant.

(A) PCR analysis on genomic DNA of At3g12480 and T-DNA in Wt, heterozygous (Htz) and homozygous (Hmz) plants of the GABI-043E02 line. (B) RT-PCR analysis of At3g12480 transcript level in Wt and homozygous plants. (C), Wt plant grown for 9 weeks in standard photoperiod conditions. (D) and (E), Homozygous GABI-043E02 plants grown for 9 and 14 weeks, respectively, in standard conditions. (F), Homozygous GABI-043E02 plant grown for 5 weeks in standard conditions and then transferred for 4 weeks in long-day conditions (16 h).

Figure 1

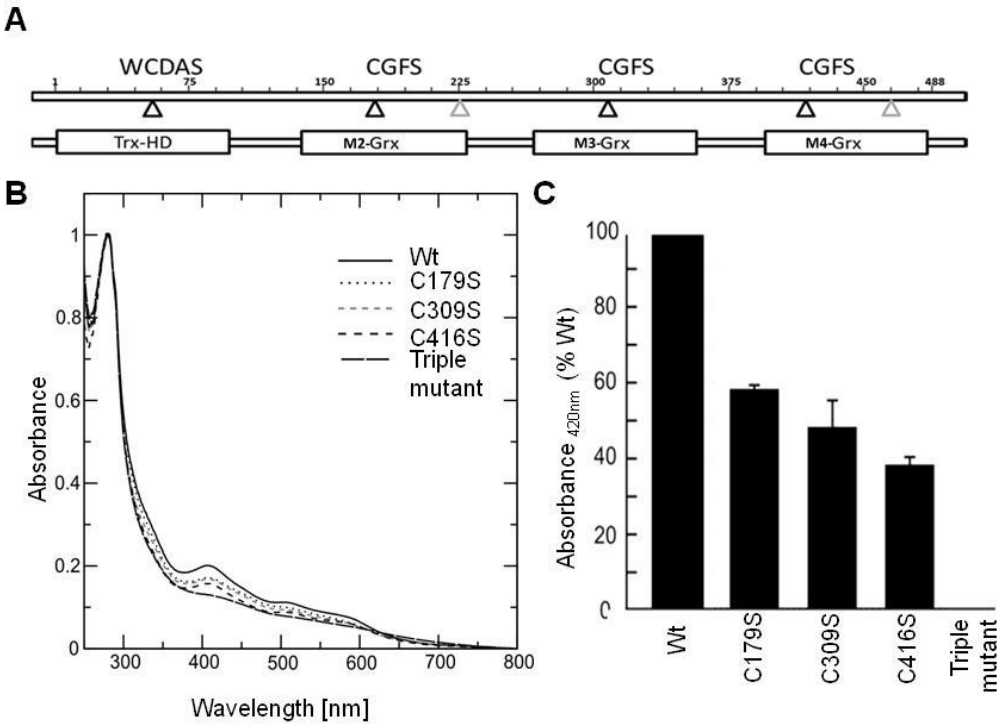
A
WCDAS
CGFS
CGFS
CGFS
1
75
150
225
300
375
450
488
Trx-HD
M2-Grx
M3-Grx
M4-Grx
B
Absorbance
Wavelength [nm]
Wt
C179S
C309S
C416S
Triple mutant
C
Absorbance 420nm (% Wt)
Wt
C179S
C309S
C416S
Triple mutant

Figure 2

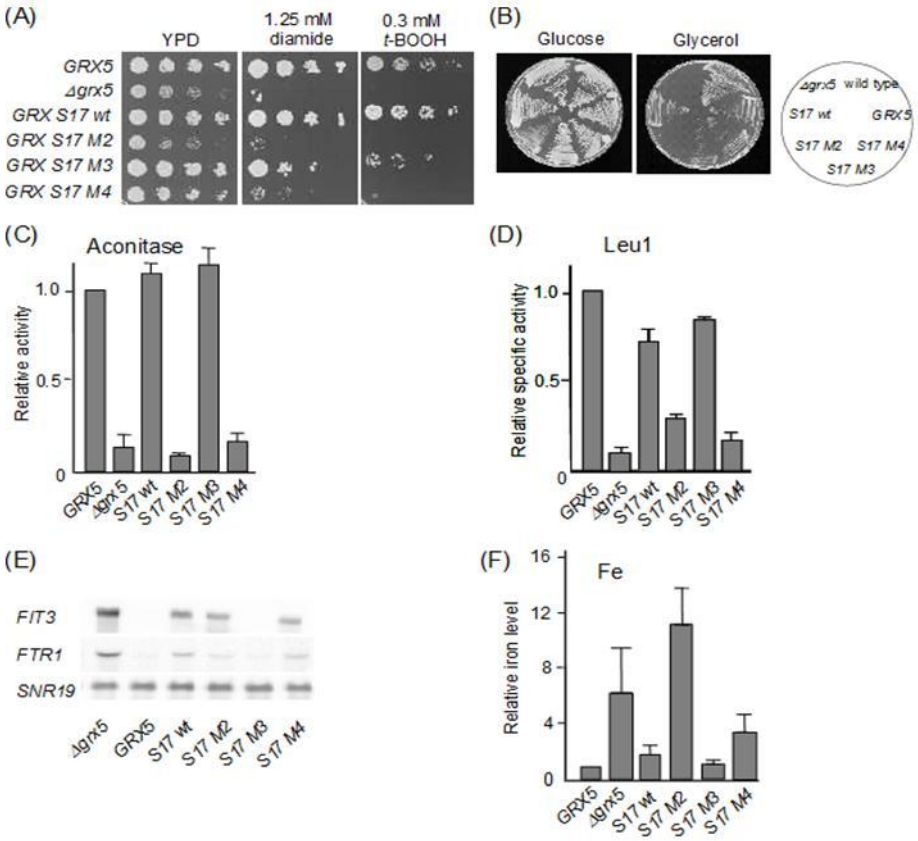
(A)
YPD
1.25 mM diamide
0.3 mM t-BOOH
GRX5
Δgrx5
GRX S17 wt
GRX S17 M2
GRX S17 M3
GRX S17 M4
(B)
Glucose
Glycerol
Δgrx5 wild type
S17 wt
GRX5
S17 M2
S17 M4
S17 M3
(C)
Aconitase
Relative activity
1.0
0.5
0
GRX5
Δgrx5
S17 wt
S17 M2
S17 M3
S17 M4
(D)
Leu1
Relative specific activity
1.0
0.5
0
GRX5
Δgrx5
S17 wt
S17 M2
S17 M3
S17 M4
(E)
FIT3
FTR1
SNR19
Δgrx5
GRX5
S17 wt
S17 M2
S17 M3
S17 M4
(F)
Fe
Relative iron level
16
12
8
4
0
GRX5
Δgrx5
S17 wt
S17 M2
S17 M3
S17 M4

Figure 3

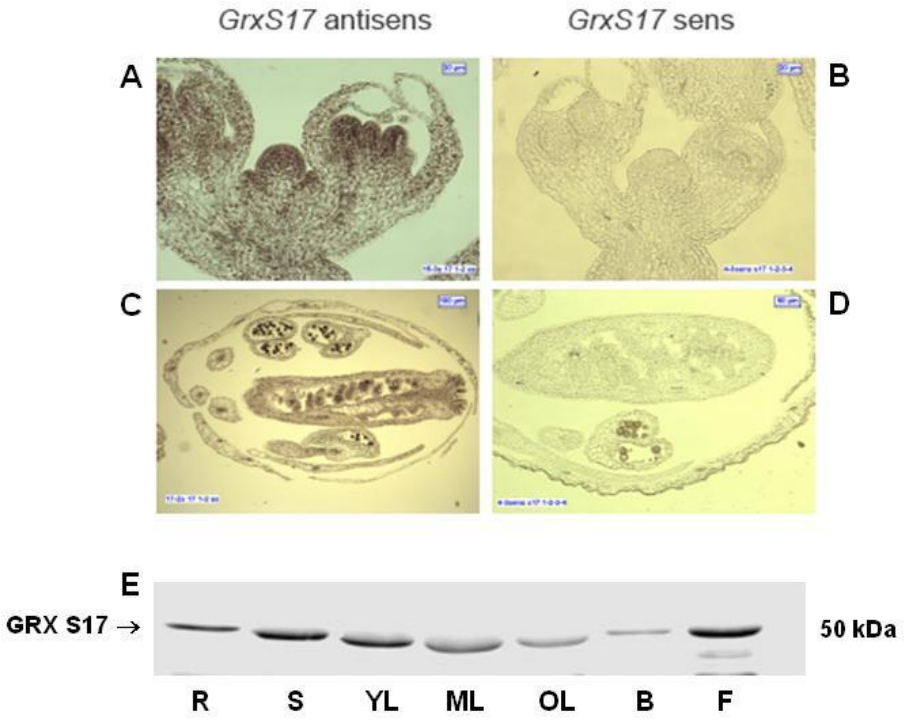
GrxS17 antisens
GrxS17 sens
A
B
C
D
E
GRX S17 →
50 kDa
R
S
YL
ML
OL
B
F

Figure 4

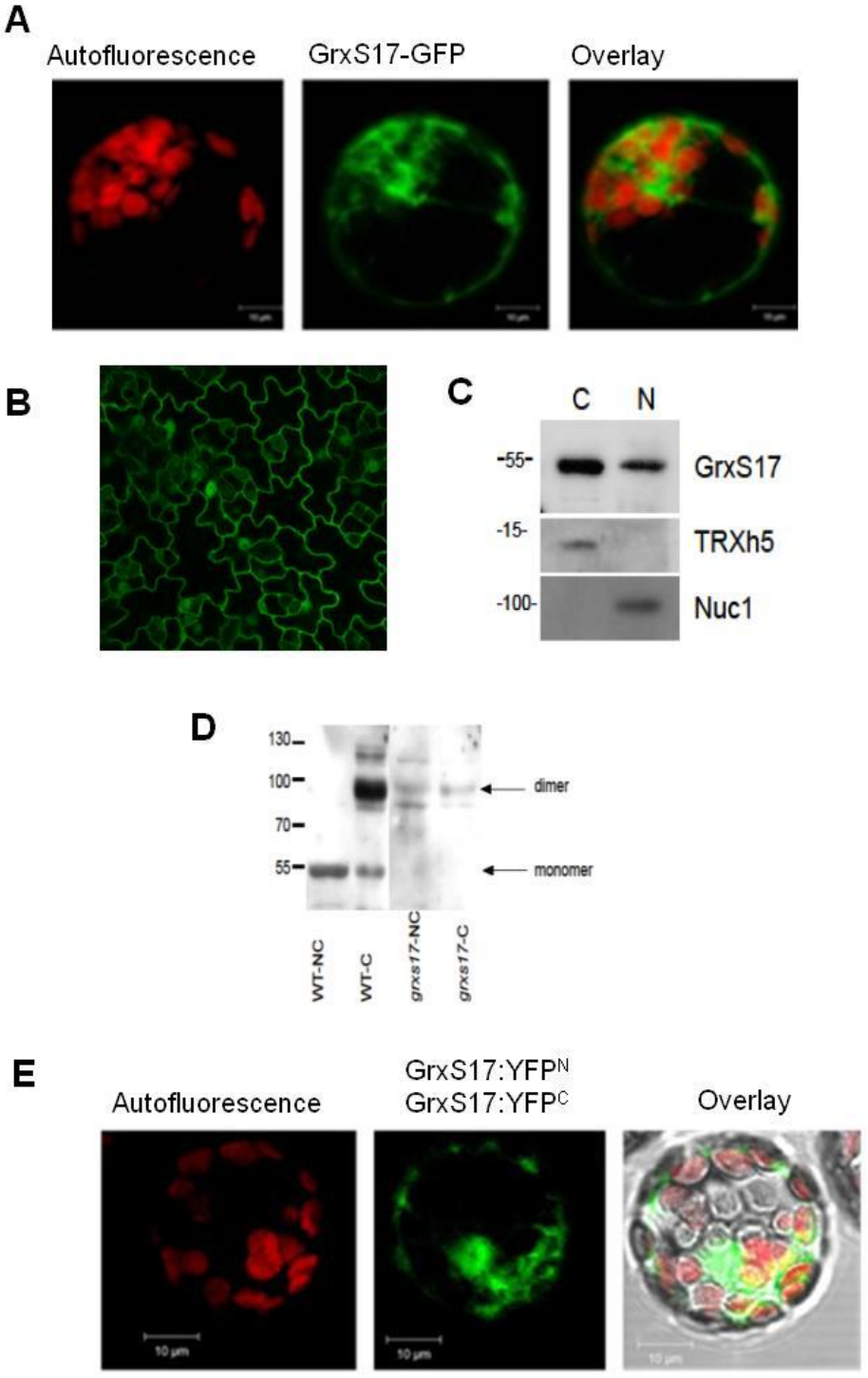
A
Autofluorescence
GrxS17-GFP
Overlay
B
C
C
N
-55-
GrxS17
-15-
TRXh5
-100-
Nuc1
D
130
100
70
55
dimer
monomer
WT-NC
WT-C
grxs17-NC
grxs17-C
E
Autofluorescence
GrxS17:YFP^N
GrxS17:YFP^C
Overlay
10 µm
10 µm
10 µm

Figure 5

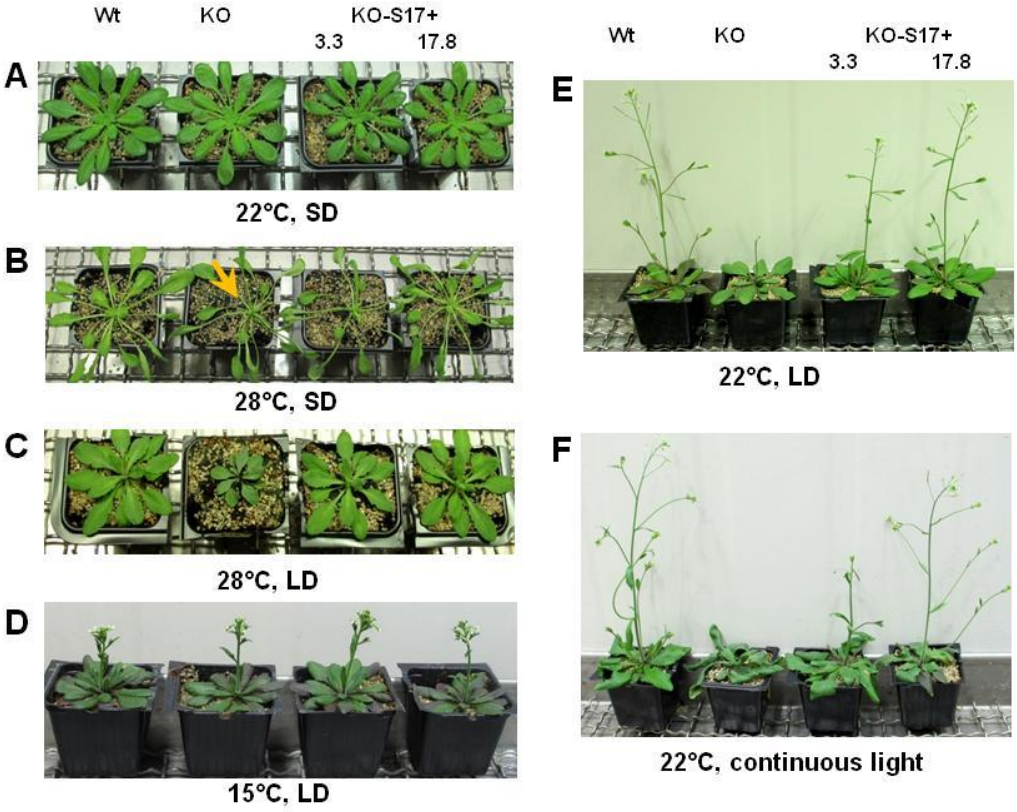
Wt
KO
KO-S17+
3.3
17.8
A
22°C, SD
B
28°C, SD
C
28°C, LD
D
15°C, LD
E
22°C, LD
F
22°C, continuous light

Figure 6

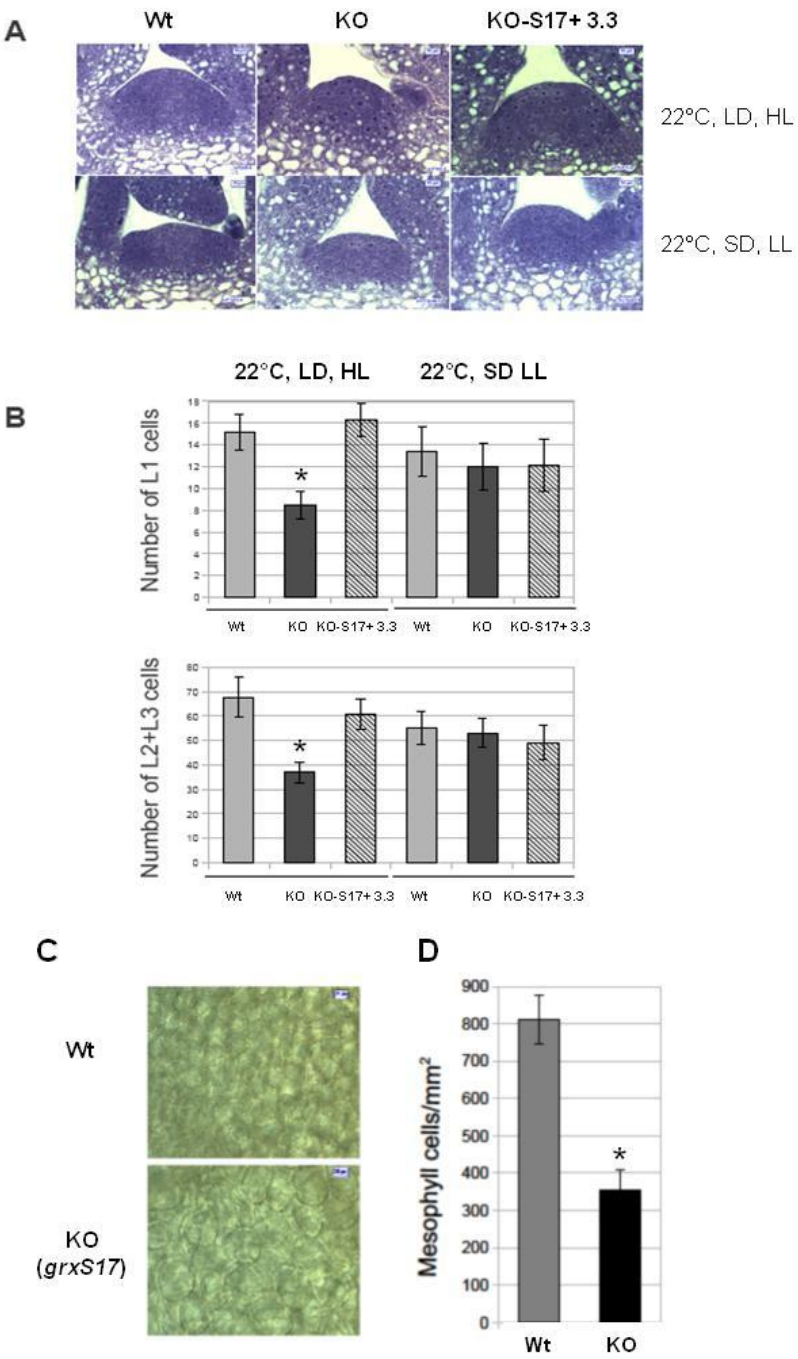
A
Wt
KO
KO-S17+ 3.3
22°C, LD, HL
22°C, SD, LL
B
22°C, LD, HL
22°C, SD LL
Number of L1 cells
Number of L2+L3 cells
Wt
KO
KO-S17+3.3
C
Wt
KO
(grxS17)
D
Mesophyll cells/mm²
Wt
KO

Figure 7

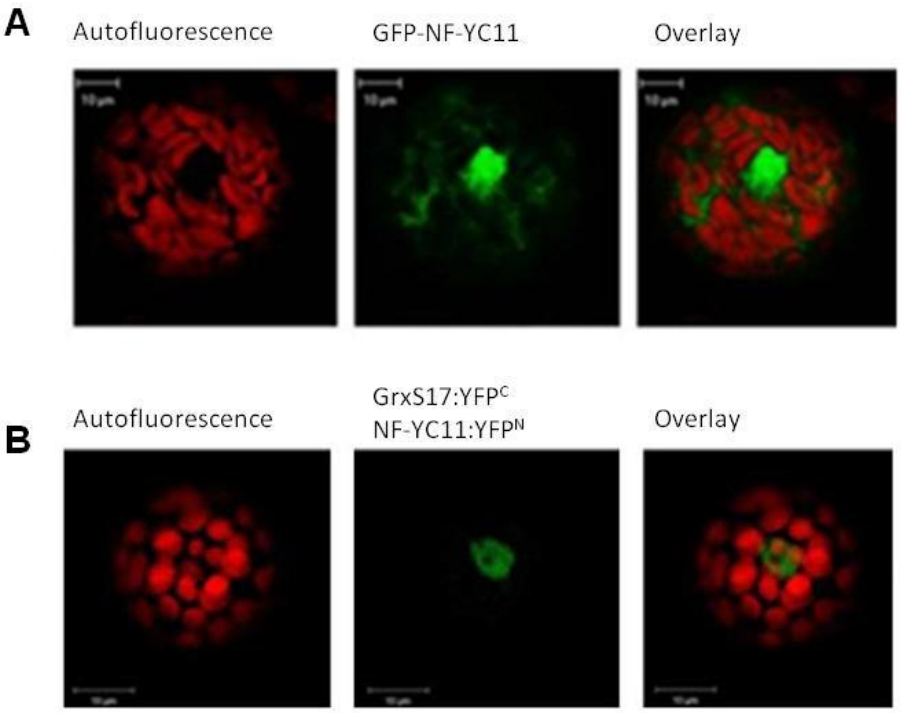
A
Autofluorescence
GFP-NF-YC11
Overlay
B
Autofluorescence
GrxS17:YFP^C
NF-YC11:YFP^N
Overlay

Figure 8

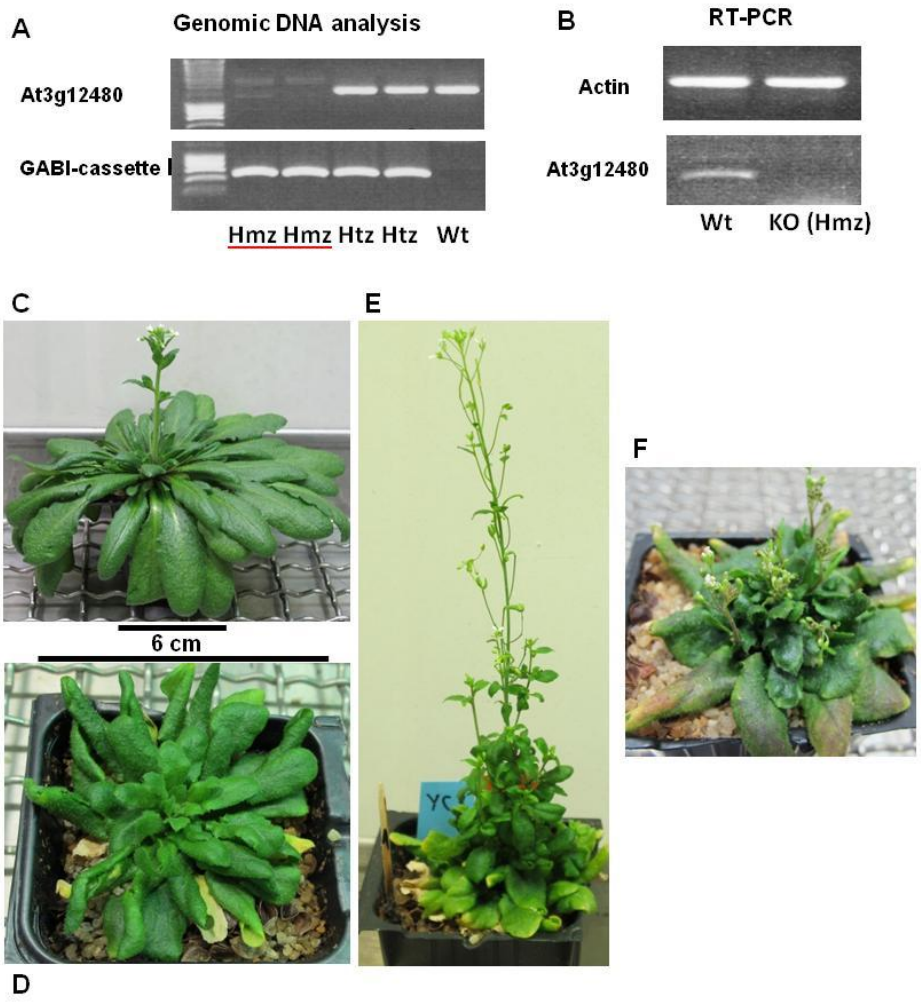
A
Genomic DNA analysis
At3g12480
GABI-cassette
Hmz Hmz Htz Htz Wt
B
RT-PCR
Actin
At3g12480
Wt KO (Hmz)
C
6 cm
D
E
F

Supplemental material

Supplemental Figure 1. . Hypothetical structure of GrxS17 and amino acid alignment of the three Grx-HD domains M2, M3, and M4 from *A. thaliana*. The structure of the single domains was modeled from known Trx/Grx proteins.

Supplemental Figure 2.

Supplemental Figure 3. Molecular characterization of plants modified in GrxS17 expression and GrxS17 protein abundance.

(A). PCR analysis of GrxS17 gene and GrxS17 cDNA in genomic DNA of Wt plants, of SALK_021301 T-DNA plants (KO $S17^-$) and of two independent lines of T-DNA plants expressing the GrxS17 cDNA under the control of the cauliflower mosaic virus 35S promoter (($S17^-/S17^+$ 3.3 and 17.8).

(B). Western analysis of Grx S17 abundance in leaf soluble proteins (20 µg per lane). Grey background in S17- lane is attributed to a non-specific signal from the large RubisCo subunit which has almost the same size as GrxS17.

Supplemental Figure 4. Activity of iron-sulphur enzymes in the *grxS17* mutant and in wild-type. (A) Phenotype of *grxS17* mutants grown under standard conditions and under heat stress in comparison with wild type (Col-0) and a weak allele of *atm3* (M29) plants known to be affected in iron-sulphur cluster assembly. Plants were grown for 7 days at 22°C. For stress treatment one batch was grown at 28°C for further 7 days, the control remained at 22°C. (B) Activities of xanthine dehydrogenase and aldehyde oxidase in leaves measured by in-gel staining in 7.5% native gels (0.15 mg protein/lane). (C) Cytosolic and mitochondrial aconitase activity measured by in-gel staining in 8% native gels containing 2% starch. The activities are shown as the percentage of the total aconitase activity in the sample. The error bars represent the difference between two measurements. (D) Total aconitase activity measured in a coupled enzyme reaction with isocitrate dehydrogenase. Activity was measured after 2 days of heat stress treatment (C,D).Wt = wild type; KO = GrxS17 knock-out line; KO-S17+ 3 (C3) and KO-S17+ 17 (C17): two independent lines of T-DNA plants expressing the GrxS17 cDNA under the control of the cauliflower mosaic virus 35S promoter.

Supplemental Figure 5. Growth and development of plants modified in GrxS17 expression as a function of light and temperature regimes. (A) Five-week old plants grown in high light conditions (500 µmol photons.m^{-2}.s^{-1}) and short day (8-h photoperiod) (22°C). (B) Three-week old plants grown in high light conditions (500 µmol photons.m^{-2}.s^{-1}) and long day (16-h photoperiod) (22°C). (C) Seven-week old plants grown for 3 weeks in standard conditions and then transferred to 15°C, long photoperiod (16 h) and high light conditions (500 µmol photons.m^{-2}.s^{-1}) for 4 weeks. Wt; wild type plants; KO: SALK_021301 T-DNA plants; KO-$S17^+$ 3.3 and KO-$S17^+$ 17.8: two independent lines of T-DNA plants expressing the GrxS17 cDNA under the control of the cauliflower mosaic virus 35S promoter.

Supplemental Figure 6: Floral development of plants modified in GrxS17 expression as a function of photoperiod length and light intensity. (A) 54-day old plants grown in standard conditions (8 h photoperiod, 200 µmol photons.m^{-2}.s^{-1} at 22°C). (B) Four-week old plants grown in high light conditions (500 µmol photons.m^{-2}.s^{-1}) and long day (16-h photoperiod) (22°C). (C) and (D) Height of the main floral spike in plants grown in standard conditions for 54 days and in high light conditions for 4 weeks, respectively. (E) and (F) Number of leaves at flowering in plants grown in standard conditions and in high light conditions, respectively. (G), Five-week old plant KO for *GrxS17* expression grown in high light conditions (500 µmol photons.m^{-2}.s^{-1}) and long day (16 h photoperiod) (22°C). Wt; Wt plants; KO: SALK_021301 T-DNA plants; KO-S17^{+} 3.3 and 17.8: two independent lines of T-DNA plants expressing the GrxS17 cDNA under the control of the cauliflower mosaic virus 35S promoter. ***, significantly different from the Wt value with $p < 0.01$ (t test).

Figure S1

```
M2   MLFMKGIPEEPRCGFSRKVVDILKEVNVDFGSFDILSDNEVREGLKKFSNWPTFPQLYCN 60
M3   MLFMKGRPEEPKCGFSGKVVEILNQEKIEFGSFDILLDDEVRQGLKVYSNWSSYPQLYVK 60
M4   MLFMKGSPDEPKCGFSSKVVKALRGENVSFGSFDILTDEEVRQGIKNFSNWPTFPQLYYK 60
     ****** *:**:**** ***. *.  ::.******* *:***:*:* :***.::**** :
M2   GELLGGADIAIAMHESGELKDAFKD 85
M3   GELMGGSDIVLEMQKSGELKKVLTE 85
M4   GELIGGCDIIMELSESGDLKATLSE 85
     ***:**.** : : :**:** .:.:
```

Figure S2

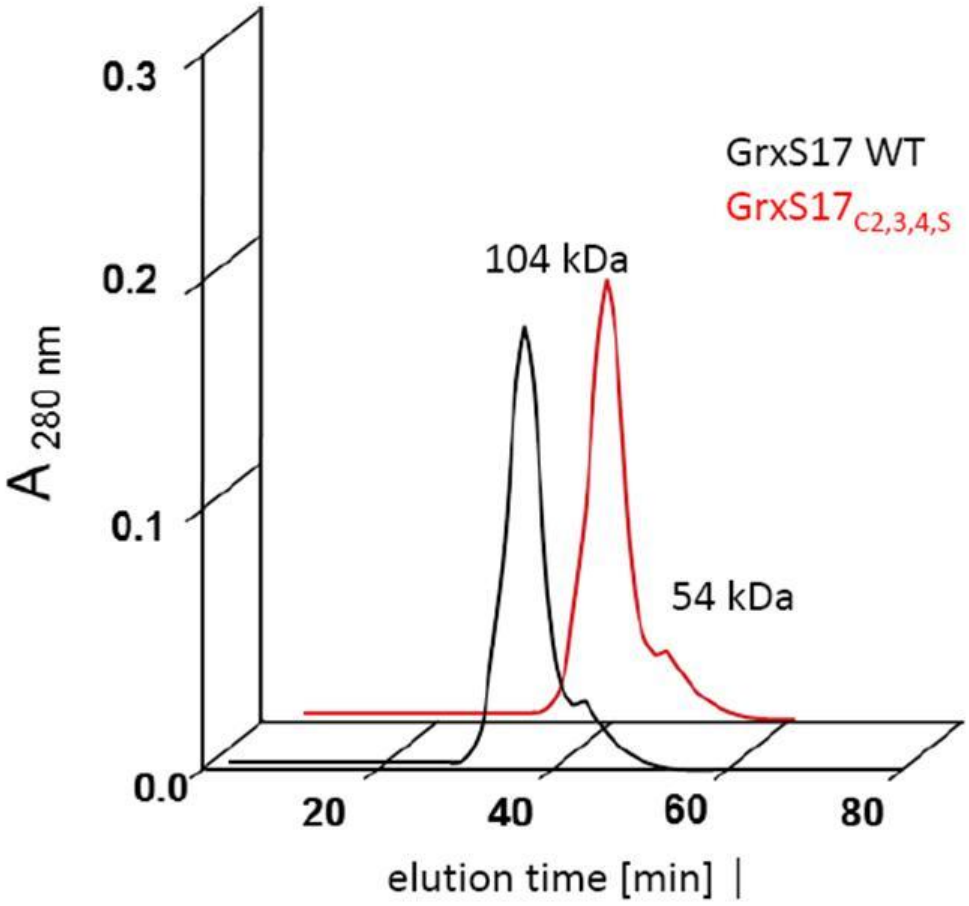
0.3
0.2
0.1
0.0
A 280 nm
GrxS17 WT
GrxS17C2,3,4,S
104 kDa
54 kDa
20
40
60
80
elution time [min]

Figure S3

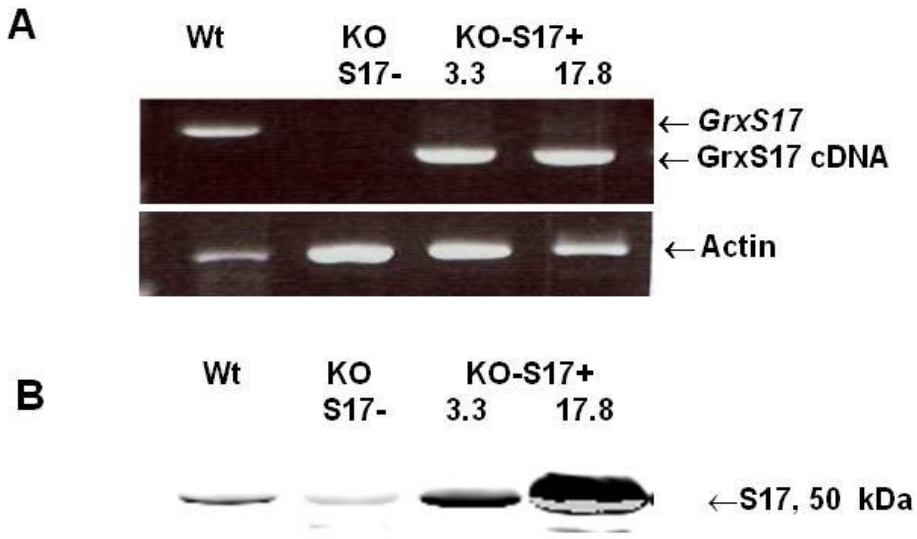
A
Wt
KO S17-
KO-S17+ 3.3
KO-S17+ 17.8
← GrxS17
← GrxS17 cDNA
← Actin
B
Wt
KO S17-
KO-S17+ 3.3
KO-S17+ 17.8
←S17, 50 kDa

Figure S4

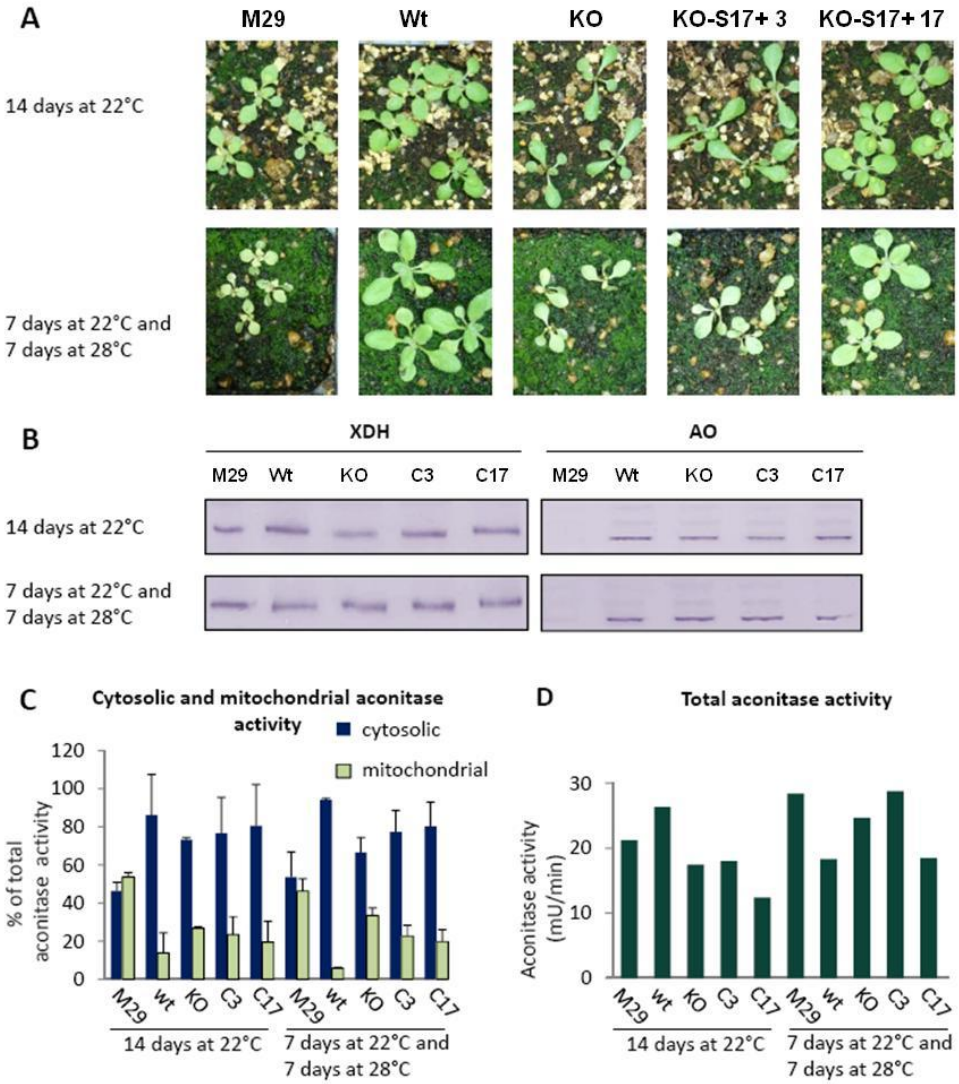
A
M29
Wt
KO
KO-S17+ 3
KO-S17+ 17
14 days at 22°C
7 days at 22°C and
7 days at 28°C
B
XDH
AO
M29 Wt KO C3 C17 M29 Wt KO C3 C17
14 days at 22°C
7 days at 22°C and
7 days at 28°C
C
Cytosolic and mitochondrial aconitase activity
cytosolic
mitochondrial
% of total aconitase activity
120
100
80
60
40
20
0
M29 wt KO C3 C17 M29 wt KO C3 C17
14 days at 22°C
7 days at 22°C and
7 days at 28°C
D
Total aconitase activity
Aconitase activity (mU/min)
30
20
10
0
M29 wt KO C3 C17 M29 wt KO C3 C17
14 days at 22°C
7 days at 22°C and
7 days at 28°C

Figure S5

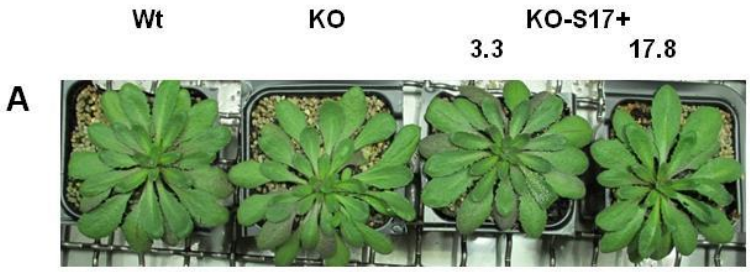

35 days at 22°C, high light (500 µmoles photons.m^{-2}.s^{-1}) and short day (8 h)

21 days at 22°C, high light (500 µmoles photons.m^{-2}.s^{-1}) and long day (14 h)

21 days at 15°C, high light (500 µmoles photons.m^{-2}.s^{-1}) and long day (16 h)
(After 18 days in control conditions)

Figure S6

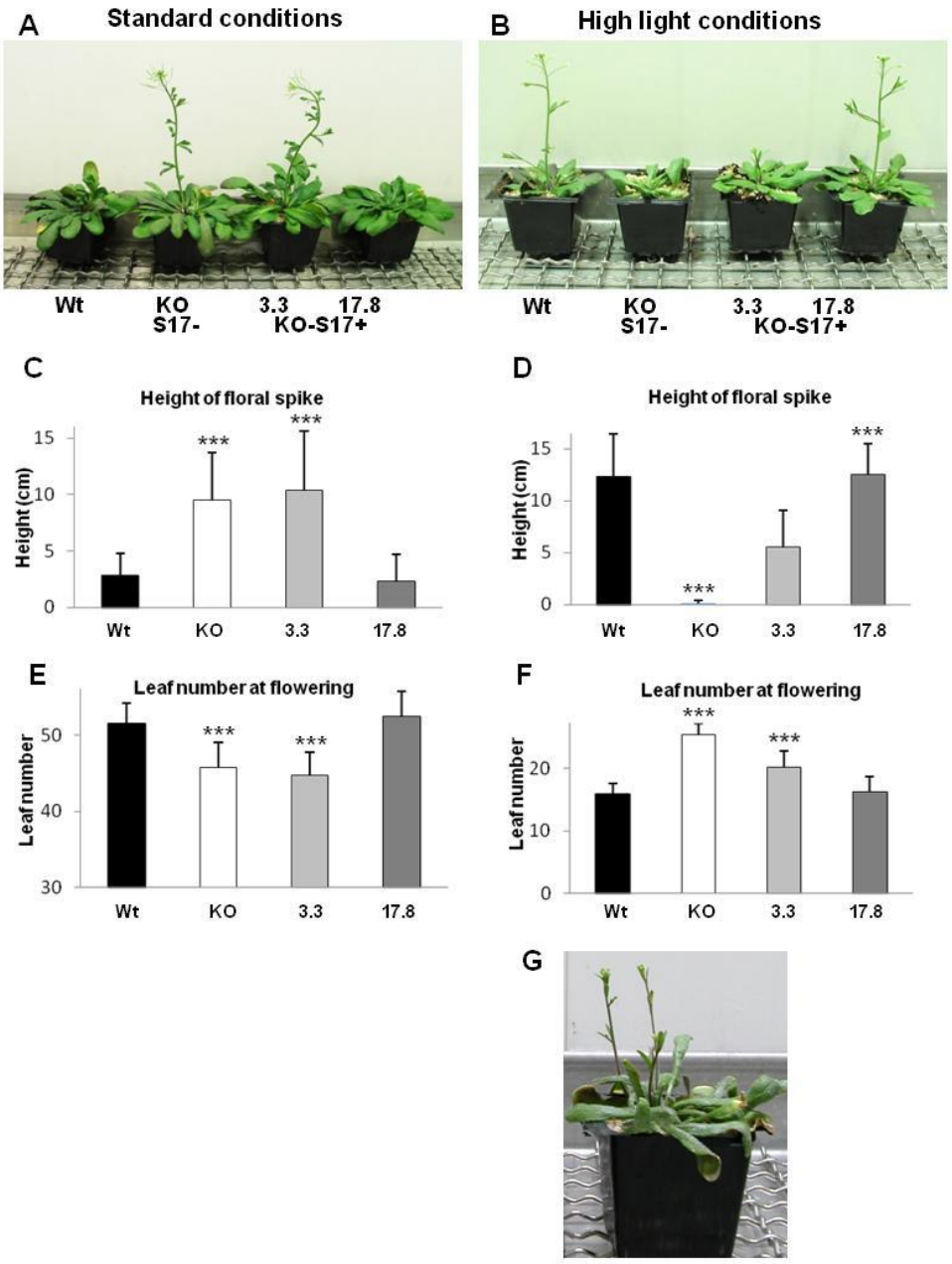
A
Standard conditions
B
High light conditions
Wt
KO S17-
3.3
17.8 KO-S17+
C
Height of floral spike
Height (cm)
D
Height of floral spike
Height (cm)
E
Leaf number at flowering
Leaf number
F
Leaf number at flowering
Leaf number
Wt
KO
3.3
17.8
***
G